3-22-2017 12:00 AM

Superantigen responsive T cells are required for nasopharyngeal infection by Streptococcus pyogenes

Joseph J. Zeppa
The University of Western Ontario

Supervisor
Dr. John McCormick
The University of Western Ontario

Graduate Program in Microbiology and Immunology
A thesis submitted in partial fulfillment of the requirements for the degree in Doctor of Philosophy

Abstract

Streptococcus pyogenes is a human-specific pathogen that is responsible for serious morbidity and mortality worldwide despite being susceptible to common antibiotics. Furthermore, there is currently no licensed vaccine available against this organism. Previous research from our laboratory implicated a critical role for superantigens in a transgenic mouse model of acute nasopharyngeal infection by *S. pyogenes*. Herein, we are able to detect superantigen production *in vivo* and establish that anti-superantigen antibodies generated by either passive immunization or active vaccination with a major histocompatibility complex II-binding interface superantigen toxoid reduces *S. pyogenes* nasopharyngeal burden. We were also able to demonstrate that this organism requires responsive Vβ-specific T cells in order to efficiently infect the upper respiratory tract. These experiments remarkably reveal that *S. pyogenes* manipulates T cells to promote infection and also supports targeting superantigens as vaccine candidates to prevent nasopharyngeal carrier and subsequent disease caused by this globally important pathogen.

Keywords

Streptococcus pyogenes; superantigens; transgenic mouse model; nasopharyngeal infection; passive immunization; vaccination; T lymphocytes

Co-Authorship Statement

This thesis includes work that has been completed by the author and previously published. These works have been reformatted to departmental guidelines and include:

Bacterial superantigens promote nasopharyngeal infection by *Streptococcus pyogenes* in a human MHC class II-dependent manner. Kasper, K. J., Zeppa, J. J., Wakabayashi, A. T., Xu, S. X., Mazzuca, D. M., Welch, I., Baroja, M. L., Kotb, M., Cairns, E., Cleary, P. P., Haeryfar, S. M. M., and McCormick, J. K. 2014. *PLoS. Pathog*. 10:e1004155.

Nasopharyngeal infection of mice with *Streptococcus pyogenes* and *in vivo* detection of superantigen activity. Zeppa, J. J., Wakabayashi, A. T., Kasper, K. J., Xu, S. X., Haeryfar, S. M. M., and McCormick, J. K. 2016. *Method. Mol. Biol.* 1396: 95-107.

Nasopharyngeal infection by *Streptococcus pyogenes* requires superantigen-responsive Vβ-specific T cells. Zeppa, J. J., Kasper, K. J., Mohorovic, I., Mazzuca, D. M., Haeryfar, S. M. M., and McCormick, J. K. Submitted.

Acknowledgments

To John, thank you for being a great mentor and supervisor. The time spent in your lab has continued to fuel my passion for research over the years, and has given me the tools to be successful in this crazy profession. I'll get back to work now!

To the members of the McCormick lab, past and present, thank you for your friendship and all of the good times. You have been a great group of people to spend an overwhelming majority of my time with.

To my thesis advisory committee members, Drs. Haeryfar and McGavin, thank you for your guidance and insightful comments on my project. It would not have been nearly as successfully without your help. Further thanks to Dr. Haeryfar for continued use of his equipment and reagents, as well as to Dr. McGavin for editing this thesis!

Thank you to The Department of Microbiology and Immunology faculty and staff. You have provided myself and countless other students with many opportunities to grow and be successful young scientists. Please continue to fuel a passion for research and all things science in the coming years!

And last but not least, a huge thank you to my friends and family. For understanding and supporting me through not only this chapter of my life, but through all of them. No words can describe how appreciative I am to have all of you in my life. Thank you.

Table of Contents

List of Tables

List of Figures

List of Appendices

List of Abbreviations

°C	degrees Celsius
× *g*	times gravity
7-AAD	7-aminoactinomycin D
µg	microgram
µl	microliter
µm	micrometer
Ab	antibody
ACK	ammonium-chloride-potassium
Amp	ampicillin
ADCC	antibody-dependent cell-mediated cytotoxicity
APC	allophycocyanin
APCs	antigen presenting cells
APSGN	acute post-streptococcal glomerulonephritis
ARF	acute rheumatic fever
BCA	bicinchoninic acid
bp	base pair
BHI	brain heart infusion
BSA	bovine serum albumin
Ca^{2+}	calcium ion
CD(*n*)	cluster of differentiation (*n*)
cDNA	complementary DNA
CDR	complementarity determining region
CFSE	carboxyfluorescein succinimidyl ester
CFU	colony forming unit
cm	centimeter
cNT	complete nasal turbinates
Cov	control of virulence
Csr	capsule synthesis regulator
CPM	counts per minute
cRPMI	complete RPMI-1640
CTL	cytotoxic T lymphocyte
Da	daltons
DAG	diacylglyceride
DALYs	disability-adjusted life years lost
DAPI	4′,6-diamidino-2-phenylindole
DC	dendritic cell
DMSO	dimethyl sulfoxide
DNA	deoxyribonucleic acid
DNase	deoxyribonuclease
dNTP	deoxyribonucleotide triphosphate
EDTA	ethylenediaminetetraacetic acid
ELISA	enzyme-linked immunosorbent assay
FACS	fluorescence-activated cell sorting
FBS	fetal bovine serum

FcγR	Fc-gamma receptor
FITC	fluorescein isothiocyanate
For	forward
FR	framework region
g	gram
G-CSF	granulocyte colony-stimulating factor
GAS	group A *Streptococcus*
GCS	group C *Streptococcus*
GFP	green fluorescent protein
GM-CSF	granulocyte macrophage colony-stimulating factor
GST	glutathione S-transferase
H&E	hematoxylin and eosin
h	hour
HBP	heptose-1,7-bisphosphate
HBSS	Hank's balanced saline solution
HEPES	4-(2-hydroxyethyl)-1-piperazineethanesulfonic acid
HLA	human leukocyte antigen
HP	human plasma
HPLC	high performance liquid chromatography
HRP	horseradish peroxidase
ICE	integrative conjugative element
IκB	inhibitor of NFκB
IKK	IκB kinase
IFN	interferon
Ig	immunoglobulin
IHC	immunohistochemistry
IL-(*n*)	interleukin-(*n*)
IM	intramuscular
IP	intraperitoneal injection
IP-10	interferon gamma-induced protein 10
IP_3	inositol triphosphate
IPTG	isopropyl-β-D-1-thiogalactopyranoside
IRDye	infrared dye
IT	intratracheal
ITAM	immunoreceptor tyrosine-based activation motif
IV	intravenous injection
IVIG	intravenous immunoglobulins
kb	kilobase
KC	keratinocyte chemoattractant
Kd	dissociation constant
kDa	kilodalton
kg	kilogram
LAT	linker for the activation of T cells
LB	Luria-Bertani broth
LIF	leukemia inhibitory factor
LIX	LPS-induced CXC chemokine

LPS	lipopolysaccharide
M	molar
M-CSF	macrophage colony-stimulating factor
MAM	*Mycoplasma arthritidis* mitogen
mAb	monoclonal antibody
Mbp	megabase pairs
MCS	multiple cloning site
MCP-1	monocyte chemoattractant protein-1
MIG	monokine induced by gamma interferon
min	minute
MIP	macrophage inflammatory protein
MHC	major histocompatability complex
mL	milliliter
mm	millimeter
mM	millimolar
MMTV	mouse mammary tumor virus
ms	millisecond
MW	molecular weight marker
NALT	nasal associated lymphoid tissue
Neo	neomycin
NF	necrotizing fasciitis
NFAT	nuclear factor of activated T cells
NFκB	nuclear factor κ light chain enhancer of B cells
ng	nanogram
NK	natural killer cell
NKT	natural killer T cell
nM	nanomolar
OB	oligonucleotide/oligosaccharide-binding
OD	optical density
O/N	overnight
PAGE	polyacrylamide gel electrophoresis
PAMP	pathogen-associated molecular pattern
PBMC	peripheral blood mononuclear cell
PBS	phosphate buffered saline
PBST	phosphate buffered saline with tween-20
PCR	polymerase chain reaction
PDB	Protein Data Bank
PE	phycoerythrin
pg	picogram
PIP_2	phosphatidylinositol 4,5-bisphosphate
PKC	protein kinase C
PLC	phospholipase C
Plg	plasminogen
Plm	plasmin
pM	picomolar
PMN	polymorphonuclear cell

PVDF	polyvinylidene difluoride
RANTES	regulated on activation, normal T cell expressed and secreted
Rev	reverse
RHD	rheumatic heart disease
RNA	ribonucleic acid
RNase	ribonuclease
RPMI-1640	Roswell Park Memorial Institute medium
rRNA	ribosomal ribonucleic acid
rSAg	recombinant superantigen
RT	room temperature
SAg	superantigen
SDS	sodium dodecyl sulphate
SDS-PAGE	sodium dodecyl sulfate polyacrylamide gel electrophoresis
SE	staphylococcal enterotoxin
sec	second
SEl	SE-like
SEM	standard error of the mean
SET	staphylococcal enterotoxin-like
SLO	streptolysin O
SLS	streptolysin S
SmeZ	streptococcal mitogenic exotoxin Z
Spe	streptococcal pyrogenic exotoxin
SSA	streptococcal superantigen
SSL	staphylococcal superantigen-like
STSS	streptococcal toxic shock syndrome
TBS	tris-buffered saline
TBST	tris-buffered saline with tween-20
TCR	T cell receptor
TCS	two-component regulatory systems
TEMED	tetramethylethylenediamine
TEV	tobacco etch virus
TGF	transforming growth factor
THY	Todd Hewitt media plus 1% (w/v) yeast extract
Thr	thrombin
TMB	Tetramethybenzidine
TNF	tumour necrosis factor
Treg	regulatory T cell
tRNA	transfer ribonucleic acid
TSB	tryptic soy broth
TSS	toxic shock syndrome
U	unit
v/v	volume per volume
Vα	variable alpha chain
Vβ	variable beta chain
VEGF	vascular endothelial growth factor
w/v	weight per volume

WHO	World Health Organization
WT	wild-type
YPM	*Yersinia pseudotuberculosis* mitogen

Chapter 1: Introduction

1 Introduction

This thesis introduction will broadly outline what is known about *S. pyogenes*. It will first examine disease manifestations from a clinical perspective followed by descriptions of the best-studied virulence factors. Animal models of infection will then be discussed which will be concluded by current vaccine approaches against this organism. Emphasis should be paid to information regarding streptococcal SAgs and their role in infectious disease as well as limitations to current vaccine approaches.

1.1 *Streptococcus pyogenes*

Streptococcus pyogenes (or Lancefield's group A streptococci; GAS) is a Gram-positive, non-motile, non-sporeforming, aerotolerant anaerobic bacterium, generally round or ovoid and 0.5 to 1 μm in diameter. It grows in pairs or chains of varying length and when grown with blood, it exhibits β-hemolysis or complete lysis of red blood cells. The only known natural reservoir for this organism are humans, and it has been shown to colonize the skin, throat, vagina and rectum [1]. *S. pyogenes* is an important human pathogen capable of causing severe diseases such as necrotizing fasciitis and streptococcal toxic shock syndrome as well as mild illnesses such as pharyngitis or impetigo [2]. Individuals can also be asymptomatic carriers of the bacterium [3]. There are numerous post-infection, non-suppurative sequelae caused by this organism including glomerulonephritis, acute rheumatic fever (ARF) and rheumatic heart disease (RHD) [2]. *S. pyogenes* bacteria remain susceptible to β-lactam antibiotics and there is currently no human-approved vaccine available.

1.2 Invasive streptococcal disease

Invasive infections are defined as the isolation of the infecting organism from a normally sterile site. In regards to *S. pyogenes*, this includes invasion into deep tissues (such as the fascia [necrotizing fasciitis; NF] or the muscle [myositis]), bacteremia and streptococcal toxic shock syndrome (STSS). In 2005, it was documented that there were over 660,000 new cases of invasive infections each year caused by *S. pyogenes* resulting in over 160,000 deaths [4]. These were overwhelmingly in developing nations and thus it is thought that this number was an underrepresentation. Data from recent decades suggest that the

incidence and severity of invasive diseases has increased and this trend seems to be continuing [4–7].

NF is an infection of the underlying human subcutaneous tissue and fascia that results in inflammation and necrosis. It can be caused by numerous other organisms, but due to commonality and severity of tissue trauma, *S. pyogenes* has been termed the 'flesh-eating bacteria'. Infection starts at an often trivial or sometimes benign site with minimal inflammation, but quickly worsens within the next 24-72 hours. A hallmark of NF is disproportionate pain to size of injury [8,9], which can help differentiate it from less severe tissue infections (impetigo, cellulitis), although differentiation is still difficult. Upon worsening, fever and severe pain become consistent, skin becomes 'dusky' and purplish, with edema occurring (filled with yellow or hemorrhagic fluid). These are all signs of the underlying necrosis, which spreads rapidly, and sloughing of the skin can be observed. Treatment consists of removal of infected tissue (debridement and pus drainage), antibiotics to treat the infection (β-lactams [penicillin] and/or protein synthesis inhibitors [clindamycin]), and aggressive supportive care (hemodynamic stabilization, nutritional supplementation and analgesic therapy) [2,10,11]. Mortality rates associated with NF are generally high, with case fatality rates reaching up to 50% in some settings [6,12–14].

STSS typically involves an invasive streptococcal infection associated with hypotension, shock and organ failure, and the clinical definition can be found in **Table 1**. Early symptoms may include pharyngitis, muscle pain, swollen lymph nodes and/or fever, followed by a sudden onset of vomiting, diarrhea, rash and hypotension. If symptoms persist, they may eventually result in multiple organ failure and potentially death. Unlike staphylococcal toxic shock syndrome (TSS), most STSS patients are bacteremic as well [15,16]. Mortality rates increase over NF and are generally between 30 and 70% [17–19]. Although the etiology of STSS is multifactorial, secreted toxins are thought to be significant contributors to the pathology [20]. Treatment of STSS is similar to NF and there is also evidence that administration of intravenous immunoglobulins (IVIG) can help reduce mortality by toxin neutralization [21,22].

1.3 Superficial and locally invasive infections

S. pyogenes is known to cause numerous superficial skin and soft tissue infections. The most common are pharyngitis (commonly known as ‘strep throat’) and pyoderma, of which there were over 600 million and 100 million incidence cases per year, respectively, as of 2005 [4]. It is possible that these infections may seed the severe and invasive diseases previously outlined, or result in post-infection sequelae as discussed below. While pharyngitis is widespread around the world, skin infections are much more common in resource poor settings due to inadequate hygiene and living conditions.

‘Strep throat’ is the most common manifestation of *S. pyogenes* infection and is also the most common cause of bacterial pharyngitis. It constitutes between 20 to 40% of all pharyngitis cases in children and between 5 to 15% in adults [23,24]. Symptoms occur abruptly and may include: sore throat (pain described as severe), moderate fever (39°C to 40.5°C), malaise, chills, headache, neck stiffness, and gastrointestinal symptoms (nausea, vomiting, abdominal pain). Examination of the throat reveals erythema and edema with purulent exudate forming on the tonsils. Cervical lymph nodes may become enlarged and tender. It is possible that fine erythematous papules become apparent on the trunk and spread towards the extremities with a sandpapery feel (scarlatiniform rash) and enlarged papillae may present on the tongue. These characteristics advance the diagnosis to ‘scarlet fever’, a similar, toxin-mediated illness associated with *S. pyogenes* [24]. These illnesses are self-limiting, and last around 8 to 10 days. However, due to the numerous potential complications associated with untreated *S. pyogenes* infections, antibiotic treatment is common which generally sees signs and symptoms subside within 24 to 48 hours.

S. pyogenes is capable of causing numerous non-life threatening skin and soft tissue infections and classification is dependent upon which layer of the skin is involved. Infection of the superficial keratin layer (impetigo), the epidermis (erysipelas) and the subcutaneous tissue (cellulitis) are all possible. Impetigo manifests as a papule with a surrounding area of erythema. Pustules arise, breakdown and form a thick crust, heal slowly, and may leave depigmented areas. Since other common skin dwelling bacteria such as *Staphylococcus aureus* more commonly cause impetigo, and are penicillin resistant, it may be difficult to discern the causative agent and treat appropriately. An FDA approved

Table 1. Streptococcal toxic shock syndrome case definition

I. Isolation of *S. pyogenes* from:	
Definite:	Probable:
Normally sterile site	Nonsterile site
and	
II. Hypotension	
and	
III. Two or more of the following:	
Renal impairment	Coagulopathy
Liver involvement	General erythematous macular rash
Tissue necrosis	Respiratory distress

From The Working Group on Severe Streptococcal Infections [19]

antibacterial, retapamulin, is also approved for treatment of methicillin-susceptible *S. aureus* and *S. pyogenes* impetigo [25].

Erysipelas is an infection of the dermis, but has lymphatic involvement. It is distinguishable by three features: the lesions are raised above the surrounding skin; a clear line of demarcation between involved and uninvolved skin; and a salmon-red colouring. Unlike impetigo, erysipelas is almost always caused by *S. pyogenes*. Upon infection, lesions begin to swell, become erythematic and become raised. If infection occurs on the face, it is common for eyes to become swollen shut. Chills and fever are also commonly associated. It is rare for infections to spread deeper and because a high proportion of cases are caused by *S. pyogenes*, penicillin is commonly used to treat these infections.

Cellulitis occurs mainly from infections of burns, wounds, or surgical incisions. Symptoms include local pain, tenderness, swelling and erythema. There may be rapid spreading into the skin, and can contrast with erysipelas because lesions are not raised and demarcation between involved and uninvolved skin is indistinct. Fever, chills and malaise may be present, and bacterial spreading to lymphatics (lymphangitis), blood (bacteremia) or both is possible. Much like impetigo, it is hard to differentiate between cellulitis caused by *S. pyogenes* and *S. aureus*. Semi-synthetic penicillinase-resistant penicillin, cephalosporin, clindamycin, linezolid or vancomycin may be used to treat cellulitis, depending on the circumstances.

1.4 Asymptomatic Carriage

Asymptomatic carriage is described as the presence of bacteria in the absence of signs or symptoms of infection. *S. pyogenes* is known to inhabit the human nasopharynx, genital mucosa, rectum, and skin in both pathogenic and benign instances. The majority of studies have studied asymptomatic colonization of the upper respiratory tract, and rates are typically around 12% for school aged children (5 to 18 years old) and much lower for adults and younger children [23,26]. Carriers do not seem to be at a higher rate of acquired immune disorders, and since they do not present with symptoms (coughing, coryza), they are found to be ineffective as transmitters. It is difficult to determine if carriers are more likely to have invasive infections because it is usually not possible to determine if a patient

was a carrier prior to an invasive infection. However, it has been shown that those suffering from invasive infections have close contacts that often contain *S. pyogenes* in the pharynx [27,28]. The asymptomatic carriage state of *S. pyogenes* remains an enigma and will probably remain so until more conclusive associations can be found.

1.5 Post-infection sequelae

In 2005, it was estimated that *S. pyogenes* was associated with over 500,000 deaths each year due to severe and invasive diseases. From a morbidity and mortality standpoint, there were over 15.6 million cases of streptococcal post-infection sequelae per year and these resulted in the highest death rates (over 233,000 deaths per year) of all GAS-associated illnesses [4]. Streptococcal post-infection sequelae arise from molecular mimicry, whereby the host's immune system not only generates a response against the invading organism, but also against self, due to bacterial factors that contain cross-reactive epitopes with human molecules. The two main molecules implicated in these types of diseases include the surface M protein and the group A carbohydrate (specifically, the dominant epitope of N-acetyl-β-D-glucosamine) [29,30].

Acute rheumatic fever (ARF) is a delayed inflammatory illness that generally appears two weeks after *S. pyogenes* pharyngitis. ARF is diagnosed based on modified Jones Criteria (**Table 2**) in which an individual with evidence of preceding *S. pyogenes* infection (positive throat culture, positive rapid streptococcal antigen test or elevated anti-streptococcal antibodies) has a combination of two major manifestations, one major and two minor manifestations or three minor manifestations (depending on whether it was an initial or recurring ARF episode). Major criteria indicate the site of inflammation (heart, joints, brain, skin and/or subcutaneous tissue) and the minor criteria demonstrate clinical or laboratory findings (fever, joint pain [arthralgia], elevated acute phase reactants [increased erythrocyte sedimentation rate and C-reactive protein] and/or prolonged PR interval on an electrocardiogram). There are more than 470,000 cases of ARF each year and the majority are in children between the ages of 5 and 14 [4]. Most cases present in poor socioeconomic and developing nations and because of that, data are thought to be underrepresented. More specifically, rates are highest among Pacific populations, specifically those of aboriginal decent [31]. Repeated streptococcal infections and exacerbation of ARF can lead to

Table 2. Modified Jones criteria for diagnosis of acute rheumatic fever

For all patient populations with evidence of preceding GAS infection	
Initial ARF	2 major manifestations OR 1 major plus 2 minor manifestations
Recurrent ARF	2 major manifestations OR 1 major and 2 minor manifestations OR 3 minor manifestations
Major Criteria	
Low-risk populations*	Moderate- and high-risk populations
• Carditis‡ • Arthritis Polyarthritis only • Chorea • Erythema marginatum • Subcutaneous nodules	• Carditis‡ • Arthritis Mono- or polyarthritis Polyarthralgia • Chorea • Erythema marginatum • Subcutaneous nodules
Minor Criteria	
Low-risk populations*	Moderate- and high-risk populations
• Polyarthralgia† • Fever (≥38.5°C) • ESR ≥60 mm in the first hour and/or CRP ≥3 mg/dL • Prolonged PR interval‡	• Monoarthralgia† • Fever (≥38°C) • ESR ≥30 mm/h and/or CRP ≥3 mg/dL • Prolonged PR interval‡

Adapted from Gewitz *et. al.* [32]

GAS, group A *Streptococcus*; ARF, acute rheumatic fever; ESR, erythrocyte sedimentation rate; CRP, C-reactive protein

*Low-risk population are those with incidence ≤2 per 100,000 school-aged children with ARF or all-age rheumatic heart disease prevalence of ≤1 per 1000 population per year

‡Clinical (based on auscultation of typical murmurs) or subclinical (based on echocardiography)

†Joint manifestations can only be considered in either the major or the minor categories but not both in the same patient

‡Can only be used if carditis is not a major criterion

sustained damage of the heart. This clinical manifestation is known as rheumatic heart disease (RHD) and can involve any heart valve, but damage to the mitral and aortic valves are most common [4]. Determinants of progression are poorly understood and initial clinical presentation can range from asymptomatic valvular dysfunction to heart failure. The severity of the initial ARF case and recurrent *S. pyogenes* infections are known to be important factors in the progression of this disease [33] which can lead to other complications including infective endocarditis, atrial fibrillation and thrombolembolic stroke [34]. RHD is the number one cause of mortality associated with *S. pyogenes* infections. The Global Burden of Disease study recently indicated that there are 33 million prevalent cases of this disease, causing more than 275,000 deaths each year and more than 9 million Disability-Adjusted Life Years (DALYs) lost [30,35–37].

Treatment for ARF is supportive, supplemented with antibiotics to treat infections and anti-inflammatory medication. Secondary prophylaxis with antibiotics reduces the risk of RHD in patients with ARF and can also slow the progression and severity of disease in patients with established RHD [38,39]. In developed countries, surgical intervention of individuals with progressed RHD is also possible.

Post-streptococcal glomerulonephritis (PSGN) is the most common cause of acute nephritis in children worldwide but can also occur in adults. It may typically occur after either pharyngitis (1 to 3 weeks) or impetigo (3 to 6 weeks) [40]. PSGN is thought to be due to inflammation as a result of deposition of complement component C3 and IgG in the kidneys. As of 2005, there were over 470,000 cases each year worldwide [4], mostly resulting from epidemics of impetigo in tropical countries [34]. Most common presentations of PSGN are haematuria and oedema with hypertension in around 60% of cases [41]. Full blown renal failure is rare, and death is seen in less than 1% of cases [4]. Usually, symptoms subside within 6-8 weeks without any treatment.

1.6 Group A *Streptococcus* Genome

Based on 19 completed genomes, the 'core' of *S. pyogenes* genome is composed of a single, ~1.8 Mbp circular chromosome with a G+C content of 38.5 ± 0.1%. There are 1,826 ± 92 protein-coding regions, 5 or 6 rRNA operons, and 57 to 67 tRNA genes [42]. A major

source of genetic variability between strains is due to mobile (or putatively mobile) genetic elements including integrative conjugative elements (ICEs) as well as phage and phage-like insertional sequences that generally harbor numerous virulence and adherence factors [43,44]. Many 'hallmark' virulence factors of *S. pyogenes* can be found on the ‘core’ genome including: M protein, the cysteine protease SpeB, the genes responsible for the production of the hyaluronic acid capsule and hemolysins, among numerous others. Genes on mobile genetic elements include DNases, antibiotic resistances and many of the streptococcal SAgs.

1.7 Streptococcal virulence factors

1.7.1 M Protein

The M protein is one of the best-studied surface molecules on Gram-positive organisms and is a major surface determinant present on *S. pyogenes*. The M protein plays a major role in virulence due to its ability to bind to numerous host factors (albumin, fibrinogen, factor H, IgG), preventing non-antibody mediated phagocytosis by PMN cells and mediating adherence to host tissues [29,45].

The M protein is a multi-domain, alpha-helical coiled-coiled dimer that is anchored to the bacterial cell wall at the C-terminus through an LPXTG motif [29,46,47]. The hypervariable N-terminus of the M protein differs amongst strains and a region of about 50 amino acids generates enough variability to aid in the classification of *S. pyogenes*. Serospecificity to this portion originally helped classify streptococci (known as M types); however, with the development of sequencing technology, a genetic classification system has been generated based on the nucleic acid sequence of this region (*emm* type) [48]. The genetic variability in this region has led to the discovery of over 200 *emm* types [49]. Based on the M6 protein – the ‘prototype’ M protein – the central region is made up of several, multiple repeat regions. Typically, the M protein is comprised of four repeat regions – designated A-D from the N- to the C-terminus – which make up the central helical rod of the M molecule. The upper A and B repeat regions are more variable between *emm* types with higher conservation in the C and D repeat regions. The C-terminus is composed of a mixture of positively and negatively charged amino acids, which are conserved amongst

many surface proteins. Just N-terminal of this is a hydrophobic core of around 15-22 amino acids (sufficient to span the cytoplasmic membrane) followed by the LPXTG consensus sequence. This sequence is recognized and cleaved by streptococcal sortase and incorporated into the cell wall.

Other M proteins structures exist and they generally contain some, but not all of the aforementioned features. Thus, *emm*-typing is not as informative in regards to sequence, predicted structure or functional domains. A closely related typing method called *emm* pattern-typing distinguishes chromosomal architecture by taking into account the presence and arrangement of *emm* genes in the chromosome [50] with evidence that *emm* types correlate with *emm* patterns [51]. The *emm* patterns have been broken down into A-C pattern (e.g. M6), D pattern (e.g. M80) which lack the A repeats in the central helical domain, and the E pattern (e.g. M77) which lacks both A and B repeats. Although the best studied pattern is A-C, they account for approximately 20 percent of isolated organisms while other patterns account for approximately 75% [52].

Importantly, there have been associations of certain M types with disease phenotypes such as pharyngitis, impetigo and post-infection autoimmune sequelae [53–57]. This disease association with typing also stems to *emm* [13,14,58] and *emm* pattern-typing whereby the majority of pharyngitis isolates were found to associate with pattern A-C and impetigo isolates belonging to pattern D, whereas Pattern E was considered to be a ‘generalist’ group [44,52,59,60]. These data indicate the complexity of *S. pyogenes* classification, but also their importance in regards to disease association and potential implication in vaccine development.

1.7.2 Capsule

The capsule of *S. pyogenes* is composed of hyaluronic acid, a linear polymer of N-acetylglucosamine and glucuronic acid. It is present on most, but not all clinical isolates in varying amounts and when present it gives the organism a mucoid colony morphology. The composition of the capsule is identical to hyaluronic acid found within the human host, which suggests that it may play a role in molecular mimicry and immune evasion. The capsule has been linked to virulence and it has been shown to increase resistance to

phagocytosis and aid in adherence to the pharynx by binding CD44 [61–64]. This is further demonstrated by the fact that hyper-encapsulated strains are frequently recovered from patients with invasive GAS infections [65]. The capsule is synthesized by the product of three genes that are found in the same operon and transcribed by the same promoter [66,67]. The *hasA*, *hasB* and *hasC* genes encode the hyaluronate synthase, UDP-glucose dehydrogenase and UDP-glucose pyrophosphorylase, respectively [68–71]. Interestingly, only *hasA* and *hasB* appears to be required for capsule expression [72]. These genes are regulated by the *covRS* (control of virulence; originally named capsule synthesis regulator [*csr*]) two component system [73]. A second regulator, *rocA* (regulator of Cov) was also shown to activate transcription of the repressor *covR* and thus has a negative impact on capsule production [74].

1.7.3 Streptococcal pyrogenic exotoxin B protease

Streptococcal pyrogenic exotoxin B (SpeB) is a secreted cysteine proteinase that was originally thought to have pyrogenic and mitogenic activity [75], but this was later shown to be due to contamination. SpeB is produced in response to starvation during late log to early stationary phase in culture, as a 40 kDa inactive zymogen [76]. It then undergoes autocatalytic cleavage and conversion to a 28 kDa active enzyme [77]. Its proteinase activity is mediated by a cysteine at position 192 whereby upon mutation, the protein loses this function [78]. SpeB is known to cleave a number of host (vitronectin [79], fibronectin [79], IL-1β precursor [80], immunoglobulins [Ig] [81], complement 3 [82], chemokines CXCL 1-7, 10-14, 16 [83]) and bacterial (M protein [84], streptococcal mitogenic exotoxin Z [SmeZ] [85], streptokinase [86]) factors [87]. This overwhelming influence on the host and bacterium would suggest that this protease plays a key role in virulence. Essentially all clinical isolate strains encode *speB* [88] and in one study, over 84% of *S. pyogenes* strains demonstrated ‘wild-type’ SpeB activity (as assessed by casein hydrolysis assay) when compared to a reference strain [89]. However, the role of SpeB in pathogenesis is still not well defined. One study examining the invasive M1T1 isolate found that administration of a $SpeB^+$ phenotypic strain into a subcutaneous murine chamber model resulted in a phase-shift to $SpeB^-$. Supernatants from $SpeB^-$ bacteria were also more immune stimulating than the parental $SpeB^+$ strain [90]. But as mentioned above, the ability of SpeB to degrade

numerous host factors could play a beneficial role during infection. Expression of SpeB is highly regulated by the two-component system CovRS in which non-phosphorylated CovR represses the expression of *speB* [2,91]. It is likely that SpeB plays numerous roles during different types of infections and further research will be required to fully understand this cysteine protease.

1.7.4 *Streptococcus pyogenes* cell envelope protease

The *S. pyogenes* cell envelope protease (SpyCEP; ScpC) is capable of cleaving all human CXC chemokines that contain the ELR motif (including the neutrophil chemotractant IL-8) [92–94]. SpyCEP is produced as a 170 kDa zymogen which undergoes autocatalytic cleavage to form two peptides which noncovalently link to form the active protease [92,95]. It can exist as either a secreted or cell-associated form and is produced throughout exponential growth [92,96]. Transcription is thought to be regulated by both the signaling peptide SilCR and the CovRS two-component regulatory system [97,98]. *In vitro* and *in vivo* models examining SpyCEP as a virulence factor are not completely conclusive, but it has been shown to mediate bacterial spread and impede clearance. Interestingly, expression of this molecule by *Lactococcus lactis* did produce hallmarks of streptococcal systemic infections [94,98–100]. To support the role of SpyCEP as a virulence factor, along with *S. pyogenes*, a number of other pathogenic streptococci also produce homologues of this protease [101].

1.7.5 Streptococcal C5a peptidase

The *S. pyogenes* C5a peptidase (ScpA) is a 130 kDa proteolytic enzyme that cleaves the complement-driven chemotaxin C5a at the PMN-binding site [102,103] which thus inhibits recruitment of phagocytic cells to the site of infection [103,104]. The *scpA* gene is controlled by the *mga* regulator [105,106] and the protein is bound to the bacterial cell surface by sortase A [107,108]. The importance of this molecule in bacterial fitness is supported by C5a peptidase homologues being found in Group B *Streptococcus*, which are thought to have arisen by horizontal gene transfer [109]. In mouse models of infection, bacterial strains without C5a peptidase were cleared more efficiently from an air sac model [104] and a nasopharyngeal infection model [110] compared to the wild-type strains.

1.7.6 Streptococcal inhibitor of complement-mediated lysis

The streptococcal inhibitor of complement-mediated lysis (SIC) is a 31 kDa extracellular protein with multiple functions. SIC inhibits the formation of the membrane attack complex [111,112], inhibits the activity of antimicrobial peptide LL-37, and also inhibits the function of lysozyme, secretory leukocyte proteinase inhibitor and defensins [113–115], the chemokine MIG (CXCL9) [116] and interferes with the activation of the contact system of the innate immune response [117]. Evidence also exists that SIC may play a role in adhesion and colonization [118,119]. Interestingly, there is high variation in *sic* between GAS strains [114,120,121] which is thought to have arisen in response to host immune pressure during epidemics to enhance survival *in vivo* [122].

1.7.7 Hemolysins

There are two major hemolysins secreted by *S. pyogenes*, Streptolysins O (SLO) and S (SLS). Both of these molecules have varying effects on a number of cell types.

SLO is a 69 kDa cholesterol-dependent, thiol-activated, pore-forming cytotoxin that is also oxygen-labile. Pore formation in a host cell membrane occurs with binding of monomers in a cholesterol-dependent manner, in which there may also be glycan involvement. This is followed by oligomerization resulting in completion of the intact pore and can lead to apoptosis of the cell by disruption of membrane integrity [123–126]. SLO and another GAS product, NAD-glycohydrolase (*S. pyogenes* NAD-glycohydrolase [SPN]; encoded by the *nga* gene) are co-transcribed and it has been shown that SLO is required for the translocation of this molecule into host cells via a 70-residue N-terminal region on SLO. Inside the cell they act synergistically to trigger cell cytotoxicity [127]. Interestingly, cholesterol and pore formation are not required for this translocation [128–130]. SLO is thought to potentially play a role in barrier penetration, whereby SLO-mediated epithelial lysis allows toxin and bacteria to gain access to sub epithelial sites [131,132]. SLO has been shown to be an important virulence factor for GAS, as mutants lacking this molecule were less virulent in murine models [126,133,134]. The presence of SLO expression in human infections is supported by the fact that SLO is highly immunogenic and anti-SLO antibody titres are used as evidence of GAS infection [135,136].

Streptolysin S (SLS) was first differentiated from SLO in 1938 by E. W. Todd, who also determined it was oxygen-stable (unlike SLO) and highly soluble in serum [137]. Later research would go on to show that a nine-gene operon (*sagA-I*) is responsible for the production of the 53 amino acid precursor (*sagA*), post-translational modification enzymes (*sagB-D*), immunity gene (*sagE*) and exporter (*sagG-I*) [138,139]. Each of these genes is required for expression of functional SLS, which is a 2.7 kDa, heterocyclic compound responsible for the β-hemolytic phenotype of GAS [140,141]. SLS cytolytic activity requires association with the bacterial cell surface or a carrier molecule [142,143] and is broad, including erythrocytes [137], leukocytes [144], platelets [145] and subcellular organelles [146,147]. SLS is related to class I bacteriocins [138] and cytolytic activity is thought to be similar to complement-mediated lysis, in which pore formation leads to osmotic lysis [148]. More recent research indicates a possible role for SLS in host cell signaling pathways at sub-lytic concentrations [149]. SLS is non-immunogenic, which is thought to be due to its post-translational modification and toxic effect on white blood cells [139]; however, neutralizing antibodies can be raised against synthetic peptide variants [150]. SLS was determined to be important in mouse models of GAS infection [151,152]; however, GAS strains with mutations in the SLS biosynthetic operon (non-hemolytic) have been shown to cause soft tissue infections, pharyngitis and otitis media [153,154].

1.7.8 Streptokinase

Streptokinase (Ska; encoded by the *ska* gene) is a 46 kDa, multi-domain protein that non-enzymatically converts the inactive zymogen plasminogen (Plg) to its proteolytically active form, plasmin (Plm) [155–157]. Conversion is thought to occur in a two-cycle pathway: (1) Trigger cycle - binding of Ska to Plg induces a conformational change in Plg resulting in the formation of an active site in the complex, where cleavage of Plg to Plm occurs. (2) Bullet cycle – Ska-Plm complex can bind a second Plg molecule which is quickly converted to Plm. One of the Plm is removed and another Plg can be bound and the cycle continues [158–160]. Variants of this protein are secreted by Group A, C and G streptococci which have functional differences and can be subdivided into two categories [161–163]. The role of Ska during infection is thought to be that activation of Plg to Plm increases dissemination by degradation of host extracellular matrix proteins both directly

and indirectly [2,29]. Ska is regulated by the two-component systems CovRS and FasBCA [91,164–167] and can be cleaved by SpeB [86]. Transgenic mice expressing human plasminogen had higher mortality when infected with GAS and susceptibility was dependent on Ska expression [168]. A novel inhibitor that reduces Ska gene expression also proved protective in this model, implicating a role for Ska in GAS pathogenesis [169].

1.7.9 Superantigens

1.7.9.1 General Introduction

The term ‘superantigen’ was first coined by Philippa Marrack and John Kappler in 1989 due to the strong and specific reactivity of this family of toxins with T cells bearing specific T cell receptor (TCR) variable-beta (Vβ) chains with little input from other variable elements [170]. These toxins, however, were previously known to have mitogenic effects towards lymphocytes [171] and were actually discovered in the 1920s by George and Gladys Dick as the causative agent in scarlet fever [172]. Following these landmark papers, there have been numerous advancements in the field of SAg research which have aided in our understanding of these toxins. These findings include the diverse number of SAgs encoded by numerous organisms, their mode of action and the role they play in many diseases.

1.7.9.2 Superantigen Diversity

Superantigenic molecules can be found in both gram-positive and -negative bacteria as well as in viruses. By far the best studied SAgs are found in the human pathogens *S. aureus* and *S. pyogenes*, but these toxins can also be found in other streptococcal species, the bacterium *Mycoplasma arthritidis* [173] and *Yersinia pseudotuberculosis* [174] as well as rabies [175], mouse mammary tumor [176] and human endogenous retro- [177,178] viruses. Due to the vast knowledge of the staphylococcal and streptococcal SAgs our primary focus will be on those toxins.

The staphylococcal SAg nomenclature is based on the ability of the toxin to also cause food poisoning (including emesis), and are thus described as staphylococcal enterotoxin (SE) or -like (SEl) molecules. The SE SAgs have been scientifically shown to induce emesis, whereas SEl toxins have similar tertiary structure but not been shown to have this

feature [179,180]. The exception to this is the SAg primarily implicated in menstrual toxic shock syndrome (TSS), TSS toxin-1 (TSST-1) [181]. Despite nomenclature being primarily based on emetic properties, all SEs, SEls and TSST-1 have the ability to activate T cells based on TCR Vβ specificity (with the exception of SEH, which targets the TCR Vα chain [182–184]). Another group of related toxins, termed the staphylococcal superantigen-like proteins (SSLs; originally named staphylococcal enterotoxin-like [SET] proteins) were shown to have high sequence similarity to the staphylococcal SAgs but were not enterotoxic or superantigenic [179,185,186]. There are currently over 20 staphylococcal SAgs and with genomes being 'mined' for these toxins, more are likely to be discovered.

Streptococcal SAgs were first named due to their ability to induce fever (e.g. streptococcal pyrogenic exotoxin [Spe]) and later based on their mitogenic (streptococcal mitogenic exotoxin [Sme]) or superantigenic (streptococcal SAg [SSA]) activities. Upon the screening of numerous streptococcal genomes (including Group A, C and G streptococci) an abundance of streptococcal SAgs and numerous alleles were discovered and subsequently characterized and named. Despite sequences being extremely similar (or the same), numerous toxins were differentially named, which caused confusion in the field of streptococcal SAg research for years. Recently, Commons *et al.* analyzed the literature and clarified a number of these errors [187]. This clarification has led to the classification of 14 streptococcal SAgs, SpeA, C, G, H, I, J, K, L, M, N, O, P, SSA and SmeZ, of which 11 are found in GAS (all except SpeN, O and P). There is also allelic diversity within specific SAgs in which 91 unique nucleotide sequences encoding complete streptococcal SAgs were found to belong to those 14 SAgs mentioned above. By far the greatest allelic diversity was discovered in SmeZ which had over 50 variants, some of which were nonfunctional due to a single base pair deletion forming a truncated protein [187–189].

Between the staphylococcal and the streptococcal SAgs, a family of toxins (termed the SAg superfamily) with highly conserved tertiary structure and apparent functional redundancy has been described [179,190]. The SAgs produced by these organisms can be categorized into five groups (Group I – V) based on their amino acid sequences. Interestingly, SAgs generally do not cluster based on the organism that produces them, indicating potential

horizontal gene transfer between organisms throughout their evolution. TSST-1, the non-emetic, causative agent of menstrual staphylococcal TSS [191], and SEl-X are the only SAgs in Group I [192]. Group II SAgs include common causes of non-menstrual TSS such as SEB, SEC [193,194] and SpeA [17]. Group III contains only staphylococcal SAgs such as SEA, SED and SEE, all of which are known to be emetic [195]. Group IV SAgs are all from streptococcal species and include the well-studied SpeC. Group V consists of mostly staphylococcal SAgs from the SEl group, other than SEI and SpeI. The differences between SAg Groups I – V are not only their amino acid sequences, but also the engagement of host immune receptors, which will be discussed below.

The majority of staphylococcal and streptococcal SAgs are found on mobile genetic elements. The staphylococcal SAgs are generally found on prophages, plasmids and pathogenicity islands (PI), discrete chromosomal accessory genetic segments harboring many virulence factors, but lacking essential genes [196–198]. The same is observed with streptococcal SAgs in that they are primarily found on phage-like elements [43,199]. In both organisms, however, there are SAgs encoded on the core genome, such as *selx* in *S. aureus* [200] and *speg*, *spej* and *smez* in *S. pyogenes* [199]. The presence of SAgs on mobile genetic elements would suggest the possibility of SAg gene movement between organisms. This has indeed been shown with streptococcal species in which SAgs on a lysogenic phage were transferred between GAS strains [201] and even to GCS [202]. These results support the idea of horizontal transfer of SAg genes between species, contributing to their evolution, as well as incorporation of these toxins into the core genome if the bacteria stand to benefit.

1.7.9.3 Superantigen structure and binding to host immune receptors

Numerous crystal structures of SAgs, either alone or in complex with immune components have been solved and have aided in our understanding of SAg interactions. For the purpose of this introduction, we will focus primarily on streptococcal SAgs. The crystal structures of SpeA [203], SpeC [204], SpeH [205], SpeI [206], SpeJ [207] and SmeZ [205] have all been solved, and for those that have not, structural modeling can be done using previously crystalized SAgs as a scaffold backbone.

The immune-stimulating properties of SAgs stems from their simultaneous interaction with the host MHC II molecules on the surface of antigen presenting cells (APCs) and TCR Vβ chains. The classical SAg structure (which pertains to most streptococcal and staphylococcal SAgs) consists of a protoxin with a secretion signal that is cleaved from the N-terminus upon export via the general Sec-dependent secretory pathway. The mature exotoxin is between 22 – 29 kDa and is stated to be highly resistant to heat, acidity and desiccation. More specifically, all classical SAgs from *S. aureus* and *S. pyogenes* follow a similar tertiary structure, in which the N-terminus contains a mixed β-barrel domain with Greek key topology also known as an oligonucleotide/oligosaccharide-binding (OB) fold. This domain binds the major histocompatibility complex (MHC) class II α-chain in a low-affinity interaction and the TCR. The C-terminus is a β-grasp fold and contains a twisted β-sheet capped by a central α4-helix. This β-grasp fold contains the zinc-dependent, high-affinity MHC binding interface for SAgs in Groups III – V. A section of the N-terminus also extends over the top of the C-terminus packing against a four-strand antiparallel twisted sheet resulting in a tight architecture which likely makes these molecules resistant to the conditions stated above (**Figure 1A**). Residues from this area are also involved in TCR interactions. The overall architecture varies slightly between SAgs, which explains their preference for certain TCR Vβ chains and MHC II interactions.

Binding of the TCR and the MHC II by SAgs differs significantly from conventional T cell activation (**Figure 1B**) and can be generally categorized based on Groups I – V. What is generally understood with TCR Vβ interaction is that binding of the complementarity-determining region (CDR) 2 loop appears to be a requirement for all staphylococcal and streptococcal SAgs and governs TCR Vβ-specificity, whereas other binding sites in the Vβ domain are responsible for stabilizing the interaction [208]. TSST-1, a Group I SAg, uniquely binds the MHC α-chain through a peptide-dependent, N-terminal low-affinity binding domain [209,210] and the TCR Vβ chain CDR2 region as well as the third framework (FR) region, in an energetically cooperative manner [208,211,212] (**Figure 1C**). Group II SAgs – including SpeA, SEB, SpeH and SSA – bind the MHC II α-chain through a peptide-independent, low-affinity, N-terminal site [213] and the TCR Vβ chain through conformational dependent mechanisms (largely independent of specific Vβ amino

Figure 1. Superantigen structure and immune complex formation.

A. Ribbon diagram of the superantigen (SAg) SpeC (PDB: 1HQR) [204] with colour-highlighted immune interaction domains. N- to C-terminus: T cell receptor (TCR; blue), low-affinity MHC class II (yellow), linking central α-helix (green) and zinc (cyan)-dependent high-affinity (red) MHC class II interacting domains. **B.** Conventional TCR (α-chain, blue; β-chain, yellow) recognition of a peptide (black) in complex with MHC class II (α-chain, red; β-chain, green) (PDB: 1FYT) [214]. **C – G.** Binding of TCR and MHC class II by representative SAgs from Groups I – V built on the backbone of SEB/MHC/TCR (PDB: 4C56) [215]. **C.** TSST-1 interacting with human TCR Vβ 2.1 (PDB: 2IJ0) [211] and HLA-DR1 MHC class II [209]. **D.** SEB interaction with TCR Vβ19 and HLA-DR1 (PDB: 4C56) [215]. **E.** SEH high-affinity MHC class II interaction with HLA-DR1 (PDB: 1HXY) [216] and TCR Vα27 (PDB: 2XNA) [183]. **F.** SpeC interaction with high-affinity MHC class II HLA-DR2a (PDB: 1HQR) [204] and human TCR Vβ2.1 (PDB: 1KTK) [217]. **G.** SEK interaction with human TCR Vβ5.1 (PDB: 2NTS) and MHC class II high-affinity interaction site based off of SEI bound with HLA-DR1 (PDB: 2G9H) [218].

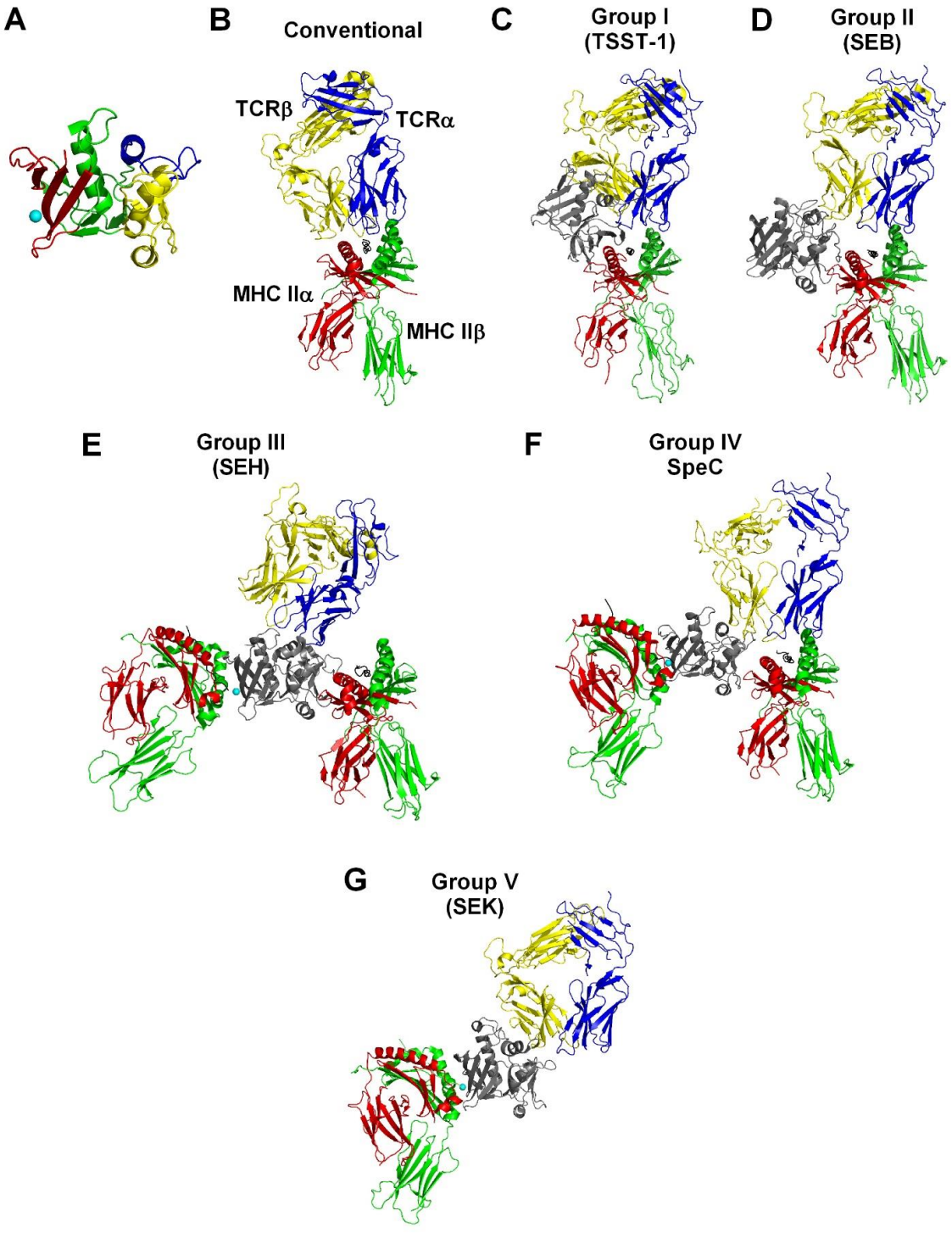
A
B
Conventional
TCRβ
TCRα
MHC IIα
MHC IIβ
C
Group I
(TSST-1)
D
Group II
(SEB)
E
Group III
(SEH)
F
Group IV
SpeC
G
Group V
(SEK)

acids side chains) restricted to CDR2 and hypervariable (HV) region 4 [217,219,220] (**Figure 1D**). Group III contains only *S. aureus* SAgs (such as SEA, SEE and SEH) and these SAgs bind MHC II with both the low- and high-affinity interactions [216,221–223]. Along with the crystal structure of SEH in complex with a TCR Vα chain [182,183] (**Figure 1E**), two other Group III SAgs have been recently crystalized with TCR Vβ to help define this interaction. SEA and SEE have highly similar amino acid sequences, structures and TCR Vβ interacting interfaces. A shallow groove in the SAg interacts mainly with the CDR2, FR3 and HV4 and to a lesser extent the CDR1 and FR4 regions of the TCR Vβ [224,225]. The Group IV SAgs are all produced by streptococci and include the well-studied SpeC. Like Group III SAgs, these toxins also contain a high-affinity MHC binding domain [204]. Our laboratory has also outlined a low-affinity binding site for SpeC, which acts similarly to the Group II SAgs [226]. Mutation of the SpeC high-affinity MHC-binding site via amino acid replacement of crucial zinc-binding residues (aspartic acid at position 203) significantly reduces, but does not extinguish, immune activation [227]. SpeC engagement of the TCR is highly specific for human TCR Vβ2.1 in that it engages all hypervariable loops (CDR 1 – 3 and HV4). There are single residue insertions in the CDR 1 and 2 loops of the human TCR Vβ2 which SpeC makes extensive networks of intermolecular contacts with [217], which are energetically and functionally important for this interaction [228] (**Figure 1F**). Lastly, Group V SAgs include mostly staphylococcal SAgs (such as SEl-K and SEI) and SpeI. The best characterization of a Group V SAg and MHC is that of SEI with HLA-DR1 in which binding occurs similarly to Group IV SAgs [218]. Probably the most unique feature of this SAg group is the existence of an additional ~15 amino acid loop between the third α-helix and the eighth β-sheet (α3-β8 loop) that has been shown to be crucial for T cell activation [206]. For SEl-K, this loop has a recognition site on the apical loop of the human TCR Vβ5.1 FR4 that is necessary for binding and required for functional activation of this T cell subset [229] (**Figure 1G**).

Another important consideration is the specificity of the SAg-TCR interaction. If a SAg targets a variety of TCR Vβ chains, then it is considered to have less specific interactions, and if it targets only one TCR Vβ chain with high affinity then it is considered very specific. The least specific SAgs (including SEB and SEC) make hydrogen bonds with the main-chain atoms of the TCR Vβ CDR2 and HV4 loops [219,220] (**Figure 1D**). Slightly higher

specificity exists for SpeA, in which it contacts more hypervariable loops than those mentioned previously and additional hydrogen bonds are formed between side-chain atoms from both TCR and SAg [217]. Upon further restriction of TCR Vβ interaction, the entire hypervariable portion of the TCR Vβ chain is engaged. The best described example would be SpeC, in which the Vβ it engages – human TCR Vβ2.1 – has non-canonical residue insertions that it also makes contacts with, providing a unique binding site [217] (**Figure 1F**). The highest specificity is seen when SAgs make contacts with unique features within the CDRs and FRs of the TCR Vβ, such is the case with TSST-1 and SEl-K [211,229] (**Figure 1C** and **1G**).

The culmination of this work is that we can now use crystal structures to visualize the full ternary complex (MHC/SAg/TCR). In fact, SEB was recently crystalized in this complex demonstrating that the SAg adopts a wedge-like position allowing for interaction of the TCR α chain with the MHC, but preventing contact with the peptide so T cell activation is peptide-independent [215] (**Figure 1D**). Although crystal structures of actual full ternary complexes do not exist for other classical SAg groups (a ternary complex involving MAM has been published [230]), we can use molecular modeling to postulate what is likely occurring. TSST-1 (Group I) generates contact with MHC and TCR as described above, but unlike SEB, there is thought to be no interaction between MHC and TCR due to the relative orientation with the SAg/MHC and the SAg/TCR interactions (**Figure 1C**). The SAgs with high-affinity, zinc-dependent MHC binding sites (SpeC, Group IV [**Figure 1F**]; SEl-K, Group V [**Figure 1G**]) are thought to bridge TCR and MHC similar to TSST-1 in that there is no actual contacts made between MHC and TCR. SpeC, which also has a low-affinity MHC site [226], is also able to bridge MHC/TCR similar to Group II (**Figure 1F**).

The last consideration of this immune complex (SAg/MHC/TCR) formation is the energetic favorability of these interactions. The optimal affinity range of MHC/TCR interactions required for T cell activation is thought to be between between 10^{-7} to 10^{-5} M [231]. Although diverse, all of the above mentioned SAg/MHC/TCR interactions are able to achieve affinities within this range [206,228,232,233], allowing these toxins to potently activate T cells, which is the currently understood biological role of SAgs.

Recently, the classical view of SAg/MHC/TCR binding has been challenged by the potential interaction of SAgs with the co-stimulatory CD28 molecule [234]. CD28 is expressed on the T cell surface and interacts with the B7 molecules CD80 and CD86 [235]. It was demonstrated that SEB binds CD28 with micromolar affinity and that this interaction was required for induction of proinflammatory cytokine genes and a structural model was also suggested with SEC [236]. A CD28 mimetic peptide was also shown to be protective in a murine lethal challenge model with SpeA and *S. pyogenes* infection [237]. A potential criticism of this model is that all data thus far have been derived from low-affinity MHC interacting SAgs, while the majority (9 of 11) of streptococcal SAgs also have a zinc-dependent, high-affinity MHC binding interface. The suggested SAg-CD28 interface would sterically hinder this interaction, and thus it is unclear whether or not CD28 interaction plays a role in immune-complex binding or if there is an alternative CD28 binding site.

1.7.9.4 Cell signaling induced by superantigens

SAgs activate far greater proportions of naïve T cells compared to classical antigen presentation due to their affinity for the MHC and specific TCR Vβ chains. Stimulation, as mentioned above, occurs by SAgs binding both the MHC II molecule on the surface of APCs and the TCR on T cells in a Vβ-dependent manner, resulting in extensive T cell clonal proliferation and activation. Individual SAgs bind different TCR Vβ repertoires that can be very specific for a single Vβ, or more promiscuous leading to a characteristic 'fingerprint' associated with that SAg. It is important to note, however, that research has also indicated TCR Vβ response can vary with stimulation strength, whereby a broader repertoire of Vβ-response can be seen at higher SAg concentrations or through presentation with an MHC molecule that binds with higher affinity [238]. Regardless, the consequence of this interaction is activation of the bound T cells and downstream signaling that results in the release of numerous cytokines into the local immune environment. SAgs have been shown to activate multiple T cell subsets including both $CD4^+$ and $CD8^+$ T cells [239], γδ T cells [240] and invariant natural killer T cells (iNKT) [241]; however, it is not known whether intracellular signaling in these subsets differs. By far, the best studied SAg-

mediated T cell activation cell-signaling pathways has been in traditional αβ T cells, which is outlined below.

Binding of SAgs to MHC and TCR are thought to induce a similar signaling cascade as normal antigen recognition. Upon interaction of the TCR/MHC (by a SAg), Lck (a src family protein tyrosine kinase associated with the cytoplasmic tail of the co-receptor molecules CD4/CD8) is thought to be dephosphorylated on a negative regulatory tyrosine (Y505) by CD45 upon recruitment of the co-receptor molecule to the TCR/CD3 complex. Lck then phosphorylates immunoreceptor tyrosine-based activation motifs (ITAMs) on the cytoplasmic tail of the CD3 complex, which becomes the site for the recruitment and activation of ZAP-70 (Syk family tyrosine kinase). Activated ZAP-70 phosphorylates tyrosine residues on the cytoplasmic portion of the transmembrane adaptor linker of activated T cells (LAT). This cascade leads to activation of phospholipase C (PLC)γ, which converts phosphatidylinositol 4,5-bisphosphate (PIP_2) to the second messengers inositol triphosphate (IP3) and diacylglycerol (DAG). IP3 is responsible for increasing intracellular Ca^{2+} and DAG activates protein kinase C (PKC) and Ras. Intracellular Ca^{2+} drives calcineurin dephosphorylation of NFAT which allows translocation to the nucleus. DAG leads to activating of the Ras/Raf-1/MEK/ERK pathway which leads to transcription factor AP-1 (Fos/Jun) translocation to the nucleus. DAG also plays a role in PKC activation which eventually leads to NF-κB (Rel and p50) translocation to the nucleus and upregulation of gene transcription. A second Lck-independent signaling pathway was also shown to be present during SAg-mediated T cell activation. The G protein Gαq11 is thought to activate another phospholipase (PLCβ), which also cleaves PIP3 into IP3 and DAG which, in turn, would continue the cascade similarly from there. T cell activation drives upregulation of activation markers (such as the IL-2 receptor α-chain; CD25), adhesion molecules and induces expression of numerous cytokines. The induction of NFAT, AP-1 and NFκB drive the expression of proinflammatory cytokines such as IL-1, IL-2, IL-6, IFNγ and TNFα [242–245].

The response of T cells to SAgs can be separated into three distinct phases: (1) activation/proliferation, (2) deletion and (3) unresponsiveness/anergy [239,246]. The aforementioned signaling cascade results in T cell proliferation (cell division) and

activation (secretion of cytokines and chemokines). This is the first phase and lasts generally from the initial hours of exposure to around two days. The newly expanded T cell subset then undergoes rapid deletion (phase 2) [247–249]. The mechanism behind this sudden decrease in cell numbers is still not entirely clear, but it is thought to be due to Fas/FasL-mediated activation-induced cell death [250]. The last phase is a prolonged state (can last for months) of unresponsiveness termed ‘anergy’, whereby the cells that did not undergo deletion are still present, but they are unable to be restimulated by SAgs and other T cell mitogens (anti-CD3 antibodies, concavalin A, etc.) [251]. This state has been extensively studied in murine models of SAg-exposure [251–255] and has been shown in human lymphocytes [256]. Importantly, depletion of specific TCR Vβ T cell subsets has been observed in humans with streptococcal diseases [257,258], indicating that this phenomenon can occur during streptococcal disease manifestation.

Although numerous cell types can act as APCs for the SAg/MHC/TCR ternary complex, the effect of different cell types as APCs remains poorly studied. It seems that SAg stimulation of APCs leads to a signaling cascade similar to that seen in traditional MHC/TCR interaction. This is similar to what was presented above whereby a tyrosine kinase (in this circumstance Syk) is phosphorylated upon immune complex interaction which results in intracellular Ca^{2+} increase due to PLC activation [259]. This has been shown to lead to cytokine expression in APCs as well including TNF, IL-6, IL-10 and IL12 as well as an increase in numerous surface markers [260,261]. When the APC is a B cell, it has been shown that SAg interaction increases MHC mRNA [262] and non-specific, polyclonal Ig response [263]. It has also been demonstrated that different SAgs interact better with specific human MHC (HLA) molecules [264–266]. These data indicate that APCs play an important role during SAg immune stimulation, and that further work is needed to elucidate the differences between this diverse group of cells and the impact they may have in disease progression.

1.7.9.5 Superantigen disease associations

Human evidence to support the involvement of SAgs in specific diseases generally comes in one of three forms: epidemiological studies showing an increase in proportion of disease associated with strains encoding specific SAg genes, serological studies detecting

seroconversion to SAgs, or TCR Vβ skewing patterns in patients that are associated with a specific SAg.

The disease originally associated with SAgs was scarlet fever, which was first shown to be caused by erythrogenic toxins – later revealed to be SAgs – produced by GAS [172]. It is thought that the rash associated with scarlet fever is the result of immune stimulation by bacterial SAgs. Although no single toxin is consistently associated with scarlet fever, SpeA, SpeC and SSA seem to have the highest correlation with the disease, generally determined by PCR amplification of the SAg genes from patient-isolated strains [267–270].

The dysregulated immune response in STSS has led to the suggestion of SAg involvement for decades. A large majority of supporting evidence involves epidemiological data that has associated GAS serotypes encoding specific SAgs with cases of STSS. Primarily, *speA* and *speC* have been associated [270–276]; however, other groups have also found other SAgs (*speJ*, *speK*, *speM* and *ssa*) to be involved [277–280]. Despite this evidence, other analyses have reported no apparent difference in SAg gene frequencies between invasive and non-invasive *S. pyogenes* isolates [281–284]. One study was able to detect SpeA in the sera from two patients with STSS [285] and another study attributed SmeZ (either alone or in combination with SpeJ) as the causative agent in STSS [20]. Lack of neutralizing antibodies has also been theorized to be a risk factor for STSS and other severe streptococcal disease. Eriksson *et al.* showed low anti-SAg antibody titres in patients with STSS and bacteremia compared with those from uncomplicated erysipelas [286], whereas Basma *et al.* showed higher neutralizing anti-SAg antibodies in those with both severe and non-severe invasive GAS disease compared to matched healthy donors [287]. Numerous studies have also detected the unique ‘fingerprint’ that SAgs leave on the TCR Vβ-repertoire, matching SAgs present in isolates from GAS severe infections to proliferation or depletion in specific TCR Vβ subsets [257,258,288]. These data, although not entirely conclusive, do suggest that SAgs play a significant role during STSS and potentially other severe and invasive GAS infections in humans.

There is also support for a superantigenic role in Kawasaki Disease, a systemic vasculitis that affects young children (generally less than 5 years old) and can lead to coronary artery damage [289]. A number of studies have analyzed TCR Vβ-skewing patterns, anti-SAg antibody titres, and PCR analysis to detect SAg in stool samples from patients, all which suggest a role for SAgs in this disease [290–296]. Some groups, however, have failed to show evidence of SAg involvement with Kawasaki Disease. These findings are mainly associated with the lack of anti-SAg antibodies [297–299] or the fact that oligoclonal expansion of B cell IgM transcripts were detected in peripheral blood of patients with Kawasaki Disease, indicating disease pathogenesis from a conventional antigen and not a SAg [300]. The overall findings seem to support a role for SAgs in the disease pathogenesis of Kawasaki Disease, but with some conflicting results and no direct mechanism available, further research will have to be done to elucidate the role for these toxins in this disease.

Guttate psoriasis is an inflammatory skin disease that is commonly associated with flare-ups after upper respiratory tract infections with β-hemolytic streptococci [301]. Some studies observe TCR Vβ-restricted T cell stimulation in the disease [302–304], but others have indicated oligoclonal T cell infiltration in psoriasis lesions suggesting a role for a more conventional antigen and potential autoimmunity [305]. It is possible that SAg-mediated activation of T cells could be driving an autoimmune response; however, further research on this topic is required.

Much like the implications for guttate psoriasis, ARF is a known post-streptococcal autoimmune sequela that can affect multiple tissues. Cross-reactive immune sera to these tissues are thought to be the etiological agent, and SAgs may potentially stimulate autoreactive immune cells. There is high correlation between M18 ARF *S. pyogenes* isolates and the *speL* and *speM* SAg genes as well as antibodies in ARF patients to these SAgs [306,307]. However, it was also shown that antibodies against SAgs did not predict susceptibility in Australian Aboriginals [308], indicating that other factors may also play a role in ARF development.

1.7.10 Other virulence factors

The above mentioned list of GAS virulence factors is by no means an exhaustive list, but does describe some of the best studied factors. *S. pyogenes* has numerous elements that contribute to virulence that are not discussed here. For more information on such factors please refer to other reviews that give a much broader view of *S. pyogenes* virulence [2,29,309].

1.8 Genetic regulation in *S. pyogenes*

The regulation of *S. pyogenes* gene expression is controlled by 13 known two-component regulatory systems (TCSs) and at least 30 stand-alone transcriptional regulators. There is extensive interplay between these elements making it an extremely complex system. For this reason, we will be focusing primarily on the best-studied virulence-associated systems and their impact on gene expression. For a more in-depth analysis, McIver and colleagues have provided excellent reviews on this topic [106,310].

The best characterized TCS in *S. pyogenes* is CovRS (formerly CsrRS). Like other TCSs, CovRS is composed of a sensor histidine kinase, CovS, that is able to sense external signals (such as Mg^{2+} and host antimicrobial peptides [311,312]) and modify a response regulator, CovR, that regulates gene expression of numerous virulence factors. Phosphorylation of CovR by CovS results in dimerization and the ability to directly bind DNA at the promoter region of targeted genes [313,314]. The CovRS TCS is known to influence up to 15% of all GAS chromosomal genes, including the hyaluronic acid capsule, SpeB cysteine protease, streptokinase and SLS [164]. CovR is generally a repressor of many virulence factors, and mutational analysis of CovRS TCSs demonstrates that a non-functioning CovRS switches *S. pyogenes* to a hypervirulent phenotype in which SpeB gene expression is reduced, and numerous virulence factors are upregulated, including SpeA and SLO [91,315]. It has been suggested that the transition from localized to systemic infections by the globally disseminated M1T1 GAS serotype is due to this CovRS mutation leading to the hypervirulent phenotype [316]. The complete role that CovRS plays during human infection is not completely understood, and since strains are still able to exist with and without a functional CovRS TCS, more research on this topic is warranted. What is known,

is that this TCS impacts a large proportion of GAS genes and a broader understanding of its influences will aid in our understanding of this complex pathogen.

‘Stand-alone’ regulators are those that control gene expression in response to outside stimulus yet the exact signal and cognate sensory element remain undefined. There are three main ‘stand-alone’ regulators in *S. pyogenes* and they include: Mga (the multiple gene regulator of GAS); RALPs (RofA-like proteins); and Rgg/RopB.

Mga was originally classified as *virR* (virulence regulator) by one group that found M protein negative M12 isolates with a mutation upstream of the *emm* gene [317]. Another group found a comparable locus in a M6 strain of GAS and called it *mry* (M protein RNA yield) [318]. It was eventually determined that these were both actually the same regulator and the culminating name was changed to Mga [319,320]. One of the two divergent *mga* alleles (*mga-1* and *mga-2*) can be found in every strain of GAS [321,322] and it is known that Mga transcriptionally activates genes during exponential growth of the organism [106]. Along with the M protein, Mga also upregulates the virulence factors ScpA and SIC, fibronectin-binding and collagen-like proteins as well as carbohydrate utilization and metabolism genes [106]. It is important to note that other pathogenic streptococci have Mga orthologs [323,324] and there is evidence that Mga plays a role in the early acute phase of infection *in vivo* [325–328].

The RALP family includes four proteins found in GAS (RofA [RALP1]; Nra [RALP2]; RALP3 and RivR [RALP4]) as well as orthologous members in other pathogenic streptococci [106,329]. All analyzed GAS strains have at least RofA or Nra, and potentially several other RALP members resulting in RALP-member and RALP-regulation variability [322,330]. Genes regulated by RALP include microbial surface components recognizing adhesive matrix molecules (MSCRAMMs; such as those for pilus biosynthesis, fibronectin-binding proteins), hemolysins (SLS), proteases (SpeB) and SAgs (SpeA) [330–333]. The RALP family is primarily involved during the transition from exponential to stationary growth and impacts host-pathogen interactions and avoidance of host cell damage [330,333,334].

The Rgg/RopB transcription regulator family of DNA-binding proteins can be found in both GAS [335,336] and closely related organisms [337–341]. This response regulator family seems to play a role in modulating virulence at times of nutritional limitation and stress. Rgg/RopB plays its largest role in post-exponential growth, but there is high strain variability in that it can impact as few as two core genes or as much as >30% of the genome [342,343]. Of the genes influenced by Rgg/RopB, there seems to be a repression of *mga*-related proteins (SIC, M protein, etc.) as well as SLO and streptokinase, and activation of virulence factors such as SpeB, the SAg SpeG, the α_2-macroglobulin-binding protein [76,343–346] and proteins involved with amino acid catabolism [344,347].

1.9 Animal models of Group A *Streptococcus* infection

No *in vitro, in situ* or *in silica* model is able to replicate the extreme complexities that exist within a host, and thus *in vivo* infection models are used in essentially all pathogenesis research. The study of *S. pyogenes* is no different, and in addition to this, a number of factors make working with this pathogen more difficult. The first issue is that GAS is a human-specific pathogen, and thus a number of its virulence factors have evolved to interact with only human immune components. Therefore, regardless of the model used, there is likely to be an issue with proper interaction of bacterial and host factors. Second, this organism can cause numerous types of infections of varying severity at different locations in the host. Consequently, numerous models are required to assess factors involved with each of these infections, resulting in further complexities. Lastly, the strain to strain variability in this organism is extensive, and thus there is no reference strain that best exemplifies all other strains. These difficulties have not stopped researchers from trying to understand this organism; on the contrary, there are numerous models from invertebrates to non-human primates that have been extremely helpful in revealing the complexities of host-pathogen interactions. The focus here will be on one of the best-studied models, the murine model, as well as the most characteristic of actual human infection, the non-human primate model.

1.9.1 Murine models of infection

Mouse models present an excellent opportunity to study host-pathogen interactions. As mammals, they contain both an innate and adaptive immune system that are similar to that of humans. In addition, they are relatively inexpensive to purchase and house, quick to reproduce, mature rapidly and there are numerous tools available to aid in the study of almost any aspect of murine biology. Mice can also be bred to select for desired traits, and can be genetically altered to express functional human genes [168,348]. For these reasons, they have been extensively used in pathogenesis research.

Murine streptococcal subcutaneous infections, pioneered by the modern ulcer and air sac models [349,350], mimic a broad range of highly inflammatory localized soft tissue lesions. Strengths include rapid bacterial proliferation and extensive recruitment of inflammatory innate immune cells which imitates what is seen in human infections [349–351]. However, a major limitation of these models is that histopathology of the infections is not the same as that observed in human manifestations due to the thinner murine epidermal layer. Also, for *S. pyogenes* pathogenesis mice may be a good model for the innate, but arguably not the adaptive, immune response since a protective immune response does not develop after resolution of the infection [352]. Regardless of the limitations, this model is considered to be one of the most versatile and useful models for studying *S. pyogenes* pathogenesis.

Murine models of systemic disease differ in their inoculation route and are generally performed by either intravenous (IV), intraperitoneal (IP) or intramuscular (IM) injections. These models are heavily used due to their technical simplicity [100,353,354], although direct inoculation into the bloodstream, peritoneal cavity or muscle bypass a crucial barrier that GAS normally must traverse. It is for this reason that intratracheal (IT) administration of bacteria has become more popular. Requirement of the bacteria to traverse the lung epithelial more closely resembles human infection whereby sepsis occurs after a localized infection in soft tissue [132,355,356]. Researchers have found that IT inoculation is more efficient at investigating the role of virulence factors in inducing systemic disease [357–359]. It is important to note that mouse strain, gender and genetics all play an important role in regards to systemic infection and the absence of adaptive immunity also does not

impact infectivity [360]. An additional implementation to better mimic human infections is the use of transgenic mice expressing human genes. Due to *S. pyogenes* being a human specific pathogen, certain virulence factors are tailored to interact with only human immune components and expression of these molecules in a murine system has been shown to increase susceptibility of mice to systemic infections [168].

As mentioned previously, SAgs are associated with TSS and administration of these toxins to mice is used as a model to study TSS. However, SAgs interact poorly with murine immune components [361] and sensitizing agents such as D-galactosamine, LPS or actinomycin were previously used to help induce this disease [362,363]. It was later found that these sensitizing agents induced a viral hepatitis-like liver injury which is not characteristic of human TSS (multi-organ dysfunction phenotype, not just a single organ) [364–367]. It was shown that mice expressing human leukocyte antigen (HLA) transgenes better replicated the human disease, and has thus become the gold-standard [368]. Numerous studies have since used this model to further develop our understanding of the role of HLA-molecules in both bacterial- and toxin-induced sepsis [264,265,369,370]. It has also been shown that different HLA types can render humans either protected or susceptible to invasive GAS infections [371], increasing the relevance of this transgenic mouse model.

The most prevalent host-pathogen interactions involving GAS are pharyngitis and nasopharyngeal asymptomatic carriage [4,23]. This indicates that the primary reservoir for *S. pyogenes* is the human upper respiratory tract, more specifically, the mucosal-associated lymphoid tissue known as Waldeyer's ring (including the tonsils). It is important to note that mice lack this tissue, but instead have a functional homologue known as the nasal-associated lymphoid tissue (NALT) inside their nostrils [372–374]. This, and the surrounding tissue (ethmoid turbinates, maxillary sinus and septum) make up what is known as the complete nasal turbinate (cNT) (**Figure 2**). Murine models of nasopharyngeal GAS infection/carriage involve administering a bolus of bacteria into the nares to seed this tissue and have been extensively used [110,354,375–377]. Numerous factors can also play a role in determining efficiency of infection, including: quantity and volume injected, duration of infection, bacterial strain, and mouse strain used. Inoculum volume is generally

Figure 2. The murine complete nasal turbine.

Coronal transverse sections of formalin-fixed mouse head stained with hematoxylin and eosin. Indicated architecture is labelled: ethmoid turbinates (ET), maxillary sinus (MS), nasal-associated lymphoid tissue (NALT) and the septum. The collective tissue environment is referred to as the complete nasal turbinates (cNT).

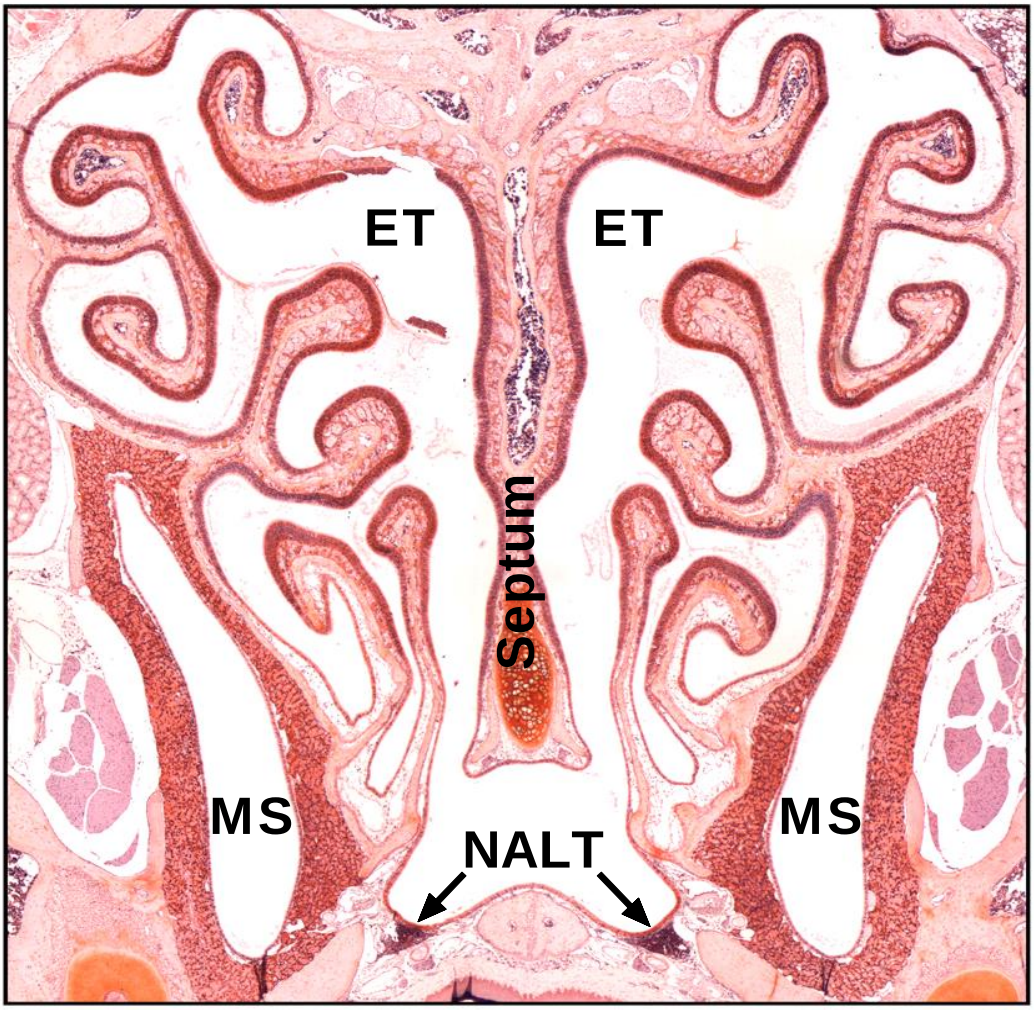
ET
ET
Septum
MS
NALT
MS

less than 20 µL as volumes greater than this have been shown to seed bacteria into the lung and cause pneumonia [376]. Duration of infections vary on amount of bacteria inoculated, but mice generally clear infections in 7-14 days, with some potentially harboring bacteria for longer [110,376,377]. Bacterial quantitation can be assessed using numerous methods: from sacrifice and tissue procurement for end point counts, nasal shedding assay (whereby nares are pressed against agar plates for bacterial enumeration) and bioluminescent imaging. The murine cNT is also an ideal location for live imaging and genetically engineered bioluminescent strains of GAS have been used in this model [375,378]. Analysis of the immune system in response to GAS nasopharyngeal infection has demonstrated a $CD4^+$ T cell-mediated clearance of bacteria that also involved neutrophils [354,379–381]. This demonstrated that both innate and adaptive immune cells can contribute to clearance of *S. pyogenes* in this model. It is important to note that the majority of intranasal infection models have used conventional laboratory mice (C57Bl/6, BALB/c, FVB, CD1, etc.) [375,376,378,379,382], however, it was recently shown that transgenic mice expressing human MHC II (HLA-DQ8) are much more susceptible to infection by *S. pyogenes* and may represent a much more relevant model [377]. However, limitations include the relatively short duration of infection/colonization, the differential architecture of the cNT from human tonsillar tissue, technical difficulty in isolating cNT tissue and the limited number of *S. pyogenes* strains that have demonstrated the ability to infect this tissue.

The limited duration of GAS nasopharyngeal infection was an issue not easily solved by making modifications to the existing model. However, since *S. pyogenes* is known to colonize the female genital tract [383–385], an alternative approach to study this host-pathogen interaction was adapted from a model previously used with other mucosal pathogens (Group B *Streptococcus* [386], *N. gonorrhoeae* [387] and *Candida albicans* [388]) using estradiol-primed conventional laboratory mice (C57Bl/6 and BALB/c) [389]. Estrous phase mice are vaginally inoculated with GAS and lavages can be taken to count bacterial load over several weeks to months. This duration, asymptomatic nature of infection, and the non-lethal measurements of bacterial burden (and cytokines) by lavage have allowed for the investigation of factors involved in longitudinal mucosal carriage of

GAS [389,390]. Limitations include strain variability, the normal microflora must be eliminated prior to colonization, and only estrogen-treated female mice can be used [389].

1.9.2 Non-human primate models of infection

Animal infection models that resemble humans, the only known reservoir for GAS, are extremely important for understanding host-pathogen interactions and testing of potential therapeutics. As close biological relatives, non-human primates are a very attractive candidate for this role. The use of baboons (*Papio cynocephalus*) [391] and cynomolgus macaques (*Macaca fascicularis*) [89,392–394] have been used to study invasive models such as sepsis and necrotizing fasciitis. Because of the highly similar anatomy and physiology, much can be garnered from these models such as relative body temperature, heart rate, blood pressure, serum chemistry, cytokine profiles and post-mortem organ analysis.

Unlike the above mentioned mouse models of colonization, non-human primates present a unique opportunity to establish a more human-like infection that develops a better representative immune response with easier access to the site of infection, larger blood and tissue samples for more analyses and importantly is more receptive to different strains of *S. pyogenes*. For decades, researchers have examined the ability of GAS to infect the oropharyngeal tissue of numerous non-human primates including: baboons [395,396], rhesus macaque (*Macaca mulatta*) [397,398], chimpanzees (*Pan*) [399,400] and cynomologus macaque [401], of which the latter is the current most common model. This is because baboons and rhesus macaques do not seem to develop symptomatic pharyngitis, but chimpanzees and cynomologus macaques do, along with most signs and symptoms (erythema, fever, tonsillar enlargement and palatal petechiae) [402,403]. In a short time, an immense amount of information about host-pathogen interaction has been discovered using these models including a dynamic humoral response during infection, genetic regulation, and energy metabolism by GAS during pharyngitis [327,392,403–407]. Despite the cost and ethical considerations, the non-human primate model remains the most comprehensive tool for studying host-pathogen interactions during *S. pyogenes* infection and colonization.

1.10 Group A streptococcal vaccines

Despite decades of research there is currently no licensed vaccine against *S. pyogenes*. The reasons for this include: concern over vaccines containing autoimmune epitopes, strain variability (surface molecule differences, infection site preference and severity, global distribution) and the primary effected population. A primary goal for vaccine development is the prevention and reduction in major GAS-associated mortality. By far the leading cause of death associated with *S. pyogenes* is autoimmune RHD [4,30,36] and an effective vaccine should aim at prevention of this disease. The epitope(s) responsible for the autoimmune response in ARF and other autoimmune sequelae have been implicated in the M protein, group A carbohydrate and hyaluronic acid capsule, among other GAS factors, which has best been reviewed by Madeline Cunningham [408,409] and Jonathan Carapetis [30]. It is for these reasons that vaccine candidates must be rigorously studied to ensure that they do not contain these epitopes. A major setback occurred in the late 1960s after a crude M protein vaccine was tested in children that resulted in ARF cases in the tested population [410,411]. This result led to a United States federal ban on GAS vaccine testing in humans, which was removed in 2006. The fact that all of the GAS autoimmune epitopes remain elusive provides a significant hurdle to vaccine development. Demonstration of M protein-type immunity against GAS has been known to be protective for decades [412], making this by far the most studied vaccine candidate. The more recent demonstration of the growing GAS *emm*-types (currently over 200) and the difference in their global distribution has made the pursuit of this vaccine less logistical for global control of this pathogen [14,49,60]. The last major concern is that approximately 95% of the population that would benefit most from a GAS vaccine live in low- and middle-income countries [4]. This produces a significant financial burden on the project as potential vaccine development companies may refrain from pursuing this due to a lack of return on investment. All of these hurdles must be overcome to generate a safe, effective and affordable GAS vaccine.

1.10.1 M protein vaccines

The realization that anti-M protein antibodies produced following natural infection could be protective against GAS infection due to promotion of phagocytosis [412,413] spurred

the investigation of using these molecules as potential vaccine candidates. Further analyses indicated that antibodies against the hypervariable N-terminus were protective and not likely to cross-react with host tissue [414]. Eventually, it was realized that protective epitopes could be linked together to create long peptides containing many protective epitopes against numerous *emm*-types. This technology led to the development of multi-valent M protein-based vaccines [414–418], of which two have made it past Phase I and Phase II clinical trials and have been shown to be both safe and effective [419,420]. Perhaps the greatest hurdle that these vaccines must overcome however, is the high variability (>200 *emm*-types) and wide distribution of the GAS *emm*-types [49]. Epidemiological data [14,58,421,422] suggests that the currently developed 30-valent vaccine [418] would protect against isolates responsible for 98% of pharyngitis cases in Canada and the U.S., 90% of invasive isolates in the U.S., and 78% of invasive isolates in Europe. Interestingly, protection against serotypes not in the vaccine were also demonstrated which may lead to significant protection in other populations [423,424]. These unexpected findings further demonstrate the potential efficacy of a multi-valent N-terminal M protein vaccine.

Another approach taken to generate M protein vaccines is the use of epitopes found on the more conserved, C-terminal region of the protein. Research has demonstrated that the C-repeat region of the M protein is highly conserved, contains protective epitopes, and thus represents a possible vaccine candidate. Original vaccine studies used the entire C-terminal region of the M6 protein [425], which future investigation later focused on specific B and T cell epitopes [426–428]. One of the best studied C-terminal vaccines is known as J8-DT, which is comprised of a stabilized M protein B cell epitope fused to the diphtheria toxoid (DT) to enhance immunogenicity [426]. Passive and active immunization has proven protective in infection models [426,429,430], long-term B cell memory is induced [431], and no host cross-reactive antibodies are generated upon vaccination [432]. Due to its success in animal models, J8-DT is currently undergoing Phase I clinical trials [433]. A second M protein conserved region vaccine candidate, known as StrepInCor, is a 55 amino acid peptide modeled after B and T cells epitopes from the C2 and C3 regions of an M5 protein [427]. Vaccination with StrepInCor demonstrated mucosal and systemic antibodies [428] which were able to opsonize several *S. pyogenes* strains [434] and protected mice from infection with no cross-reactivity to cardiac proteins or other tissues [435,436].

Despite promising *in vivo* animal efficacy, there have been no human clinical trials as of yet.

1.10.2 Streptococcal superantigen-based vaccines

The known association of SAgs with TSS led to investigations of whether or not toxoid (inactive) molecules could be used in vaccinations to prevent the onset of the disease. Vaccination with TCR and/or MHC II binding site mutant SAg toxoids were non-lethal, stimulated antibody responses, and were protective in a rabbit model of TSS [437,438]. Vaccination of HLA-DQ8 mice with either toxoid SpeA alone or fused to inactive SpeB generated antibodies that protected mice from lethal wild-type SpeA challenge, and the fusion vaccine also significantly increased survival in a *S. pyogenes* sepsis model [439]. This protective antibody phenotype is supported by the fact that IVIG contains neutralizing anti-SAg antibodies and administration of IVIG in humans has been shown to reduce mortality in cases of STSS [21,22,440]. However, the efficacy of IVIG therapy for the treatment of invasive streptococcal disease remains controversial [441,442]. With new understandings of SAgs and their role in both severe/invasive diseases as well as acute uncomplicated infections and asymptomatic colonization [245], further study is warranted in using toxoid SAgs as potential vaccine candidates.

1.10.3 Other vaccine candidates

Although M protein based vaccines are the only candidates that have made it into clinical trials, numerous other antigens have undergone pre-clinical, animal model protection analysis including: SpeB [439,443]; the GAS carbohydrate [444]; C5a peptidase [110,382,445,446], SpyCEP [92], fibronectin-binding protein [447] and others [381,433,448]. Analysis of current GAS vaccines would indicate that we are close to having strain-specific vaccines available, but still well behind in the development of a globally-protective GAS vaccine. Numerous antigens have proven protective in animal models of infections and it would seem most likely that a full protective vaccine would come from a multi-component vaccine including multiple M protein serotypes and numerous other antigens. However, there is a difficulty in acquiring funding to pursue Phase I clinical trials for human safety and efficacy of these vaccines. More resources

should be allocated towards the development of GAS vaccines, as it would have a major impact on prevention of worldwide, GAS-associated morbidity and mortality.

1.11 Rationale and Hypothesis

On a global scale, *S. pyogenes* is a major cause of morbidity as well as mortality, and there is currently no licensed vaccine against this organism [4,433]. Recently, our laboratory has determined that streptococcal SAgs play not only an important role in severe diseases, but also in nasopharyngeal infection establishment [449]. In this model, *S. pyogenes* MGAS8232, an M18 rheumatic fever clinical isolate [306], was efficient at infecting the cNT of transgenic mice expressing human MHC II (HLA) but not conventional C57Bl/6 mice. Using genetic knockout and complementation, this infection was also found to be dependent on the SAg SpeA. In the work to be described, we speculate that in the above mentioned model, *in vivo* production of SAgs by *S. pyogenes* can be detected using flow cytometric analysis of the T cell activation marker CD25 on SAg-targeted, but not other, T cell subsets in the local immune environment. This SAg-dependent infection phenotype also led us to hypothesize that anti-SAg antibodies – provided by either passive immunization or active vaccination with an attenuated SpeA toxoid – would be protective in a murine model of GAS upper respiratory tract infection. Finally, since it is known that Vβ-specific T cell activation is a hallmark of SAg activity, we propose that these T cells are required to be present and functional for *S. pyogenes* nasopharyngeal infection.

Chapter 2: Materials and Methods

2 Materials and Methods

All solutions and media were made using water purified with a MilliQ filtration system (EMD Millipore; Darmstadt, Germany).

2.1 Ethics statements

The use of primary human lymphocytes was reviewed and approved by Western University's Research Ethics Board (REB) for Health Sciences Research Involving Human Subjects (**Appendix 1**). Informed written consent was obtained from all donors. All animal experiments were completed under Animal Use Protocol (AUP) Number 2011-088 in accordance with the Canadian Council on Animal Care Guide to the Care and Use of Experimental Animals, and was approved by the Animal Use Subcommittee at Western University (London, ON, Canada) (**Appendix 2**).

2.2 Bacterial growth conditions

A complete list of bacterial strains used in this study can be found in **Table 3**.

2.2.1 *Escherichia coli*

E. coli strains were grown in Luria-Burtani (LB; EMD Millipore) broth, containing 1.5% (w/v) agar (Thermo Fisher Scientific Inc.; Waltham, MA, USA) when required, aerobically at 37°C. For cultures containing pET28 or pET41 plasmids, cultures were supplemented with 50 μg mL^{-1} kanamycin (Sigma-Aldrich Canada Co.; Oakville, ON, Canada). A complete list of plasmids used in this study can be found in **Table 4**. Frozen stock cultures were stored in LB broth plus 25% (v/v) glycerol.

2.2.2 *Streptococcus pyogenes*

S. pyogenes strains were grown statically at 37°C in Todd Hewitt broth (Becton Dickinson [BD] Biosciences; Franklin Lakes, NJ, USA) supplemented with 1% (w/v) yeast extract (BD Biosciences) (THY). For solid media preparation, 1.5% (w/v) agar (Thermo Fisher Scientific) was added to broth. To restore capsule, *S. pyogenes* MGAS8232 was grown in THY broth supplemented with 5% (v/v) human plasma (HP). Human plasma was collected from healthy donors and diluted 1:1 in Roswell Park Memorial Institute (RPMI; Life

Table 3: Bacterial strains used in this study

Strain	Description	Source
Escherichia coli		
XL1 Blue	Cloning Strain *recA1 endA1 gyrA96 thi-1 hsdR17 supE44 relA1 lac* [F′*proABlacI*^{q}*ZΔM15 Tn10* (Tet^{r})]	Stratagene
BL21 (DE3)	Protein Expression Strain F^{-} *ompT hsdS*$_{B}$(r_{B}^{-}, m_{B}^{-}) *gal dcm* (DE3)	Novagen
Streptococcus pyogenes		
MGAS8232	M18 strain isolated from patient with acute rheumatic fever	[306]
SF370	M1 strain isolated from wound of infected patient	[450]
Streptococcus pneumoniae		
P1121	Serotype 23F derived from nasopharyngeal human carriage of strain P833	Dawn Bowdish [451–453]

Table 4: Plasmids used in this study

Plasmid	Description[a]	Source
pET-28a(+)	Protein expression vector; N-terminal His•Tag®/thrombin cut site; Kan^r	Novagen
pET-28a(+)::TEV	pET-28a(+) plasmid with modified TEV protease cleavage site; Kan^r	McCormick Lab
pET-41a(+)	Protein expression vector; N-terminal GST•Tag/His•Tag®; Kan^r	Novagen
pET-41a(+)::TEV	pET-41a(+) plasmid with modified TEV protease cleavage site; Kan^r	[228]
pET-28a(+)::TEV::*speA*	*speA* inserted into *Nco*I and *Bam*HI of pET-28a::TEV; Kan^r	[377]
pET-28a(+)::TEV::$speA_{N20A}$	Asn to Ala at mutation position 20 in *speA*; Kan^r	This Study
pET-28a(+)::TEV::$speA_{L41/42A}$	Leu to Ala mutation at positions 41 and 42 in *speA*; Kan^r	This study
pET-28a(+)::TEV::$speA_{Y100A}$	Tyr to Ala mutation at position 100 in *speA*; Kan^r	[377,454]
pET-28a(+)::TEV::$speA_{N20A/Y100A}$	Asn (at position 20) and Tyr (at position 100) to Ala mutations in *speA*; Kan^r	This Study
pET-28a(+)::TEV::$speA_{TRI}$	Leu (at positions 41 and 42) and Tyr (at position 100) to Ala mutations in *speA*; Kan^r	This Study
pET-28a(+)::TEV::$speA_{TETRA}$	Asn (at position 20), Leu (positions 41 and 42) and Tyr (at position 100) to Ala mutations in *speA*; Kan^r	This Study
pET-28a(+)::$speA_{HEXA}$	Gln to His at position 19, Asn to Asp at position 20, Leu to Ala at positions 41 and 42, Asp to Asn at position 45 and Cys to Ser at position 98 mutations in *speA*; Kan^r	[437]

pET-28a(+)::TEV *speA*$_{HEXA}$	*speA* mutant from Roggiani *et al.* [437] inserted into *Nco*I and *Bam*HI of pET-28a::TEV; Kan^r	This Study
pET-41a(+)::TEV:: *speC*	*speC* gene inserted into *Nco*I and *Bam*HI of pET-41a::TEV; Kan^r	[208]
pET-28a(+)::TEV:: *speG*	*speG* inserted into *Nco*I and *Bam*HI of pET-28a::TEV; Kan^r	[377]
pET-28a(+)::TEV:: *speH*	*speH* inserted into *Nco*I and *Bam*HI of pET-28a::TEV; Kan^r	McCormick Lab
pET-28a(+)::TEV:: *speI*	*speI* inserted into *Nco*I and *Bam*HI of pET-28a::TEV; Kan^r	[206]
pET-28a(+)::TEV:: *speJ*	*speJ* inserted into *Nco*I and *Bam*HI of pET-28a::TEV; Kan^r	McCormick Lab
pET-28a(+)::TEV:: *speK*	*speK* inserted into *Nco*I and *Bam*HI of pET-28a::TEV; Kan^r	McCormick Lab
pET-28a(+):: *speL*	*speL* inserted into *Nco*I and *Bam*HI of pET-28a; Kan^r	[377]
pET-28a(+):: *speM*	*speM* inserted into *Nco*I and *Bam*HI of pET-28a; Kan^r	[377]
pET-28a(+):: *ssa*	*ssa* inserted into *Nco*I and *Bam*HI of pET-28a; Kan^r	McCormick Lab
pET-41a(+)::TEV:: *smeZ*	*smeZ* gene inserted into *Nco*I and *Bam*HI of pET-41a::TEV; Kan^r	[377]
pET-28a(+)::TEV:: *seb*	*seb* inserted into *Nco*I and *Bam*HI of pET-28a::TEV; Kan^r	[455]

[a] Abbreviations: Kan^r, kanamycin resistance; TEV, tobacco etch virus protease cleavage site

Technologies Inc.; Carlsbad, CA, USA) 1640 media. THY media with 5% (v/v) HP was sterilized by 0.2 µM filtration (Pall Life Sciences; Port Washington, NY, USA). Frozen stock cultures were created by addition of 20% (v/v) glycerol to THY media.

2.2.3 *Streptococcus pneumoniae*

S. pneumoniae was grown in Tryptic Soy broth (TSB; BD Biosciences) statically at 37°C in 5% CO_2. Frozen stocks were prepared by addition of 20% (v/v) glycerol into TSB media.

2.3 Growth curves

S. pyogenes and *S. pneumoniae* strains were grown from -80°C freezer stocks and subcultured twice (1%) in their respective medias (THY and TSB) at the appropriate conditions stated above. Overnight culture optical densities at 600 nm (OD_{600}) were corrected to a value of ~0.05 in 100 mL of media. Bacteria were grown in appropriate conditions and OD_{600} readings were measured every hour using a spectrophotometer (DU® 530 Life Sciences UV/Vis Spectrophotometer; Beckman Coulter Canada LP; Mississauga, ON, Canada). Once a logarithmic growth phase was determined, the growth curve was repeated with serial dilution and spot plating during this phase. Bacterial counts were used to generate a linear relationship between OD_{600} and bacterial concentration, with a line of best fit and equation of the slope for bacterial preparation for infection.

2.4 Deoxyribonucleic acid

2.4.1 Plasmid isolation from *E. coli*

Plasmid DNA was isolated from 5 mL of pelleted *E. coli* after growth to stationary phase (O/N aerobic growth at 37°C). Pelleted bacteria were treated using QIAprep spin miniprep kit (Qiagen; Hilden, Germany) or E. Z. N. A. kit (Omega Bio-Tek; Norcross, GA, USA) as per manufacturer's instructions. Plasmid DNA was eluted in sterile water. A complete list of plasmids can be found in **Table 4**.

2.4.2 Genomic DNA isolation from murine tissue

Genomic DNA was prepared according to The Jackson Laboratory (Bar Harbor, ME, USA). Briefly, mouse ears were notched for identification purposes prior to being weaned (approximately two weeks after birth). Removed tissue was stored at -20°C until use.

Tissue was added to 75 µL of 25 mM NaOH, 0.2 mM EDTA and placed in a thermocycler at 98°C for 1 hour followed by a reduction to 15°C until proceeding to the next step. An addition of 75 µL of 40 mM Tris HCl (pH 5.5) was then made prior to centrifugation at 4,000 × *g* for 3 minutes. The supernatant was then used as template for polymerase chain reaction.

2.4.3 Polymerase chain reaction

All primers used in this study were generated by Sigma-Aldrich and are listed in **Table 5**. Primers were resuspended to a final concentration of 100 µM in MilliQ water. Reactions were comprised of 1 × high fidelity buffer (Thermo Fisher Scientific), 2 mM magnesium chloride ($MgCl_2$; Thermo Fisher Scientific), 3 mM deoxyribonucleotide triphosphate (dNTP) mixture (Roche Diagnostics; Risch-Rotkreuz, Switzerland), 10 pM each of forward and reverse primer, at least 1 pg of low complexity (plasmid) or 50 ng of high complexity (genomic) DNA and 0.02 units mL^{-1} of Phusion High-Fidelity DNA polymerase (Thermo Fisher Scientific). All reactions were completed on a Peltier Thermocycler PTC-200 (MJ Research, Waterdown, MA, USA). Reactions were visualized (see below) and products were purified using a QIAquick PCR Purification kit (Qiagen) according to the manufacturer's instructions and eluted in sterile MilliQ water.

2.4.3.1 Plasmid mutagenesis and gene amplification

Cycling for megaprimer plasmid mutagenesis and general gene amplification was as follows: 98°C for 5 minutes as an initial denaturing step; 98°C for 30 seconds, 0.5°C per second ramp to 53°C annealing, 53°C for 30 seconds, 0.5°C per second ramp to 72°C for amplification, 72°C for 4 minutes and 0.5°C ramp to 98°C, repeat for a total of 32 cycles. The final extension step was 72°C for 5 minutes and reactions were set to 4°C before removal from thermocycler.

2.4.3.2 Mouse genotyping

Cycling for mouse genotypes were as follows: Initial denaturing step at 98°C for 4 minutes and 30 seconds. Cycle begins with 98°C denaturing for 20 seconds, annealing at 50°C for 45 seconds, amplification at 72°C for 15 seconds; repeat cycle 29 times. Final extension

Table 5: Primers used in this study

Primer	Sequence (5′ – 3′)[a]	Purpose
T7 promoter	TAA TAC GAC TCA CTA TAG GG	Sequencing
T7 reverse	CGC CAG GGT TTT CCC AGT CAC GAC	Sequencing
*Nco*I His TEV *speA* For	CCC CCA TGG GCA GCA GCC ATC ATC ATC ATC ATC ACA GCA GCG GCG AAA ACT TGT ATT TCC AAG GCC AAC AAG ACC CCG ATC CAA GCC A	Gene amplification
*Bam*HI *speA* Rev	CCC GGA TCC TTA CTT GGT TGT TAG GTA GAC TTC AAT	Gene amplification
speA N20A For	AAA AAC CTT CAA **GCA** ATA TAT TTT CTT	Mutagenesis
speA N20A Rev	AAG AAA ATA TAT **TGC** TTG AAG GTT TTT	Mutagenesis
speA L41/42A For	TCT GTT GAT CAA **GCA GCA** TCT CAC GAT TTA	Mutagenesis
speA L41/42A Rev	TAA ATC GTG AGA **TGC TGC** TTG ATC AAC AGA	Mutagenesis
DQA (1027) For	GAA GAC ATT GTG GCT GAC CAT GTT GCC	Mouse genotype
DQA (1029) Rev	AGC ACA GCG ATG TTT GTC AGT GCA AAT TGC GG	Mouse genotype
DQ8b (vA) For	AGG ATT TGG TGT ACC AGT TTA AGG GCA T	Mouse genotype
DQ8b (vii) Rev	TGC AAG GTC GTG CGG AGC TCC AA	Mouse genotype
DR4A (1101) For	GGA GAT AGT GGA ACT TGC GG	Mouse genotype
DR4A (1104) Rev	CCG ATC ACC AAT GTA CCT CC	Mouse genotype
DR4B (1098) For	GTT TCT TGG AGC AGG TTA AAC A	Mouse genotype

DR4B (1099) Rev	CTG CAC TGT GAA GCT CTC AC	Mouse genotype

[a] Underlined nucleotides represent restriction enzyme recognition sites; bolded nucleotides represented mutated amino acids

was completed at 72°C for 4 minutes, and reactions were set to 4°C until removed from thermocycler.

2.4.4 Visualization

UltraPure™ Agarose (Invitrogen, Life Technologies Inc.) at 1% or 2% (w/v) in 40 mM Tris-acetate, 1mM EDTA (TAE) buffer was used to visualize DNA. Samples were mixed 5:1 with DNA loading dye (40% [v/v] glycerol, 0.25% [w/v] bromophenol blue [International Biotechnologies; New Haven, CT, USA]) prior to gel loading. Electrophoresis was performed for 1 hour at 100 V (Bio-Rad Laboratories Inc.; Hercules, CA, USA). A standard DNA molecular weight ladder (1 Kb; Invitrogen) was included in each gel as a size marker. Agarose gels were stained with 0.05% (v/v) ethidium bromide (EMD) in TAE buffer for approximately 20 minutes and visualized using ultraviolet light (Gel Doc™, Bio-Rad Laboratories Inc.).

2.4.5 Gel extraction

DNA was visualized as stated above and excised from agarose gel under ultraviolet light using a scalpel. Extracted DNA was purified using QIAquick Gel Extraction Kit (Qiagen) according to the manufacturer's protocol. DNA was eluted using sterile MilliQ water.

2.4.6 Quantification

DNA was quantified using a NanoDrop 1000 Spectrophotometer (Thermo Fisher Scientific Inc.).

2.5 Molecular cloning

2.5.1 Restriction enzyme digestion

Restriction enzyme digestions of DNA were completed as per the manufacturer's instructions (New England BioLabs Inc.; Ipswich, MA, USA or Roche Diagnostics). Briefly, target DNA with 1 U enzyme μg^{-1} DNA in enzyme-specific buffer and 1 × bovine serum albumin (New England BioLabs Inc.) were incubated for 2.5 hours at 37°C. Reactions were visualized (see above) compared to uncut controls, and purified using QIAquick PCR Purification kit (Qiagen) as per manufacturer's instructions and eluted with sterile MilliQ water.

2.5.2 DNA ligation

Appropriate concentrations (100 ng:1 ng, vector:insert; 1:1 molar ratio) of purified, restriction enzyme digested DNA products were mixed with 1 × T4 Ligase Buffer and 40 U T4 DNA Ligase (New England BioLabs Inc.) and incubated at 16°C for 1 hour. Ligation reactions were directly transformed into rubidium chloride competent *E. coli* (see below).

2.5.3 Preparation of rubidium chloride competent *E. coli*

Appropriate *E. coli* culture grown in LB media aerobically overnight at 37°C (stationary phase) were subcultured 1:100 into 100 mL PSI broth (5 g/L Bacto yeast extract [BD Biosciences], 20 g/L Bacto Tryptone [BD Biosciences], 5 g/L magnesium sulphate, pH 7.6) and grown to OD_{600} 0.48. Cultures were incubated on ice for 15 minutes followed by centrifugation at 4°C for 5 minutes at 5,000 × *g*. The cell pellet was resuspended in 40 mL TfbI buffer (30 mM potassium acetate, 100 mM rubidium chloride, 10 mM calcium chloride, 50 mM manganese chloride, 15% [v/v] glycerol, pH 5.8) and incubated on ice for 15 minutes. Cells were centrifuged again as mentioned above. The pellet was then resuspended in 4 mL TfbII buffer (75 mM calcium chloride, 10 mM 3-(N-morpholino) propanesulfonic acid [MOPS], 10 mM rubidium chloride, 15% [v/v] glycerol, pH 6.5) and aliquots were store at -80°C until use.

2.5.4 Transformation of competent cells

Ligation reactions (see above) were transformed into rubidium chloride competent *E. coli* using a heat-shock method. Competent cells were thawed on ice, ligation reaction (~10 µL) was added and cells were incubated for 30 minutes on ice. Cells were then placed in a 42°C water bath for 45 seconds and subsequently placed on ice for 2 minutes. Cells then had 0.9 mL LB broth added and were incubated aerobically for 1 hour at 37°C. Transformed cultures were then spread plated (200 µL) on LB agar with appropriate antibiotics (according to transformed plasmid; see **Table 2**) and grown overnight at 37°C.

2.6 Sequencing of DNA

Sequencing was completed by the Sequencing Facility at the John P. Robarts Research Institute at Western University in London, Ontario, Canada. Sequencing was completed with either provided or designated primers (**Table 3**).

2.7 Protein production

2.7.1 Bacterial protein expression

E. coli BL21 (DE3) containing the appropriate pET expression construct (**Figure 3A**) was inoculated from freezer stock into LB broth containing appropriate antibiotic (**Table 2**). The culture was then grown aerobically overnight at 37°C. Overnight culture was subcultured 1:100 into 1L LB broth containing appropriate antibiotic and grown for 3 hours aerobically at 37°C. The bacterial culture was then induced with 200 µM isopropyl β-D-1-thiogalactopyranoside (IPTG) and grown aerobically overnight at room temperature (~25°C). The overnight culture was pelleted at 3,500 × *g* for 10 minutes and resuspended in 10 mL of 20 mM Tris base, 200 mM sodium chloride pH 7.5 buffer containing 10 µL DNaseI (Sigma-Aldrich) and 50 µL of 10 mg mL^{-1} lysozyme (Thermo Fisher Scientific Inc.) and incubated on ice for 1 hour with shaking. The bacteria was then sonicated for 3 rounds with 50 pulses each, 40% duty cycle and output 4 on a Branson Sonifier (Emerson Industrial Automation; Eden Prairie, MN, USA) with icing between each round. Sonicated product was then centrifuged at 10,000 × *g* at 4°C for 10 minutes and the supernatant was collected for gravity nickel column purification.

2.7.2 Metal affinity column chromatography protein purification

Supernatants from bacterial lysates were added to a charged (100 mM nickel sulphate) Ni-NTA affinity column (Novagen, EMD Millipore) and washed with 20 mM Tris base, 200 mM sodium chloride pH 7.5 buffer containing increasing concentrations of imidazole (5 mL each; 30 mM, 60 mM and 200 mM Imidazole). Fractions were analyzed by sodium dodecyl sulphate polyacrylamide gel electrophoresis (SDS-PAGE; see below) (**Figure 3B**) and fractions found to contain an abundance of the protein of interest were pooled and dialyzed in 1 L of 20 mM Tris base, 200 mM sodium chloride pH 7.5 three times for 1 hour per litre. The N-terminal His_6 tags were removed from the proteins by addition of either

Figure 3. Superantigen plasmid constructs and protein purification.

A. All wild-type and toxoid SAg genes were cloned in either pET28a or pET41a expression plasmids with the indicated purification and cleavage tags. **B – D.** Protein expression was induced using IPTG from *E. coli* BL21 (DE3) and SAgs were purified from cell lysate using nickel-affinity column chromatography. **B.** Cell lysates were applied to a $NiSO_4$-charged column and fractions were eluted using increasing concentrations of imidazole. SAg-containing fractions were pooled, dialysed to remove imidazole and incubated with the appropriate cleaving enzyme. **C.** The sample was again passed through a charged nickel column to remove cleaved His_6 tags and His_6-tagged TEV. **D.** Fractions of purified, cleaved SAg were collected and dialyzed into appropriate buffer and diluted to the required concentration. All visualization was done using 12% v/v SDS-PAGE. FT, flowthrough; W, wash; P, purified SAg protein. Column labels indicate concentration of imidazole in the wash buffers.

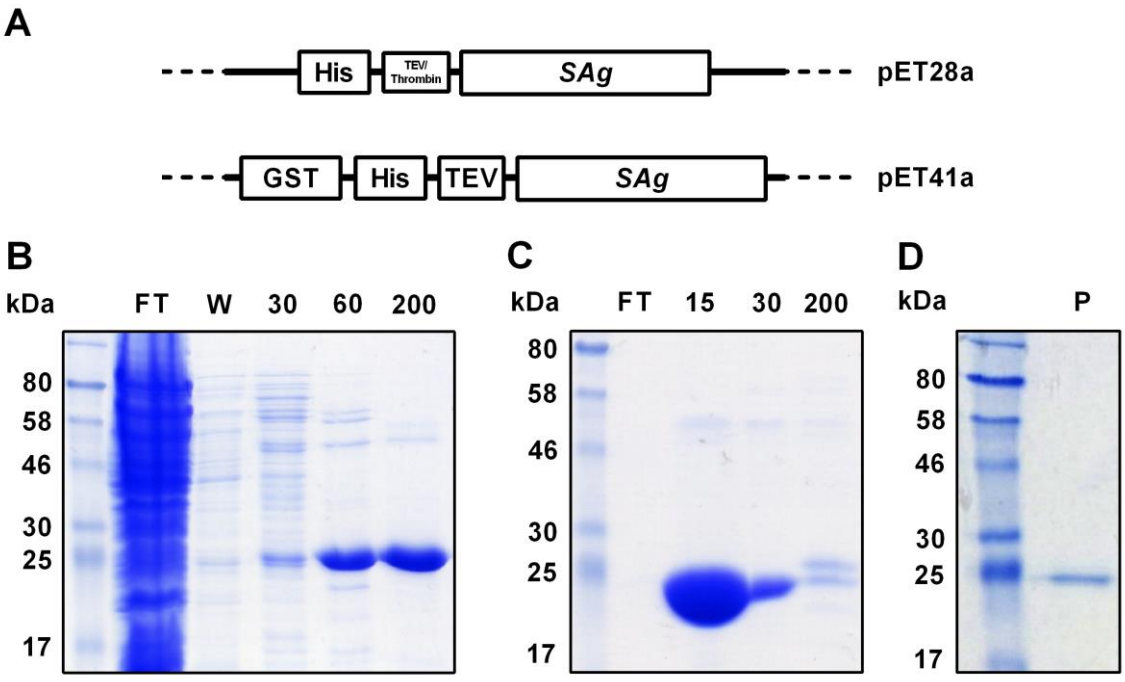
A
His
TEV/ Thrombin
SAg
pET28a
GST
His
TEV
SAg
pET41a
B
kDa
FT
W
30
60
200
80
58
46
30
25
17
C
kDa
FT
15
30
200
80
58
46
30
25
17
D
kDa
P
80
58
46
30
25
17

autoinactivation-resistant His_7-TEV [456] or thrombin for 24 hours at room temperature. The protein solution was then reapplied to a charged Ni-NTA affinity column (Novagen, EMD Millipore) to remove His_7-TEV and obtain a purified protein sample (**Figure 3C**). Pure protein was then dialyzed three times against 1 L of 150 mM sodium chloride, pH 7.4 for one hour per litre. Homogeneity was assessed by SDS-PAGE (see below) (**Figure 3D**).

2.7.3 Protein quantitation

Concentration of purified protein was determined using Pierce™ BCA Protein Assay kit (Thermo Fisher Scientific Inc.) according to manufacturer's instructions. Briefly, the protein of interest was mixed with working reagent, bicinchoninic acid (BCA), for colourimetric detection of protein at an optical density of 562 nm. The protein of interest concentration was then determined by comparing with various concentrations of a reference protein, BSA. Optical density was read using a Synergy™ H4 Hybrid Multi-Mode Microplate Reader (BioTek, Fisher Scientific Inc.).

2.8 Protein visualization

2.8.1 Sodium dodecyl sulphate polyacrylamide gel electrophoresis

Protein samples were mixed 3:1 with 4 × Laemmeli buffer (240 mM Tris-HCl pH 6.8, 8% [w/v] sodium dodecyl sulphate [SDS], 40% [v/v] glycerol, 0.01% [w/v] bromophenol blue, 1% [v/v] β-mercaptoethanol) and boiled for 5 minutes. Samples were then loaded into 15% polyacrylamide resolving gels (15% [v/v] acrylamide/bisacrylamide [37.5:1] aqueous solution, 0.25% [v/v] 1.5 M Tris-HCl pH 8.8, 0.1% [w/v] SDS, 0.1 % [w/v] ammonium persulfate [APS], 0.15% [v/v] tetramethylethylenediamine [TEMED]) with 5% polyacrylamide stacking gel (5 % [v/v] acrylamide/bisacrylamide [37.5:1] aqueous solution, 25% [v/v] 0.5 M Tris-HCl pH 6.8, 1.3% [w/v] SDS, 0.1 % [w/v] APS, 0.2% [v/v] TEMED) and run for 50 minutes at 200 V (Mini-PROTEAN System, Bio-Rad Laboratories Inc.) using Tris-Glycine electrophoresis buffer (192 mM glycine, 25 mM Tris, 0.1% [w/v] SDS, pH 8.3). Polyacrylamide gels were stained for 1 hour with staining solution (45% [v/v] methanol, 10% [v/v] glacial acetic acid, 0.1% [w/v] Coomassie Brilliant Blue R-250 [Bio-Rad Laboratories Inc.) and immediately placed in destain solution (45% [v/v] methanol, 10% [v/v] glacial acetic acid) several times until background staining was

resolved. To estimatre protein molecular weight, samples were compared to Prestained Broad Range P7708S Protein Marker (New England BioLabs Inc.) or BLUeye Protein Ladder (GeneDireX Inc., Taiwan).

2.8.2 Western blot

To probe for specific proteins, contents from SDS-PAGE gel (prior to staining procedure) were transferred onto polyvinylidine difluoride (PVDF) membrane (EMD Millipore). To accomplish this, PVDF membrane was first incubated in 100% methanol for 5 minutes, followed by immersion in Western blot transfer buffer (20% [v/v] methanol, 48 mM Tris base, 39 mM glycine, 0.037% [w/v] SDS) for 5 minutes. The prepared PVDF membrane and SDS-PAGE gel were then assembled together in a Mini Trans-Blot® Cell (Bio-Rad Laboratories Inc.) with Western blot transfer buffer and electroblotted for 1 hour at 100 V or overnight at 25 V with a cold block. The PVDF membrane was then blocked for 30 minutes with 5% (w/v) skim milk powder in Tris buffered saline (TBS; 100 mM Tris, 1.5 M sodium chloride, pH 7.5). Post-blocking, the membrane was incubated for 1 hour with primary antibody (polyclonal rabbit anti-SAg; ProSci; see below; **Table 6**) diluted 1:10,000 in 1% (w/v) skim milk in TBS. To remove residual antibody, PVDF membrane was washed three times in TBS with 0.01% (v/v) tween-20 (TBS-T) for 5 minutes per wash. IRDye800-conjugated goat anti-rabbit (Rockland Inc.; Limerick, PA, USA) secondary antibody was diluted 1:10,000 in 1% (w/v) skim milk powder in TBS and incubated with the PVDF membrane for 1 hour, shielded from light at room temperature. The membrane was washed three times with TBS-T as mentioned previously, and imaged on a LI-COR® Odyssey Imaging System (LI-COR Biosciences; Lincoln, NE, USA).

2.9 Antibody generation

Purified SAg toxins in 150 mM sodium chloride (pH 7.5), were sent to ProSci Inc. (Poway, CA, USA) for production of polyclonal rabbit anti-SAg antibodies. New Zealand White rabbits were injected with 200 µg of SAg with complete Freund's adjuvant at week 0, and boosted with 100 µg SAg with incomplete Freund's adjuvant at weeks 2, 4 and 6. Serum was collected at week 0, 5 and 7 with terminal bleed taken at week 8. Serum samples were

Table 6: Antibodies and dyes used in this study

Target	Fluorophore/Conjugate	Clone	Source
Passive Immunization/Western Blot			
SpeA	N/A	Polyclonal (Rabbit)	ProSci
SpeC	N/A	Polyclonal (Rabbit)	ProSci
Anti-Rabbit IgG	IRDye800	Polyclonal (Donkey)	Rockland
T cell Depletion			
CD4	N/A	GK1.5	BioXCell
CD8	N/A	YTS169.4	BioXCell
KLH	N/A	LTF-2	BioXCell
Vβ4	N/A	KT4	BioXCell
Vβ8	N/A	F23.1	BioXCell
Flow Cytometry – Mouse			
CD3ε	APC	145-2C11	eBioscience
CD4	APC-eFluor 780	GK1.5	eBioscience
CD8a	PE	53-6.7	eBioscience
CD25	PE	7D4	BD Pharmingen
TCR Vβ3	FITC	KJ25	BD Pharmingen
TCR Vβ4	FITC	KT4	BD Pharmingen
TCR Vβ8.1/8.2	FITC	KJ16	eBioscience
Flow Cytometry – Human			
7-AAD	N/A	N/A	eBioscience
CD3	APC	UCHT1	BD Pharmingen
CD4	BV 711	RPA-T4	BioLegend
CD8	Alexa Fluor 700	RPA-T8	BD Pharmingen
CD25	PE	M-A251	BD Pharmingen
PD-1	BV 421	EH12.2H7	BioLegend
ELISA – Antibody Titre			
Anti-Mouse IgG	HRP	Polyclonal (Goat)	Sigma-Aldrich
Anti-Mouse IgM	HRP	Polyclonal (Goat)	Rockland

assessed for anti-SAg antibody titre using enzyme-linked immunosorbent assay (ELISA; see below), aliquoted and stored at -80°C until use.

2.10 *In vivo* experiments

2.10.1 Mice

Other than size, there were no gender differences (bacterial load, response to SAgs, etc.) between male and female mice between any of the strains used in this study. It was therefore determined that when possible equal numbers of male and female mice would be used in each group, however, this was not a requirement for experimentation.

2.10.1.1 Housing and breeding

Mice were bred and housed in the West Valley Barrier Facility (Western University, London, ON, Canada) and moved to the Animal Holding Facility on the sixth floor of the Dental Sciences Building (Western University, London, ON, Canada) for undertaking of experiments. In both facilities mice were housed under specific pathogen-free conditions with food and water *ad libitum*.

2.10.1.2 Strains utilized

A list of all mice used in this study can be found in **Table 7**. C57Bl/6 mice expressing the transgenic major histocompatibility complex (MHC) class II human leukocyte antigen (HLA)-DR4 and DQ8 were obtained from the Kotb Laboratory and have been previously described [348,369,457]. Mice expressing the DQ8 gene alone were outbred from HLA-DR4/DQ8 by selecting for mice containing only the HLA-DQ8 allele. Conventional C57Bl/6 mice were obtained from The Jackson Laboratory.

2.10.2 Passive immunization

HLA-DQ8 mice 12-14 weeks of age were injected in the intraperitoneal cavity with 500 µL of rabbit anti-SAg serum -24 and -2 hours prior to nasopharyngeal infection with *S. pyogenes* (see below).

Table 7. Mouse strains used in this study

Strain	Characteristic	Source
C57Bl/6	Inbred black mouse	Jackson Laboratories (Bar Harbor, ME, USA)
HLA-DR4/DQ8	C57Bl/6 mice null for endogenous $H2^b$ MHC class II and transgenic for human HLA-DR4 and HLA-DQ8	[369]; McCormick lab breeding colony
HLA-DQ8	C57Bl/6 mice null for endogenous $H2^b$ MHC class II and transgenic for human HLA-DQ8	McCormick lab breeding colony

2.10.3 Vaccination experiments

Vaccination of 6-8 week old HLA-DR4/DQ8 mice has been previously described [377]. Briefly, mice received 1 µg (unless otherwise stated) SAg or toxoid in 200 µL (100 µL 150 mM sodium chloride, pH 7.5; 100 µL Imject™ Alum Adjuvant [Thermo Fisher Scientific]) subcutaneously under isoflurane anesthetic. Control mice received only saline solution and adjuvant. Injections were received on day 0, 14 and 28, and mice were bled via saphenous vein on day 42 to assess antibody titre (see below). Mice were weighed on day 0 prior to injection, day 7, 21 and 42 to determine if SAg injection had any effect on weight gain. To assess T cell responsiveness post-vaccination, spleens were removed on day 43 and subjected to an activation assay (see below). Where applicable, nasopharyngeal infection occurred on day 43 (see below).

2.10.4 T cell depletion

Murine depletion of T cells has been previously described [458]. In brief, HLA-DQ8 mice received 300 µg of anti-CD4 (GK1.5; BioXCell; West Lebanon, NH, USA), anti-CD8 (YTS169.4; BioXCell) or isotype control (LTF-2; BioXCell) alone or in combination in 500 µL of PBS, pH 7.5. Injections were received on day -7, -6 and -1. On day 0, mice were either sacrificed for lymph node procurement and flow cytometric analysis or streptococcal infection (see below).

2.10.5 Murine nasopharyngeal infection

Mice were given 2 mg ml^{-1} neomycin sulphate *ad libitum* in their drinking water two days prior to infection to reduce the nasal microbiota. Regardless of infecting bacteria, mice were sacrificed 48 hours post infection and cNT, blood, spleen, liver, kidneys, lungs and heart were removed for bacterial enumeration and cytokine analysis where indicated.

2.10.5.1 *S. pyogenes* preparation and inoculation

Preparation of *S. pyogenes* MGAS8232 for inoculation has been previously described [377,459]. In brief, *S. pyogenes* MGAS8232 was grown from freezer stock (see above) in THY broth statically at 37°C and subcultured 1:100 for two days. On the third day, the bacteria was subcultured (7%) into 100 mL of pre-warmed THY broth and grown until an

OD_{600} of ~0.3. Using the equation generated from the bacterial growth curve (see above), the appropriate volume containing 1×10^9 CFU was centrifuged at 2,000 × g for 7 minutes and the supernatant was removed. The bacterial pellet was transferred to a new container and spun at 21,000 × *g* for one minute. The residual supernatant was removed and the pellet was resuspended in 1 mL Hanks' Balanced Saline Solution (HBSS; Wisent Bioproducts Inc.; Saint-Bruno, QU, Canada) and spun as above. The supernatant was again removed and the pellet was reconstituted in 150 µL HBSS for murine inoculation. One dose was serially diluted and plated to determine the concentration of bacterial inoculum. Mice from one of the above mentioned experimental methodologies were then anesthetized using ^{Pr} FORANE (isoflurane, USP; Baxter Corporation; Mississauga, ON, Canada) and 7.5 µL of bacterial inoculum was administered to each nostril. The mice were then allowed to recover from the anesthetic and monitored for the duration of the experiment. Inoculation with *S. pyogenes* SF370 was completed as above with the following modification: after being grown from the freezer stock, the bacteria were directly subcultured (7% v/v) into 100 mL pre-warmed THY media without two days of subculturing.

2.10.5.2 *S. pneumoniae* preparation and inoculation

Nasal inoculation of *S. pneumoniae* was prepared similarly to Puchta *el al*. [460]. Briefly, *S. pneumoniae* was grown from freezer stock in 10 mL TSB at 37°C with 5% CO_2 overnight. The overnight growth was subcultured (7%) in 100 mL TSB and grown as above until an OD_{600} ~0.3 was reached. Using the generated equation (see above), the appropriate volume containing 1×10^8 CFU was spun at 15,000 × g for 1 minute. The supernatant was removed and the pellet was resuspended in 100 µL of PBS, pH 7.5. One dose was serially diluted and plated to determine the concentration of bacterial inoculum. T cell depleted or isotype control treated mice were then anesthetized using ^{Pr} FORANE (isoflurane, USP; Baxter Corporation; Mississauga, ON, Canada) and 5 µL of bacterial inoculum was administered to each nostril. The mice were then allowed to recover from the anesthetic and monitored for the duration of the experiment.

2.11 Antibody titre analysis

Antibody titres were determined using ELISA. Wells of a Corning Costar 9018 (Corning; Corning, NY, USA) 96-well high-bind plate were coated with 100 µL of indicated SAg (10 µg mL^{-1}) in coating carbonate buffer (affymetrix eBioscience; Thermo Fischer Scientific**)** and was left at room temperature overnight in a humidified chamber. Plates were subsequently washed twice with distilled water. Plates were then blocked with PBS containing 1% (w/v) bovine serum albumin (BSA) and 0.05% (v/v) tween-20 for 2 hours at room temperature and washed as above. Mouse serum samples were diluted starting at 1:100 in PBS containing 0.1% (w/v) BSA and 0.05% (v/v) tween-20 to a final volume of 100 µL per well followed by two-fold serial dilutions down the plate until a final dilution of 1:204,800 was reached. Plates were incubated at room temperature for 2 hours and washed three time in wash buffer (PBS containing 0.05% v/v tween-20) followed by three washes with distilled water. Goat anti-mouse horseradish peroxidase (HRP)-conjugated secondary antibody (Sigma-Aldrich) was added at a dilution of 1:10,000 to a final volume of 100 µL/well and incubated at room temperature for 2 hours. Plates were washed 5 times as above and developed by adding 100 µL/well of 3, 3′, 5, 5′ Tetramethybenzidine (TMB; BD Biosciences) for 15 minutes. Colour change was halted by addition of 50 µL of 1 M H_2SO_4 and plates were read at OD_{450} with OD_{570} subtraction. Positive antibody titre was calculated as the reciprocal of the lowest serum dilution with readings four-fold above background.

2.12 *Ex vivo* experiments

2.12.1 Cell preparation

2.12.1.1 Murine splenocytes

Spleens were procured from euthanized mice and immediately stored on ice in 5 mL of HBSS. Spleens were pressed through a sterile 0.2 µm nylon mesh filter and the single-cell suspension was centrifuged at 450 × *g* for 5 minutes. The supernatant was removed and the pellet was loosened via racking. Red blood cells were lysed by addition of 1 mL ammonium chloride potassium (ACK) lysing buffer (Thermofisher Scientific Inc.) for 30 seconds. To stop the lysis reaction, 10 mL of PBS, pH 7.5 was added and the cells were spun as above. Cells were resuspended in 7 mL PBS buffer and sieved through nylon mesh filter as above

to remove cell debris. The filter was washed with an additional 7 mL PBS to ensure collection of all living cells. The collected sample was spun as above, the supernatant was discarded, and the pellet was racked, and then resuspended in 4 mL of complete RPMI (cRPMI) media (RPMI-1640 [Life Technologies Inc.] supplemented with 0.1 mM minimal essential medium non-essential amino acids [Life Technologies Inc.], 10% [v/v] heat-inactivated fetal bovine serum [Sigma-Aldrich], 100 units mL^{-1} penicillin [Life Technologies Inc.], 100 µg mL^{-1} streptomycin [Life Technologies Inc.], 1 mM sodium pyruvate [Life Technologies Inc.], and 2 mM L-glutamine [Life Technologies Inc.]). Live cells were counted using Trypan Blue (Life Technologies Inc.) exclusion and resuspended to a concentration as required for the indicated assay.

2.12.1.2 Murine lymph nodes

Cervical lymph nodes were procured from anaesthetized mice and immediately homogenized in 5 mL of ice-cold PBS, pH 7.5 using a glass homogenizer. Cells were processed as above, however, no ACK lysing buffer was required.

2.12.1.3 Human peripheral blood mononuclear cells

Blood was obtained from healthy donors with ethics approval (**Appendix 1**). Whole blood was mixed with pre-warmed RPMI-1640 (Life Technologies Inc.) in a 1:1 ratio. The blood mixture was added to room-temperature Ficoll (GE Healthcare; Fairfield, CT, USA) in a 1:2 (blood : Ficoll) ratio. Tubes were spun for 30 minutes at 913 × *g* and stopping was done without the aid of a break. The PBMC layer was carefully transferred to a new tube and washed with RPMI (Life Technologies Inc.) three times. With each wash, spin intensity decreased (514, 329, and 185 × *g*, respectively with break). Cells were resuspended in cRPMI and live cells were counted using Trypan Blue exclusion and diluted to the appropriate concentration as required for the indicated assay.

2.12.2 T cell activation assay

Cells were seeded at 2×10^5 cells per well in a 96-well plate. SAgs at indicated concentrations were added, and cells were incubated at 37°C with 5% CO_2 for 18 hours. Cells were spun, and supernatant was removed and stored at -20°C until further experimentation. To assess activation, IL-2 was measured using ELISA (mouse IL-2

ELISA Ready-Set-Go! Kit [eBioscience Inc.] or human IL-2 ELISA Kit [BD Biosciences Inc.]) according to the manufacturer's instructions. Briefly, Corning Costar 9018 (Corning) 96-well high-bind plates were coated overnight at 4°C with appropriate capture antibody in supplied carbonate capture buffer. Plates were washed twice with wash buffer (PBS with 0.05% [v/v] tween-20) and blocked for 2 hours at room temperature with assay diluent. Plates were washed as above and supernatant from stimulated cells was added (murine splenocyte supernatant added neat; human PBMC supernatant diluted 1:4 with assay diluent) and incubated at room temperature for one hour. Plates were washed as above three times, and detection cocktail was added (primary antibody-biotin and avidin-horse radish peroxidase conjugates were incubated together in assay diluent for 30 minutes prior to addition to 96-well plate) for one hour. Plates were washed five times as above, and supplied TMB was added for 15 minutes prior to colour change stoppage by addition of 1 M H_2SO_4. All plates were read on a Synergy H4 plate reader (BioTek Instruments Inc.) by assessing absorbance at OD_{450} and subtracting OD_{570}. Concentrations were determined by comparing supernatant concentrations to supplied standards, and limit of detection was 3.125 ng mL^{-1} for murine IL-2 and 7.8 ng mL^{-1} for human IL-2.

2.12.3 Flow cytometry

Isolated cells were aliquoted at a concentration of 1×10^6 cells per tube, centrifuged at 450 × *g* for 5 minutes, supernatant was removed, pellet was resuspended by racking and washed in 2 mL of FACS wash buffer (PBS supplemented with 2% [v/v] fetal bovine serum and 0.01% [w/v] sodium azide). Cells were spun again as above, supernatant was removed, and cells were resuspended as above. Cells were incubated with appropriate concentrations of fluorophore-conjugated antibodies or cell viability dyes according to the manufacturer's instructions for 30 minutes at 4°C or on ice protected from light. In low-light conditions, samples were washed three times as above, resuspended in 400 µL of FACS wash buffer, and read on an LSR II Flow Cytometer (BD Biosciences Inc.).

2.12.4 T cell proliferation assay

T cell proliferation was measured from human PBMCs using the CellTrace™ carboxyfluorescein succinimidyl ester (CFSE) cell proliferation kit (Thermo Fisher

Scientific Inc.) as per the manufacturer's instructions. Briefly, 10×10^6 cells were resuspended in 37°C pre-warmed RPMI-1640 (Life Technologies Inc.) and a 5 mM CellTrace™ CFSE stock solution was created by diluting the stock solution with dimethyl sulfoxide (DMSO). The CFSE solution is added to the cells to generate a final concentration of 10 µM and cells are incubated in a water bath protected from light at 37°C for 10 minutes with gentle mixing at 5 minutes. Cell labelling was stopped by addition of 30 mL of 4°C cRPMI, and the cell mixture was incubated on ice for 5 minutes. The cells were spun at 403 × g for 10 minutes and resuspended in cRPMI. Cells were aliquoted at 8×10^5 cells per tube, and stimulated with varying concentrations of SAg or untreated control. Polymixin B was then added to a final concentration of 2 µg mL^{-1} and cells were incubated at 37°C with 5% CO_2 for 5 days before flow cytometry analysis using a LSR II Flow Cytometer (BD Biosciences Inc.).

2.13 Multiplex cytokine array

Cytokine and chemokine concentrations were determined from the cNT of HLA-DQ8 mice treated with LTF-2 (isotype control), GK1.5 (anti-mouse CD4), YT169.4 (anti-mouse CD8) or a combination of GK1.5 and YTS169.4 and infected with either *S. pyogenes* MGAS8232 or *S. pneumoniae* P1121. *S. pyogenes* infected HLA-DR4/DQ8 mice from wild-type SpeA and SEB vaccination groups, and a sham group, were also assessed. Uninfected HLA-DR4/DQ8 cNT homogenates were tested as a background control. Mutiplex cytokine array (Mouse Cytokine/Chemokine Array 31-Plex) was performed by Eve Technologies (Calgary, AB, Canada) and heat maps were generated using Matrix2png [461]. The data is shown as average cytokine response from 3-4 mice per group normalized to the highest concentration as 100% between all groups. Statistical analysis was completed by the appropriate test within groups (**Appendix 4**).

2.14 Statistical analysis

Data was analyzed using unpaired Student's *t*-test, one-way analysis of variance (ANOVA) with Dunnett's multiple comparisons post-hoc test or two-way ANOVA with Tukey's or Dunnett's multiple comparison post-hoc test, as indicated. A value of *P* less than 0.05 was

determined to be statistically significant and all analyses were completed using Prism software (GraphPad Software, Inc.; La Jolla, CA, USA).

Chapter 3: Results

3 Results

3.1 Generation and purification of wild-type and SpeA toxoid superantigens

Wild-type SAg expression constructs, and select mutant toxoid constructs, were previously designed by members of the McCormick laboratory (**Table 4**). Constructs were generated in either the expression construct pET28a or pET41a, with either a TEV protease or thrombin cleavage site between the His_6-Tag and the SAg gene (**Figure 3A**). Proteins were expressed by IPTG induction in *E. coli* BL21 (DE3), and purified from cell lysate using two-step nickel-affinity column chromatography (**Figure 3B-D**). For all SpeA mutant toxoids (except $SpeA_{HEXA}$) that had not been previously generated, megaprimer PCR amplification was used with the appropriate primers (**Table 5**) (**Figure 4A**). $SpeA_{HEXA}$ was previously generated and published [437] without a TEV cleavage site between the His_6-Tag and the SAg gene. This construct was generated by amplifying the $SpeA_{HEXA}$ gene from the original construct using primers that added the nucleic acid sequence for a His_6-Tag, TEV protease cleave site with appropriate restriction enzyme sites for cloning into the pET28a expression vector (**Table 5**; **Figure 4B**).

To supplement the previously designed MHC II binding site SpeA toxoid ($SpeA_{Y100A}$) [454], numerous other toxoids were generated using megaprimer PCR (**Figure 4A**) including: a TCR-binding interface toxoid ($SpeA_{N20A}$); a toxoid containing both N20A and Y100A amino acid substitutions ($SpeA_{N20A/Y100A}$); a further attenuate MHC II toxoid which combined the Y100A substitution with two additional substitutions at this interface (L41A and L42A; designated $SpeA_{TRI}$); as well as a toxoid that contained all the aforementioned substitutions (N20A/L41A/L42A/Y100A; designated $SpeA_{TETRA}$). The choice of the amino acid mutations were based upon previously published literature describing the attenuation of SpeA by the addition of these mutations [437,439,462]. SAg structures and relevant mutations were observed visually using PyMOL (The PyMOL Molecular Graphics System, Version 1.8 Schrödinger, LLC.). To generate the ribbon diagram, SEB in complex with TCR and MHC class II (4C56) [215] was used as a scaffold. The SpeA (1FNU) [203], HLA-DQ8 (1JK8) [463] and murine TCR vβ8 (1SBB) [220] constructs were superimposed onto the corresponding structures from the SEB ternary complex (**Figure 5**).

Figure 4. Polymerase chain methodology for the generation of SpeA toxoids.

A. Mutant SpeA derivatives were generated by PCR amplification from *speA* housed in the pET28a expression plasmid. Forward and reverse primers spanned the area of interest and contained the appropriate nucleic acid changes to result in desired amino acid substitutions, with flanking upstream and downstream regions left complementary to the wild-type gene. Amplification of the construct using these primers resulted in a product containing the desired substitution. Restriction enzyme digestion with *Dpn*I eradicated the parent plasmid and left only the desired toxoid construct, which could then be directly transformed into chemically-competent *Escherichia coli* and circularized by host DNA repair mechanisms. **B.** $SpeA_{HEXA}$ was provided by a collaborator and has been previously described [437]. The plasmid housing the $speA_{HEXA}$ gene did not have the desired purification or cleavage tags, so the gene was moved to a new expression plasmid using megaprimer PCR amplification. A forward primer containing the desired restriction enzyme cut site, 6x His-Tag and tobacco etch virus (TEV) protease cleavage site as well as 5′ sequence overlap to $speA_{HEXA}$ were used in combination with a reverse primer that had a second restriction enzyme cute site and 3′ overlap. Amplified gene product and empty pET28a expression plasmid were digested with indicated restriction enzymes, ligated together and transformed into desired chemically-competent *E. coli* strains. All transformants were selected for on media containing specific antibiotics and toxoid product sequences were confirmed using DNA sequencing.

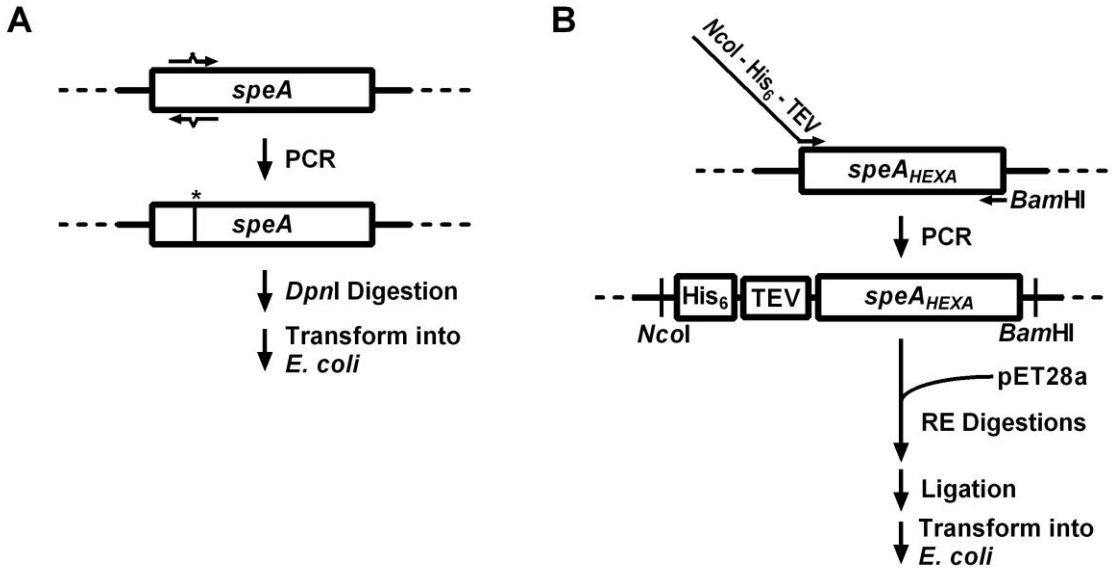
A
speA
PCR
*
speA
DpnI Digestion
Transform into
E. coli
B
NcoI - His6 - TEV
speAHEXA
BamHI
PCR
His6
TEV
speAHEXA
NcoI
BamHI
pET28a
RE Digestions
Ligation
Transform into
E. coli

Figure 5. Visualization of SpeA toxoid amino acid substitutions.

A. Ribbon diagram cartoon of the SpeA crystal structure (grey) (1FNU) [203] in complex with murine TCR Vβ8 (yellow) (1SBB) [220] (α-chain, blue) and MHC class II HLA-DQ8 (α-chain, red; β-chain, green) (1JK8) [463] was generated using the published TCR/SEB/MHCII trimolecular complex (4C56) [215] as a scaffold. **B.** and **C.** Inset box shows an up-close view of the SpeA immune complex interaction interface with highlighted amino acids (cyan) substituted in (**B**) $SpeA_{HEXA}$ (Q19H/N20D/L41A/L42A/D45N/C98S) and (**C**) $SpeA_{TETRA}$ (N20A/L41A/L42A/Y100A). Images were generated with PyMOL (The PyMOL Molecular Graphics System, Version 1.8 Schrödinger, LLC.).

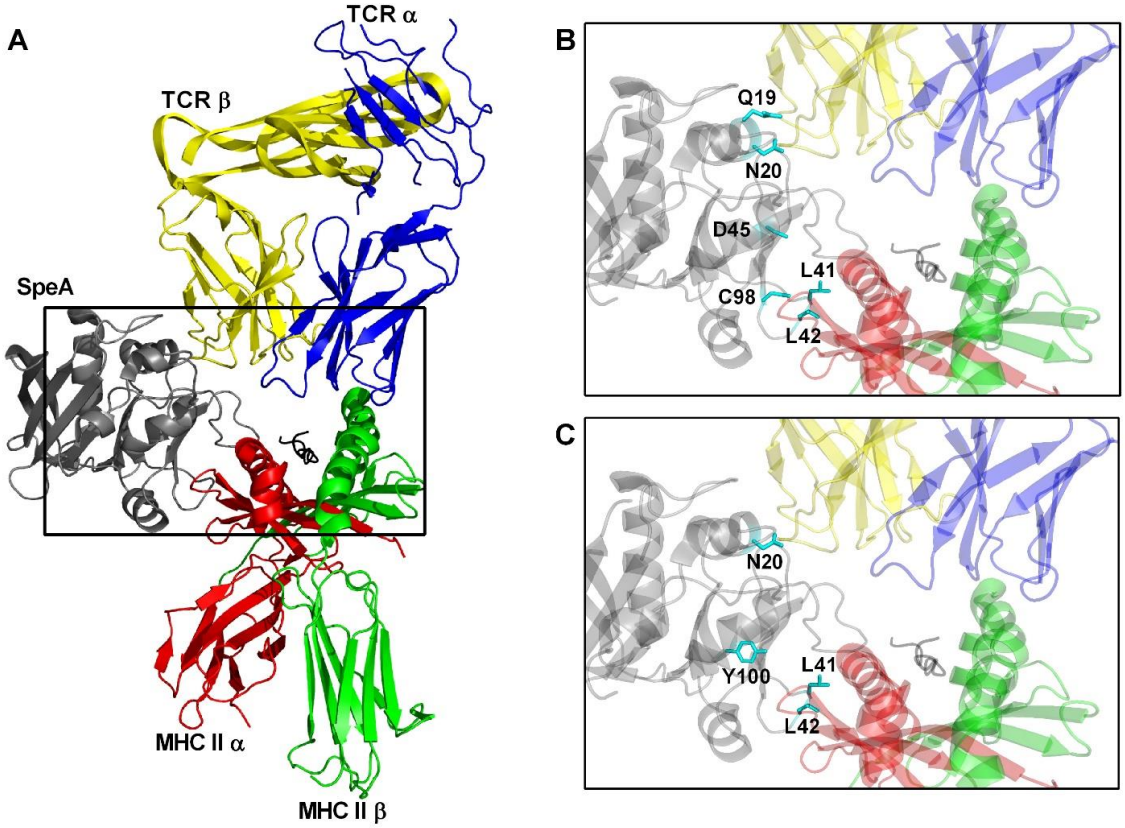
A
TCR α
TCR β
SpeA
MHC II α
MHC II β
B
Q19
N20
D45
L41
C98
L42
C
N20
Y100
L41
L42

To generate purified SAg protein, cell lysate from induced bacterial strains that contained the desired SAg expression plasmids was applied to charged nickel resin column. His_6-tagged proteins were eluted from the column with increasing concentration of imidazole (**Figure 3A**). SDS-PAGE gels were used to determine fractions containing the desired protein which were subsequently dialyzed to remove imidazole and the His_6-Tag was removed by addition of either autoinactivation-resistant His_7::TEV [456] or thrombin depending on the construct (**Table 4**). Samples were again passed over a charged nickel column to removed purification tags and HIS_7::TEV (**Figure 3C**). SAgs were isolated in wash or low imidazole concentrations and confirmed by size comparison on an SDS-PAGE (approximately 25kDa). Pure samples were dialyzed into a saline solution for future experimentation (**Figure 3D**).

3.2 Evaluation of superantigen function on immune cells

3.2.1 Human PBMC proliferation, activation and anergy induced by wild-type superantigens

The ability of purified wild-type SAgs to activate, cause proliferation and induce anergy in human PBMCs was assessed using flow cytometry (**Figure 6**). Cells were isolated from a healthy human donor and incubated with increasing concentrations of SAgs for 5 days. Proliferation was based on dilution of CFSE within dividing cells (**Figure 6B**), activation was based upon expression of CD25 (**Figure 6C**) and anergy was based upon expression of PD-1 (**Figure 6D**). All SAgs were able to activate, proliferate and induce anergy in both $CD4^+$ and $CD8^+$ cells, however, this donor was a low responder to SpeA and SSA.

A second marker of activation – IL-2 – was also measured. Human PBMCs from the same donor were incubated with increasing concentrations of SAgs for 18 hours and IL-2 from culture supernatants were measured. Similar to the results above, it was demonstrated that all SAgs could activate human PBMCs, and it was noted that this donor was a low responder to SpeA and SSA (**Figure 6E**).

Figure 6. Activation of human T cells by recombinant streptococcal superantigens. Human peripheral blood mononuclear cells (PBMCs) were isolated from a healthy donor via Ficoll gradient centrifugation and stimulated with increasing concentrations of each streptococcal SAgs to assess their ability to proliferate, activate and induce markers of anergy in cells. **A.** Purified streptococcal SAgs were visualized using 12% SDS-PAGE. **B – D.** Human PBMCs were incubated with the indicated concentrations of SAg for five days. Cells were then analyzed by flow cytometry to assess (**B**) proliferation ($CFSE^{Low}$), (**C**) activation ($CD25^{+}$) and (**D**) anergy ($PD\text{-}1^{+}$) of $CD3^{+}$ $CD4^{+}$ or $CD3^{+}$ $CD8^{+}$ cells. Data represent singular values. (**E**) PBMCs were also incubated with indicated concentrations of SAg for 18 hours to assess activation based on supernatant IL-2 concentration as determined by ELISA. Data represent the mean of triplicate values. SAgs are colour-coded as indicated in the legend.

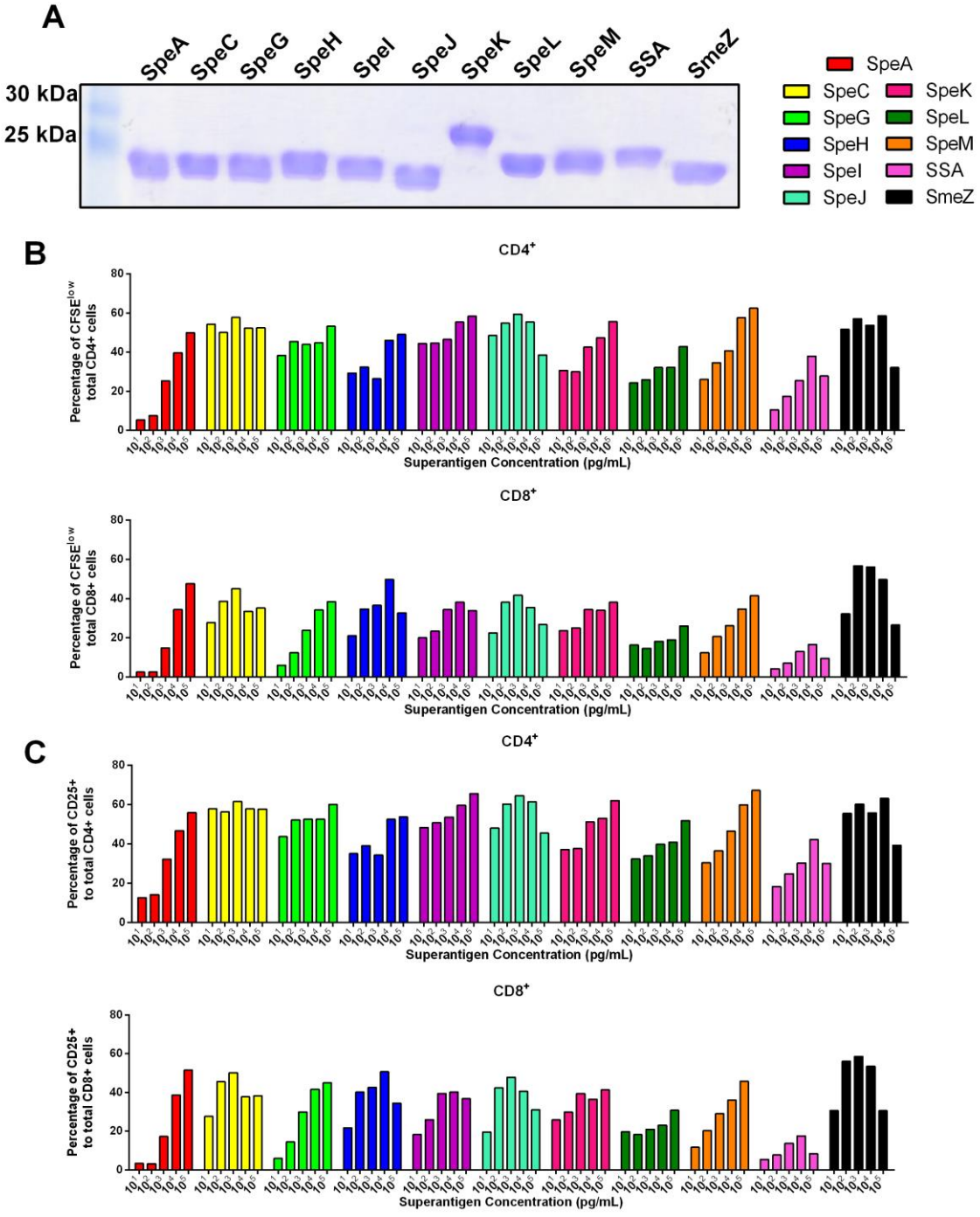
A
SpeA
SpeC
SpeG
SpeH
SpeI
SpeJ
SpeK
SpeL
SpeM
SSA
SmeZ
30 kDa
25 kDa
B
CD4+
Percentage of CFSElow total CD4+ cells
Superantigen Concentration (pg/mL)
CD8+
Percentage of CFSElow total CD8+ cells
Superantigen Concentration (pg/mL)
C
CD4+
Percentage of CD25+ to total CD4+ cells
Superantigen Concentration (pg/mL)
CD8+
Percentage of CD25+ to total CD8+ cells
Superantigen Concentration (pg/mL)

D

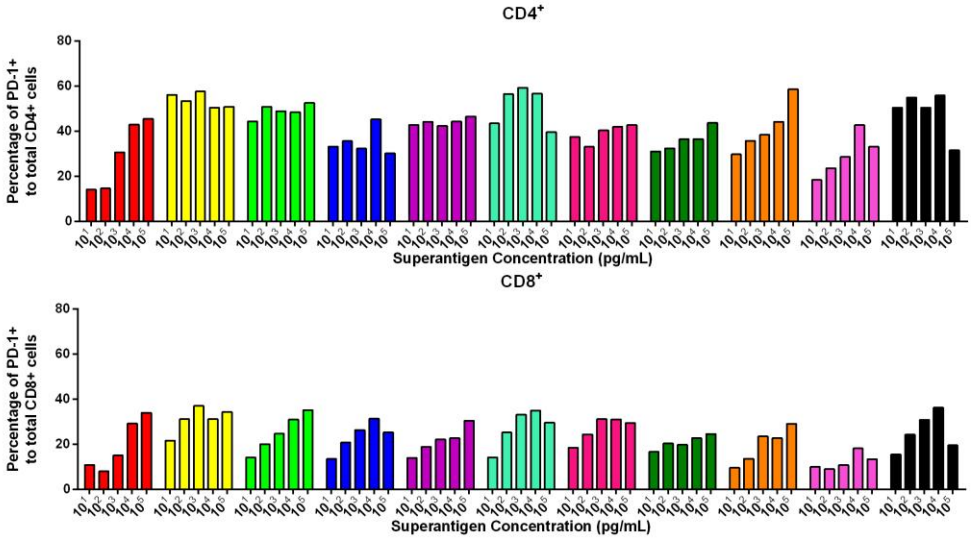
CD4+
Percentage of PD-1+ to total CD4+ cells
0
20
40
60
80
Superantigen Concentration (pg/mL)
CD8+
Percentage of PD-1+ to total CD8+ cells
0
20
40
60
80
Superantigen Concentration (pg/mL)

E

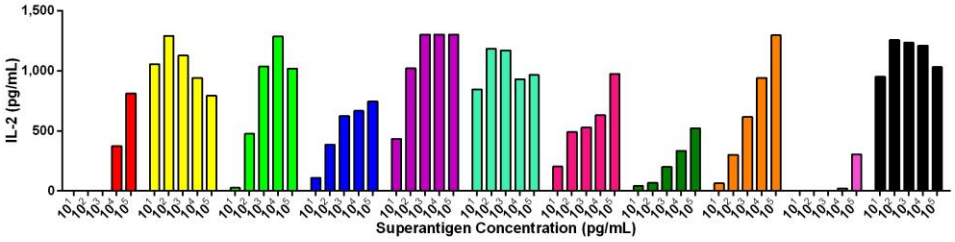
IL-2 (pg/mL)
0
500
1,000
1,500
Superantigen Concentration (pg/mL)

3.2.2 Evaluation of activation potential by wild-type superantigens on murine splenocytes

The ability of SAgs to activate conventional C57Bl/6 and transgenic HLA-DR4/DQ8 mice was evaluated. Splenocytes from both mouse strains were stimulated with increasing concentrations of SAgs and culture supernatants were analyzed for IL-2 using ELISA. In contrast to humans, conventional C57Bl/6 mice were only stimulated by SpeH, SpeI and to a lesser extent SpeL, SpeM and SmeZ (**Figure 7A**). HLA-DR4/DQ8 transgenic mice were slightly more sensitive to the above mentioned SAgs, but were also stimulated by SpeA (**Figure 7B**). In comparison to human cells (**Figure 6**), the murine cells were stimulated to a much lower magnitude comparing overall concentrations of IL-2 in culture supernatant.

3.3 Confirmation of MHC II dependence during *S. pyogenes* infection

Previous work from our laboratory has demonstrated the requirement for murine expression of human MHC II for efficient nasopharyngeal infection by *S. pyogenes* [449]. To confirm this finding, conventional C57Bl/6, HLA-DQ8 or HLA-DR4/DQ8 mice were infected with *S. pyogenes* MGAS8232. As previously shown, conventional C57Bl/6 mice were poorly infected by this strain of Group A *Streptococcus*, whereas mice expressing HLA-DQ8 (or -DR4/DQ8) had a significantly higher bacterial load at 48 hours (**Figure 8A**).

A second strain of *S. pyogenes* was tested for this MHC II dependence phenotype. *S. pyogenes* SF370 was inoculated into C57Bl/6 and HLA-DQ8 mice and nasopharyngeal bacterial load was assessed. Conventional C57Bl/6 mice were shown to harbor significantly less bacteria than their HLA-DQ8-exressing counterparts, confirming human MHC II dependence during infection for this strain of Group A *Streptococcus* (**Figure 8B**).

3.4 *In vivo* detection of superantigen expression

Our laboratory has elucidated the importance of the SAg SpeA for nasopharyngeal infection by *S. pyogenes* MGAS8232 of HLA-DR4/DQ8 transgenic mice [449]. To determine if SpeA was expressed and could be detected by subsequent lymphocyte activation *in vivo*, mice were infected with either wild-type or *S. pyogenes* MGAS8232

Figure 7. Conventional and transgenic mouse T cell responses to streptococcal superantigens.

Splenocytes from (**A**) conventional C57Bl/6 or (**B**) transgenic mice which lack endogenous murine MHC class II but express HLA-DR4 and HLA-DQ8 were stimulated with indicated concentrations of streptococcal SAgs for 18 hours. Culture supernatants were then analyzed for IL-2 using ELISA as a marker of T cell activation. Data represent the mean ± SEM of triplicate values from a single mouse. SAgs are colour-coded as indicated in the legend.

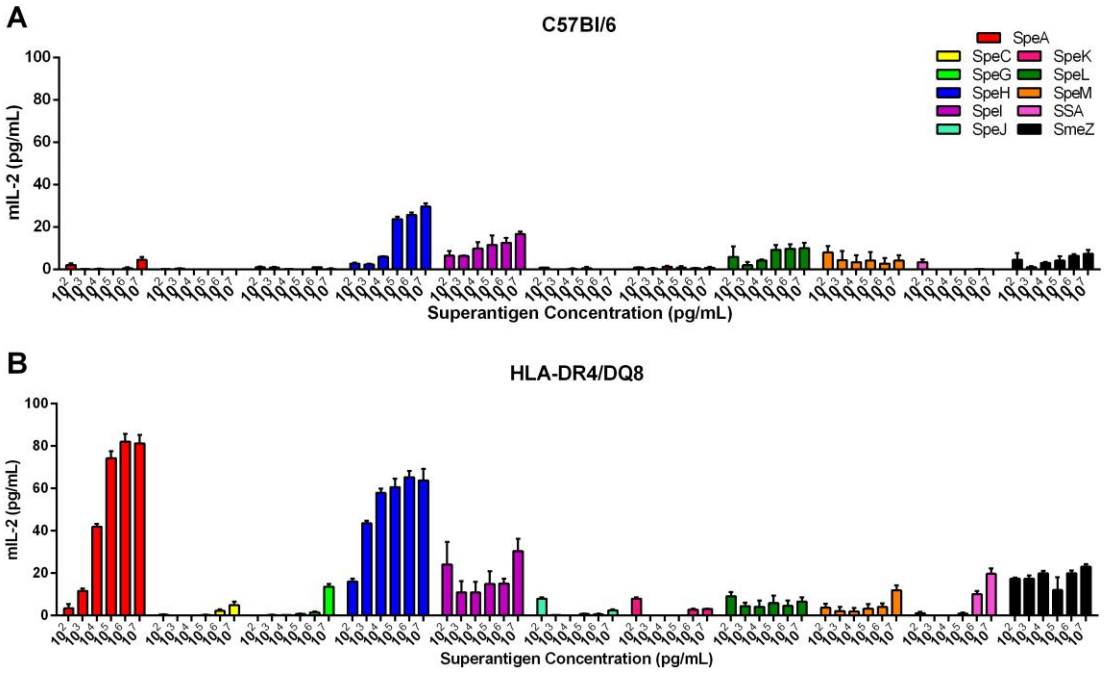
A
C57Bl/6
SpeA
SpeC
SpeK
SpeG
SpeL
SpeH
SpeM
SpeI
SSA
SpeJ
SmeZ
mIL-2 (pg/mL)
Superantigen Concentration (pg/mL)
B
HLA-DR4/DQ8
mIL-2 (pg/mL)
Superantigen Concentration (pg/mL)

Figure 8. Efficient nasopharyngeal infection by *S. pyogenes* requires transgenic expression of human MHC class II molecules.

Conventional C57Bl/6 or transgenic mice expressing the indicated human leukocyte antigen MHC class II molecules were intranasally infected with 10^8 CFU of either (**A**) *S. pyogenes* MGAS8232 or (**B**) *S. pyogenes* SF370 for 48 hours. Data points represent CFU from the cNT of individual mice. Horizontal bars represent the mean. Horizontal dotted line indicates the theoretical limit of detection. Significance determined by (**A**) one-way ANOVA with Tukey's post-hoc test (***, $P < 0.001$) or (**B**) Student's *t* test (*, $P < 0.05$).

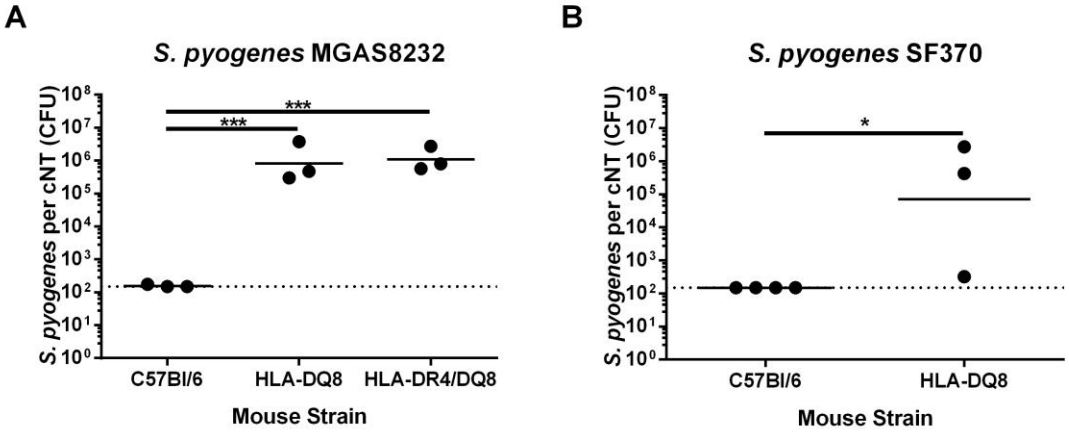
A
S. pyogenes MGAS8232
S. pyogenes per cNT (CFU)
***
***
C57Bl/6
HLA-DQ8
HLA-DR4/DQ8
Mouse Strain
B
S. pyogenes SF370
S. pyogenes per cNT (CFU)
*
C57Bl/6
HLA-DQ8
Mouse Strain

Δ*speA* and cervical lymph nodes were removed at 48 hours post-infection. SpeA-targeted lymphocytes were stained for activation markers and were compared to a non-targeted internal control. Using flow cytometry, live lymphocytes were gated first using forward and side scatter. Cells expressing $CD3^+$ surface antigen were then gated. Expression of the activation marker $CD25^+$ on SpeA-targeted T cell subset expressing the TCR Vβ8 chain was compared this to an internal control (TCR Vβ3 expressing T cells) (**Figure 9A**). It was demonstrated that between the two strains, there was no significant difference in the percentage of $CD3^+$ TCR $V\beta^+$ subsets (**Figure 9B**), however, there was a significant difference in the percentage of TCR $V\beta8^+$ $CD25^+$ T cells (targeted by SpeA) but not the non-SpeA targeted subset (TCR Vβ3) (**Figure 9C**). This data was also supplemented with cNT counts and which again demonstrated the importance of SpeA in our nasopharyngeal infection model (**Figure 9D**).

3.5 Anti-superantigen passive immunization protects mice from *S. pyogenes* infection

To assess whether anti-SAg antibodies could be protective against *S. pyogenes* MGAS8232 nasopharyngeal infection, a passive immunization experiment was designed. HLA-DQ8 transgenic mice were administered hyper-immune serum from previously immunized rabbits containing antibodies to either SpeA or control serum containing anti-SpeC antibodies, as deletion of *speC* from *S. pyogenes* MGAS8232 had no effect on the infection phenotype [377]. After passive transfer, mice were infected with *S. pyogenes* MGAS8232 and sacrificed 48 hours later (**Figure 10A**). Murine cNT was removed to assess nasopharyngeal bacterial burden and blood was drawn to examine antibody titres. Mice treated with anti-SpeA immune serum had significantly reduced bacterial load compared to control serum (**Figure 10B**). In addition, Western blot analysis demonstrated that the rabbit serum was specific for each SAg, and that the serum was not cross-reactive between SpeA and SpeC (**Figure 10 C**). As expected, protected mice had significantly higher anti-SpeA antibodies present in their blood, and the lack of cross-reactivity was confirmed by ELISA (**Figure 10 D** and **E**). These results indicate that anti-SAg antibodies can be protective in a *S. pyogenes* nasopharyngeal infection model.

Figure 9. Detection of superantigen-dependent Vβ-specific T cell activation *in vivo*. Flow cytometric analysis of HLA-DR4/DQ8 cervical lymph node cells and cNT bacterial counts 48 hours post-infection with wild-type *S. pyogenes* MGAS8232 or MGAS823 ΔSpeA ($n \geq 4$ for each group). **A.** Cells were first gated on live lymphocytes using FSC and SSC followed by gating on $CD3^+$ cells and either $V\beta3^+$ $CD25^+$ or $V\beta8^+$ $CD25^+$ cells. **B.** Percentages of $V\beta3^+$ and $V\beta8^+$ subsets were compared between groups. **C.** Percentages of $V\beta^+$ $CD25^+$ cells were compared between groups. **D.** Data points represent CFU from the cNT of individual mice. Horizontal bars represent the mean. Horizontal dotted line indicates the theoretical limit of detection. Significance determined by Student's *t* test (**, $P < 0.01$; ***, $P < 0.001$).

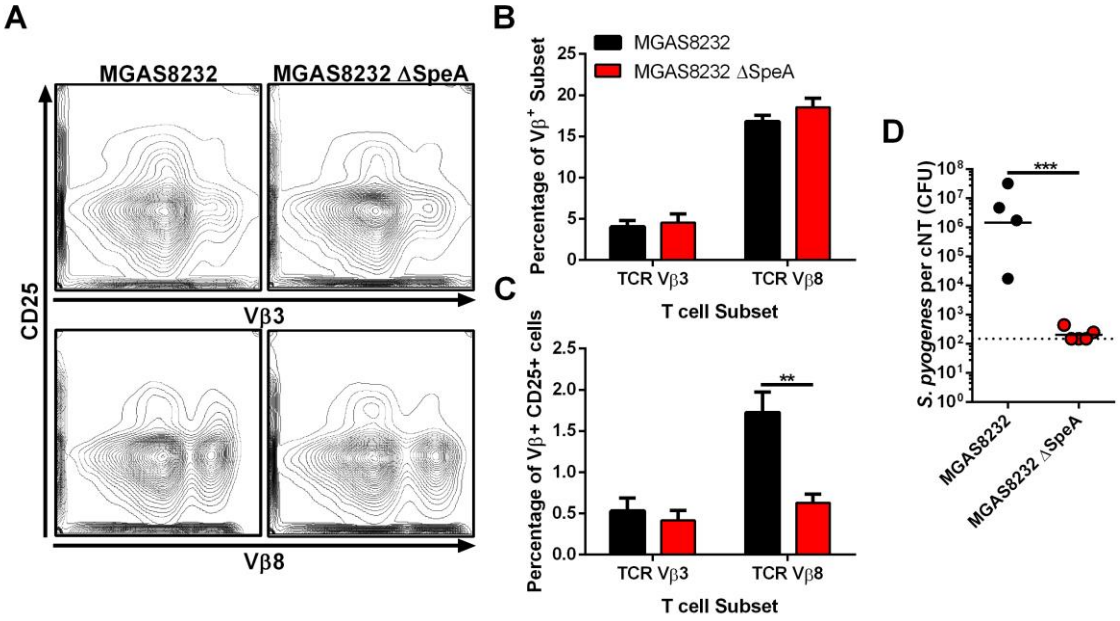
A
MGAS8232
MGAS8232 ΔSpeA
CD25
Vβ3
Vβ8
B
MGAS8232
MGAS8232 ΔSpeA
Percentage of Vβ+ Subset
TCR Vβ3
TCR Vβ8
T cell Subset
C
Percentage of Vβ+ CD25+ cells
**
TCR Vβ3
TCR Vβ8
T cell Subset
D
S. pyogenes per cNT (CFU)
***
MGAS8232
MGAS8232 ΔSpeA

Figure 10. Passive immunization with hyper-immune anti-SpeA rabbit serum reduces the burden of *S. pyogenes* MGAS8232 in the nasopharynx.

A. Passive immunization schedule. **B.** Nasal challenge of HLA-DQ8 transgenic mice with 10^8 CFU *S. pyogenes* MGAS8232 after passive immunization with rabbit anti-SpeA or anti-SpeC serum. Data points represent CFU from the cNT of individual mice at 48 hours. Horizontal bars represent the mean. The horizontal dotted line indicates the theoretical limit of detection. **C.** Recombinant SAg (15% SDS-PAGE; top panel) and Western blot (bottom two panels). **D** and **E**. Serum IgG antibody titres determined using ELISA from HLA-DQ8 mice ($n \geq 4$) passively immunized with indicated treatment. Plates were coated with 100 µL of 10 µg mL^{-1} SpeA (**D**) or SpeC (**E**). Bars represent the mean ± SEM. Colours correspond throughout the figure as follows: α-SpeA, red; α-SpeC, yellow. Significance determined by unpaired Student's *t* test (*, $P < 0.05$; **, $P < 0.01$).

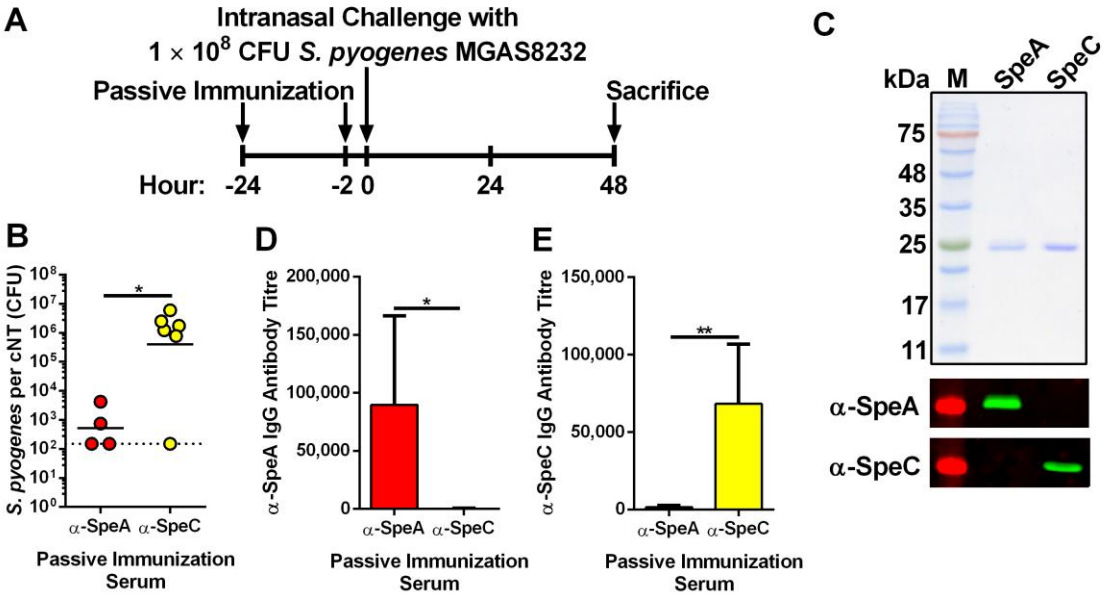
A
Intranasal Challenge with
1 × 10^8 CFU S. pyogenes MGAS8232
Passive Immunization
Sacrifice
Hour: -24 -2 0 24 48
B
S. pyogenes per cNT (CFU)
*
α-SpeA α-SpeC
Passive Immunization Serum
D
α-SpeA IgG Antibody Titre
200,000
150,000
100,000
50,000
0
*
α-SpeA α-SpeC
Passive Immunization Serum
E
α-SpeC IgG Antibody Titre
150,000
100,000
50,000
0
**
α-SpeA α-SpeC
Passive Immunization Serum
C
kDa M SpeA SpeC
75
48
35
25
17
11
α-SpeA
α-SpeC

3.6 Evaluation of differing SpeA concentrations for vaccine dosage

Since it was previously determined that SpeA was required for efficient murine nasopharyngeal infection by *S. pyogenes* MGAS8232 and that its activating potential could be detected *in vivo*, we decided to target this SAg for our vaccination studies. To determine an optimal concentration for SAg vaccination, three groups of HLA-DR4/DQ8 transgenic mice were administered different concentrations (100 ng, 1 µg or 10 µg) of SpeA with alum adjuvant. Mice received subcutaneous injections under isoflurane anesthetic on day 0, 14 and 28 with blood being drawn via saphenous vein on day 42 to assess antibody titres (**Figure 11A**). Weight was also monitored on day 0 prior to the first injection, and on day 7, 21 and 42 to determine if there was a detrimental effect on weight gain by wild-type SpeA injections. Mice were then infected with *S. pyogenes* MGAS8232, and the bacterial burden was assessed. The only vaccination dose to show a significant protective effect was 1 µg although there were trends at both the low and the high doses (**Figure 11B**). Interestingly, there was no statistical difference in anti-SpeA IgG titres either, however, an increased trend was noted in the 10 µg treatment group (**Figure 11C**). Consistent with the non-invasive nature of the model [449], *S. pyogenes* was below the limit of detection in the blood, spleen, kidneys, liver and heart (**Figure 12A-E**). Control lungs had two cases of *S. pyogenes* detection above the limit of detection, but these counts were not statistically different compared to any other treatment group (**Figure 12F**). All treatment group weights increased during the vaccine regimen, and there was no difference between groups (**Figure 12G**).

3.7 Wild-type superantigen vaccination protection stems from reduced and unresponsive T cell subsets

After it was concluded that 1 µg of SpeA was the optimal tested dose that reduced murine nasopharyngeal bacterial burden compared to our control group, this concentration was used for the remainder of our vaccine experimentation. The observation that significant antibody titres were not present in our protective SpeA dose (**Figure 11C**) made us consider an alternative explanation for this protective phenotype. SAgs are known to interact with both T cells and antigen presenting cells; however, their impact on T cells has been more rigorously studied. Thus, we sought to examine the effects of our wild-type

Figure 11. Assessing effective dose of SpeA superantigen vaccination.

A. Superantigen vaccination protocol. **B.** HLA-DR4/DQ8 transgenic mice were vaccinated with the SpeA at the indicated concentration and intranasally infected with 10^8 CFU *S. pyogenes* MGAS8232 for 48 hours post-vaccination. Data points represent CFU from the cNT of individual mice. Horizontal bars represent the mean. Horizontal dotted line indicates the theoretical limit of detection. **C.** Serum was collected 24 hours prior to infection and used to assess antibody titre using ELISA ($n \geq 4$). Data represented as the mean ± SEM. Significance determined by one-way ANOVA with Dunnett's post-hoc test (*, $P < 0.05$).

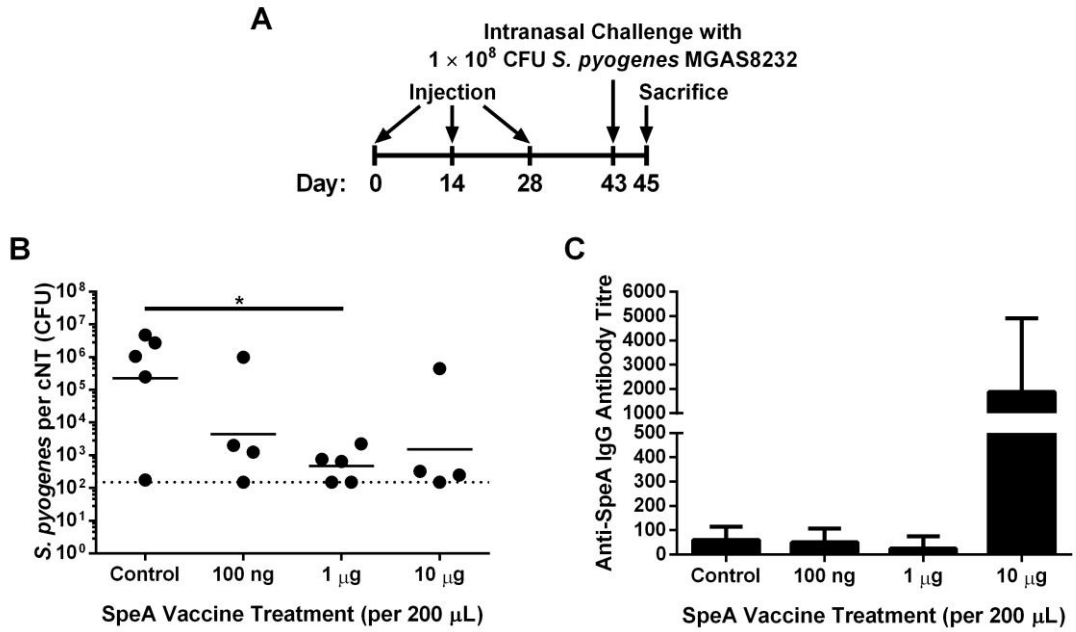
A
Intranasal Challenge with
1 × 10^8 CFU S. pyogenes MGAS8232
Injection
Sacrifice
Day: 0 14 28 43 45
B
S. pyogenes per cNT (CFU)
*
Control
100 ng
1 μg
10 μg
SpeA Vaccine Treatment (per 200 μL)
C
Anti-SpeA IgG Antibody Titre
Control
100 ng
1 μg
10 μg
SpeA Vaccine Treatment (per 200 μL)

Figure 12. Nasopharyngeal infection by *S. pyogenes* MGAS8232 is not invasive and vaccination with SpeA does not alter weight gain.

A – F. HLA-DR4/DQ8 transgenic mice were vaccinated three times over a 28-day period and infected two weeks post-vaccination with 10^8 CFU of *S. pyogenes* MGAS8232. Mice were sacrificed 48 hours post-infection and indicated organs were removed, homogenized and plated to assess bacterial burden. Data points represent CFU indicated organs of individual mice. Horizontal bars represent the mean. Horizontal dotted line indicates the theoretical limit of detection. A one-way ANOVA with Dunnett's post-hoc test was used to evaluate significance. **G.** Mice ($n \geq 4$) were weighed on indicated days to assess impact of SAg vaccination. Data represented as the mean ± SEM. Significance was assessed using a two-way ANOVA with Dunnett's post-hoc test.

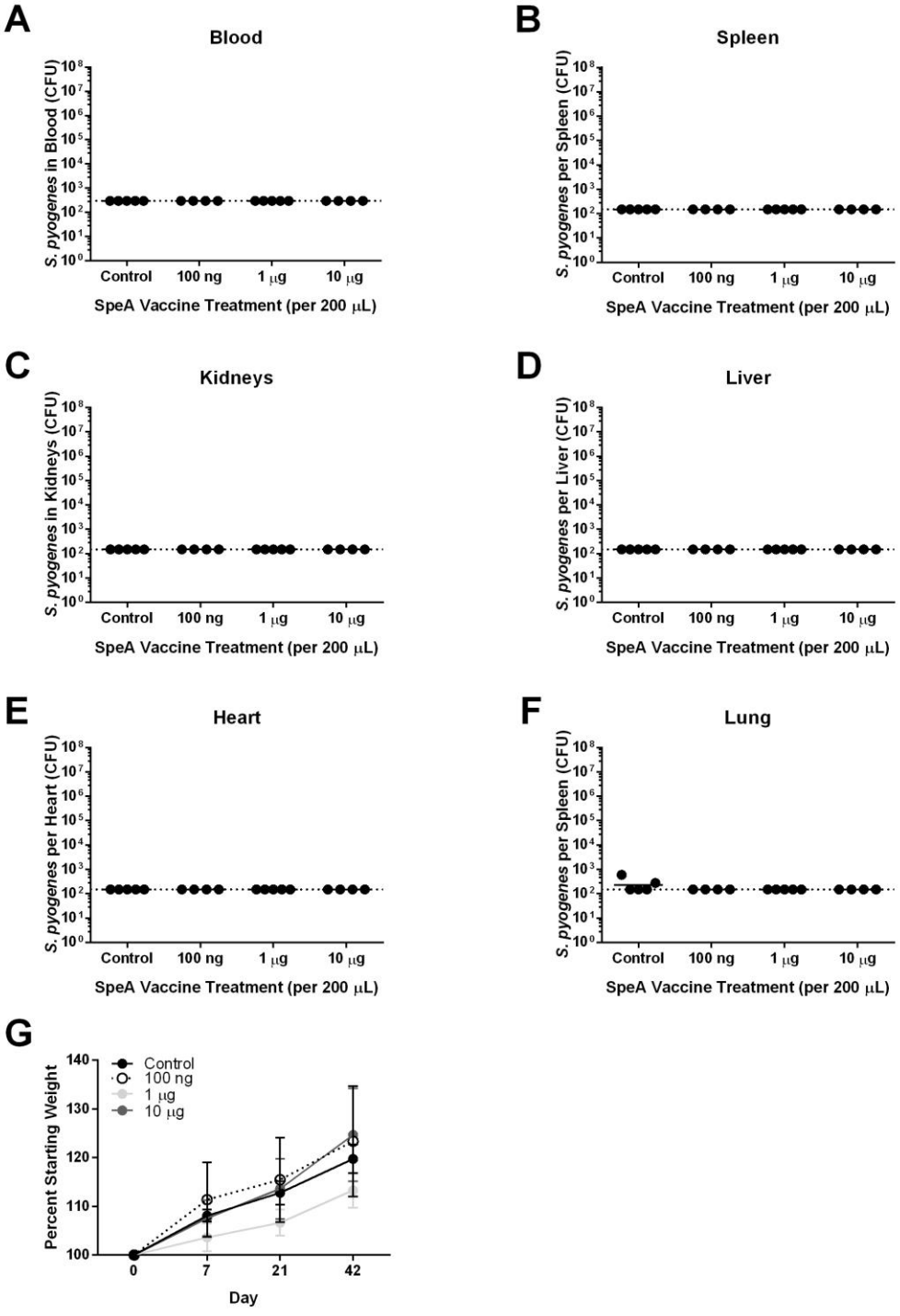
A
Blood
S. pyogenes in Blood (CFU)
Control
100 ng
1 μg
10 μg
SpeA Vaccine Treatment (per 200 μL)
B
Spleen
S. pyogenes per Spleen (CFU)
C
Kidneys
S. pyogenes in Kidneys (CFU)
D
Liver
S. pyogenes per Liver (CFU)
E
Heart
S. pyogenes per Heart (CFU)
F
Lung
S. pyogenes per Spleen (CFU)
G
Percent Starting Weight
Day

SpeA vaccine treatment on Vβ8$^+$ T cells known to be targeted by SpeA. Two additional SAg controls were included in these analyses. Staphylococcal enterotoxin B (SEB) is a SAg that is produced by *S. aureus,* and also primarily targets Vβ8$^+$ T cells. SpeC is a streptococcal SAg that is unable to activate murine T cells due to an inability to interact with murine TCRs [464] and was thus used as a negative control. SEB and SpeC were purified (**Figure 13A**) and their ability to stimulate transgenic HLA-DR4/DQ8 mouse splenocytes was assessed. It was confirmed that SEB has similar stimulation potential to SpeA, and SpeC had no stimulation potential at the highest concentration tested (**Figure 13B**).

Following the above mentioned vaccination protocol in our transgenic HLA-DR4/DQ8 mice, *S. pyogenes* MGAS8232 nasopharyngeal bacterial burden was assessed. Mice treated with either SpeA or SEB wild-type SAgs had significantly reduced bacterial loads compared to both control groups (**Figure 13C**). In order to exclude the possibility of antibody-mediated protection, anti-SpeA IgG titres were assessed across all groups and it was shown no treatment generated titres above our saline/alum adjuvant control (**Figure 13D**). Splenocytes from the above mentioned groups were analyzed by flow cytometry to assess the impact of SAg vaccination on specific TCR Vβ subsets. CD3$^+$ TCR Vβ8$^+$ and TCR Vβ3$^+$ (internal control) T cells subsets were compared between groups. There was a relative decrease of detectable TCR Vβ8$^+$ T cells in SpeA and SEB treated mice compared to control treated mice, but no difference in TCR Vβ3$^+$ T cells (**Figure 14A** and **B**). T cell responsiveness was also tested by SAg stimulation of vaccinated mouse splenocytes. Splenocytes from control-, SpeA- and SEB-vaccinated mice were processed and re-stimulated with either TCR Vβ8$^+$ targeting SAgs (SpeA and SEB) or streptococcal mitogenic exotoxin Z (SmeZ), a SAg that targets TCR Vβ11$^+$ T cells (an unaffected T cell subset) that was used as an internal control. Mice treated with either TCR Vβ8$^+$-targeting SAg had an impaired ability to be stimulated by TCR Vβ8$^+$-targeting SAgs compared to control-treated mice (**Figure 14C** and **D**). All groups were able to be stimulated by TCR Vβ11$^+$-targeting SAg SmeZ; however, SpeA and SEB treated mice seemed to respond better to this SAg (**Figure 14E**). This data suggests that wild-type SpeA- and SEB-vaccinated mice had impaired TCR Vβ8$^+$ T cells, but other subsets (i.e. Vβ11) remained responsive. This impairment also correlated with *in vivo* protection from *S. pyogenes*

Figure 13. Vaccination with wild-type TCR Vβ8-targeting superantigens is protective against nasopharyngeal infection by *S. pyogenes* MGAS8232 but does not appear to be antibody mediated.

A. Purified SAgs visualized using 12% SDS-PAGE. **B.** Activation assay measuring the ability of purified SAgs to stimulate HLA-DR4/DQ8 murine splenocytes as determined by IL-2 production. Data represented as the mean ± SEM of triplicate values from a single mouse. **C.** HLA-DR4/DQ8 mice were vaccinated with either a saline control and adjuvant or the indicated SAgs as previously described. Mice were intranasally infected with 10^8 CFU of *S. pyogenes* MGAS8232 and sacrificed 48 hours later. Data points represent CFU from the cNT of individual mice. Horizontal bars represent the mean. Horizontal dotted line indicates the theoretical limit of detection. **D.** Serum was collected 24 hours prior to infection and used to assess antibody titre using ELISA ($n \geq 4$). SpeA cNT and serum IgG levels are the same as those reported in Figure 11 for mice vaccinated with 1 µg of SpeA. Colours correspond to: control, black; SpeA, red; SEB, blue and SpeC, yellow. Data represented as the mean ± SEM. Significance determined by one-way ANOVA with Dunnett's post-hoc test (***, $P < 0.001$).

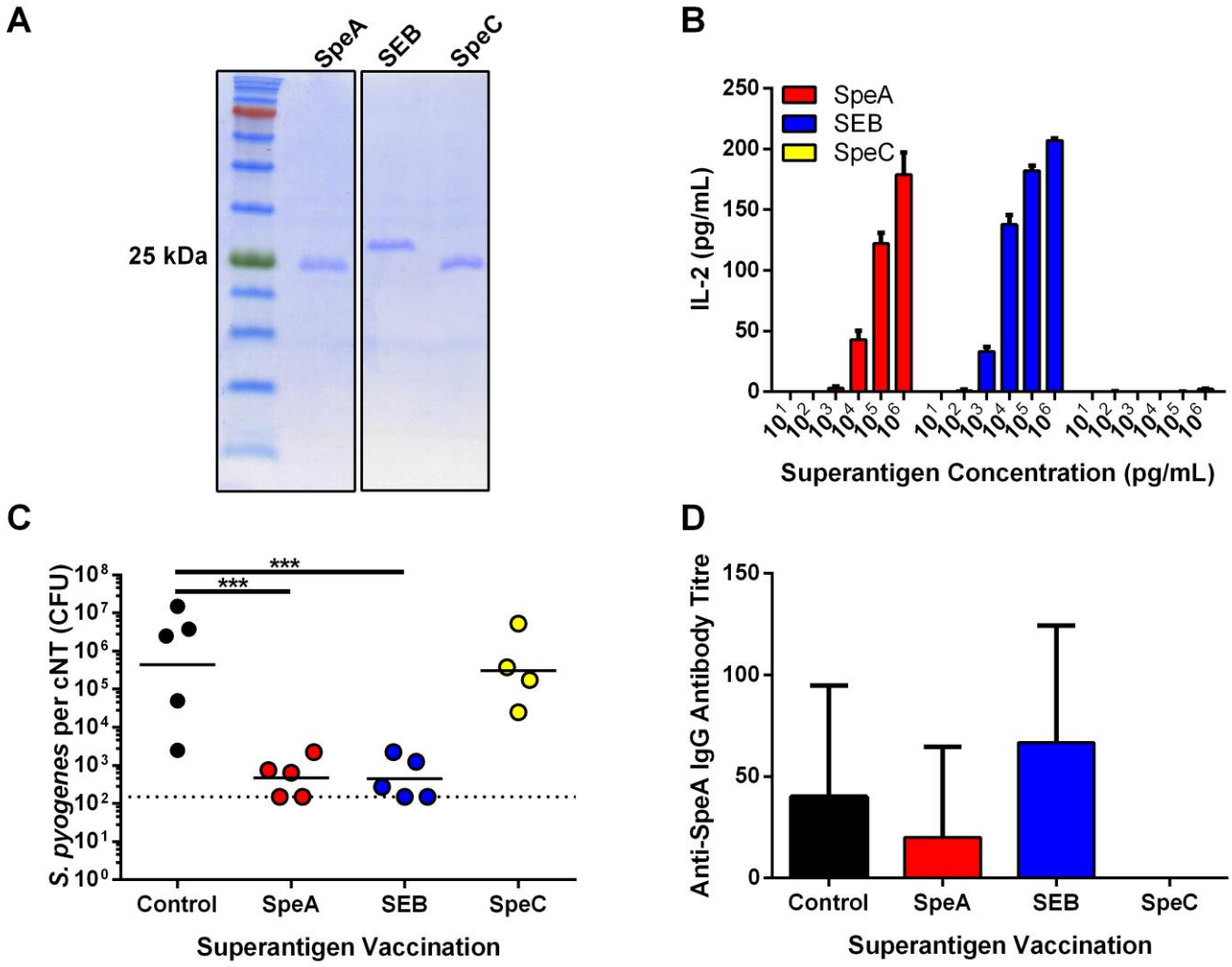
A
SpeA
SEB
SpeC
25 kDa
B
SpeA
SEB
SpeC
IL-2 (pg/mL)
Superantigen Concentration (pg/mL)
C
S. pyogenes per cNT (CFU)
***
***
Control
SpeA
SEB
SpeC
Superantigen Vaccination
D
Anti-SpeA IgG Antibody Titre
Control
SpeA
SEB
SpeC
Superantigen Vaccination

Figure 14. SpeA- and SEB-vaccinated mice have impaired Vβ8+ T cells.

A and **B**. Flow cytometric analysis of splenocytes at day 43 post-SAg vaccination (n = 4 for each group). **A**. Representative flow plots for each treatment group stained for CD3 (APC) and either Vβ3 or Vβ8 (FITC). Staining of Vβ3 and Vβ8 are from the same mouse. Each sample was first gated on lymphocyte population based on FSC and SSC before gating on $CD3^+$ $V\beta^+$ population. **B.** Percentage of $CD3^+$ $V\beta3^+$ or $CD3^+$ $V\beta8^+$ T cell subset for each treatment group (control, black; SpeA, red; SEB, blue). Data are shown as mean ± SEM. Significance determined by two-way ANOVA with Dunnett's multiple comparison post-hoc test (*, $P < 0.05$; ***, $P < 0.001$).**C – E.** HLA-DR4/DQ8 mouse splenocyte IL-2 activation assay post vaccination with control (●), SpeA (▲) or SEB (▼) (n = 3 for each group). Treated mouse splenocytes were stimulated with increasing concentrations of SAgs targeting specific TCR Vβ subsets (**C**) SpeA, Vβ8; (**D**) SEB, Vβ8; (**E**) SmeZ, Vβ11. Stimulation occurred for 18 hours and culture supernatants were analyzed for IL-2 using ELISA as a readout for T cell activation. Data is shown as the mean ± SEM of triplicate values from each mouse.

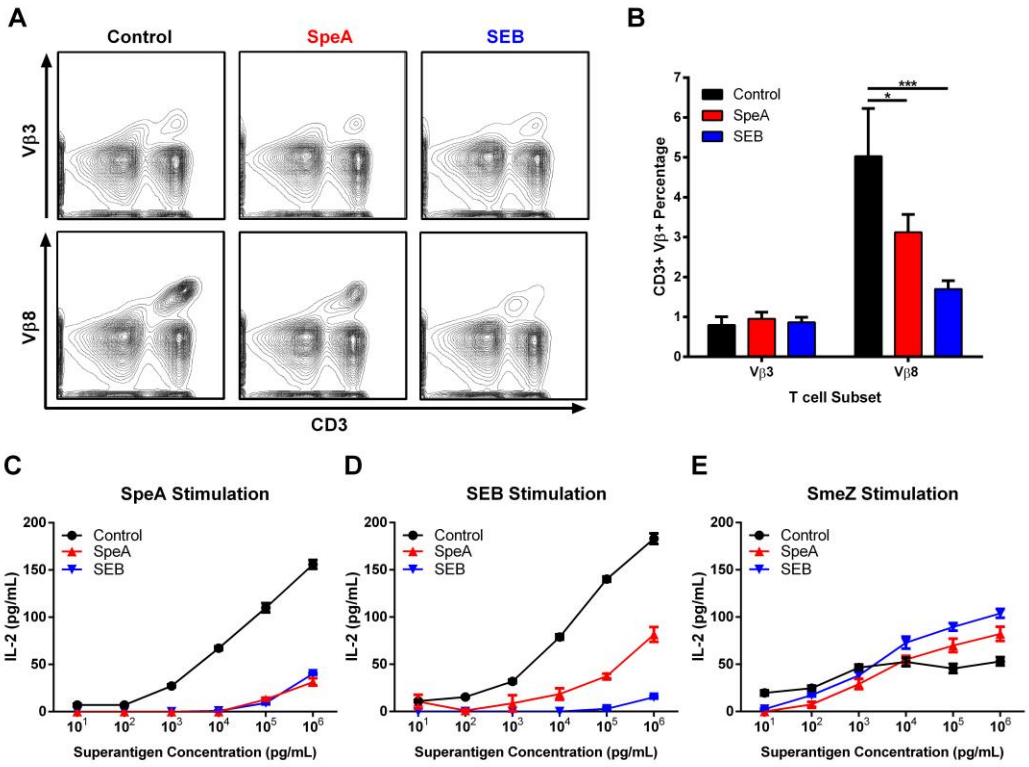
A
Control
SpeA
SEB
Vβ3
Vβ8
CD3
B
Control
SpeA
SEB
***
*
CD3+ Vβ+ Percentage
Vβ3
Vβ8
T cell Subset
C
SpeA Stimulation
D
SEB Stimulation
E
SmeZ Stimulation
IL-2 (pg/mL)
Superantigen Concentration (pg/mL)

nasopharyngeal infection indicating that wild-type vaccine protection likely stems from rendering specific SAg-targeted T cell subsets unresponsive.

3.8 Superantigen toxoid vaccination can induce protective antibodies *in vivo*

3.8.1 Vaccination with $SpeA_{Y100A}$ elicits a protective but bimodal phenotype

Discovery that passive immunization with anti-SAg antibodies could reduce *S. pyogenes* bacterial load in a murine nasopharyngeal infection model prompted us to test whether vaccination with SAgs could generate protective antibodies. However, vaccination with wild-type SpeA did not generate significant anti-SAg antibodies (**Figure 13D**) whereas protection from this vaccination procedure stemmed from rendering a specific T cell subset unresponsiveness (**Figure 14**), indicating that an alternative approach must be taken to generate protective anti-SAg antibodies. To assess whether attenuated SAgs would be able to generate antibodies upon vaccination, a previously generated SpeA variant with a mutated MHC II interface – $SpeA_{Y100A}$ – [454] was used. It was first shown that $SpeA_{Y100A}$ had reduced capacity to activate HLA-DR4/DQ8 murine splenocytes (as determined through IL-2 production) compared to its wild-type counterpart (**Figure 15A**). Next, transgenic HLA-DR4/DQ8 mice vaccinated with $SpeA_{Y100A}$ had significantly reduced bacterial load in their nasopharynx when infected with *S. pyogenes* MGAS8232 (**Figure 15B**). Upon assessment of antibody titres, it was discovered that despite the protective effects in mice, only a fraction (3/5) elicited a high anti-SpeA IgG antibody response (**Figure 15C**). Flow cytometric analysis of $SpeA_{Y100A}$-vaccinated mouse splenocytes indicated that there was no reduction of $V\beta8^+$ T cells compared to control-vaccinated mice (**Figure 15D**). However, we were able to show, using our previously described T cell responsiveness assay (**Figure 14C-E**), that in circumstances where vaccination with $SpeA_{Y100A}$ resulted in minimal anti-SpeA antibodies production (**Figure 16A**), $V\beta8^+$ T cells were poorly responsive, similar to what was shown with wild-type SpeA-vaccinated mice (**Figure 16B** and **C**). In contract, $SpeA_{Y100A}$-vaccinated mice that generated high anti-SpeA antibody titres had more responsive $V\beta8^+$ T cells similar to control-vaccinated mice (**Figure 16B** and **C**). Both low and high anti-SpeA antibody producing mouse splenocytes had similar responsiveness to the TCR $V\beta11^+$-targeting SAg SmeZ (**Figure 16D**) which was used as an internal control to indicate that irrelevant TCR Vβ subsets were not

Figure 15. Vaccination with either SpeA$_{Y100A}$ or SpeA$_{HEXA}$ does not yield consistent antibody-mediated protection.

A. Activation assay measuring ability of wild-type or toxoid SAg to stimulate HLA-DR4/DQ8 murine splenocytes as determined by IL-2 production. Data represented as the mean ± SEM of triplicate values from a single mouse. **B.** HLA-DR4/DQ8 mice were vaccinated with either a saline control or the indicated SAg toxoid. Mice were intranasally infected with 10^8 CFU of *S. pyogenes* MGAS8232 and sacrificed 48 hours later. Data points represent CFU from the cNT of individual mice. Horizontal bars represent the mean. Horizontal dotted line indicates limit of detection. **C.** Serum was collected 24 hours prior to infection and used to assess IgG antibody titres using ELISA ($n \geq 5$). Data represented as the mean ± SEM. Significance determined by one-way ANOVA with Dunnett's post-hoc test (*, $P < 0.05$; **, $P < 0.01$). **D.** Flow cytometric analysis of splenocytes at day 43 post-SAg vaccination ($n \geq 3$ for each group). Treatment groups were stained for CD3 (APC) and either Vβ3 or Vβ8 (FITC). Each sample was first gated on live lymphocyte population based on FSC and SSC before gating on $CD3^+$ $V\beta^+$ population. Data represents percentage of $CD3^+$ $V\beta3^+$ or $CD3^+$ $V\beta8^+$ T cell subset for each treatment group. Data are shown as mean ± SEM. Control Vβ percentage data is replicated from Figure 14B. Statistical significance was assessed by two-way ANOVA with Dunnett's multiple comparison post-hoc test.

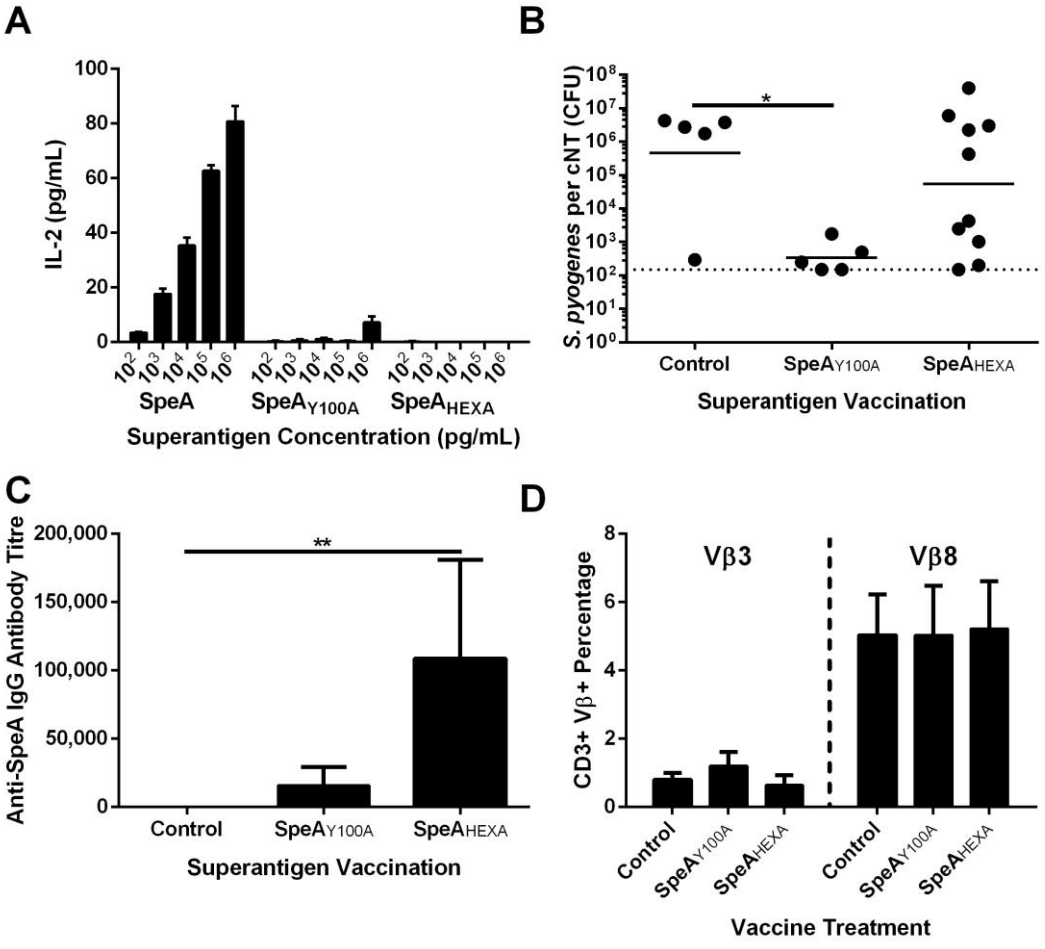
A
IL-2 (pg/mL)
100
80
60
40
20
0
10^2 10^3 10^4 10^5 10^6
SpeA
SpeA$_{Y100A}$
SpeA$_{HEXA}$
Superantigen Concentration (pg/mL)
B
S. pyogenes per cNT (CFU)
10^8 10^7 10^6 10^5 10^4 10^3 10^2 10^1 10^0
*
Control
SpeA$_{Y100A}$
SpeA$_{HEXA}$
Superantigen Vaccination
C
Anti-SpeA IgG Antibody Titre
200,000
150,000
100,000
50,000
0
**
Control
SpeA$_{Y100A}$
SpeA$_{HEXA}$
Superantigen Vaccination
D
CD3+ Vβ+ Percentage
8
6
4
2
0
Vβ3
Vβ8
Control
SpeA$_{Y100A}$
SpeA$_{HEXA}$
Control
SpeA$_{Y100A}$
SpeA$_{HEXA}$
Vaccine Treatment

Figure 16. SpeA$_{Y100A}$ vaccination elicits a bimodal antibody phenotype.

A. Two HLA-DR4/DQ8 mice were vaccinated with SpeA$_{Y100A}$ and antibody titre against wild-type SpeA was determined by ELISA. **B – D**. The SpeA$_{Y100A}$-vaccinated HLA-DR4/DQ8 mouse splenocytes were stimulated separately with increasing concentrations of two TCR Vβ8^{+}-targeting SAgs, SpeA (**B**) and SEB (**C**), and a TCR Vβ11^{+}-targeting SAg, SmeZ (**D**), as an internal control. Incubation occurred for 18 hours and IL-2 was measured from splenocyte culture supernatants as a marker for T cell activation. For comparison purposes, control (●) and SpeA (●) curves were added from Figure 14C-E. The SpeA$_{Y100A}$-vaccinated mice with low antibody titre (■) and with high antibody titre (▲) were assessed for their ability to respond to exogenous SAgs (n = 1 repeated in triplicate for each group). Data is shown as the mean.

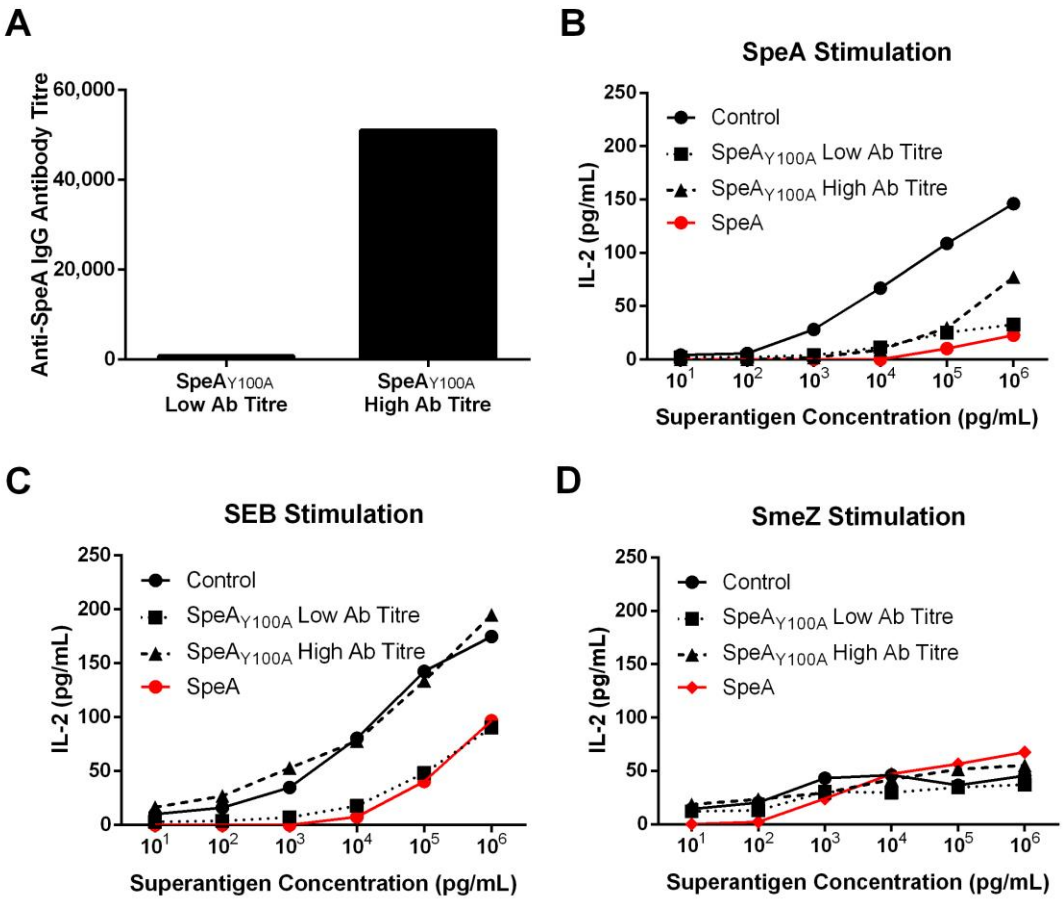
A
Anti-SpeA IgG Antibody Titre
60,000
40,000
20,000
0
SpeAY100A Low Ab Titre
SpeAY100A High Ab Titre
B
SpeA Stimulation
IL-2 (pg/mL)
250
200
150
100
50
0
Control
SpeAY100A Low Ab Titre
SpeAY100A High Ab Titre
SpeA
10^1 10^2 10^3 10^4 10^5 10^6
Superantigen Concentration (pg/mL)
C
SEB Stimulation
IL-2 (pg/mL)
Control
SpeAY100A Low Ab Titre
SpeAY100A High Ab Titre
SpeA
Superantigen Concentration (pg/mL)
D
SmeZ Stimulation
IL-2 (pg/mL)
Control
SpeAY100A Low Ab Titre
SpeAY100A High Ab Titre
SpeA
Superantigen Concentration (pg/mL)

impacted by the vaccination protocol. This data suggests that vaccination with $SpeA_{Y100A}$ can result in two protective phenotypes: a low anti-SpeA antibody titre with unresponsive TCR $V\beta8^+$ T cells that protects similarly to wild-type SpeA vaccination, or a high anti-SpeA antibody titres where T cell subsets are responsive and protection is antibody-mediated.

3.8.2 $SpeA_{HEXA}$ induces high antibody titres but is not consistently protective

Our previous finding that $SpeA_{Y100A}$ was still able to impair T cell responsiveness led us to attempt vaccination with a further attenuated SpeA variant. It was previously shown that a SpeA toxoid with six amino acid substitutions – $SpeA_{HEXA}$ – was protective in a rabbit model of STSS [437]. We sought to determine if vaccination with this molecule would be protective in our streptococcal murine nasopharyngeal infection model. $SpeA_{HEXA}$ was unable to activate HLA-DR4/DQ8 transgenic murine splenocytes at even the highest concentration tested (**Figure 15A**). Upon vaccination, only 50% of mice had reduced bacteria load in the cNT (**Figure 15B**), despite all mice having consistently high anti-SpeA antibody titres (**Figure 15C**). Assessment of T cell subsets using flow cytometry revealed no differences in $V\beta3^+$ or $V\beta8^+$ T cell subsets compared to control-vaccinated mice (**Figure 15D**). This data demonstrates that the six amino acid substitutions of $SpeA_{HEXA}$ render it unable to activate T cells and consistently generate high anti-SpeA antibody titres *in vivo*; however, the antibodies generated were not reliably protective in our model of *S. pyogenes* nasopharyngeal infection.

3.8.3 $SpeA_{TRI}$ generates high antibody titres and is consistently protective

Due to the bimodal protection phenotype of $SpeA_{Y100A}$ and the ~50% efficacy of $SpeA_{HEXA}$ when used as a vaccine, a minimalistic approach was taken to generating an inactive SpeA toxoid that contained as few amino acid substitutions as possible and provided consistent protection and high antibody titres. Previous data has shown that the asparagine at position 20 is crucial for SpeA interacting with the TCR [437,462], and the leucine residues at positions 41 and 42 have been previously shown to be important for interaction with MHC II [437,439]. These residues were thus mutated to alanine using primer-based site-directed mutagenesis both separately and in tandem to generate four new mutants. $SpeA_{N20A}$,

$SpeA_{N20A/Y100A}$, $SpeA_{TRI}$ (L41A/L42A/Y100A) and $SpeA_{TETRA}$ (N20A/L41A/L42A/Y100A) each were shown to have drastically reduced capacity to activate murine splenocytes compared to wild-type SpeA (**Figure 17A**). Each of these mutants was then tested in our vaccination regimen to assess protection from *S. pyogenes* nasopharyngeal challenge (**Figure 17B**) and antibody titres (**Figure 17C** and **D**). Interestingly, despite all mutants having reduced superantigenic activity, only $SpeA_{TRI}$ generated both consistent protection and high anti-SpeA IgG antibody titres. $SpeA_{N20A}$ failed to both protect mice or generate an anti-SpeA antibody response. $SpeA_{N20A/Y100A}$ had ~50% protection rate and a variable anti-SpeA IgG profile. The mice that were protected from infection by $SpeA_{N20A/Y100A}$ vaccination were shown to have a higher anti-SpeA IgG titre, whereas mice with higher bacterial load had low anti-SpeA antibody titres. These data suggest that when this $SpeA_{N20A/Y100A}$ vaccination does yield high anti-SpeA antibody titres, the mice are protected (**Appendix 3**). Vaccination with $SpeA_{TETRA}$, which contains all of the mutations of $SpeA_{TRI}$ in addition to N20A, trended to produce enhanced, but not significantly higher anti-SpeA IgG antibody titres (**Figure 17C**) with inconsistent protection (5/8) (**Figure 17B**). In conclusion, the most successful toxoid that consistently generated high anti-SAg antibody titres was $SpeA_{TRI}$ that had amino acid substitutions only within the MHC II binding interface.

3.9 Depletion of $CD4^+$ and $CD8^+$ T cells reduce *S. pyogenes* burden

Our finding that vaccination with wild-type SpeA and SEB generated unresponsive T cell subsets that ultimately led to protection in these mice led us to assess whether these cells were required for infection establishment by *S. pyogenes*. To determine this, we sought to deplete specific T cell subsets using a previously published depletion strategy [458] (**Figure 18A**) and subsequently assess the impact on nasopharyngeal infection. To confirm the depletion potential of these antibodies, transgenic HLA-DQ8 mice were administered three doses of T cell-depleting antibody, or isotype control, and cervical lymph nodes were subjected to flow cytometry to assess T cell subset abundance. Lymphocytes were gated using forward and side scatter, and $CD4^+$ and $CD8^+$ T cell subsets were analyzed (**Figure 18B**). Compared to the isotype control, administration of T cell-depleting antibodies

Figure 17. Further mutations within the MHC II binding interface of SpeA generates high IgG antibody titres and is protective.

A. Activation assay measuring ability of wild-type or toxoid SAgs to stimulate HLA-DR4/DQ8 murine splenocytes as determined by IL-2 production. Data represented as the mean ± SEM of triplicate values from a single mouse. **B.** HLA-DR4/DQ8 mice were vaccinated with a saline control or the indicated SpeA toxoid as previously described. Mice were intranasally infected with 10^8 CFU of *S. pyogenes* MGAS8232 and sacrificed 48 hours later. Data points represent CFU from the cNT of individual mice. Horizontal bars represent the mean. Horizontal dotted line indicates the theoretical limit of detection. **C.** Serum was collected 24 hours prior to infection and used to assess IgG antibody titres using ELISA ($n \geq 3$). Data is represented as the mean ± SEM. Significance determined by one-way ANOVA with Dunnett's post-hoc test (*, $P < 0.05$; **, $P < 0.01$). SpeA IL-2 activation assay (Figure 15), cNT and IgG (Figure 11; designated 1 µg therein) are repeated values**;** IL-2 activation assay, cNT and Ig data for control, $SpeA_{Y100A}$ and $SpeA_{HEXA}$ data are repeated from Figure 15.

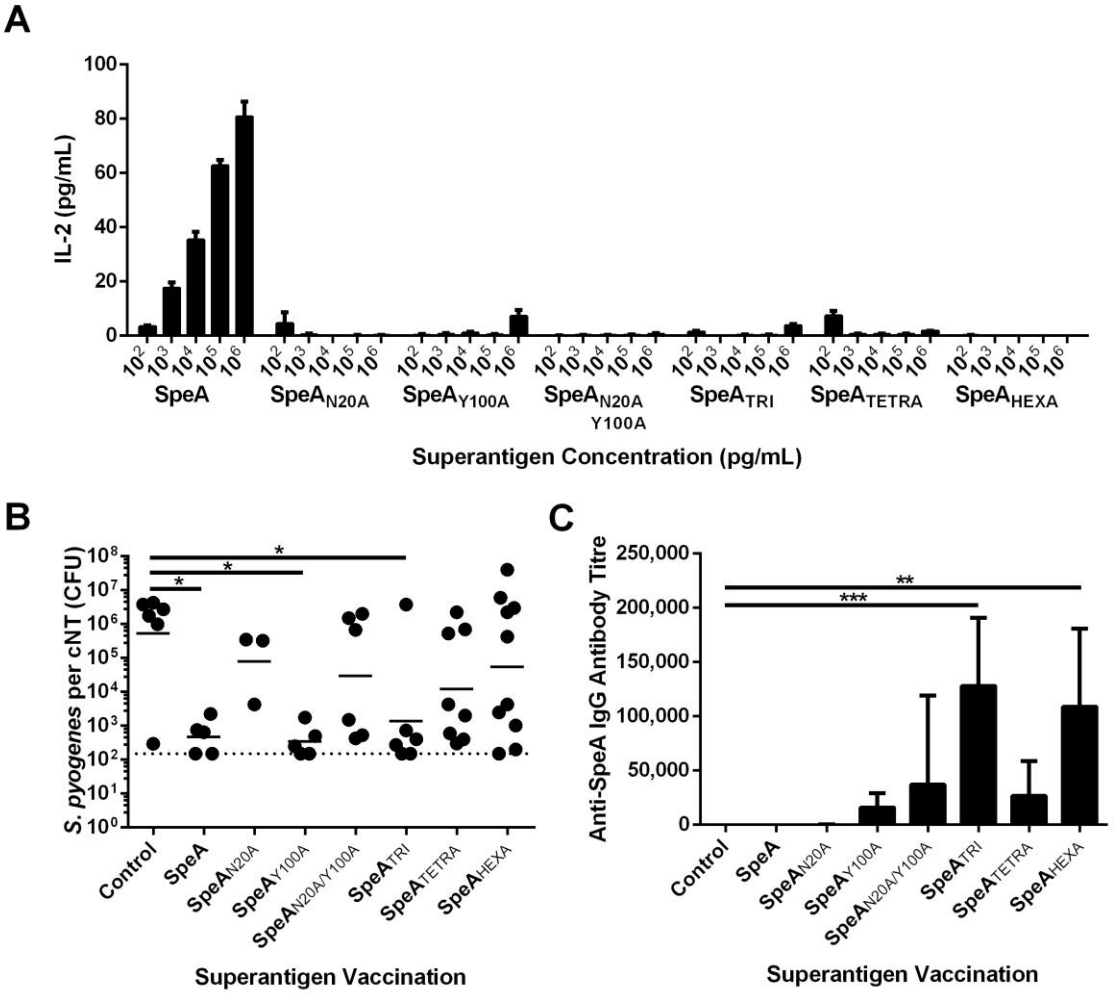
A
IL-2 (pg/mL)
100
80
60
40
20
0
SpeA
SpeA N20A
SpeA Y100A
SpeA N20A Y100A
SpeA TRI
SpeA TETRA
SpeA HEXA
Superantigen Concentration (pg/mL)
B
S. pyogenes per cNT (CFU)
Control
SpeA
SpeA N20A
SpeA Y100A
SpeA N20A/Y100A
SpeA TRI
SpeA TETRA
SpeA HEXA
Superantigen Vaccination
C
Anti-SpeA IgG Antibody Titre
250,000
200,000
150,000
100,000
50,000
0
Superantigen Vaccination

Figure 18. Depletion of CD4+ and CD8+ T cells reduces *S. pyogenes* nasopharyngeal bacterial load.

A. T cell depletion protocol. **B** and **C.** Flow cytometric analysis of cervical lymph node populations at day 0 post T cell depletion (n = 3 per group). **B.** Representative flow plots for each treatment group stained for CD4 (APC-efluor 780) and CD8 (PE). Each sample had the lymphocytes first gated upon using FSC and SSC. **C.** Percentage of $CD4^+$ and $CD8^+$ cells to total lymphocyte population in both treatment groups. Data are shown as mean ± SEM. Significance determined by Student's t test (***, $P < 0.001$). **D.** Nasal challenge of transgenic mice expressing HLA-DQ8 with 10^8 CFU *S. pyogenes* MGAS8232 post-injection with indicated treatments. Data points represent CFU from the complete nasal turbinates (cNT) of individual mice 48 hours post-infection. Horizontal bars represent the mean. The horizontal dotted line indicates limit of detection. Significance determined by one-way ANOVA with Dunnett's multiple comparisons post-hoc test (*, $P < 0.05$; **, $P < 0.01$).

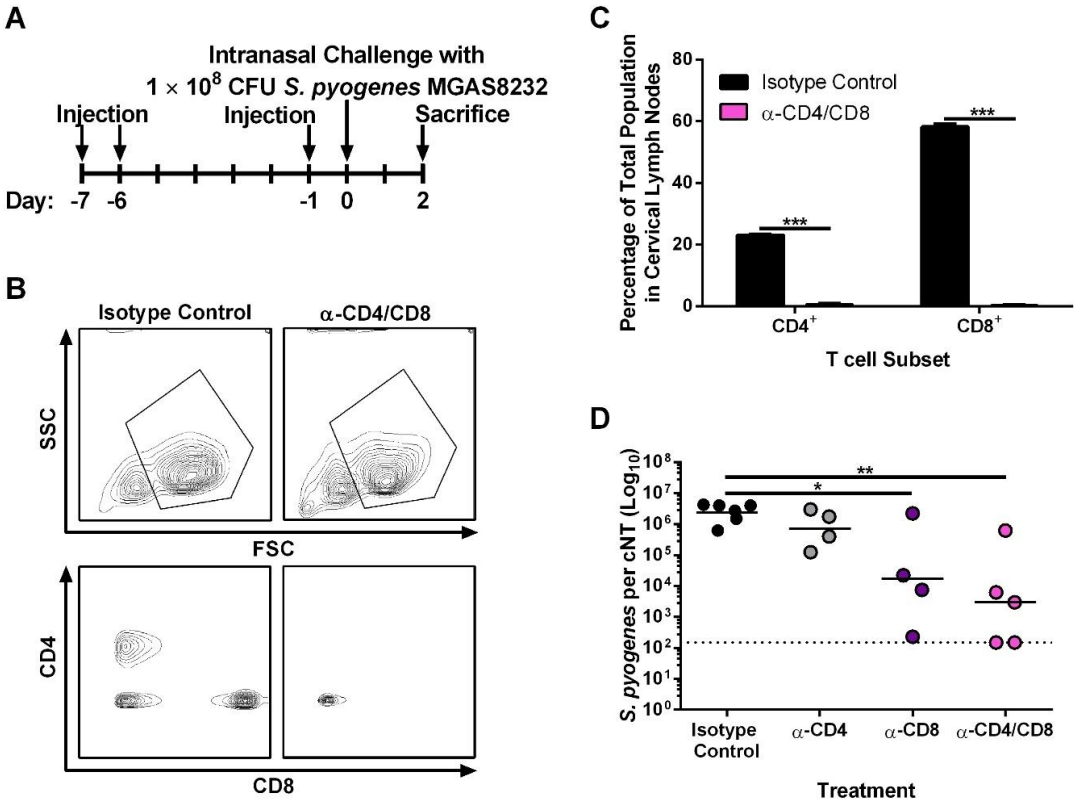
A
Intranasal Challenge with
1 × 10^8 CFU S. pyogenes MGAS8232
Injection
Injection
Sacrifice
Day: -7 -6 -1 0 2
B
Isotype Control
α-CD4/CD8
SSC
FSC
CD4
CD8
C
Percentage of Total Population in Cervical Lymph Nodes
Isotype Control
α-CD4/CD8
***
***
CD4+
CD8+
T cell Subset
D
S. pyogenes per cNT (Log10)
**
*
Isotype Control
α-CD4
α-CD8
α-CD4/CD8
Treatment

significantly reduced the $CD4^+$ and $CD8^+$ subsets (**Figure 18C**). Next, mice were again administered T cell-depleting antibodies as described above, but were infected with *S. pyogenes* MGAS8232 for 48 hours. Mice were then sacrificed and cNT bacterial load was assessed. Depletion of $CD8^+$ alone, but not $CD4^+$ T cells significantly reduced *S. pyogenes* nasopharyngeal bacterial load; however, the greatest reduction was observed upon depletion of both subsets (**Figure 18D**). These results support the requirement for $CD4^+$ and $CD8^+$ T cell subsets during *S. pyogenes* nasopharyngeal infection.

3.10 $CD4^+$ and $CD8^+$ T cell subset depletion has no impact on *S. pneumoniae* P1121 bacterial load

To determine whether the above-mentioned T cell depletion phenotype was specific to *S. pyogenes*, another human-specific nasopharyngeal colonizer – *Streptococcus pneumoniae* – was tested for its ability to infect T cell-depleted mice. We first assessed whether the ability of *S. pneumoniae* to infect the nasopharynx of mice was human MHC II-dependent. Both conventional C57Bl/6 and transgenic HLA-DR4/DQ8 mice were intranasally infected with *S. pneumoniae* P1121 and bacterial load in the cNT was evaluated. It was demonstrated that both strains of mice had high bacterial load 48 hours post-infection; however, HLA-DR4/DQ8 mice did have a statistically higher bacterial yield (**Figure 19A**). It was also shown that bacterial load was below the detectable limit in all but one lung sample (**Figure 19B**) and in the blood (**Figure 19C**). The cNT bacterial burden was also comparable to those seen in *S. pyogenes* infected HLA-DQ8 transgenic mice (**Figure 8A**). Next, the impact of T cell depletion was measured. HLA-DQ8 mice were treated with T cell depleting or isotype control antibodies as above, and mice were infected intranasally with *S. pneumoniae* P1121. T cell depletion had no impact on infection (**Figure 20A**). To ensure that the inoculation dose did not result in pneumonia or bacteremia, lung and blood samples were plated for bacterial enumeration. It was determined that only one T cell depleted mouse had bacteria above the detectable limit in the lungs but this was not significantly different compared with control mice (**Figure 20B**). There were no bacteria in the blood above the detectable limit (**Figure 20C**). This data supports the notion that the conventional T cell subset dependence phenotypes observed in *S. pyogenes* MGAS8232 are not common to all human upper respiratory tract-infecting organisms.

Figure 19. C57Bl/6 and HLA-DR4/DQ8 nasopharyngeal infection by *S. pneumoniae*. Conventional C57Bl/6 or HLA-DR4/DQ8 mice were intranasally infected with 10^7 CFU of *S. pneumoniae* P1121 for 48 hours. Mice were then sacrificed and cNT (**A**), lung (**B**) and blood (**C**) were extracted, processed and plated for bacterial enumeration. Data points represent CFU from indicated tissue of individual mice 48 hours post-infection. Horizontal bars represent the mean. The horizontal dotted line indicates limit of detection. Significance was determined by Student's *t* test (*, $P < 0.05$).

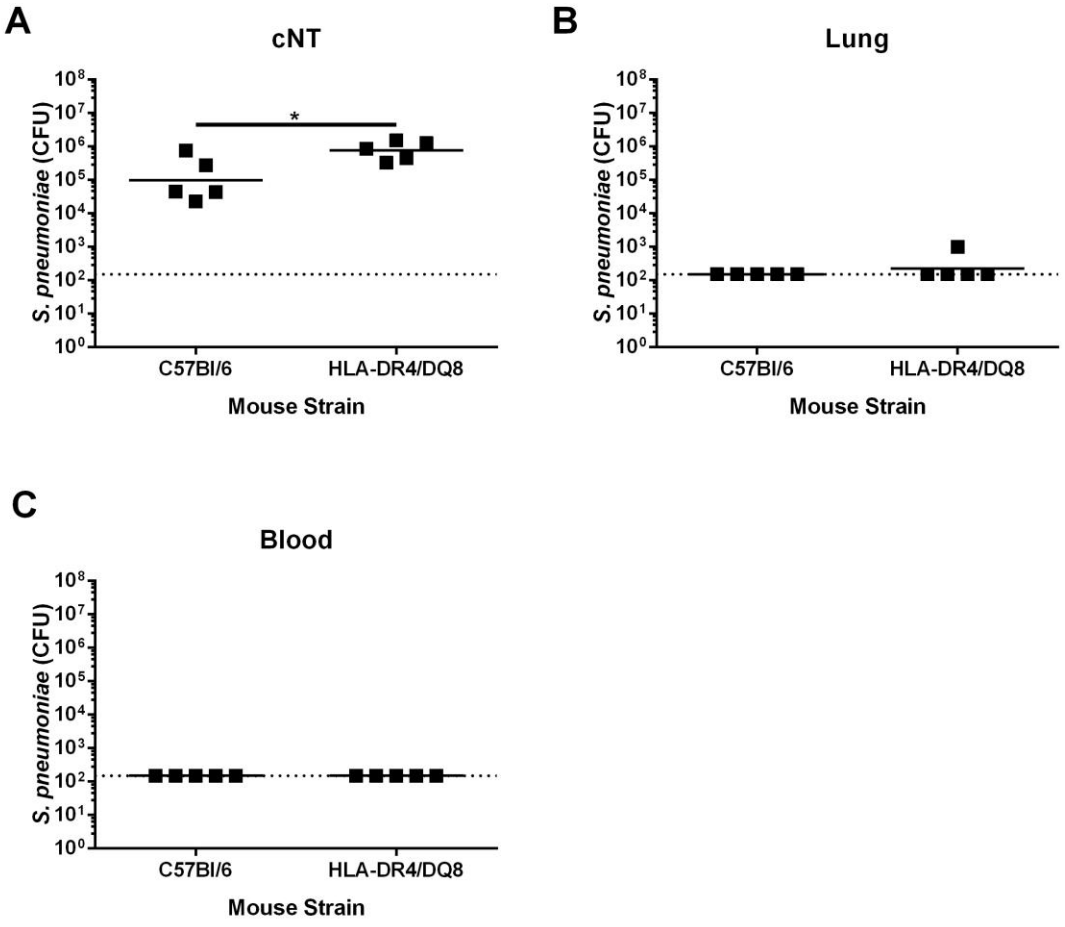
A
cNT
S. pneumoniae (CFU)
10^8
10^7
10^6
10^5
10^4
10^3
10^2
10^1
10^0
*
C57Bl/6
HLA-DR4/DQ8
Mouse Strain
B
Lung
S. pneumoniae (CFU)
C57Bl/6
HLA-DR4/DQ8
Mouse Strain
C
Blood
S. pneumoniae (CFU)
C57Bl/6
HLA-DR4/DQ8
Mouse Strain

Figure 20. Depletion of conventional T cells has no impact on *S. pneumoniae* nasopharyngeal infection.

HLA-DR4/DQ8 mice were treated with isotype control (black) or α-CD4 (GK1.5) and α-CD8 (YTS 169.4) depleting antibodies (pink) and intranasally infected with 10^7 CFU *S. pneumoniae* P1121. Mice were sacrificed 48 hours later and cNT (**A**), lung (**B**) and blood (**C**) were isolated, processed, and plated for bacterial enumeration. Data points represent CFU from indicated tissue of individual mice 48 hours post-infection. Horizontal bars represent the mean. The horizontal dotted line indicates the theoretical limit of detection. Statistical analysis was completed using Student's *t* test.

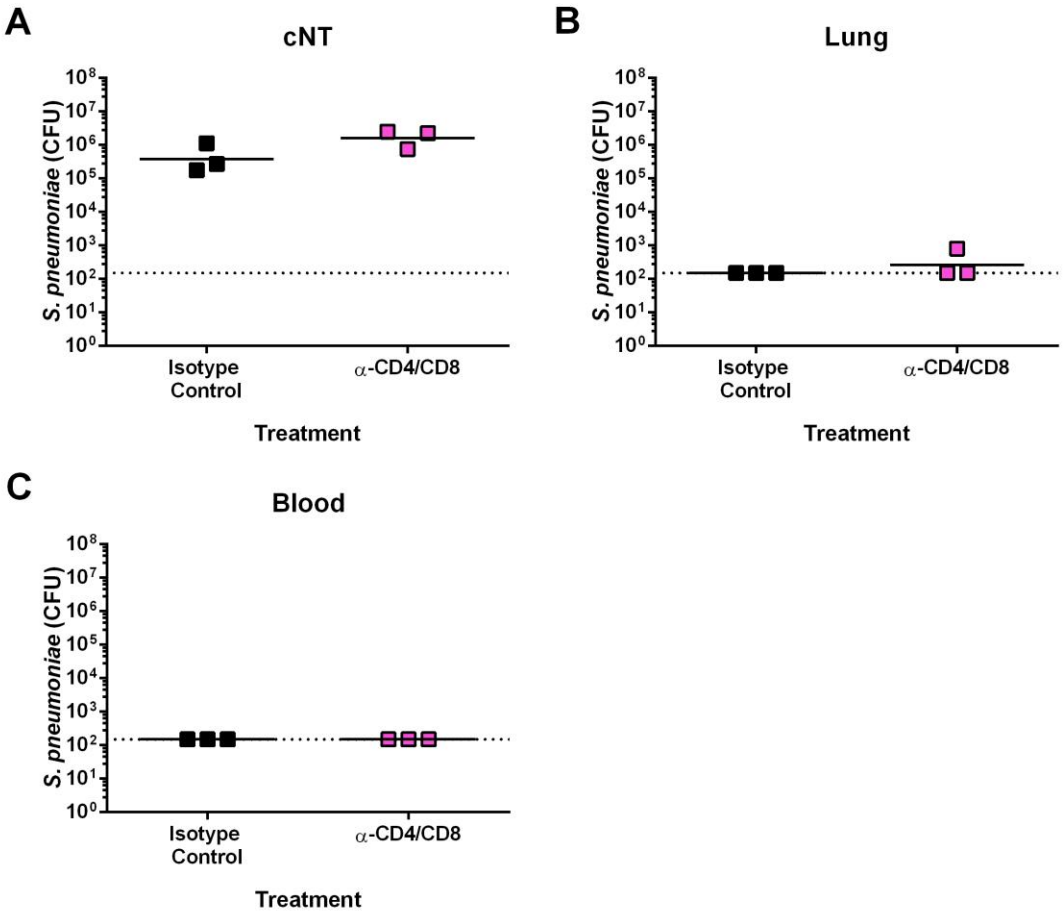
A
cNT
B
Lung
C
Blood
S. pneumoniae (CFU)
Isotype Control
α-CD4/CD8
Treatment

3.11 Responsive T cells are required for robust cytokine response during *S. pyogenes* nasopharyngeal infection

To assess the cytokine and chemokine environment during SAg-rendered unresponsiveness and T cell depletion followed by infection, supernatants from the cNT of treated and infected mice were analyzed by multiplex cytokine array to test for the presence of 32 cytokines. Statistical analyses were completed on individual cytokines within treatment and infection groups. Any cytokine that showed a significant difference within any of the treatment groups was included in the heat map for all groups. To compare the cytokines between groups, the heat map displays individual cytokine concentrations between all treatment groups which were normalized so that the highest concentration was 100% (**Figure 21**). Quantitative data is shown in **Appendix 4**. For *S. pyogenes* infections, the most robust cytokine response can be seen in the sham-vaccinated (saline plus alum adjuvant) or the isotype control (LTF-2) treated mice and includes: Th1-type cytokines (TNFα, IL-1β and IL-12 [p70]); Th2-type cytokines (IL-4); Th17-type cytokines (IL-6 and IL-17); chemokines (KC, IP-10, MCP-1, MIP-1α, MIP-1β, MIP-2 and LIF); and growth factors (G-CSF and M-CSF) (**Figure 21B** and **C**; **Appendix 4**). Conversely, mice with T cell subsets that were unresponsive to SpeA, either by wild-type SpeA or wild-type SEB vaccination, or treatment with CD4 (GK1.5) and CD8 (YTS 169.4) T cell-depleting antibodies (**Figure 21B** and **C**) had cytokine profiles similar to uninfected mice (**Figure 21A**). These results are in stark contrast to mice treated with isotype control or CD4 and CD8 T cell-depleting antibodies and infected with *S. pneumoniae* (**Figure 21D**). T cell depleted mice infected with *S. pneumoniae* demonstrated higher cytokine/chemokine responses compared to isotype control treated mice. These elevated molecules included: Th1-type cytokines (TNFα, IL-1α and IL-12 [p70]); Th2-type cytokines (IL-4); Th17-type cytokines (IL-6 and IL-17); and chemokines (KC, IP-10, MCP-1, MIG and LIF) (**Figure 21D**). There were also numerous cytokines that were either not different between any groups or did not conform to any obvious trends (**Appendix 4**). These results suggest that the presence of responsive T cells plays an important role in modulating the nasopharyngeal cytokine environment during *S. pyogenes* infections, which differs greatly from that during infection with *S. pneumoniae*.

Figure 21. Impact of superantigen-vaccination and T cell depletion on the murine nasopharyngeal cytokine microenvironment following infection by *S. pyogenes* MGAS8232.

HLA-expressing mice were either uninfected (**A**), vaccinated (**B**) or underwent T cell depleting antibody treatment (**C** and **D**) prior to infection with either 10^8 CFU of *S. pyogenes* MGAS8232 (**B** and **C**) or 10^7 *S. pneumoniae* P1121 (**D**) for 48 hours. Mice were sacrificed and supernatant from cNT homogenates were procured for cytokine and chemokine analysis. Data shown represents the mean cNT cytokine response that displayed significant differences within any group. Values for each individual cytokine were normalized to have the highest cytokine value as 100% ($n \geq 3$ mice per group). Corresponding quantitative data and statistical analyses are shown in **Appendix 4**.

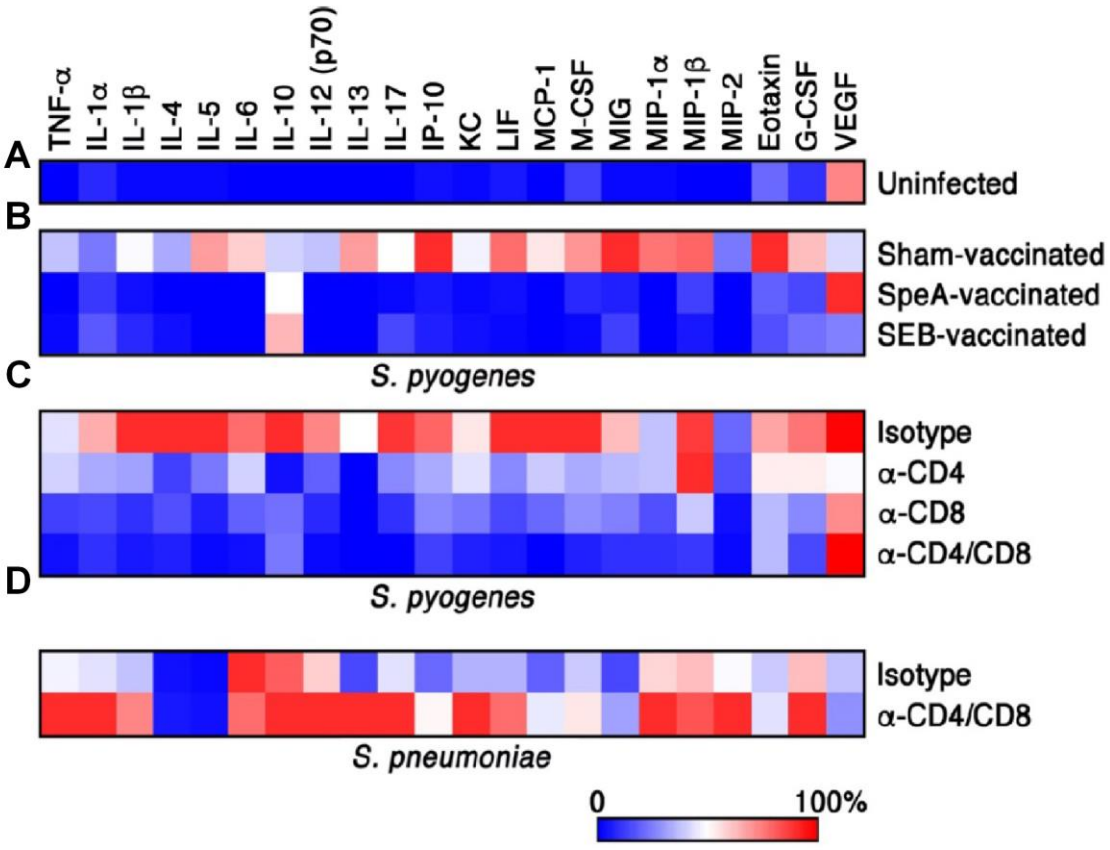
TNF-α
IL-1α
IL-1β
IL-4
IL-5
IL-6
IL-10
IL-12 (p70)
IL-13
IL-17
IP-10
KC
LIF
MCP-1
M-CSF
MIG
MIP-1α
MIP-1β
MIP-2
Eotaxin
G-CSF
VEGF
A
Uninfected
B
Sham-vaccinated
SpeA-vaccinated
SEB-vaccinated
C
S. pyogenes
Isotype
α-CD4
α-CD8
α-CD4/CD8
D
S. pyogenes
Isotype
α-CD4/CD8
S. pneumoniae
0
100%

Chapter 4: Discussion

4 Discussion

The primary barrier to preventing the greater than 500,000 deaths cause by GAS each year [4] is the lack of a safe and effective vaccine. Although this topic has been extensively studied for decades, there are numerous deterrents which have prevented this crucial prophylactic from being developed, including the lack of monetary incentive (due to this organism being a primary burden on developing, low income nations) and the potential for developing a cross-reactive immune response upon immunization with bacterial components leading to autoimmune sequelae [433,465]. The most promising vaccine candidate thus far is a multivalent M protein-based vaccine that targets 26 of the most common pharyngitis, invasive and rheumatogenic serotypes, and this vaccine has now undergone phase I and II clinical trials [419] and a reformatted 30-valent vaccine has undergone phase I trials [418,433]. The choice to target the M protein as a potential vaccine component stems from experiments completed over 50 years ago in pioneering studies by Rebecca Lancefield who demonstrated type-specific protective immunity in mice and subsequently showed that in humans, bactericidal M protein antibodies persisted for years after GAS infection [412]. Despite these findings, an overarching concern with M protein-based vaccines is that there are over 200 known streptococcal *emm*-types with varying distributions worldwide [49], presenting a possible complication of vaccine coverage and the likelihood of selecting for *emm*-types not present in the vaccine. Recent findings have shown that the 30-valent vaccine would protect against the majority of invasive- and pharyngitis-associated *emm*-types in North America and Europe [14,58,421,422] and does produce cross-reactive antibodies that target other *emm*-types [423,424]. This furthers the potential of M protein-based vaccines, but it is considered unlikely that a universally protective vaccine will ever arise from just targeting the M protein. Our belief is that a vaccine that targets multiple bacterial components that are known to be crucial to the establishment and/or maintenance of infection and survival of the organism *in vivo* would be a more successful candidate.

Streptococcal infection of the throat, skin and/or mucosa often precedes autoimmune sequelae [12,29,466], which results in the largest burden of GAS-associated disease [4,467]. Therefore, prevention of bacterial colonization and infection would largely prevent

this disease burden. Previous findings from our laboratory that GAS SAgs are required for efficient acute nasopharyngeal infection [377], and our demonstration herein that SAgs are expressed during infection establishment (**Figure 9**) led us to consider these toxins as potential vaccine candidates. One major benefit to the use of SAgs as vaccine candidates is that there are only 11 known Group A streptococcal SAgs [187]. This makes the generation of a pan-SAg vaccine more feasible compared to targeting the greater than 200 streptococcal *emm*-types. There is also data showing that administration of IVIG, which contain SAg-neutralizing antibodies [468], may reduce patient mortality in some settings [22,469,470], providing support for anti-SAg antibody-mediated protection against *S. pyogenes* in humans. Although it has been noted that numerous SAgs have multiple alleles, these generally differ in just a few amino acids [245], and thus it is probable that antibodies generated against one allele would cross-react. The one documented exception to this is SmeZ, in which there are over 50 variants [187]. Current analysis indicated that all tested variants still target human TCR V$\beta8^+$ cells, and those that do not are truncated and inactive [205], which indicates that if antibodies towards the TCR-targeting interface of SmeZ could be generated, this would likely neutralize most, if not all, active SmeZ variants.

Our vaccine analysis focused on SpeA, the only critical SAg in our human transgenic mouse model of *S. pyogenes* MGAS8232 upper respiratory tract infection [377]. A goal of this project was thus to produce a SpeA-based vaccine that generated antibody-mediated protection in our nasopharyngeal infection model. Previous studies have used SpeA toxoids as vaccine candidates [437,439] in severe and invasive disease, but not in the context of nasopharyngeal infection or other non-invasive models. Our passive immunization experiments show conclusively that anti-SpeA antibodies can be protective in *S. pyogenes* nasopharyngeal infection (**Figure 10**). Although treatment with wild-type SpeA was protective (**Figure 13C**), this was not antibody-mediated (**Figure 13D**), and instead was due to rendering TCR V$\beta8^+$ T cells unresponsive (**Figure 14**). Although protective in our animal model, vaccinating with wild-type SAgs would never be plausible for human use. This would primarily be due to the fact that SAgs are potent toxins that are capable of causing severe diseases – such as TSS – at extremely low concentrations and could also potentially drive an autoimmune response. Also, protection stemmed from rendering T cell subsets unresponsive, and thus individuals receiving a wild-type SAg vaccination may

invoke some level of protection against *S. pyogenes* infection, but may also be more susceptible to infections normally controlled by functioning T cells, such as viral infection. Nevertheless, this finding led us to pursue testing of attenuated SpeA toxoids in our vaccination model. Previously described mutants $SpeA_{Y100A}$ [454] and $SpeA_{HEXA}$ [437] that were tested in this vaccination model did not satisfy the above mentioned criteria due to protection stemming partially from unresponsive T cells (**Figure 15B** and **16**) or consistent, yet non-protective anti-SpeA antibody titres (**Figure 15B** and **C**), respectively. These findings led us to further analyze SpeA TCR and MHC class II binding site mutants, whereby we determined a further attenuated MHC II binding site mutant, $SpeA_{TRI}$, was able to generate consistently high anti-SpeA antibody titres and consistent protection (**Figure 17B** and **C**).

Mutation of asparagine at position 20 impacts the SpeA-TCR Vβ interacting interface (**Figure 5C**). Interestingly, incorporation of this amino acid substitution alone or in tandem with other substitutions generated a SpeA toxoid that failed to generate consistent protection in our *S. pyogenes* nasopharyngeal infection model (**Figure 17B**). Furthermore, $SpeA_{N20A}$ was incapable of activating murine T cells at all concentrations tested (**Figure 17A**) and did not induce anti-SpeA IgG antibodies (**Figure 17C**). SAgs have been recognized for their ability to suppress antibody production [254,471]; however, this was previously reported to be primarily through T cell-mediated perforin- and Fas-FasL-dependent B cell apoptosis [472–474]. Since $SpeA_{N20A}$ no longer has T cell activating potential (**Figure 17A**), this suggests an alternative, T cell-independent mechanism for antibody suppression, possibly mediated through direct MHC II binding. This is further supported by $SpeA_{TRI}$, which has only amino substitutions at the MHC II binding interface and produces a robust and protective antibody response (**Figure 17B** and **C**). Vaccination with toxoids containing mutations at both TCR and MHC II interacting interfaces ($SpeA_{TETRA}$ and $SpeA_{HEXA}$) resulted in a similar bimodal protection phenotype (**Figure 17B**). The exact reasons for this phenotype have not yet been elucidated, but it is possible that these amino acid substitutions removed a key epitope located within the TCR binding site which prevented generation of SpeA-neutralizing antibodies. Alternatively, TCR binding site mutant SAgs may not be appropriately trafficked to B cell germinal centers which would prevent a robust Ab response. Further experimentation will be required to

elucidate the mechanism of T cell-independent antibody suppression, as well as the lack of protection from antibodies that can bind the wild-type toxin. However, our discovery of $SpeA_{TRI}$ and its effectiveness as a vaccine against GAS further support toxoid SAgs as potential vaccine candidates to be used in a multi-component vaccine.

The mammalian adaptive immune system is known to be a critical component for protecting the host against infection. More specifically, T lymphocytes are known to be crucial components, aiding in the removal of viruses and intracellular pathogens, as well as modulating of immune microenvironments and stimulating antibody production by B cells. Through extremely diverse TCRs, T cells can recognize an astonishing number of peptides when presented on MHC molecules. It is thus not surprising that T cells are beneficial to the host in numerous infection models including those involving *Mycobacterium tuberculosis* [475], *Haemophilus influenza* [476], *Salmonella enterica* serovar Typhimurium [477] and *Listeria monocytogenes* [458]. Interestingly, in the case of *S. pyogenes*, a robust nasopharyngeal infection required the presence of SAg-responsive T cells. Vaccination with wild-type SpeA and SEB unexpectedly protected mice from *S. pyogenes* nasopharyngeal infection without the generation of anti-SAg antibodies (**Figure 13C** and **D**). We were able to show that this protection was due to rendering specific SAg-targeted Vβ T cells unresponsive (**Figure 14**). Depleting $CD4^+$ and $CD8^+$ T cells via antibody administration was also shown to be detrimental to GAS infection of the upper respiratory tract (**Figure 18**). Interestingly, removal of $CD8^+$ T cells alone impaired nasopharyngeal infection (**Figure 18D**); however, SAgs are able to activate both $CD4^+$ and $CD8^+$ T cells (**Figure 6C**), and thus we suspect that although both cells likely contribute to this phenotype, $CD8^+$ T cells may be more numerically dominant within this environment (**Figure 18C**). Since we were able to detect activation of SpeA-targeted $V\beta8^+$ T cells *in vivo* during *S. pyogenes* nasopharyngeal infection (**Figure 9**), and previous work from our laboratory indicates that both host expression of human MHC II (HLA-DQ8) and expression of SpeA are critical for *S. pyogenes* infection [377], this work supports that *S. pyogenes* requires Vβ-specific and functional T cells to promote upper respiratory tract infection.

This *S. pyogenes* T cell-dependent infection phenotype was shown to be in contrast to infection with *S. pneumoniae*, another Gram-positive, human nasopharyngeal colonizer that can disseminate from this site to cause a wide variety of invasive diseases [451,452,460]. Importantly, *S. pneumoniae* does not produce any known SAgs and thus its ability to colonize and infect the upper respiratory tract is completely independent of these toxins. *S. pneumoniae* was shown to infect HLA-DQ8 transgenic mice better than C57Bl/6 mice (**Figure 19A**), however, both infection groups harbored ~5 logs of bacteria or more, on average, and thus it appears that the role MHC II plays in this infection model is minimal and not as pronounced as with *S. pyogenes* (**Figure 8**). Active immunity against *S. pneumoniae* nasopharyngeal infection has been shown to be mediated by $CD4^+$ T cells [478], however, depletion of this T cell subset did not impact bacterial load at 48 hours (**Figure 20A**). This result was not unexpected, as mice were naïve to *S. pneumoniae* infection and the infection timeframe was too short to mount an adaptive immune response. These results demonstrate that although both organisms colonize a similar niche, their mechanisms for doing so appear to be very different.

Inflammation is a hallmark of the host response to an invading pathogen and generally acts to recruit factors that promote the clearance of the assaulting organism. In the presence of functioning T cells, when *S. pyogenes* had high bacterial load (**Figure 13C** and **18D**), a robust cytokine and chemokine response was observed in the nasopharyngeal environment (**Figure 21B, C** and **Appendix 4**). Conversely, when bacterial load in the murine cNT was decreased by SpeA or SEB vaccination (**Figure 13C**) or $CD4^+$ and $CD8^+$ T cell depletion (**Figure 18D**), the cytokine and chemokine profile mimicked that of uninfected mice (**Figure 21A, B, C** and **Appendix 4**). There was no significant impact on *S. pneumoniae* bacterial load upon $CD4^+$ and $CD8^+$ T cell depletion; however, a trend of increased CFUs was observed in T cell depleted mice (**Figure 20A**), accompanied by an enhanced cytokine response (**Figure 21D**). These results indicated that there is a consistent inflammatory signature when bacterial load is high. If an organism is able to avoid mucocilliary clearance mechanisms, its next goal is to adhere to the underlying epithelial surface [479]. This binding would theoretically also engage pattern recognition receptors of the innate immune system resulting in inflammation [480]. Since inflammatory cytokine levels were comparable in wild-type SAg vaccinated (SpeA and SEB), T cell-depleted (CD4 and CD8

together), as well as uninfected mice, this would indicate that in the absence of SAg-driven T cell activation, *S. pyogenes* cannot initiate even the earliest steps of nasopharyngeal colonization. Taken further, it can be hypothesized that this early inflammatory response is favorable for the bacteria and could provide a suitable environment for it to flourish.

There are other examples of bacteria-generated inflammation that appear to aid in the establishment of infection. *Neisseria gonorrhoeae* has been shown to secrete the modified sugar heptose-1,7-bisphosphate (HBP) as a novel pathogen-associated molecular pattern (PAMP) that is recognized by innate immune receptors in host cells, leading to an inflammatory response [481–483]. All analyzed Gram-negative organisms can produce HBP, but *Neisseria* species were found to release this sugar during growth [481], implicating an 'intent' by the organism to cause this immune response. It is currently unknown as to why this organism in particular liberates this molecule, but it does have interesting implications in pathogen-intended inflammation. Lupp *et al.* were also able to show that inflammation in a murine model of infectious colitis benefitted the infecting bacteria by eliminating the endogenous microflora and supporting the growth of introduced aerobic bacteria [484]. In a model of murine chronic otitis media, nontypeable *Haemophilus influenzae* was found to persist for up to two months in a cytokine rich environment of IL-1β, TNF-α, IL-10 and transforming growth factor (TGF)-β. Upon removal of T regulatory (T_{reg}) cells, a ~3 log reduction of bacteria was demonstrated [485]. Although SAgs can induce T_{reg} cells [486,487], our data does not suggest a T_{reg}-dependent phenotype as IL-10 was uniformly very low (<10 pg/mL) (**Appendix 4**) in all experimental conditions, and infection with *S. pyogenes* induced a prominent IL-6 and IL-17 response (**Figure 21**; **Appendix 4**). Therefore, our data suggests a more redundant role for $CD4^+$ and $CD8^+$ T cells. Both *S. pyogenes* and *H. influenzae* are regularly found in cases of human recurrent acute tonsillitis and tonsillar hypertrophy [488] and these patients are known to have an increase in IL-1α, IL-1β and TNF-α secreting cells in their tonsillar tissue [489]. Tonsillar cells from these patients re-stimulated with heat killed *H. influenzae* or *S. pyogenes* similarly had an increase in these, and other, Th1 cytokines [490]. These cytokines were also observed when the *S. pyogenes* bacterial load was high in the cNT of infected mice (control vaccinated and isotype control treated mice; **Figure 21B** and **C**). All

of these data suggest that certain organisms many induce an inflammatory environment upon infection to assist the microbe in the early stages of infection.

A major question that has yet to be answered is what biological role do SAgs play in the life cycle of *S. pyogenes*. SAgs have been primarily associated with severe and invasive diseases [187], however, the high conservation and apparent functional redundancy of these toxins indicate that they may play a more important role in *S. pyogenes* biology. Our findings support the hypothesis that SAgs are critical factors at the early stage of nasopharyngeal infection. Upon introduction into the upper respiratory tract, GAS upregulates numerous virulence and colonization factors, including SAgs. This has been well documented *in vivo* during the early colonization phase in a non-human primate model of GAS pharyngitis [327]. Secreted SAgs would likely interact with T cells and APCs in the local lymph node environments such as the Waldeyer's ring in humans or the NALT in the murine nasopharynx. This would stimulate a local inflammatory response driven by T lymphocyte activation, which may perform a number of crucial tasks for the bacterium including: suppression of innate phagocytic cell recruitment or function; expose important binding receptors on host cells; enhance nutrient acquisition by the pathogen; and/or inhibit members of the endogenous microbiota to reduce competition (**Figure 22**). Interestingly, previously published work from our laboratory has indicated a different role for SAg toxins during *S. aureus* nasopharyngeal infection. *S. aureus* SAg knockout strains were shown to have higher bacterial densities in the nasal cavity compared to wild-type counterparts, indicating a role for SAgs in regulating bacterial densities during colonization [491]. The specific benefits gained by both *S. pyogenes* and *S. aureus* manipulation of the local immune environment by producing SAgs remains incompletely understood, but future research will further elucidate the mechanistic role(s) that these toxins play in both organisms biology.

This thesis provides valuable insight into the host-pathogen interaction of *S. pyogenes*, however, there are limitations to this study. First and foremost, GAS is a human-specific pathogen, and although our model does well represent nasopharyngeal infection, it is still not completely analogous to a human infection. Future studies should assess antibody-mediated protection and T cell dependence in a more longitudinal model representing

colonization (vaginal colonization [389]) and/or a more human-like model (non-human primate [403]). Another limitation was that we were only able to test one strain of *S. pyogenes*. Future studies should analyze other isolates, such as the endemic *emm*1 strain (MGAS5005 [492] or 5448 [90,493]). Vaccine analysis focused primarily on the SAg SpeA. It will be important to assess other streptococcal SAgs and confirm that mutations to the MHC interacting interface will confer a similar protective phenotype upon vaccination. Lastly, many of the experiments herein used a minimal number of animals to reach statistical significance. Although this was due to limitations in murine colony breeding, it was noted that future work should run statistical power tests to determine the appropriate number of animals to use in each experiment and do everything possible to reach that number of samples per group.

To conclude, within this work, we were able to detect expression of the SAg SpeA *in vivo* during *S. pyogenes* nasopharyngeal infection, further implicating the role of these toxins at this critical juncture of host-pathogen interaction. Numerous SpeA toxoid variants were also designed and generated to assess their ability to generate protective SAg-specific antibodies *in vivo*. Antibody-mediated protection was successfully demonstrated against *S. pyogenes* nasopharyngeal infection using both passive immunization and vaccination with a SpeA MHC II binding interface variant, $SpeA_{TRI}$. Vaccination of mice with wild-type SAgs and T cell depletion experiments were able to demonstrate that *S. pyogenes* requires responsive Vβ-specific T cells in order to infect the cNT, a phenotype to our knowledge that is completely unique to a bacterial pathogen. We were also able to show that in the presence of T cells, *S. pyogenes* infection correlates with a robust cytokine response that was completely absent when T cells are unresponsive or depleted. This implicates a T cell-driven cytokine environment that is necessary for the establishment of infection. To our knowledge, this thesis presents the first use of a toxoid SAg to generate antibody-mediated protection against *S. pyogenes* nasopharyngeal infection. From this work, there is now a template to generate other SAg toxoids that can be used to create a potential vaccine containing all streptococcal SAgs, which offers a different approach to current vaccine strategies against *S. pyogenes*. Additionally, this work helps to guide the future of SAg research, from a toxin that causes severe disease to a tool used by bacteria to establish

Figure 22. Proposed mechanism of superantigen benefit to *S. pyogenes*.

S. pyogenes (group A *streptococcus*; GAS) gains access to the nasopharynx of its host and quickly up-regulates virulence factors including SAgs (**1**). SAgs traverse the epithelium to the local lymph environment such as Waldery's ring in humans or the NALT in mice (**2**). In the local lymph environment SAgs are able to activate both T cells (T) and antigen presenting cells (APC) via interacting with the TCR and MHC II, respectively, which leads to cytokine and chemokine production from both cell subset (**3**). Numerous bacterial benefits are possible from cytokine and chemokine production including: suppression of innate immune cell recruitment/function; exposure of binding receptors; enhanced nutrient acquisition; and removal of endogenous competing microflora (**4**). These outcomes would then allow the bacteria to survive and prosper in the nasopharynx.

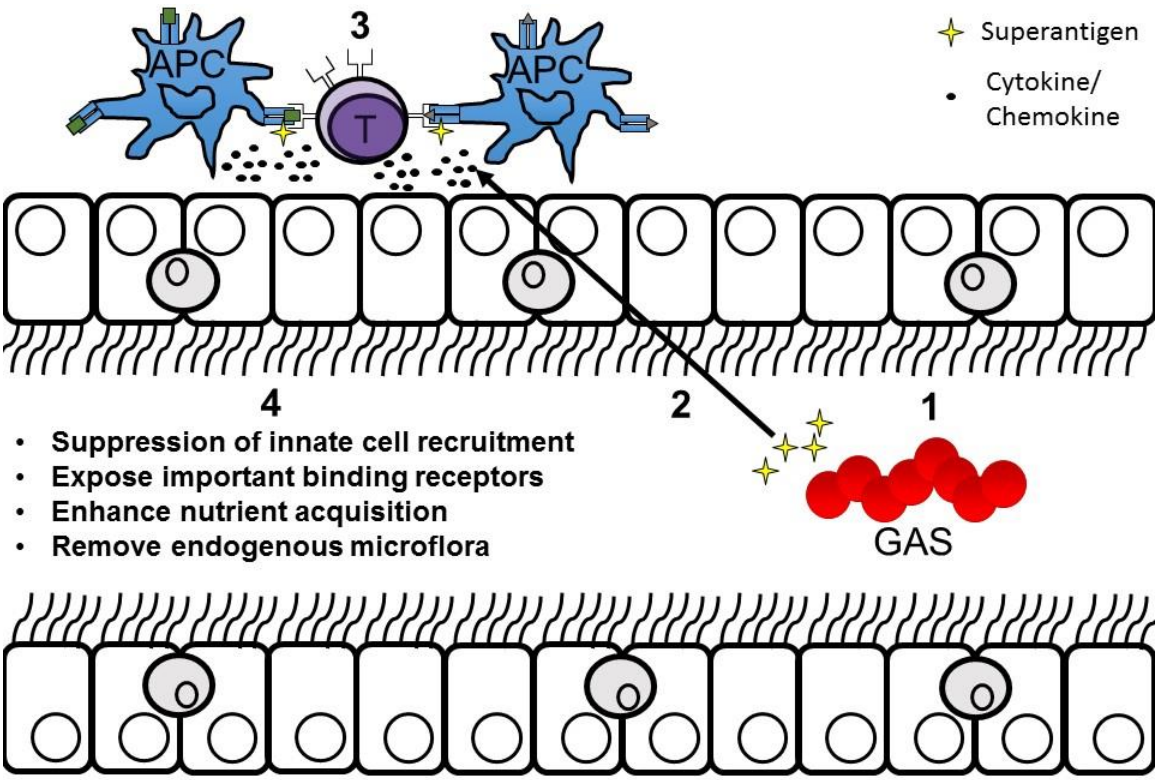
APC
3
T
APC
Superantigen
Cytokine/
Chemokine
4
2
1
• Suppression of innate cell recruitment
• Expose important binding receptors
• Enhance nutrient acquisition
• Remove endogenous microflora
GAS

infection. Analyzing SAgs from this perspective may have wide-reaching implications on the numerous organisms and viruses that utilize these truly unique proteins.

References

1. Whiley RA, Hardie JM. *Streptococcus*. Bergey's Manual of Systematics of Archaea and Bacteria. Chichester, UK: John Wiley & Sons, Ltd; 2015. pp. 1–86. doi:10.1002/9781118960608.gbm00612
2. Walker MJ, Barnett TC, McArthur JD, Cole JN, Gillen CM, Henningham A, et al. Disease manifestations and pathogenic mechanisms of group a *Streptococcus*. Clin Microbiol Rev. 2014;27: 264–301. doi:10.1128/CMR.00101-13
3. Tanz RR, Shulman ST. Chronic pharyngeal carriage of group A streptococci. Pediatr Infect Dis J. 2007;26: 175–6. doi:10.1097/01.inf.0000255328.19808.be
4. Carapetis JR, Steer AC, Mulholland EK, Weber M. The global burden of group A streptococcal diseases. Lancet Infect Dis. 2005;5: 685–94. doi:10.1016/S1473-3099(05)70267-X
5. Cone LA, Woodard DR, Schlievert PM, Tomory GS. Clinical and bacteriologic observations of a toxic shock-like syndrome due to *Streptococcus pyogenes*. N Engl J Med. 1987;317: 146–9. doi:10.1056/NEJM198707163170305
6. O'Brien KL, Beall B, Barrett NL, Cieslak PR, Reingold A, Farley MM, et al. Epidemiology of invasive group a *Streptococcus* disease in the United States, 1995-1999. Clin Infect Dis. 2002;35: 268–76. doi:10.1086/341409
7. Gaworzewska E, Colman G. Changes in the pattern of infection caused by *Streptococcus pyogenes*. Epidemiol Infect. 1988;100: 257–69. Available: http://www.ncbi.nlm.nih.gov/pubmed/3128449
8. Chelsom J, Halstensen A, Haga T, Høiby EA. Necrotising fasciitis due to group A streptococci in western Norway: incidence and clinical features. Lancet (London, England). 1994;344: 1111–5. doi:10.1016/S0140-6736(94)90629-7
9. Dahl PR, Perniciaro C, Holmkvist KA, O'Connor MI, Gibson LE. Fulminant group A streptococcal necrotizing fasciitis: clinical and pathologic findings in 7 patients. J Am Acad Dermatol. 2002;47: 489–92. doi:10.1067/mjd.2002.120536
10. Steer AC, Lamagni TL, Curtis N, Carapetis JR. Invasive group a streptococcal disease: epidemiology, pathogenesis and management. Drugs. 2012;72: 1213–27. doi:10.2165/11634180-000000000-00000
11. Young MH, Engleberg NC, Mulla ZD, Aronoff DM. Therapies for necrotising fasciitis. Expert Opin Biol Ther. 2006;6: 155–65. doi:10.1517/14712598.6.2.155
12. Steer AC, Carapetis JR, Nolan TM, Shann F. Systematic review of rheumatic heart disease prevalence in children in developing countries: the role of environmental factors. J Paediatr Child Health. 2002;38: 229–34. Available: http://www.ncbi.nlm.nih.gov/pubmed/12047688
13. Lamagni TL, Darenberg J, Luca-Harari B, Siljander T, Efstratiou A, Henriques-Normark B, et al. Epidemiology of severe *Streptococcus pyogenes* disease in Europe. J Clin Microbiol. 2008;46: 2359–67. doi:10.1128/JCM.00422-08
14. O'Loughlin RE, Roberson A, Cieslak PR, Lynfield R, Gershman K, Craig A, et al.

The epidemiology of invasive group A streptococcal infection and potential vaccine implications: United States, 2000-2004. Clin Infect Dis. 2007;45: 853–62. doi:10.1086/521264

15. Stevens DL. Streptococcal toxic-shock syndrome: spectrum of disease, pathogenesis, and new concepts in treatment. Emerg Infect Dis. 1995;1: 69–78. doi:10.3201/eid0103.950301

16. Shimizu Y. Streptococcal toxic shock-like syndrome. Intern Med. 2000;39: 195–6. Available: http://www.ncbi.nlm.nih.gov/pubmed/10772119

17. Stevens DL, Tanner MH, Winship J, Swarts R, Ries KM, Schlievert PM, et al. Severe group A streptococcal infections associated with a toxic shock-like syndrome and scarlet fever toxin A. N Engl J Med. 1989;321: 1–7. doi:10.1056/NEJM198907063210101

18. Eriksson BK, Andersson J, Holm SE, Norgren M. Epidemiological and clinical aspects of invasive group A streptococcal infections and the streptococcal toxic shock syndrome. Clin Infect Dis. 1998;27: 1428–36. Available: pm:9868656

19. Defining the group A streptococcal toxic shock syndrome. Rationale and consensus definition. The Working Group on Severe Streptococcal Infections. JAMA. 1993;269: 390–1. Available: http://www.ncbi.nlm.nih.gov/pubmed/8418347

20. Proft T, Sriskandan S, Yang LPH, Fraser JD. Superantigens and streptococcal toxic shock syndrome. Emerg Infect Dis. 2003;9: 1211–8. doi:10.3201/eid0910.030042

21. Stegmayr B, Björck S, Holm S, Nisell J, Rydvall A, Settergren B. Septic shock induced by group A streptococcal infection: clinical and therapeutic aspects. Scand J Infect Dis. 1992;24: 589–97. doi:10.3109/00365549209054644

22. Kaul R, McGeer A, Norrby-Teglund A, Kotb M, Schwartz B, O'Rourke K, et al. Intravenous immunoglobulin therapy for streptococcal toxic shock syndrome--a comparative observational study. The Canadian Streptococcal Study Group. Clin Infect Dis. 1999;28: 800–7. doi:10.1086/515199

23. Shaikh N, Leonard E, Martin JM. Prevalence of streptococcal pharyngitis and streptococcal carriage in children: a meta-analysis. Pediatrics. 2010;126: e557–e564. doi:10.1542/peds.2009-2648

24. Ebell MH, Smith MA, Barry HC, Ives K, Carey M. The rational clinical examination. Does this patient have strep throat? JAMA. 2000;284: 2912–8. doi:10.1001/jama.284.22.2912

25. Yang LPH, Keam SJ. Retapamulin: a review of its use in the management of impetigo and other uncomplicated superficial skin infections. Drugs. 2008;68: 855–73. Available: http://www.ncbi.nlm.nih.gov/pubmed/18416589

26. Strömberg A, Schwan A, Cars O. Throat carrier rates of beta-hemolytic streptococci among healthy adults and children. Scand J Infect Dis. 1988;20: 411–7. Available: http://www.ncbi.nlm.nih.gov/pubmed/3194709

27. Weiss K, Laverdière M, Lovgren M, Delorme J, Poirier L, Béliveau C. Group A *Streptococcus* carriage among close contacts of patients with invasive infections. Am J Epidemiol. 1999;149: 863–8. Available: http://www.ncbi.nlm.nih.gov/pubmed/10221323

28. DeMuri GP, Wald ER. The Group A Streptococcal Carrier State Reviewed: Still an Enigma. J Pediatric Infect Dis Soc. 2014;3: 336–42. doi:10.1093/jpids/piu030

29. Cunningham MW. Pathogenesis of group A streptococcal infections. Clin Microbiol Rev. 2000;13: 470–511. Available: http://cmr.asm.org/cgi/content/abstract/13/3/470

30. Carapetis JR, Beaton A, Cunningham MW, Guilherme L, Karthikeyan G, Mayosi BM, et al. Acute rheumatic fever and rheumatic heart disease. Nat Rev Dis Prim. 2016;2: 15084. doi:10.1038/nrdp.2015.84

31. Jaine R, Baker M, Venugopal K. Epidemiology of acute rheumatic fever in New Zealand 1996-2005. J Paediatr Child Health. 2008;44: 564–71. doi:10.1111/j.1440-1754.2008.01384.x

32. Gewitz MH, Baltimore RS, Tani LY, Sable CA, Shulman ST, Carapetis J, et al. Revision of the Jones Criteria for the diagnosis of acute rheumatic fever in the era of Doppler echocardiography: a scientific statement from the American Heart Association. Circulation. 2015;131: 1806–18. doi:10.1161/CIR.0000000000000205

33. Carapetis JR, Currie BJ, Mathews JD. Cumulative incidence of rheumatic fever in an endemic region: a guide to the susceptibility of the population? Epidemiol Infect. 2000;124: 239–44. doi:10.1017/S0950268800003514

34. Martin WJ, Steer AC, Smeesters PR, Keeble J, Inouye M, Carapetis JR, et al. Post-infectious group A streptococcal autoimmune syndromes and the heart. Autoimmun Rev. Elsevier B.V.; 2015;14: 710–25. doi:10.1016/j.autrev.2015.04.005

35. Murray CJL, Vos T, Lozano R, Naghavi M, Flaxman AD, Michaud C, et al. Disability-adjusted life years (DALYs) for 291 diseases and injuries in 21 regions, 1990-2010: a systematic analysis for the Global Burden of Disease Study 2010. Lancet (London, England). 2012;380: 2197–223. doi:10.1016/S0140-6736(12)61689-4

36. GBD 2013 Mortality and Causes of Death Collaborators. Global, regional, and national age-sex specific all-cause and cause-specific mortality for 240 causes of death, 1990-2013: a systematic analysis for the Global Burden of Disease Study 2013. Lancet (London, England). Elsevier Ltd; 2015;385: 117–71. doi:10.1016/S0140-6736(14)61682-2

37. Global Burden of Disease Study 2013 Collaborators. Global, regional, and national incidence, prevalence, and years lived with disability for 301 acute and chronic diseases and injuries in 188 countries, 1990-2013: a systematic analysis for the Global Burden of Disease Study 2013. Lancet (London, England). 2015;386: 743–800. doi:10.1016/S0140-6736(15)60692-4

38. Lue HC, Chen CL, Wei H, Okuni M, Mabilangan LM, Dharmasakti D, et al. The natural history of rheumatic fever and rheumatic heart disease in the Orient. Jpn Heart J. 1979;20: 237–52. Available: http://www.ncbi.nlm.nih.gov/pubmed/459093

39. Rheumatic Fever and Rheumatic Heart Disease: report of a WHO Expert Consultation. Geneva, Switzerland: World Health Organization; 2001.

40. Nordstrand A, Norgren M, Holm SE. Pathogenic mechanism of acute post-streptococcal glomerulonephritis. Scand J Infect Dis. 1999;31: 523–37. doi:10.1080/00365549950164382

41. Marshall CS, Cheng AC, Markey PG, Towers RJ, Richardson LJ, Fagan PK, et al. Acute post-streptococcal glomerulonephritis in the Northern Territory of Australia: a review of 16 years data and comparison with the literature. Am J Trop Med Hyg. 2011;85: 703–10. doi:10.4269/ajtmh.2011.11-0185

42. Maruyama F, Watanabe T, Nakagawa I. *Streptococcus pyogenes* Genomics [Internet]. *Streptococcus pyogenes*: Basic Biology to Clinical Manifestations. 2016. Available: http://www.ncbi.nlm.nih.gov/pubmed/26866228

43. Beres SB, Musser JM. Contribution of exogenous genetic elements to the group A *Streptococcus* metagenome. PLoS One. 2007;2: e800. doi:10.1371/journal.pone.0000800

44. Bessen DE, McShan WM, Nguyen S V, Shetty A, Agrawal S, Tettelin H. Molecular epidemiology and genomics of group A *Streptococcus*. Infect Genet Evol. Elsevier B.V.; 2015;33: 393–418. doi:10.1016/j.meegid.2014.10.011

45. Metzgar D, Zampolli A. The M protein of group A *Streptococcus* is a key virulence factor and a clinically relevant strain identification marker. Virulence. 2011;2: 402–12. doi:10.4161/viru.2.5.16342

46. Phillips GN, Flicker PF, Cohen C, Manjula BN, Fischetti V a. Streptococcal M protein: alpha-helical coiled-coil structure and arrangement on the cell surface. Proc Natl Acad Sci U S A. 1981;78: 4689–93. doi:10.1073/pnas.78.8.4689

47. Fischetti V a, Pancholi V, Schneewind O. Conservation of a hexapeptide sequence in the anchor region of surface proteins from gram-positive cocci. Mol Microbiol. 1990;4: 1603–5. doi:10.1111/j.1365-2958.1990.tb02072.x

48. Beall B, Facklam R, Thompson T. Sequencing emm-specific PCR products for routine and accurate typing of group A streptococci. J Clin Microbiol. 1996;34: 953–8. Available: http://www.ncbi.nlm.nih.gov/pubmed/8815115

49. Steer AC, Law I, Matatolu L, Beall BW, Carapetis JR. Global emm type distribution of group A streptococci: systematic review and implications for vaccine development. Lancet Infect Dis. Elsevier Ltd; 2009;9: 611–6. doi:10.1016/S1473-3099(09)70178-1

50. Hollingshead SK, Readdy TL, Yung DL, Bessen DE. Structural heterogeneity of the emm gene cluster in group A streptococci. Mol Microbiol. 1993;8: 707–17. Available: http://www.ncbi.nlm.nih.gov/pubmed/8332063

51. McGregor KF, Spratt BG, Kalia A, Bennett A, Bilek N, Beall B, et al. Multilocus sequence typing of *Streptococcus pyogenes* representing most known emm types and distinctions among subpopulation genetic structures. J Bacteriol. 2004;186: 4285–94. doi:10.1128/JB.186.13.4285-4294.2004

52. McMillan DJ, Drèze P, Vu T, Bessen DE, Guglielmini J, Steer andrew C, et al. Updated model of group A *Streptococcus* M proteins based on a comprehensive worldwide study. Clin Microbiol Infect. 2013;19: E222-9. doi:10.1111/1469-0691.12134

53. Anthony BF, Kaplan EL, Wannamaker LW, Chapman SS. The dynamics of streptococcal infections in a defined population of children: serotypes associated with skin and respiratory infections. Am J Epidemiol. 1976;104: 652–66. Available: http://www.ncbi.nlm.nih.gov/pubmed/793381

54. Wannamaker LW. Differences between streptococcal infections of the throat and of the skin (second of two parts). N Engl J Med. 1970;282: 78–85. doi:10.1056/NEJM197001082820206

55. Stollerman GH. Rheumatogenic and nephritogenic streptococci. Circulation. 1971;43: 915–21. doi:10.1227/01.NEU.0000335789.61773.C5

56. Bessen DE, Sotir CM, Readdy TL, Hollingshead SK. Genetic correlates of throat and skin isolates of group A streptococci. J Infect Dis. 1996;173: 896–900. doi:10.1093/infdis/173.4.896

57. Bessen DE, Veasy LG, Hill HR, Augustine NH, Fischetti VA. Serologic evidence for a class I group A streptococcal infection among rheumatic fever patients. J Infect Dis. 1995;172: 1608–11. Available: http://www.ncbi.nlm.nih.gov/pubmed/7594728

58. Shulman ST, Tanz RR, Kabat W, Kabat K, Cederlund E, Patel D, et al. Group A streptococcal pharyngitis serotype surveillance in North America, 2000-2002. Clin Infect Dis. 2004;39: 325–32. doi:10.1086/421949

59. Bessen DE, Kumar N, Hall GS, Riley DR, Luo F, Lizano S, et al. Whole-genome association study on tissue tropism phenotypes in group A *Streptococcus*. J Bacteriol. 2011;193: 6651–6663. doi:10.1128/JB.05263-11

60. Bessen DE, Carapetis JR, Beall B, Katz R, Hibble M, Currie BJ, et al. Contrasting molecular epidemiology of group A streptococci causing tropical and nontropical infections of the skin and throat. J Infect Dis. 2000;182: 1109–16. doi:10.1086/315842

61. Cywes C, Stamenkovic I, Wessels MR. CD44 as a receptor for colonization of the pharynx by group A *Streptococcus*. J Clin Invest. 2000;106: 995–1002. doi:10.1172/JCI10195

62. Wessels MR, Bronze MS. Critical role of the group A streptococcal capsule in pharyngeal colonization and infection in mice. Proc Natl Acad Sci U S A. 1994;91: 12238–42. Available: http://www.ncbi.nlm.nih.gov/pubmed/7991612

63. Foley MJ, Wood WB. Studies on the pathogenicity of group A streptococci. II.

The antiphagocytic effects of the M protein and the capsular gel. J Exp Med. 1959;110: 617–28. Available: http://www.ncbi.nlm.nih.gov/pubmed/13823728

64. Dale JB, Washburn RG, Marques MB, Wessels MR. Hyaluronate capsule and surface M protein in resistance to opsonization of group A streptococci. Infect Immun. 1996;64: 1495–501. Available: http://www.ncbi.nlm.nih.gov/pubmed/8613352

65. Stollerman GH, Dale JB. The importance of the group a *Streptococcus* capsule in the pathogenesis of human infections: a historical perspective. Clin Infect Dis. 2008;46: 1038–45. doi:10.1086/529194

66. Dougherty BA, van de Rijn I. Molecular characterization of a locus required for hyaluronic acid capsule production in group A streptococci. J Exp Med. 1992;175: 1291–9. doi:10.1084/jem.175.5.1291

67. Crater DL, van de Rijn I. Hyaluronic acid synthesis operon (has) expression in group A streptococci. J Biol Chem. 1995;270: 18452–8. Available: http://www.ncbi.nlm.nih.gov/pubmed/7629171

68. Dougherty BA, van de Rijn I. Molecular characterization of hasA from an operon required for hyaluronic acid synthesis in group A streptococci. J Biol Chem. 1994;269: 169–75. Available: http://www.ncbi.nlm.nih.gov/pubmed/8276791

69. DeAngelis PL, Papaconstantinou J, Weigel PH. Molecular cloning, identification, and sequence of the hyaluronan synthase gene from group A *Streptococcus pyogenes*. J Biol Chem. 1993;268: 19181–4. Available: http://www.ncbi.nlm.nih.gov/pubmed/8366070

70. Dougherty BA, van de Rijn I. Molecular characterization of hasB from an operon required for hyaluronic acid synthesis in group A streptococci. Demonstration of UDP-glucose dehydrogenase activity. J Biol Chem. 1993;268: 7118–24. Available: http://www.ncbi.nlm.nih.gov/pubmed/8463246

71. Crater DL, Dougherty BA, van de Rijn I. Molecular characterization of hasC from an operon required for hyaluronic acid synthesis in group A streptococci. Demonstration of UDP-glucose pyrophosphorylase activity. J Biol Chem. 1995;270: 28676–80. Available: http://www.ncbi.nlm.nih.gov/pubmed/7499387

72. Ashbaugh CD, Albertí S, Wessels MR. Molecular analysis of the capsule gene region of group A *Streptococcus*: the hasAB genes are sufficient for capsule expression. J Bacteriol. 1998;180: 4955–9. Available: http://www.ncbi.nlm.nih.gov/pubmed/9733702

73. Levin JC, Wessels MR. Identification of csrR/csrS, a genetic locus that regulates hyaluronic acid capsule synthesis in group A *Streptococcus*. Mol Microbiol. 1998;30: 209–19. doi:10.1046/j.1365-2958.1998.01057.x

74. Biswas I, Scott JR. Identification of rocA, a positive regulator of covR expression in the group A *Streptococcus*. J Bacteriol. 2003;185: 3081–90. doi:10.1128/JB.185.10.3081

75. Gerlach D, Knöll H, Köhler W, Ozegowski JH, Hríbalova V. Isolation and

characterization of erythrogenic toxins. V. Communication: identity of erythrogenic toxin type B and streptococcal proteinase precursor. Zentralbl Bakteriol Mikrobiol Hyg A. 1983;255: 221–33. Available: http://www.ncbi.nlm.nih.gov/pubmed/6359775

76. Chaussee MS, Phillips ER, Ferretti JJ. Temporal production of streptococcal erythrogenic toxin B (streptococcal cysteine proteinase) in response to nutrient depletion. Infect Immun. 1997;65: 1956–9. Available: http://www.ncbi.nlm.nih.gov/pubmed/9125588

77. Liu TY, Elliott SD. Streptococcal proteinase: The zymogen to enzyme transformation. J Biol Chem. 1965;240: 1138–42. Available: http://www.ncbi.nlm.nih.gov/pubmed/14284716

78. Musser JM, Stockbauer K, Kapur V, Rudgers GW. Substitution of cysteine 192 in a highly conserved *Streptococcus pyogenes* extracellular cysteine protease (interleukin 1beta convertase) alters proteolytic activity and ablates zymogen processing. Infect Immun. 1996;64: 1913–7. Available: http://www.ncbi.nlm.nih.gov/pubmed/8675287

79. Kapur V, Topouzis S, Majesky MW, Li LL, Hamrick MR, Hamill RJ, et al. A conserved *Streptococcus pyogenes* extracellular cysteine protease cleaves human fibronectin and degrades vitronectin. Microb Pathog. 1993;15: 327–46. doi:10.1006/mpat.1993.1083

80. Kapur V, Majesky MW, Li LL, Black RA, Musser JM. Cleavage of interleukin 1 beta (IL-1 beta) precursor to produce active IL-1 beta by a conserved extracellular cysteine protease from *Streptococcus pyogenes*. Proc Natl Acad Sci U S A. 1993;90: 7676–80. doi:10.1073/pnas.90.16.7676

81. Collin M, Olsén A. Effect of SpeB and EndoS from *Streptococcus pyogenes* on human immunoglobulins. Infect Immun. 2001;69: 7187–9. doi:10.1128/IAI.69.11.7187-7189.2001

82. Kuo C-F, Lin Y-S, Chuang W-J, Wu J-J, Tsao N. Degradation of complement 3 by streptococcal pyrogenic exotoxin B inhibits complement activation and neutrophil opsonophagocytosis. Infect Immun. 2008;76: 1163–9. doi:10.1128/IAI.01116-07

83. Egesten A, Olin AI, Linge HM, Yadav M, Mörgelin M, Karlsson A, et al. SpeB of *Streptococcus pyogenes* differentially modulates antibacterial and receptor activating properties of human chemokines. PLoS One. 2009;4: e4769. doi:10.1371/journal.pone.0004769

84. Raeder R, Woischnik M, Podbielski A, Boyle MD. A secreted streptococcal cysteine protease can cleave a surface-expressed M1 protein and alter the immunoglobulin binding properties. Res Microbiol. 1998;149: 539–48. doi:10.1016/S0923-2508(99)80001-1

85. Nooh MM, Aziz RK, Kotb M, Eroshkin A, Chuang W-J, Proft T, et al. Streptococcal mitogenic exotoxin, SmeZ, is the most susceptible M1T1 streptococcal superantigen to degradation by the streptococcal cysteine protease, SpeB. J Biol Chem. 2006;281: 35281–8. doi:10.1074/jbc.M605544200

86. Svensson MD, Sjöbring U, Luo F, Bessen DE. Roles of the plasminogen activator streptokinase and the plasminogen-associated M protein in an experimental model for streptococcal impetigo. Microbiology. 2002;148: 3933–45. doi:10.1099/00221287-148-12-3933

87. Nelson DC, Garbe J, Collin M. Cysteine proteinase SpeB from *Streptococcus pyogenes* - a potent modifier of immunologically important host and bacterial proteins. Biol Chem. 2011;392: 1077–88. doi:10.1515/BC.2011.208

88. Yu CE, Ferretti JJ. Frequency of the erythrogenic toxin B and C genes (speB and speC) among clinical isolates of group A streptococci. Infect Immun. 1991;59: 211–5. Available: http://www.ncbi.nlm.nih.gov/pubmed/1987034

89. Olsen RJ, Raghuram A, Cantu C, Hartman MH, Jimenez FE, Lee S, et al. The majority of 9,729 group A *Streptococcus* strains causing disease secrete SpeB cysteine protease: pathogenesis implications. Infect Immun. 2015;83: 4750–8. doi:10.1128/IAI.00989-15

90. Aziz RK, Pabst MJ, Jeng A, Kansal R, Low DE, Nizet V, et al. Invasive M1T1 group A *Streptococcus* undergoes a phase-shift in vivo to prevent proteolytic degradation of multiple virulence factors by SpeB. Mol Microbiol. 2004;51: 123–34. doi:10.1046/j.1365-2958.2003.03797.x

91. Treviño J, Perez N, Ramirez-Peña E, Liu Z, Shelburne SA, Musser JM, et al. CovS simultaneously activates and inhibits the CovR-mediated repression of distinct subsets of group A *Streptococcus* virulence factor-encoding genes. Infect Immun. 2009;77: 3141–9. doi:10.1128/IAI.01560-08

92. Zingaretti C, Falugi F, Nardi-Dei V, Pietrocola G, Mariani M, Liberatori S, et al. *Streptococcus pyogenes* SpyCEP: a chemokine-inactivating protease with unique structural and biochemical features. FASEB J. 2010;24: 2839–48. doi:10.1096/fj.09-145631

93. Edwards RJ, Taylor GW, Ferguson M, Murray S, Rendell N, Wrigley A, et al. Specific C-terminal cleavage and inactivation of interleukin-8 by invasive disease isolates of *Streptococcus pyogenes*. J Infect Dis. 2005;192: 783–90. doi:10.1086/432485

94. Hidalgo-Grass C, Mishalian I, Dan-Goor M, Belotserkovsky I, Eran Y, Nizet V, et al. A streptococcal protease that degrades CXC chemokines and impairs bacterial clearance from infected tissues. EMBO J. 2006;25: 4628–37. doi:10.1038/sj.emboj.7601327

95. Fritzer A, Noiges B, Schweiger D, Rek A, Kungl AJ, von Gabain A, et al. Chemokine degradation by the Group A streptococcal serine proteinase ScpC can be reconstituted in vitro and requires two separate domains. Biochem J. 2009;422: 533–42. doi:10.1042/BJ20090278

96. Turner CE, Kurupati P, Jones MD, Edwards RJ, Sriskandan S. Emerging role of the interleukin-8 cleaving enzyme SpyCEP in clinical *Streptococcus pyogenes* infection. J Infect Dis. 2009;200: 555–63. doi:10.1086/603541

97. Salim KY, de Azavedo JC, Bast DJ, Cvitkovitch DG. Regulation of sagA, siaA

and scpC by SilCR, a putative signaling peptide of *Streptococcus pyogenes*. FEMS Microbiol Lett. 2008;289: 119–25. doi:10.1111/j.1574-6968.2008.01375.x

98. Sumby P, Zhang S, Whitney AR, Falugi F, Grandi G, Graviss E a, et al. A chemokine-degrading extracellular protease made by group A *Streptococcus* alters pathogenesis by enhancing evasion of the innate immune response. Infect Immun. 2008;76: 978–85. doi:10.1128/IAI.01354-07

99. Kurupati P, Turner CE, Tziona I, Lawrenson RA, Alam FM, Nohadani M, et al. Chemokine-cleaving *Streptococcus pyogenes* protease SpyCEP is necessary and sufficient for bacterial dissemination within soft tissues and the respiratory tract. Mol Microbiol. 2010;76: 1387–97. doi:10.1111/j.1365-2958.2010.07065.x

100. Sjölinder H, Lövkvist L, Plant L, Eriksson J, Aro H, Jones A, et al. The ScpC protease of *Streptococcus pyogenes* affects the outcome of sepsis in a murine model. Infect Immun. 2008;76: 3959–66. doi:10.1128/IAI.00128-08

101. Lawrenson RA, Sriskandan S. Cell Envelope Proteinase A (*Streptococcus*). Handbook of Proteolytic Enzymes. Elsevier; 2013. pp. 3195–3202. doi:10.1016/B978-0-12-382219-2.00704-3

102. Cleary PP, Prahbu U, Dale JB, Wexler DE, Handley J. Streptococcal C5a peptidase is a highly specific endopeptidase. Infect Immun. 1992;60: 5219–23. Available: http://www.ncbi.nlm.nih.gov/pubmed/1452354

103. Wexler DE, Chenoweth DE, Cleary PP. Mechanism of action of the group A streptococcal C5a inactivator. Proc Natl Acad Sci U S A. 1985;82: 8144–8. Available: http://www.pubmedcentral.nih.gov/articlerender.fcgi?artid=391459&tool=pmcentrez&rendertype=abstract

104. Ji Y, McLandsborough L, Kondagunta A, Cleary PP. C5a peptidase alters clearance and trafficking of group A streptococci by infected mice. Infect Immun. 1996;64: 503–10. Available: http://www.ncbi.nlm.nih.gov/pubmed/8550199

105. Simpson WJ, LaPenta D, Chen C, Cleary PP. Coregulation of type 12 M protein and streptococcal C5a peptidase genes in group A streptococci: evidence for a virulence regulon controlled by the virR locus. J Bacteriol. 1990;172: 696–700. Available: http://www.ncbi.nlm.nih.gov/pubmed/2404953

106. McIver KS. Stand-alone response regulators controlling global virulence networks in *Streptococcus pyogenes*. Contrib Microbiol. Basel: KARGER; 2009;16: 103–19. doi:10.1159/000219375

107. O'Connor SP, Cleary PP. Localization of the streptococcal C5a peptidase to the surface of group A streptococci. Infect Immun. 1986;53: 432–4. Available: http://www.ncbi.nlm.nih.gov/pubmed/3525415

108. Barnett TC, Scott JR. Differential recognition of surface proteins in *Streptococcus pyogenes* by two sortase gene homologs. J Bacteriol. 2002;184: 2181–91. doi:10.1128/JB.184.8.2181-2191.2002

109. Chmouryguina I, Suvorov A, Ferrieri P, Cleary PP. Conservation of the C5a

peptidase genes in group A and B streptococci. Infect Immun. 1996;64: 2387–90. Available: http://www.ncbi.nlm.nih.gov/pubmed/8698456

110. Ji Y, Carlson B, Kondagunta A, Cleary PP. Intranasal immunization with C5a peptidase prevents nasopharyngeal colonization of mice by the group A *Streptococcus*. Infect Immun. 1997;65: 2080–7. Available: http://www.pubmedcentral.nih.gov/articlerender.fcgi?artid=175287&tool=pmcentrez&rendertype=abstract

111. Akesson P, Sjöholm AG, Björck L. Protein SIC, a novel extracellular protein of *Streptococcus pyogenes* interfering with complement function. J Biol Chem. 1996;271: 1081–8. doi:10.1074/jbc.271.2.1081

112. Fernie-King BA, Seilly DJ, Willers C, Würzner R, Davies A, Lachmann PJ. Streptococcal inhibitor of complement (SIC) inhibits the membrane attack complex by preventing uptake of C567 onto cell membranes. Immunology. 2001;103: 390–8. doi:10.1046/j.1365-2567.2001.01249.x

113. Frick I-M, Akesson P, Rasmussen M, Schmidtchen A, Björck L. SIC, a secreted protein of *Streptococcus pyogenes* that inactivates antibacterial peptides. J Biol Chem. 2003;278: 16561–6. doi:10.1074/jbc.M301995200

114. Fernie-King BA, Seilly DJ, Binks MJ, Sriprakash KS, Lachmann PJ. Streptococcal DRS (distantly related to SIC) and SIC inhibit antimicrobial peptides, components of mucosal innate immunity: a comparison of their activities. Microbes Infect. 2007;9: 300–7. doi:10.1016/j.micinf.2006.12.006

115. Fernie-King BA, Seilly DJ, Davies A, Lachmann PJ. Streptococcal inhibitor of complement inhibits two additional components of the mucosal innate immune system: secretory leukocyte proteinase inhibitor and lysozyme. Infect Immun. 2002;70: 4908–16. doi:10.1128/IAI.70.9.4908-4916.2002

116. Egesten A, Eliasson M, Johansson HM, Olin AI, Morgelin M, Mueller A, et al. The CXC chemokine MIG/CXCL9 is important in innate immunity against *Streptococcus pyogenes*. J Infect Dis. 2007;195: 684–93. doi:10.1086/510857

117. Frick I-M, Shannon O, Åkesson P, Mörgelin M, Collin M, Schmidtchen A, et al. Antibacterial activity of the contact and complement systems is blocked by SIC, a protein secreted by *Streptococcus pyogenes*. J Biol Chem. 2011;286: 1331–40. doi:10.1074/jbc.M110.178350

118. Hoe NP, Ireland RM, DeLeo FR, Gowen BB, Dorward DW, Voyich JM, et al. Insight into the molecular basis of pathogen abundance: group A *Streptococcus* inhibitor of complement inhibits bacterial adherence and internalization into human cells. Proc Natl Acad Sci U S A. 2002;99: 7646–51. doi:10.1073/pnas.112039899

119. Lukomski S, Hoe NP, Abdi I, Rurangirwa J, Kordari P, Liu M, et al. Nonpolar inactivation of the hypervariable streptococcal inhibitor of complement gene (sic) in serotype M1 *Streptococcus pyogenes* significantly decreases mouse mucosal colonization. Infect Immun. 2000;68: 535–42. doi:10.1128/IAI.68.2.535-542.2000

120. Stockbauer KE, Grigsby D, Pan X, Fu YX, Mejia LM, Cravioto A, et al.

Hypervariability generated by natural selection in an extracellular complement-inhibiting protein of serotype M1 strains of group A *Streptococcus*. Proc Natl Acad Sci U S A. 1998;95: 3128–33. doi:10.1073/pnas.95.6.3128

121. Mejia LM, Stockbauer KE, Pan X, Cravioto A, Musser JM. Characterization of group A *Streptococcus* strains recovered from Mexican children with pharyngitis by automated DNA sequencing of virulence-related genes: unexpectedly large variation in the gene (sic) encoding a complement-inhibiting protein. J Clin Microbiol. 1997;35: 3220–4. Available: http://www.ncbi.nlm.nih.gov/pubmed/9399523

122. Hoe NP, Nakashima K, Lukomski S, Grigsby D, Liu M, Kordari P, et al. Rapid selection of complement-inhibiting protein variants in group A *Streptococcus* epidemic waves. Nat Med. 1999;5: 924–9. doi:10.1038/11369

123. Bhakdi S, Tranum-Jensen J, Sziegoleit A. Mechanism of membrane damage by streptolysin-O. Infect Immun. 1985;47: 52–60. Available: http://www.ncbi.nlm.nih.gov/pubmed/3880730

124. Shewell LK, Harvey RM, Higgins MA, Day CJ, Hartley-Tassell LE, Chen AY, et al. The cholesterol-dependent cytolysins pneumolysin and streptolysin O require binding to red blood cell glycans for hemolytic activity. Proc Natl Acad Sci U S A. 2014;111: E5312-20. doi:10.1073/pnas.1412703111

125. Tweten RK. Cholesterol-dependent cytolysins, a family of versatile pore-forming toxins. Infect Immun. 2005;73: 6199–209. doi:10.1128/IAI.73.10.6199-6209.2005

126. Timmer AM, Timmer JC, Pence MA, Hsu L-C, Ghochani M, Frey TG, et al. Streptolysin O promotes group A *Streptococcus* immune evasion by accelerated macrophage apoptosis. J Biol Chem. 2009;284: 862–71. doi:10.1074/jbc.M804632200

127. Madden JC, Ruiz N, Caparon MG. Cytolysin-mediated translocation (CMT): a functional equivalent of type III secretion in gram-positive bacteria. Cell. 2001;104: 143–52. Available: http://www.ncbi.nlm.nih.gov/pubmed/11163247

128. Mozola CC, Caparon MG. Dual modes of membrane binding direct pore formation by Streptolysin O. Mol Microbiol. 2015;97: 1036–50. doi:10.1111/mmi.13085

129. Mozola CC, Magassa N, Caparon MG. A novel cholesterol-insensitive mode of membrane binding promotes cytolysin-mediated translocation by Streptolysin O. Mol Microbiol. 2014; 1–13. doi:10.1111/mmi.12786

130. Magassa N, Chandrasekaran S, Caparon MG. *Streptococcus pyogenes* cytolysin-mediated translocation does not require pore formation by streptolysin O. EMBO Rep. 2010;11: 400–5. doi:10.1038/embor.2010.37

131. Brosnahan AJ, Mantz MJ, Squier C a, Peterson ML, Schlievert PM. Cytolysins augment superantigen penetration of stratified mucosa. J Immunol. 2009;182: 2364–73. doi:10.4049/jimmunol.0803283

132. Reglinski M, Sriskandan S. The contribution of group A streptococcal virulence determinants to the pathogenesis of sepsis. Virulence. 2014;5: 127–36.

doi:10.4161/viru.26400

133. Ato M, Ikebe T, Kawabata H, Takemori T, Watanabe H. Incompetence of neutrophils to invasive group A *Streptococcus* is attributed to induction of plural virulence factors by dysfunction of a regulator. PLoS One. 2008;3: e3455. doi:10.1371/journal.pone.0003455

134. Zhu L, Olsen RJ, Lee JD, Porter AR, DeLeo FR, Musser JM. Contribution of Secreted NADase and Streptolysin O to the Pathogenesis of Epidemic Serotype M1 *Streptococcus pyogenes* Infections. Am J Pathol. Elsevier Inc; 2016; 1–10. doi:10.1016/j.ajpath.2016.11.003

135. Burke RJ, Chang C. Diagnostic criteria of acute rheumatic fever. Autoimmun Rev. Elsevier B.V.; 2014;13: 503–7. doi:10.1016/j.autrev.2014.01.036

136. Zegeye N, Asrat D, Woldeamanuel Y, Habte A, Gedlu E, Tønjum T, et al. Throat culture positivity rate and antibiotic susceptibility pattern of beta-hemolytic streptococci in children on secondary prophylaxis for rheumatic heart disease. BMC Infect Dis. BMC Infectious Diseases; 2016;16: 510. doi:10.1186/s12879-016-1841-3

137. Todd EW. The differentiation of two distinct serological varieties of streptolysin, streptolysin O and streptolysin S. J Pathol Bacteriol. 1938;47: 423–445. doi:10.1002/path.1700470307

138. Nizet V, Beall B, Bast DJ, Datta V, Kilburn L, Low DE, et al. Genetic locus for streptolysin S production by group A *Streptococcus*. Infect Immun. 2000;68: 4245–54. Available: http://www.ncbi.nlm.nih.gov/pubmed/10858242

139. Molloy EM, Cotter PD, Hill C, Mitchell DA, Ross RP. Streptolysin S-like virulence factors: the continuing sagA. Nat Rev Microbiol. 2011;9: 670–81. doi:10.1038/nrmicro2624

140. Datta V, Myskowski SM, Kwinn LA, Chiem DN, Varki N, Kansal RG, et al. Mutational analysis of the group A streptococcal operon encoding streptolysin S and its virulence role in invasive infection. Mol Microbiol. 2005;56: 681–95. doi:10.1111/j.1365-2958.2005.04583.x

141. Lee SW, Mitchell DA, Markley AL, Hensler ME, Gonzalez D, Wohlrab A, et al. Discovery of a widely distributed toxin biosynthetic gene cluster. Proc Natl Acad Sci U S A. 2008;105: 5879–84. doi:10.1073/pnas.0801338105

142. Ginsburg I. Is streptolysin S of group A streptococci a virulence factor? APMIS. 1999;107: 1051–9. doi:10.1111/j.1699-0463.1999.tb01509.x

143. Theodore TS, Calandra GB. Streptolysin S activation by lipoteichoic acid. Infect Immun. 1981;33: 326–8. Available: http://www.ncbi.nlm.nih.gov/pubmed/7021426

144. Hryniewicz W, Pryjma J. Effect of streptolysin S on human and mouse T and B lymphocytes. Infect Immun. 1977;16: 730–3. Available: http://www.ncbi.nlm.nih.gov/pubmed/302239

145. Bernherimer AW, Schwartz LL. Effect of staphylococcal and other bacterial toxins

on platelets in vitro. J Pathol Bacteriol. 1965;89: 209–23. Available: http://www.ncbi.nlm.nih.gov/pubmed/14263463

146. Keiser H, Weissmann G, Bernheimer AW. Studies on lysosomes. IV. Solubilization of enzymes during mitochondiral swelling and disruption of lysosomes by streptolysin S and other hemolytic agents. J Cell Biol. 1964;22: 101–13. Available: http://www.ncbi.nlm.nih.gov/pubmed/14195604

147. Bernheimer AW, Schwartz LL. Lysosomal disruption by bacterial toxins. J Bacteriol. 1964;87: 1100–4. doi:10.1117/12.2234235

148. Carr A, Sledjeski DD, Podbielski A, Boyle MD, Kreikemeyer B. Similarities between complement-mediated and streptolysin S-mediated hemolysis. J Biol Chem. 2001;276: 41790–6. doi:10.1074/jbc.M107401200

149. Flaherty R a., Puricelli JM, Higashi DL, Park CJ, Lee SW. Streptolysin S Promotes Programmed Cell Death and Enhances Inflammatory Signaling in Epithelial Keratinocytes during Group A *Streptococcus* Infection. Infect Immun. 2015;83: 4118–33. doi:10.1128/IAI.00611-15

150. Dale JB, Chiang EY, Hasty DL, Courtney HS. Antibodies against a synthetic peptide of SagA neutralize the cytolytic activity of streptolysin S from group A streptococci. Infect Immun. 2002;70: 2166–70. doi:10.1128/IAI.70.4.2166

151. Sierig G, Cywes C, Wessels MR, Ashbaugh CD. Cytotoxic effects of streptolysin o and streptolysin s enhance the virulence of poorly encapsulated group a streptococci. Infect Immun. 2003;71: 446–55. doi:10.1128/IAI.71.1.446-455.2003

152. Betschel SD, Borgia SM, Barg NL, Low DE, De Azavedo JC. Reduced virulence of group A streptococcal Tn916 mutants that do not produce streptolysin S. Infect Immun. 1998;66: 1671–9. Available: http://www.ncbi.nlm.nih.gov/pubmed/9529097

153. Jantsch J, Gerlach RG, Ensser A, Dahesh S, Popp I, Heeg C, et al. Severe soft tissue infection caused by a non-beta-hemolytic *Streptococcus pyogenes* strain harboring a premature stop mutation in the sagC gene. J Clin Microbiol. 2013;51: 1962–5. doi:10.1128/JCM.00175-13

154. Yoshino M, Murayama SY, Sunaoshi K, Wajima T, Takahashi M, Masaki J, et al. Nonhemolytic *Streptococcus pyogenes* isolates that lack large regions of the sag operon mediating streptolysin S production. J Clin Microbiol. 2010;48: 635–8. doi:10.1128/JCM.01362-09

155. Marcum JA, Kline DL. Species specificity of streptokinase. Comp Biochem Physiol B. 1983;75: 389–94. doi:10.1016/0305-0491(83)90345-0

156. Damaschun G, Damaschun H, Gast K, Gerlach D, Misselwitz R, Welfle H, et al. Streptokinase is a flexible multi-domain protein. Eur Biophys J. 1992;20: 355–61. doi:10.1007/BF00196594

157. Wang X, Lin X, Loy JA, Tang J, Zhang XC. Crystal structure of the catalytic domain of human plasmin complexed with streptokinase. Science. 1998;281: 1662–5. doi:10.1126/science.281.5383.1662

158. Boxrud PD, Bock PE. Coupling of conformational and proteolytic activation in the kinetic mechanism of plasminogen activation by streptokinase. J Biol Chem. 2004;279: 36642–9. doi:10.1074/jbc.M405265200

159. Boxrud PD, Fay WP, Bock PE. Streptokinase binds to human plasmin with high affinity, perturbs the plasmin active site, and induces expression of a substrate recognition exosite for plasminogen. J Biol Chem. 2000;275: 14579–89. doi:10.1074/jbc.275.19.14579

160. Nolan M, Bouldin SD, Bock PE. Full time course kinetics of the streptokinase-plasminogen activation pathway. J Biol Chem. 2013;288: 29482–93. doi:10.1074/jbc.M113.477935

161. Huang TT, Malke H, Ferretti JJ. Heterogeneity of the streptokinase gene in group A streptococci. Infect Immun. 1989;57: 502–6. Available: http://www.ncbi.nlm.nih.gov/pubmed/2643572

162. Huang TT, Malke H, Ferretti JJ. The streptokinase gene of group A streptococci: cloning, expression in Escherichia coli, and sequence analysis. Mol Microbiol. 1989;3: 197–205. Available: http://www.ncbi.nlm.nih.gov/pubmed/2668686

163. McArthur JD, McKay FC, Ramachandran V, Shyam P, Cork AJ, Sanderson-Smith ML, et al. Allelic variants of streptokinase from *Streptococcus pyogenes* display functional differences in plasminogen activation. FASEB J. 2008;22: 3146–53. doi:10.1096/fj.08-109348

164. Graham MR, Smoot LM, Migliaccio CAL, Virtaneva K, Sturdevant DE, Porcella SF, et al. Virulence control in group A *Streptococcus* by a two-component gene regulatory system: global expression profiling and in vivo infection modeling. Proc Natl Acad Sci U S A. 2002;99: 13855–60. doi:10.1073/pnas.202353699

165. Kreikemeyer B, Boyle MD, Buttaro BA, Heinemann M, Podbielski A. Group A streptococcal growth phase-associated virulence factor regulation by a novel operon (Fas) with homologies to two-component-type regulators requires a small RNA molecule. Mol Microbiol. 2001;39: 392–406. doi:10.1046/j.1365-2958.2001.02226.x

166. Malke H, Steiner K. Control of streptokinase gene expression in group A & C streptococci by two-component regulators. Indian J Med Res. 2004;119 Suppl: 48–56. Available: http://www.ncbi.nlm.nih.gov/pubmed/15232162

167. Steiner K, Malke H. Dual control of streptokinase and streptolysin S production by the covRS and fasCAX two-component regulators in *Streptococcus dysgalactiae* subsp. *equisimilis*. Infect Immun. 2002;70: 3627–36. doi:10.1128/IAI.70.7.3627-3636.2002

168. Sun H, Ringdahl U, Homeister JW, Fay WP, Engleberg NC, Yang AY, et al. Plasminogen is a critical host pathogenicity factor for group A streptococcal infection. Science. 2004;305: 1283–1286. doi:10.1126/science.1101245

169. Sun H, Xu Y, Sitkiewicz I, Ma Y, Wang X, Yestrepsky BD, et al. Inhibitor of streptokinase gene expression improves survival after group A *Streptococcus* infection in mice. Proc Natl Acad Sci U S A. 2012;109: 3469–74.

doi:10.1073/pnas.1201031109

170. White J, Herman A, Pullen a M, Kubo R, Kappler JW, Marrack PC. The V beta-specific superantigen staphylococcal enterotoxin B: stimulation of mature T cells and clonal deletion in neonatal mice. Cell. 1989;56: 27–35. Available: http://www.ncbi.nlm.nih.gov/pubmed/2521300

171. Barsumian EL, Schlievert PM, Watson DW. Nonspecific and specific immunological mitogenicity by group A streptococcal pyrogenic exotoxins. Infect Immun. 1978;22: 681–8. Available: http://www.ncbi.nlm.nih.gov/pubmed/365764

172. Dick GF, Dick GH. Landmark article Jan 26, 1924: The etiology of scarlet fever. By George F. Dick and Gladys Henry Dick. JAMA. 1983;250: 3096. Available: http://www.ncbi.nlm.nih.gov/pubmed/6358561

173. Cole BC, Atkin CL. The *Mycoplasma arthritidis* T-cell mitogen, MAM: a model superantigen. Immunol Today. 1991;12: 271–6. doi:10.1016/0167-5699(91)90125-D

174. Ito Y, Abe J, Yoshino K, Takeda T, Kohsaka T. Sequence analysis of the gene for a novel superantigen produced by *Yersinia pseudotuberculosis* and expression of the recombinant protein. J Immunol. 1995;154: 5896–906. Available: http://www.ncbi.nlm.nih.gov/pubmed/7751634

175. Lafon M, Scott-Algara D, Marche PN, Cazenave P a, Jouvin-Marche E. Neonatal deletion and selective expansion of mouse T cells by exposure to rabies virus nucleocapsid superantigen. J Exp Med. 1994;180: 1207–15. Available: http://www.pubmedcentral.nih.gov/articlerender.fcgi?artid=2191690&tool=pmcentrez&rendertype=abstract

176. Choi Y, Kappler JW, Marrack P. A superantigen encoded in the open reading frame of the 3’ long terminal repeat of mouse mammary tumour virus. Nature. 1991;350: 203–7. doi:10.1038/350203a0

177. Perron H, Jouvin-Marche E, Michel M, Ounanian-Paraz A, Camelo S, Dumon A, et al. Multiple sclerosis retrovirus particles and recombinant envelope trigger an abnormal immune response in vitro, by inducing polyclonal Vbeta16 T-lymphocyte activation. Virology. 2001;287: 321–32. doi:10.1006/viro.2001.1045

178. Sutkowski N, Conrad B, Thorley-Lawson D a, Huber BT. Epstein-Barr virus transactivates the human endogenous retrovirus HERV-K18 that encodes a superantigen. Immunity. 2001;15: 579–89. doi:http://dx.doi.org/10.1016/S1074-7613(01)00210-2

179. Xu SX, McCormick JK. Staphylococcal superantigens in colonization and disease. Front Cell Infect Microbiol. 2012;2: 52. doi:10.3389/fcimb.2012.00052

180. Krakauer T, Pradhan K, Stiles BG. Staphylococcal Superantigens Spark Host-Mediated Danger Signals. Front Immunol. 2016;7: 23. doi:10.3389/fimmu.2016.00023

181. Schlievert PM, Shands KN, Dan BB, Schmid GP, Nishimura RD. Identification and characterization of an exotoxin from *Staphylococcus aureus* associated with

toxic-shock syndrome. J Infect Dis. 1981;143: 509–16. Available: http://www.ncbi.nlm.nih.gov/pubmed/6972418

182. Petersson K, Pettersson H, Skartved NJ, Walse B, Forsberg G. Staphylococcal enterotoxin H induces V alpha-specific expansion of T cells. J Immunol. 2003;170: 4148–4154. doi:10.4049/jimmunol.170.8.4148

183. Saline M, Rödström KEJ, Fischer G, Orekhov VY, Karlsson BG, Lindkvist-Petersson K. The structure of superantigen complexed with TCR and MHC reveals novel insights into superantigenic T cell activation. Nat Commun. 2010;1: 119. doi:10.1038/ncomms1117

184. Pumphrey N, Vuidepot A, Jakobsen B, Forsberg G, Walse B, Lindkvist-Petersson K. Cutting edge: Evidence of direct TCR alpha-chain interaction with superantigen. J Immunol. 2007;179: 2700–4. doi:10.4049/jimmunol.179.5.2700

185. Williams RJ, Ward JM, Henderson B, Poole S, O'Hara BP, Wilson M, et al. Identification of a novel gene cluster encoding staphylococcal exotoxin-like proteins: characterization of the prototypic gene and its protein product, SET1. Infect Immun. 2000;68: 4407–15. doi:10.1128/IAI.68.8.4407-4415.2000

186. Fraser JD, Proft T. The bacterial superantigen and superantigen-like proteins. Immunol Rev. 2008;225: 226–43. doi:10.1111/j.1600-065X.2008.00681.x

187. Commons RJ, Smeesters PR, Proft T, Fraser JD, Robins-Browne R, Curtis N. Streptococcal superantigens: categorization and clinical associations. Trends Mol Med. Elsevier Ltd; 2014;20: 48–62. doi:10.1016/j.molmed.2013.10.004

188. Proft T, Moffatt SL, Weller KD, Paterson A, Martin D, Fraser JD. The streptococcal superantigen SMEZ exhibits wide allelic variation, mosaic structure, and significant antigenic variation. J Exp Med. 2000;191: 1765–76. doi:10.1084/jem.191.10.1765

189. Turner CE, Sommerlad M, McGregor K, Davies FJ, Pichon B, Chong DLW, et al. Superantigenic activity of emm3 *Streptococcus pyogenes* is abrogated by a conserved, naturally occurring smeZ mutation. PLoS One. 2012;7: e46376. doi:10.1371/journal.pone.0046376

190. McCormick JK, Yarwood JM, Schlievert PM. Toxic shock syndrome and bacterial superantigens: an update. Annu Rev Microbiol. 2001;55: 77–104. doi:10.1146/annurev.micro.55.1.77

191. Schlievert PM, Jablonski LM, Roggiani M, Sadler I, Callantine S, Mitchell DT, et al. Pyrogenic toxin superantigen site specificity in toxic shock syndrome and food poisoning in animals. Infect Immun. 2000;68: 3630–4. doi:10.1128/IAI.68.6.3630-3634.2000.Updated

192. Brosnahan AJ, Schlievert PM. Gram-positive bacterial superantigen outside-in signaling causes toxic shock syndrome. FEBS J. 2011;278: 4649–67. doi:10.1111/j.1742-4658.2011.08151.x

193. Schlievert PM. Staphylococcal enterotoxin B and toxic-shock syndrome toxin-1 are significantly associated with non-menstrual TSS. Lancet (London, England).

1986;1: 1149–50. Available: http://www.ncbi.nlm.nih.gov/pubmed/2871397

194. Bohach G a, Fast DJ, Nelson RD, Schlievert PM. Staphylococcal and streptococcal pyrogenic toxins involved in toxic shock syndrome and related illnesses. Crit Rev Microbiol. 1990;17: 251–72. doi:10.3109/10408419009105728

195. Argudín MÁ, Mendoza MC, Rodicio MR. Food poisoning and *Staphylococcus aureus* enterotoxins. Toxins (Basel). 2010;2: 1751–73. doi:10.3390/toxins2071751

196. Ruzin A, Lindsay J, Novick RP. Molecular genetics of SaPI1--a mobile pathogenicity island in *Staphylococcus aureus*. Mol Microbiol. 2001;41: 365–77. doi:mmi2488 [pii]

197. Bae T, Baba T, Hiramatsu K, Schneewind O. Prophages of *Staphylococcus aureus* Newman and their contribution to virulence. Mol Microbiol. 2006;62: 1035–47. doi:10.1111/j.1365-2958.2006.05441.x

198. Baba T, Takeuchi F, Kuroda M, Yuzawa H, Aoki K, Oguchi A, et al. Genome and virulence determinants of high virulence community-acquired MRSA. Lancet (London, England). 2002;359: 1819–27. doi:10.1016/S0140-6736(02)08713-5

199. Friães A, Pinto FR, Silva-Costa C, Ramirez M, Melo-Cristino J. Superantigen gene complement of *Streptococcus pyogenes*--relationship with other typing methods and short-term stability. Eur J Clin Microbiol Infect Dis. 2013;32: 115–25. doi:10.1007/s10096-012-1726-3

200. Wilson GJ, Seo KS, Cartwright RA, Connelley T, Chuang-Smith ON, Merriman JA, et al. A novel core genome-encoded superantigen contributes to lethality of community-associated MRSA necrotizing pneumonia. PLoS Pathog. 2011;7: e1002271. doi:10.1371/journal.ppat.1002271

201. Johnson LP, Schlievert PM, Watson DW. Transfer of group A streptococcal pyrogenic exotoxin production to nontoxigenic strains of lysogenic conversion. Infect Immun. 1980;28: 254–7. Available: http://www.ncbi.nlm.nih.gov/pubmed/6991440

202. Vojtek I, Pirzada Z a, Henriques-Normark B, Mastny M, Janapatla RP, Charpentier E. Lysogenic transfer of group A *Streptococcus* superantigen gene among Streptococci. J Infect Dis. 2008;197: 225–34. doi:10.1086/524687

203. Earhart C a, Vath GM, Roggiani M, Schlievert PM, Ohlendorf DH. Structure of streptococcal pyrogenic exotoxin A reveals a novel metal cluster. Protein Sci. 2000;9: 1847–1851.

204. Li Y, Li H, Dimasi N, McCormick JK, Martin R, Schuck P, et al. Crystal structure of a superantigen bound to the high-affinity, zinc-dependent site on MHC class II. Immunity. 2001;14: 93–104.

205. Arcus VL, Proft T, Sigrell J a, Baker HM, Fraser JD, Baker EN. Conservation and variation in superantigen structure and activity highlighted by the three-dimensional structures of two new superantigens from *Streptococcus pyogenes*. J Mol Biol. 2000;299: 157–168. doi:10.1006/jmbi.2000.3725

206. Brouillard J-NP, Günther S, Varma AK, Gryski I, Herfst C a, Rahman a KMN, et

al. Crystal structure of the streptococcal superantigen SpeI and functional role of a novel loop domain in T cell activation by group V superantigens. J Mol Biol. 2007;367: 925–34. doi:10.1016/j.jmb.2007.01.024

207. Baker HM, Proft T, Webb PD, Arcus VL, Fraser JD, Baker EN. Crystallographic and mutational data show that the streptococcal pyrogenic exotoxin J can use a common binding surface for T-cell receptor binding and dimerization. J Biol Chem. 2004;279: 38571–6. doi:10.1074/jbc.M406695200

208. Nur-ur Rahman a KM, Bonsor D a, Herfst C a, Pollard F, Peirce M, Wyatt AW, et al. The T cell receptor beta-chain second complementarity determining region loop (CDR2beta governs T cell activation and Vbeta specificity by bacterial superantigens. J Biol Chem. 2011;286: 4871–81. doi:10.1074/jbc.M110.189068

209. Kim J, Urban RG, Strominger JL, Wiley DC. Toxic shock syndrome toxin-1 complexed with a class II major histocompatibility molecule HLA-DR1. Science. 1994;266: 1870–4. Available: http://www.ncbi.nlm.nih.gov/pubmed/7997880

210. Wen R, Cole GA, Surman S, Blackman MA, Woodland DL. Major histocompatibility complex class II-associated peptides control the presentation of bacterial superantigens to T cells. J Exp Med. 1996;183: 1083–92. Available: http://www.ncbi.nlm.nih.gov/pubmed/8642250

211. Moza B, Varma AK, Buonpane R a, Zhu P, Herfst C a, Nicholson MJ, et al. Structural basis of T-cell specificity and activation by the bacterial superantigen TSST-1. EMBO J. 2007;26: 1187–97. doi:10.1038/sj.emboj.7601531

212. Moza B, Buonpane RA, Zhu P, Herfst CA, Rahman AKMN, McCormick JK, et al. Long-range cooperative binding effects in a T cell receptor variable domain. Proc Natl Acad Sci U S A. 2006;103: 9867–72. doi:10.1073/pnas.0600220103

213. Jardetzky TS, Brown JH, Gorga JC, Stern LJ, Urban RG, Chi YI, et al. Three-dimensional structure of a human class II histocompatibility molecule complexed with superantigen. Nature. 1994;368: 711–8. doi:10.1038/368711a0

214. Hennecke J, Carfi A, Wiley DC. Structure of a covalently stabilized complex of a human alphabeta T-cell receptor, influenza HA peptide and MHC class II molecule, HLA-DR1. EMBO J. 2000;19: 5611–24. doi:10.1093/emboj/19.21.5611

215. Rödström KEJ, Elbing K, Lindkvist-Petersson K. Structure of the Superantigen Staphylococcal Enterotoxin B in Complex with TCR and Peptide-MHC Demonstrates Absence of TCR-Peptide Contacts. J Immunol. 2014;193: 1998–2004. doi:10.4049/jimmunol.1401268

216. Petersson K, Håkansson M, Nilsson H, Forsberg G, Svensson LA, Liljas A, et al. Crystal structure of a superantigen bound to MHC class II displays zinc and peptide dependence. EMBO J. 2001;20: 3306–12. doi:10.1093/emboj/20.13.3306

217. Sundberg EJ, Li H, Llera AS, McCormick JK, Tormo J, Schlievert PM, et al. Structures of two streptococcal superantigens bound to TCR beta chains reveal diversity in the architecture of T cell signaling complexes. Structure. 2002;10: 687–99. Available: http://www.ncbi.nlm.nih.gov/pubmed/12015151

218. Fernández MM, Guan R, Swaminathan CP, Malchiodi EL, Mariuzza RA. Crystal structure of staphylococcal enterotoxin I (SEI) in complex with a human major histocompatibility complex class II molecule. J Biol Chem. 2006;281: 25356–64. doi:10.1074/jbc.M603969200

219. Fields BA, Malchiodi EL, Li H, Ysern X, Stauffacher C V, Schlievert PM, et al. Crystal structure of a T-cell receptor beta-chain complexed with a superantigen. Nature. 1996;384: 188–92. doi:10.1038/384188a0

220. Li H, Llera A, Tsuchiya D, Leder L, Ysern X, Schlievert PM, et al. Three-dimensional structure of the complex between a T cell receptor beta chain and the superantigen staphylococcal enterotoxin B. Immunity. 1998;9: 807–16. doi:10.1016/S1074-7613(00)80646-9

221. Abrahmsén L, Dohlsten M, Segrén S, Björk P, Jonsson E, Kalland T. Characterization of two distinct MHC class II binding sites in the superantigen staphylococcal enterotoxin A. EMBO J. 1995;14: 2978–86. Available: http://www.ncbi.nlm.nih.gov/pubmed/7542584

222. Hudson KR, Tiedemann RE, Urban RG, Lowe SC, Strominger JL, Fraser JD. Staphylococcal enterotoxin A has two cooperative binding sites on major histocompatibility complex class II. J Exp Med. 1995;182: 711–20. Available: http://www.ncbi.nlm.nih.gov/pubmed/7650479

223. Petersson K, Thunnissen M, Forsberg G, Walse B. Crystal structure of a SEA variant in complex with MHC class II reveals the ability of SEA to crosslink MHC molecules. Structure. 2002;10: 1619–26. doi:10.1016/S0969-2126(02)00895-X

224. Rödström KEJ, Regenthal P, Lindkvist-Petersson K. Structure of Staphylococcal Enterotoxin E in Complex with TCR Defines the Role of TCR Loop Positioning in Superantigen Recognition. PLoS One. 2015;10: e0131988. doi:10.1371/journal.pone.0131988

225. Rödström KEJ, Regenthal P, Bahl C, Ford A, Baker D, Lindkvist-Petersson K. Two common structural motifs for TCR recognition by staphylococcal enterotoxins. Sci Rep. Nature Publishing Group; 2016;6: 25796. doi:10.1038/srep25796

226. Kasper KJ, Xi W, Rahman AKMN-U, Nooh MM, Kotb M, Sundberg EJ, et al. Molecular requirements for MHC class II alpha-chain engagement and allelic discrimination by the bacterial superantigen streptococcal pyrogenic exotoxin C. J Immunol. 2008;181: 3384–92. doi:10.4049/jimmunol.181.5.3384

227. Patterson KG. Development of a Novel Humanized Single Chain Antibody-Streptococcal Superantigen-Derived Immunotherapy Targeting the 5T4 Oncofetal Antigen [Internet]. The University of Western Ontario. 2015. Available: http://ir.lib.uwo.ca/etd/3398

228. Rahman AKMN, Herfst CA, Moza B, Shames SR, Chau LA, Bueno C, et al. Molecular basis of TCR selectivity, cross-reactivity, and allelic discrimination by a bacterial superantigen: integrative functional and energetic mapping of the SpeC-Vbeta2.1 molecular interface. J Immunol. 2006;177: 8595–603.

doi:10.4049/jimmunol.177.12.8595

229. Günther S, Varma AK, Moza B, Kasper KJ, Wyatt AW, Zhu P, et al. A novel loop domain in superantigens extends their T cell receptor recognition site. J Mol Biol. 2007;371: 210–21. doi:10.1016/j.jmb.2007.05.038

230. Wang L, Zhao Y, Li Z, Guo Y, Jones LL, Kranz DM, et al. Crystal structure of a complete ternary complex of TCR, superantigen and peptide-MHC. Nat Struct Mol Biol. 2007;14: 169–71. doi:10.1038/nsmb1193

231. Davis MM, Boniface JJ, Reich Z, Lyons D, Hampl J, Arden B, et al. Ligand recognition by alpha beta T cell receptors. Annu Rev Immunol. 1998;16: 523–44. doi:10.1146/annurev.immunol.16.1.523

232. Andersen PS, Schuck P, Sundberg EJ, Geisler C, Karjalainen K, Mariuzza RA. Quantifying the energetics of cooperativity in a ternary protein complex. Biochemistry. 2002;41: 5177–84. doi:10.1021/bi0200209

233. Buonpane R a, Moza B, Sundberg EJ, Kranz DM. Characterization of T cell receptors engineered for high affinity against toxic shock syndrome toxin-1. J Mol Biol. 2005;353: 308–21. doi:10.1016/j.jmb.2005.08.041

234. Kaempfer R, Arad G, Levy R, Hillman D, Nasie I, Rotfogel Z. CD28: direct and critical receptor for superantigen toxins. Toxins (Basel). 2013;5: 1531–42. doi:10.3390/toxins5091531

235. Riley JL, June CH. The CD28 family: a T-cell rheostat for therapeutic control of T-cell activation. Blood. 2005;105: 13–21. doi:10.1182/blood-2004-04-1596

236. Arad G, Levy R, Nasie I, Hillman D, Rotfogel Z, Barash U, et al. Binding of superantigen toxins into the CD28 homodimer interface is essential for induction of cytokine genes that mediate lethal shock. PLoS Biol. 2011;9: e1001149. doi:10.1371/journal.pbio.1001149

237. Ramachandran G, Tulapurkar ME, Harris KM, Arad G, Shirvan A, Shemesh R, et al. A peptide antagonist of CD28 signaling attenuates toxic shock and necrotizing soft-tissue infection induced by *Streptococcus pyogenes*. J Infect Dis. 2013;207: 1869–77. doi:10.1093/infdis/jit104

238. Llewelyn MJ, Sriskandan S, Terrazzini N, Cohen J, Altmann DM. The TCR Vbeta signature of bacterial superantigens spreads with stimulus strength. Int Immunol. 2006;18: 1433–41. doi:10.1093/intimm/dxl076

239. MacDonald HR, Baschieri S, Lees RK. Clonal expansion precedes anergy and death of V beta 8+ peripheral T cells responding to staphylococcal enterotoxin B in vivo. Eur J Immunol. 1991;21: 1963–6. doi:10.1002/eji.1830210827

240. Morita CT, Li H, Lamphear JG, Rich RR, Fraser JD, Mariuzza RA, et al. Superantigen recognition by gammadelta T cells: SEA recognition site for human Vgamma2 T cell receptors. Immunity. 2001;14: 331–44. Available: http://www.ncbi.nlm.nih.gov/pubmed/11290341

241. Hayworth JL, Mazzuca DM, Maleki Vareki S, Welch I, McCormick JK, Haeryfar SMM. CD1d-independent activation of mouse and human iNKT cells by bacterial

superantigens. Immunol Cell Biol. Nature Publishing Group; 2012;90: 699–709. doi:10.1038/icb.2011.90

242. Bueno C, Criado G, McCormick JK, Madrenas J. T cell signalling induced by bacterial superantigens. Chem Immunol Allergy. 2007;93: 161–80. doi:10.1159/0000100894

243. Huang Y, Wange RL. T cell receptor signaling: beyond complex complexes. J Biol Chem. 2004;279: 28827–30. doi:10.1074/jbc.R400012200

244. Louis-Dit-Sully C, Blumenthal B, Duchniewicz M, Beck-Garcia K, Fiala GJ, Beck-García E, et al. Activation of the TCR complex by peptide-MHC and superantigens. EXS. 2014;104: 9–23. doi:10.1007/978-3-0348-0726-5_2

245. Proft T, Fraser JD. Streptococcal Superantigens: Biological properties and potential role in disease [Internet]. *Streptococcus pyogenes*: Basic Biology to Clinical Manifestations. 2016. Available: http://www.ncbi.nlm.nih.gov/pubmed/26866236

246. Langley RJ, Renno T. Superantigens. eLS. Chichester, UK: John Wiley & Sons, Ltd; 2011. pp. 1–9. doi:10.1002/9780470015902.a0001216.pub2

247. Kawabe Y, Ochi A. Programmed cell death and extrathymic reduction of Vbeta8+ CD4+ T cells in mice tolerant to *Staphylococcus aureus* enterotoxin B. Nature. 1991;349: 245–8. doi:10.1038/349245a0

248. Mccormack JE, Callahan JE, Kappler J, Marrack PC. Profound Deletion of Mature T Cells in vivo by Chronic Exposure to Exogenous Superantigens. J Immunol. 1993;150: 3785–3792.

249. Wahl C, Miethke T, Heeg K, Wagner H. Clonal deletion as direct consequence of an in vivo T cell response to bacterial superantigen. Eur J Immunol. 1993;23: 1197–200. doi:10.1002/eji.1830230536

250. Ettinger R, Panka DJ, Wang JK, Stanger BZ, Ju ST, Marshak-Rothstein A. Fas ligand-mediated cytotoxicity is directly responsible for apoptosis of normal CD4+ T cells responding to a bacterial superantigen. J Immunol. 1995;154: 4302–8. Available: http://www.ncbi.nlm.nih.gov/pubmed/1341

251. Muraille E, De Smedt T, Andris F, Pajak B, Armant M, Urbain J, et al. Staphylococcal enterotoxin B induces an early and transient state of immunosuppression characterized by V beta-unrestricted T cell unresponsiveness and defective antigen-presenting cell functions. J Immunol. 1997;158: 2638–47. Available: http://www.ncbi.nlm.nih.gov/pubmed/9058796

252. Janik DK, Lee WT. Staphylococcal Enterotoxin B (SEB) Induces Memory CD4 T Cell Anergy in vivo and Impairs Recall Immunity to Unrelated Antigens. J Clin Cell Immunol. 2015;6: 1–8. doi:10.4172/2155-9899.1000346

253. Watson ARO, Janik DK, Lee WT. Superantigen-induced CD4 memory T cell anergy. I. Staphylococcal enterotoxin B induces Fyn-mediated negative signaling. Cell Immunol. Elsevier Inc.; 2012;276: 16–25. doi:10.1016/j.cellimm.2012.02.003

254. Lussow a R, MacDonald HR. Differential effects of superantigen-induced

"anergy" on priming and effector stages of a T cell-dependent antibody response. Eur J Immunol. 1994;24: 445–449. doi:10.1002/eji.1830240227

255. Kawabe Y, Ochi A. Selective anergy of V beta 8+,CD4+ T cells in *Staphylococcus* enterotoxin B-primed mice. J Exp Med. 1990;172: 1065–1070. doi:10.1084/jem.172.4.1065

256. O'Hehir RE, Lamb JR. Induction of specific clonal anergy in human T lymphocytes by *Staphylococcus aureus* enterotoxins. Proc Natl Acad Sci U S A. 1990;87: 8884–8. Available: http://www.ncbi.nlm.nih.gov/pubmed/1978940

257. Watanabe-Ohnishi R, Low DE, McGeer A, Stevens DL, Schlievert PM, Newton D, et al. Selective depletion of V beta-bearing T cells in patients with severe invasive group A streptococcal infections and streptococcal toxic shock syndrome. Ontario Streptococcal Study Project. J Infect Dis. 1995;171: 74–84. Available: http://www.ncbi.nlm.nih.gov/pubmed/7798684

258. Michie C, Scott A, Cheesbrough J, Beverley P, Pasvol G. Streptococcal toxic shock-like syndrome: evidence of superantigen activity and its effects on T lymphocyte subsets in vivo. Clin Exp Immunol. 1994;98: 140–4. Available: http://www.ncbi.nlm.nih.gov/pubmed/7923873

259. Kanner SB, Grosmaire LS, Blake J, Schieven GL, Masewicz S, Odum N, et al. ZAP-70 and p72syk are signaling response elements through MHC class II molecules. Tissue Antigens. 1995;46: 145–54. Available: http://www.ncbi.nlm.nih.gov/pubmed/8525473

260. Sähr A, Förmer S, Hildebrand D, Heeg K. T-cell activation or tolerization: the Yin and Yang of bacterial superantigens. Front Microbiol. 2015;6: 1153. doi:10.3389/fmicb.2015.01153

261. Hopkins PA, Fraser JD, Pridmore AC, Russell HH, Read RC, Sriskandan S. Superantigen recognition by HLA class II on monocytes up-regulates toll-like receptor 4 and enhances proinflammatory responses to endotoxin. Blood. 2005;105: 3655–62. doi:10.1182/blood-2004-07-2523

262. Mooney NA, Ju L, Brick-Ghannam C, Charron DJ. Bacterial superantigen signaling via HLA class II on human B lymphocytes. Mol Immunol. 1994;31: 675–81. Available: http://www.ncbi.nlm.nih.gov/pubmed/8028602

263. Stohl W, Xu D, Zang S, Kim KS, Li L, Hanson JA, et al. In vivo staphylococcal superantigen-driven polyclonal Ig responses in mice: dependence upon CD4(+) cells and human MHC class II. Int Immunol. 2001;13: 1291–300. Available: http://www.ncbi.nlm.nih.gov/pubmed/11581174

264. Llewelyn M, Sriskandan S, Peakman M, Ambrozak DR, Douek DC, Kwok WW, et al. HLA class II polymorphisms determine responses to bacterial superantigens. J Immunol. 2004;172: 1719–26. Available: http://www.ncbi.nlm.nih.gov/pubmed/14734754

265. Norrby-Teglund A, Nepom GT, Kotb M. Differential presentation of group A streptococcal superantigens by HLA class II DQ and DR alleles. Eur J Immunol. 2002;32: 2570–7. doi:10.1002/1521-4141(200209)32:9<2570::AID-

IMMU2570>3.0.CO;2-E

266. Rajagopalan G, Polich G, Sen MM, Singh M, Epstein BE, Lytle AK, et al. Evaluating the role of HLA-DQ polymorphisms on immune response to bacterial superantigens using transgenic mice. Tissue Antigens. 2008;71: 135–45. doi:10.1111/j.1399-0039.2007.00986.x

267. Davies MR, Holden MT, Coupland P, Chen JHK, Venturini C, Barnett TC, et al. Emergence of scarlet fever *Streptococcus pyogenes* emm12 clones in Hong Kong is associated with toxin acquisition and multidrug resistance. Nat Genet. 2015;47: 84–7. doi:10.1038/ng.3147

268. Silva-Costa C, Carriço J a, Ramirez M, Melo-Cristino J. Scarlet fever is caused by a limited number of *Streptococcus pyogenes* lineages and is associated with the exotoxin genes ssa, speA and speC. Pediatr Infect Dis J. 2014;33: 306–10. doi:10.1097/INF.0000000000000088

269. Tyler SD, Johnson WM, Huang JC, Ashton FE, Wang G, Low DE, et al. Streptococcal erythrogenic toxin genes: detection by polymerase chain reaction and association with disease in strains isolated in Canada from 1940 to 1991. J Clin Microbiol. 1992;30: 3127–31. Available: http://www.ncbi.nlm.nih.gov/pubmed/1452695

270. Yu CE, Ferretti JJ. Molecular epidemiologic analysis of the type A streptococcal exotoxin (erythrogenic toxin) gene (speA) in clinical *Streptococcus pyogenes* strains. Infect Immun. 1989;57: 3715–9. Available: http://www.ncbi.nlm.nih.gov/pubmed/2553612

271. Talkington DF, Schwartz B, Black CM, Todd JK, Elliott J, Breiman RF, et al. Association of phenotypic and genotypic characteristics of invasive *Streptococcus pyogenes* isolates with clinical components of streptococcal toxic shock syndrome. Infect Immun. 1993;61: 3369–74. Available: http://www.ncbi.nlm.nih.gov/pubmed/8335368

272. Hauser AR, Stevens DL, Kaplan EL, Schlievert PM. Molecular analysis of pyrogenic exotoxins from *Streptococcus pyogenes* isolates associated with toxic shock-like syndrome. J Clin Microbiol. 1991;29: 1562–7. Available: http://www.ncbi.nlm.nih.gov/pubmed/1684795

273. Cleary PP, Kaplan EL, Handley JP, Wlazlo A, Kim MH, Hauser AR, et al. Clonal basis for resurgence of serious *Streptococcus pyogenes* disease in the 1980s. Lancet (London, England). 1992;339: 518–21. Available: http://www.ncbi.nlm.nih.gov/pubmed/1346879

274. Carapetis JR, Robins-Browne R, Martin D, Shelby-James T, Hogg G. Increasing severity of invasive group A streptococcal disease in Australia: clinical and molecular epidemiological features and identification of a new virulent M-nontypeable clone. Clin Infect Dis. 1995;21: 1220–7. doi:10.1093/clinids/21.5.1220

275. Reichardt W, Müller-Alouf H, Alouf JE, Köhler W. Erythrogenic toxins A, B and C: occurrence of the genes and exotoxin formation from clinical *Streptococcus*

pyogenes strains associated with streptococcal toxic shock-like syndrome. FEMS Microbiol Lett. 1992;100: 313–22. doi:10.1016/0378-1097(92)90227-F

276. Vlaminckx BJM, Mascini EM, Schellekens J, Schouls LM, Paauw A, Fluit AC, et al. Site-specific manifestations of invasive group a streptococcal disease: type distribution and corresponding patterns of virulence determinants. J Clin Microbiol. 2003;41: 4941–9. doi:10.1128/JCM.41.11.4941

277. Ikebe T, Wada A, Inagaki Y, Sugama K, Suzuki R, Tanaka D, et al. Dissemination of the phage-associated novel superantigen gene speL in recent invasive and noninvasive *Streptococcus pyogenes* M3/T3 isolates in Japan. Infect Immun. 2002;70: 3227–33. doi:10.1128/IAI.70.6.3227-3233.2002

278. Murakami J, Kawabata S, Terao Y, Kikuchi K, Totsuka K, Tamaru A, et al. Distribution of emm genotypes and superantigen genes of *Streptococcus pyogenes* isolated in Japan, 1994-9. Epidemiol Infect. 2002;128: 397–404. doi:10.1017/S0950268802006854

279. Friães A, Pinto FR, Silva-Costa C, Ramirez M, Melo-Cristino J. Group A streptococci clones associated with invasive infections and pharyngitis in Portugal present differences in emm types, superantigen gene content and antimicrobial resistance. BMC Microbiol. 2012;12: 280. doi:10.1186/1471-2180-12-280

280. Lintges M, van der Linden M, Hilgers R-D, Arlt S, Al-Lahham A, Reinert RR, et al. Superantigen genes are more important than the emm type for the invasiveness of group A *Streptococcus* infection. J Infect Dis. 2010;202: 20–8. doi:10.1086/653082

281. Descheemaeker P, Van Loock F, Hauchecorne M, Vandamme P, Goossens H. Molecular characterisation of group A streptococci from invasive and non-invasive disease episodes in Belgium during 1993-1994. J Med Microbiol. 2000;49: 467–71. doi:10.1099/0022-1317-49-5-467

282. Haukness HA, Tanz RR, Thomson RB, Pierry DK, Kaplan EL, Beall B, et al. The heterogeneity of endemic community pediatric group a streptococcal pharyngeal isolates and their relationship to invasive isolates. J Infect Dis. 2002;185: 915–20. doi:10.1086/339407

283. Hsueh PR, Wu JJ, Tsai PJ, Liu JW, Chuang YC, Luh KT. Invasive group A streptococcal disease in Taiwan is not associated with the presence of streptococcal pyrogenic exotoxin genes. Clin Infect Dis. 1998;26: 584–9. Available: http://www.ncbi.nlm.nih.gov/pubmed/9524827

284. Mylvaganam H, Bjorvatn B, Osland A. Distribution and sequence variations of selected virulence genes among group A streptococcal isolates from western Norway. APMIS. 2000;108: 771–8. Available: http://www.ncbi.nlm.nih.gov/pubmed/11211972

285. Sriskandan S, Moyes D, Cohen J. Detection of circulating bacterial superantigen and lymphotoxin-alpha in patients with streptococcal toxic-shock syndrome. Lancet (London, England). 1996;348: 1315–6. Available: http://www.ncbi.nlm.nih.gov/pubmed/8909404

286. Eriksson BK, Andersson J, Holm SE, Norgren M. Invasive group A streptococcal infections: T1M1 isolates expressing pyrogenic exotoxins A and B in combination with selective lack of toxin-neutralizing antibodies are associated with increased risk of streptococcal toxic shock syndrome. J Infect Dis. 1999;180: 410–8. doi:10.1086/314872

287. Basma H, Norrby-Teglund A, Guedez Y, McGeer A, Low DE, El-Ahmedy O, et al. Risk factors in the pathogenesis of invasive group A streptococcal infections: role of protective humoral immunity. Infect Immun. 1999;67: 1871–7. Available: http://www.ncbi.nlm.nih.gov/pubmed/10085030

288. Thomas D, Perpoint T, Dauwalder O, Lina G, Floccard B, Richard J-C, et al. In vivo and in vitro detection of a superantigenic toxin Vbeta signature in two forms of streptococcal toxic shock syndrome. Eur J Clin Microbiol Infect Dis. 2009;28: 671–6. doi:10.1007/s10096-008-0671-7

289. Takahashi K, Oharaseki T, Yokouchi Y. Update on etio and immunopathogenesis of Kawasaki disease. Curr Opin Rheumatol. 2014;26: 31–6. doi:10.1097/BOR.0000000000000010

290. Abe J, Kotzin BL, Jujo K, Melish ME, Glode MP, Kohsaka T, et al. Selective expansion of T cells expressing T-cell receptor variable regions V beta 2 and V beta 8 in Kawasaki disease. Proc Natl Acad Sci U S A. 1992;89: 4066–70. Available: http://www.pubmedcentral.nih.gov/articlerender.fcgi?artid=525633&tool=pmcentrez&rendertype=abstract

291. Konishi N, Baba K, Abe J, Maruko T, Waki K, Takeda N, et al. A case of Kawasaki disease with coronary artery aneurysms documenting *Yersinia pseudotuberculosis* infection. Acta Paediatr. 1997;86: 661–4. Available: http://www.ncbi.nlm.nih.gov/pubmed/9202805

292. Yoshioka T, Matsutani T, Iwagami S, Toyosaki-Maeda T, Yutsudo T, Tsuruta Y, et al. Polyclonal expansion of TCRBV2- and TCRBV6-bearing T cells in patients with Kawasaki disease. Immunology. 1999;96: 465–72. doi:10.1046/j.1365-2567.1999.00695.x

293. Matsubara K, Fukaya T, Miwa K, Shibayama N, Nigami H, Harigaya H, et al. Development of serum IgM antibodies against superantigens of *Staphylococcus aureus* and *Streptococcus pyogenes* in Kawasaki disease. Clin Exp Immunol. 2006;143: 427–34. doi:10.1111/j.1365-2249.2006.03015.x

294. Suenaga T, Suzuki H, Shibuta S, Takeuchi T, Yoshikawa N. Detection of multiple superantigen genes in stools of patients with Kawasaki disease. J Pediatr. Mosby, Inc.; 2009;155: 266–70. doi:10.1016/j.jpeds.2009.03.013

295. Brogan PA, Shah V, Clarke LA, Dillon MJ, Klein N. T cell activation profiles in Kawasaki syndrome. Clin Exp Immunol. 2008;151: 267–74. doi:10.1111/j.1365-2249.2007.03567.x

296. Nagata S, Yamashiro Y, Ohtsuka Y, Shimizu T, Sakurai Y, Misawa S, et al. Heat shock proteins and superantigenic properties of bacteria from the gastrointestinal

tract of patients with Kawasaki disease. Immunology. 2009;128: 511–20. doi:10.1111/j.1365-2567.2009.03135.x

297. Gupta-Malhotra M, Viteri-Jackson A, Thomas W, Zabriskie JB. Antibodies to highly conserved peptide sequence of staphylococcal and streptococcal superantigens in Kawasaki disease. Exp Mol Pathol. 2004;76: 117–21. doi:10.1016/j.yexmp.2003.12.003

298. Morita A, Imada Y, Igarashi H, Yutsudo T. Serologic evidence that streptococcal superantigens are not involved in the pathogenesis of Kawasaki disease. Microbiol Immunol. 1997;41: 895–900. Available: http://www.ncbi.nlm.nih.gov/pubmed/9444333

299. Nomura Y, Yoshinaga M, Masuda K, Takei S, Miyata K. Maternal antibody against toxic shock syndrome toxin-1 may protect infants younger than 6 months of age from developing Kawasaki syndrome. J Infect Dis. 2002;185: 1677–80. doi:10.1086/340513

300. Lee HH, Park IH, Shin J-S, Shin JS, Kim DS. Immunoglobulin V(H) chain gene analysis of peripheral blood IgM-producing B cells in patients with Kawasaki disease. Yonsei Med J. 2009;50: 493–504. doi:10.3349/ymj.2009.50.4.493

301. Nahary L, Tamarkin A, Kayam N, Sela S, Fry L, Baker B, et al. An investigation of antistreptococcal antibody responses in guttate psoriasis. Arch Dermatol Res. 2008;300: 441–9. doi:10.1007/s00403-008-0866-x

302. Leung DYM, Travers JB, Giorno R, Norris DA, Skinner R, Aelion J, et al. Evidence for a streptococcal superantigen-driven process in acute Guttate psoriasis. J Clin Invest. 1995;96: 2106–2112. doi:10.1172/JCI118263

303. Lewis HM, Baker BS, Bokth S, Powles a V, Garioch JJ, Valdimarsson H, et al. Restricted T-cell receptor V beta gene usage in the skin of patients with guttate and chronic plaque psoriasis. Br J Dermatol. 1993;129: 514–20. Available: http://www.ncbi.nlm.nih.gov/pubmed/8251347

304. Davison SC, Allen MH, Mallon E, Barker JN. Contrasting patterns of streptococcal superantigen-induced T-cell proliferation in guttate vs. chronic plaque psoriasis. Br J Dermatol. 2001;145: 245–51. doi:10.1046/j.1365-2133.2001.04341.x

305. Valdimarsson H, Thorleifsdottir RH, Sigurdardottir SL, Gudjonsson JE, Johnston A. Psoriasis--as an autoimmune disease caused by molecular mimicry. Trends Immunol. 2009;30: 494–501. doi:10.1016/j.it.2009.07.008

306. Smoot JC, Barbian KD, Van Gompel JJ, Smoot LM, Chaussee MS, Sylva GL, et al. Genome sequence and comparative microarray analysis of serotype M18 group A *Streptococcus* strains associated with acute rheumatic fever outbreaks. Proc Natl Acad Sci U S A. 2002;99: 4668–73. doi:10.1073/pnas.062526099

307. Smoot LM, McCormick JK, Smoot JC, Hoe NP, Strickland I, Cole RL, et al. Characterization of two novel pyrogenic toxin superantigens made by an acute rheumatic fever clone of *Streptococcus pyogenes* associated with multiple disease outbreaks. Infect Immun. 2002;70: 7095–104. doi:10.1128/IAI.70.12.7095

308. Yang LPH, Eriksson BKG, Harrington Z, Curtis N, Lang S, Currie BJ, et al. Variations in the protective immune response against streptococcal superantigens in populations of different ethnicity. Med Microbiol Immunol. 2006;195: 37–43. doi:10.1007/s00430-005-0245-6

309. Hynes W, Sloan M. Secreted Extracellular Virulence Factors [Internet]. *Streptococcus pyogenes*: Basic Biology to Clinical Manifestations. 2016. Available: http://www.ncbi.nlm.nih.gov/pubmed/26866214

310. Vega LA, Malke H, McIver KS. Virulence-Related Transcriptional Regulators of *Streptococcus pyogenes* [Internet]. *Streptococcus pyogenes*: Basic Biology to Clinical Manifestations. 2016. Available: http://www.ncbi.nlm.nih.gov/pubmed/26866215

311. Gryllos I, Levin JC, Wessels MR. The CsrR/CsrS two-component system of group A *Streptococcus* responds to environmental Mg2+. Proc Natl Acad Sci U S A. 2003;100: 4227–32. doi:10.1073/pnas.0636231100

312. Gryllos I, Tran-Winkler HJ, Cheng M-F, Chung H, Bolcome R, Lu W, et al. Induction of group A *Streptococcus* virulence by a human antimicrobial peptide. Proc Natl Acad Sci U S A. 2008;105: 16755–60. doi:10.1073/pnas.0803815105

313. Miller AA, Engleberg NC, DiRita VJ. Repression of virulence genes by phosphorylation-dependent oligomerization of CsrR at target promoters in S. *pyogenes*. Mol Microbiol. 2001;40: 976–90. doi:10.1046/j.1365-2958.2001.02441.x

314. Gusa AA, Gao J, Stringer V, Churchward G, Scott JR. Phosphorylation of the group A Streptococcal CovR response regulator causes dimerization and promoter-specific recruitment by RNA polymerase. J Bacteriol. 2006;188: 4620–6. doi:10.1128/JB.00198-06

315. Engleberg NC, Heath A, Miller A, Rivera C, DiRita VJ. Spontaneous mutations in the CsrRS two-component regulatory system of *Streptococcus pyogenes* result in enhanced virulence in a murine model of skin and soft tissue infection. J Infect Dis. 2001;183: 1043–54. doi:10.1086/319291

316. Cole JN, Barnett TC, Nizet V, Walker MJ. Molecular insight into invasive group A streptococcal disease. Nat Rev Microbiol. Nature Publishing Group; 2011;9: 724–736. doi:10.1038/nrmicro2648

317. Spanier JG, Jones SJ, Cleary PP. Small DNA deletions creating avirulence in *Streptococcus pyogenes*. Science. 1984;225: 935–8. Available: http://www.ncbi.nlm.nih.gov/pubmed/6089334

318. Caparon MG, Scott JR. Identification of a gene that regulates expression of M protein, the major virulence determinant of group A streptococci. Proc Natl Acad Sci U S A. 1987;84: 8677–81. doi:10.1073/pnas.84.23.8677

319. Chen C, Bormann N, Patrick Cleary P. VirR and Mry are homologous trans-acting regulators of M protein and C5a peptidase expression in group A streptococci. MGG Mol Gen Genet. 1993;241–241: 685–693. doi:10.1007/BF00279912

320. Scott JR, Cleary PP, Caparon MG, Kehoe M, Heden L, Musser JM, et al. New name for the positive regulator of the M protein of group A *Streptococcus*. Mol Microbiol. 1995;17: 799. Available: http://www.ncbi.nlm.nih.gov/pubmed/8801432

321. Podbielski A. Ubiquitous occurrence of virR and scpA genes in group A streptococci. Med Microbiol Immunol. 1992;181: 227–40. doi:10.1007/BF00215768

322. Bessen DE, Manoharan A, Luo F, Wertz JE, Robinson DA. Evolution of transcription regulatory genes is linked to niche specialization in the bacterial pathogen *Streptococcus pyogenes*. J Bacteriol. 2005;187: 4163–72. doi:10.1128/JB.187.12.4163-4172.2005

323. Geyer A, Schmidt KH. Genetic organisation of the M protein region in human isolates of group C and G streptococci: two types of multigene regulator-like (mgrC) regions. Mol Gen Genet. 2000;262: 965–76. Available: http://www.ncbi.nlm.nih.gov/pubmed/10660058

324. Vahling CM, McIver KS. Domains required for transcriptional activation show conservation in the mga family of virulence gene regulators. J Bacteriol. 2006;188: 863–73. doi:10.1128/JB.188.3.863-873.2006

325. Musser JM, DeLeo FR. Toward a genome-wide systems biology analysis of host-pathogen interactions in group A *Streptococcus*. Am J Pathol. American Society for Investigative Pathology; 2005;167: 1461–72. doi:10.1016/S0002-9440(10)61232-1

326. Terao Y, Kawabata S, Kunitomo E, Murakami J, Nakagawa I, Hamada S. Fba, a novel fibronectin-binding protein from *Streptococcus pyogenes*, promotes bacterial entry into epithelial cells, and the fba gene is positively transcribed under the Mga regulator. Mol Microbiol. 2001;42: 75–86. doi:10.1046/j.1365-2958.2001.02579.x

327. Virtaneva K, Porcella SF, Graham MR, Ireland RM, Johnson C a, Ricklefs SM, et al. Longitudinal analysis of the group A *Streptococcus* transcriptome in experimental pharyngitis in cynomolgus macaques. Proc Natl Acad Sci U S A. 2005;102: 9014–9019.

328. Kihlberg BM, Cooney J, Caparon MG, Olsén A, Björck L. Biological properties of a *Streptococcus pyogenes* mutant generated by Tn916 insertion in mga. Microb Pathog. 1995;19: 299–315. doi:10.1016/S0882-4010(96)80003-9

329. Granok AB, Parsonage D, Ross RP, Caparon MG. The RofA binding site in *Streptococcus pyogenes* is utilized in multiple transcriptional pathways. J Bacteriol. 2000;182: 1529–40. doi:10.1128/JB.182.6.1529-1540.2000

330. Podbielski A, Woischnik M, Leonard BA, Schmidt KH. Characterization of nra, a global negative regulator gene in group A streptococci. Mol Microbiol. 1999;31: 1051–64. doi:10.1046/j.1365-2958.1999.01241.x

331. Patti JM, Höök M. Microbial adhesins recognizing extracellular matrix macromolecules. Curr Opin Cell Biol. 1994;6: 752–8. Available: http://www.ncbi.nlm.nih.gov/pubmed/7833055

332. Kreikemeyer B, Beckert S, Braun-Kiewnick A, Podbielski A. Group A streptococcal RofA-type global regulators exhibit a strain-specific genomic presence and regulation pattern. Microbiology. 2002;148: 1501–11. doi:10.1099/00221287-148-5-1501

333. Beckert S, Kreikemeyer B, Podbielski A. Group A streptococcal rofA gene is involved in the control of several virulence genes and eukaryotic cell attachment and internalization. Infect Immun. 2001;69: 534–7. doi:10.1128/IAI.69.1.534-537.2001

334. Molinari G, Rohde M, Talay SR, Chhatwal GS, Beckert S, Podbielski A. The role played by the group A streptococcal negative regulator Nra on bacterial interactions with epithelial cells. Mol Microbiol. 2001;40: 99–114. doi:10.1046/j.1365-2958.2001.02373.x

335. Chaussee MS, Ajdic D, Ferretti JJ. The rgg gene of *Streptococcus pyogenes* NZ131 positively influences extracellular SPE B production. Infect Immun. 1999;67: 1715–22. Available: http://www.ncbi.nlm.nih.gov/pubmed/10085009

336. Lyon WR, Gibson CM, Caparon MG. A role for trigger factor and an rgg-like regulator in the transcription, secretion and processing of the cysteine proteinase of *Streptococcus pyogenes*. EMBO J. 1998;17: 6263–75. doi:10.1093/emboj/17.21.6263

337. Sulavik MC, Tardif G, Clewell DB. Identification of a gene, rgg, which regulates expression of glucosyltransferase and influences the Spp phenotype of *Streptococcus gordonii* Challis. J Bacteriol. 1992;174: 3577–86. Available: http://www.ncbi.nlm.nih.gov/pubmed/1534326

338. Fujiwara T, Hoshino T, Ooshima T, Sobue S, Hamada S. Purification, characterization, and molecular analysis of the gene encoding glucosyltransferase from *Streptococcus* oralis. Infect Immun. 2000;68: 2475–83. Available: http://www.pubmedcentral.nih.gov/articlerender.fcgi?artid=97449&tool=pmcentrez&rendertype=abstract

339. Vickerman MM, Sulavik MC, Clewell DB. Oral streptococci with genetic determinants similar to the glucosyltransferase regulatory gene, rgg. Infect Immun. 1995;63: 4524–7. Available: http://www.ncbi.nlm.nih.gov/pubmed/7591096

340. Qi F, Chen P, Caufield PW. Purification and biochemical characterization of mutacin I from the group I strain of *Streptococcus* mutans, CH43, and genetic analysis of mutacin I biosynthesis genes. Appl Environ Microbiol. 2000;66: 3221–9. doi:10.1128/AEM.66.8.3221-3229.2000

341. Sanders JW, Leenhouts K, Burghoorn J, Brands JR, Venema G, Kok J. A chloride-inducible acid resistance mechanism in {{\textless}i{\textgreater}Lactococcus} lactis{\textless}/i{\textgreater} and its regulation. Mol Microbiol. 1998;27: 299–310. doi:10.1046/j.1365-2958.1998.00676.x

342. Dmitriev A V, McDowell EJ, Chaussee MS. Inter- and intraserotypic variation in the *Streptococcus pyogenes* Rgg regulon. FEMS Microbiol Lett. 2008;284: 43–51. doi:10.1111/j.1574-6968.2008.01171.x

343. Dmitriev A V., McDowell EJ, Kappeler K V., Chaussee MA, Rieck LD, Chaussee MS. The Rgg regulator of *Streptococcus pyogenes* influences utilization of nonglucose carbohydrates, prophage induction, and expression of the NAD-glycohydrolase virulence operon. J Bacteriol. 2006;188: 7230–41. doi:10.1128/JB.00877-06

344. Chaussee MS, Somerville G a, Reitzer L, Musser JM. Rgg coordinates virulence factor synthesis and metabolism in *Streptococcus pyogenes*. J Bacteriol. 2003;185: 6016–24. doi:10.1128/JB.185.20.6016

345. Chaussee MS, Watson RO, Smoot JC, Musser JM. Identification of Rgg-regulated exoproteins of *Streptococcus pyogenes*. Infect Immun. 2001;69: 822–31. doi:10.1128/IAI.69.2.822-831.2001

346. Chaussee MS, Sylva GL, Sturdevant DE, Smoot LM, Graham MR, Watson RO, et al. Rgg influences the expression of multiple regulatory loci to coregulate virulence factor expression in *Streptococcus pyogenes*. Infect Immun. 2002;70: 762–70. doi:10.1128/IAI.70.2.762

347. Chaussee MA, Callegari EA, Chaussee MS. Rgg regulates growth phase-dependent expression of proteins associated with secondary metabolism and stress in *Streptococcus pyogenes*. J Bacteriol. 2004;186: 7091–9. doi:10.1128/JB.186.21.7091-7099.2004

348. Cheng S, Baisch J, Krco C, Savarirayan S, Hanson J, Hodgson K, et al. Expression and function of HLA-DQ8 (DQA1*0301/DQB1*0302) genes in transgenic mice. Eur J Immunogenet. 1996;23: 15–20. Available: http://www.ncbi.nlm.nih.gov/pubmed/8834919

349. Bunce C, Wheeler L, Reed G, Musser JM, Barg N. Murine model of cutaneous infection with gram-positive cocci. Infect Immun. 1992;60: 2636–40. Available: http://www.ncbi.nlm.nih.gov/pubmed/1612733

350. Raeder R, Boyle MD. Association between expression of immunoglobulin G-binding proteins by group A streptococci and virulence in a mouse skin infection model. Infect Immun. 1993;61: 1378–84. Available: http://www.ncbi.nlm.nih.gov/pubmed/8454339

351. Schrager HM, Rheinwald JG, Wessels MR. Hyaluronic acid capsule and the role of streptococcal entry into keratinocytes in invasive skin infection. J Clin Invest. 1996;98: 1954–8. doi:10.1172/JCI118998

352. Bisno AL, Gaviria JM. Murine model of recurrent group G streptococcal cellulitis: no evidence of protective immunity. Infect Immun. 1997;65: 4926–30. Available: http://www.ncbi.nlm.nih.gov/pubmed/9393777

353. J FM, Smith MR, Wood WB. Studies on the pathogenicity of group A Streptococci. I. Its relation to surface phagocytosis. J Exp Med. 1959;110: 603–16. Available: http://www.ncbi.nlm.nih.gov/pubmed/13823727

354. Dileepan T, Linehan JL, Moon JJ, Pepper M, Jenkins MK, Cleary PP. Robust antigen specific th17 T cell response to group A *Streptococcus* is dependent on IL-6 and intranasal route of infection. PLoS Pathog. 2011;7: e1002252.

doi:10.1371/journal.ppat.1002252

355. Wong CJ, Stevens DL. Serious group a streptococcal infections. Med Clin North Am. 2013;97: 721–36, xi–xii. doi:10.1016/j.mcna.2013.03.003

356. Rantala S, Vuopio-Varkila J, Vuento R, Huhtala H, Syrjänen J. Clinical presentations and epidemiology of beta-haemolytic streptococcal bacteraemia: a population-based study. Clin Microbiol Infect. 2009;15: 286–8. doi:10.1111/j.1469-0691.2008.02672.x

357. Roberts S, Scott JR, Husmann LK, Zurawski CA. Murine models of *Streptococcus pyogenes* infection. Curr Protoc Microbiol. 2006;Chapter 9: Unit 9D.5. doi:10.1002/9780471729259.mc09d05s02

358. Husmann LK, Dillehay DL, Jennings VM, Scott JR. *Streptococcus pyogenes* infection in mice. Microb Pathog. 1996;20: 213–24. doi:10.1006/mpat.1996.0020

359. Husmann LK, Yung DL, Hollingshead SK, Scott JR. Role of putative virulence factors of *Streptococcus pyogenes* in mouse models of long-term throat colonization and pneumonia. Infect Immun. 1997;65: 1422–30. Available: http://www.ncbi.nlm.nih.gov/pubmed/9119483

360. Medina E, Goldmann O, Rohde M, Lengeling A, Chhatwals GS. Genetic Control of Susceptibility to Group A Streptococcal Infection in Mice. J Infect Dis. 2001;184: 846–852. doi:10.1086/323292

361. Lavoie PM, Thibodeau J, Erard F, Sékaly RP. Understanding the mechanism of action of bacterial superantigens from a decade of research. Immunol Rev. 1999;168: 257–69. doi:10.1111/j.1600-065X.1999.tb01297.x

362. Lowell GH, Kaminski RW, Grate S, Hunt RE, Charney C, Zimmer S, et al. Intranasal and intramuscular proteosome-staphylococcal enterotoxin B (SEB) toxoid vaccines: immunogenicity and efficacy against lethal SEB intoxication in mice. Infect Immun. 1996;64: 1706–1713.

363. Chen JY, Qiao Y, Komisar JL, Baze WB, Hsu IC, Tseng J. Increased susceptibility to staphylococcal enterotoxin B intoxication in mice primed with actinomycin D. Infect Immun. 1994;62: 4626–31. Available: http://www.ncbi.nlm.nih.gov/pubmed/7927730

364. Keppler D, Decker K. Studies on the mechanism of galactosamine-1-phosphate and its inhibition of UDP-glucose pyrophosphorylase. Eur J Biochem. 1969;10: 219–25. Available: http://www.ncbi.nlm.nih.gov/pubmed/5823097

365. Keppler D, Lesch R, Reutter W, Decker K. Experimental hepatitis induced by D-galactosamine. Exp Mol Pathol. 1968;9: 279–90. doi:10.1016/0014-4800(68)90042-7

366. Record CO, Alberti KG, Williamson DH. Metabolic studies in experimental liver disease resulting from D(+)-galactosamine administration. Biochem J. 1972;130: 37–44. Available: http://www.pubmedcentral.nih.gov/articlerender.fcgi?artid=1174298&tool=pmcentrez&rendertype=abstract

367. Silverstein R. D-galactosamine lethality model: scope and limitations. J Endotoxin Res. 2004;10: 147–62. doi:10.1179/096805104225004879

368. Tilahun AY, Marietta E V, Wu T-T, Patel R, David CS, Rajagopalan G. Human leukocyte antigen class II transgenic mouse model unmasks the significant extrahepatic pathology in toxic shock syndrome. Am J Pathol. 2011;178: 2760–2773. doi:10.1016/j.ajpath.2011.02.033

369. Nooh MM, El-Gengehi N, Kansal R, David CS, Kotb M. HLA transgenic mice provide evidence for a direct and dominant role of HLA class II variation in modulating the severity of streptococcal sepsis. J Immunol. 2007;178: 3076–83. Available: http://www.ncbi.nlm.nih.gov/pubmed/17312154

370. Sriskandan S, Unnikrishnan M, Krausz T, Dewchand H, Van Noorden S, Cohen J, et al. Enhanced susceptibility to superantigen-associated streptococcal sepsis in human leukocyte antigen-DQ transgenic mice. J Infect Dis. 2001;184: 166–173.

371. Kotb M, Norrby-Teglund A, McGeer A, El-Sherbini H, Dorak MT, Khurshid A, et al. An immunogenetic and molecular basis for differences in outcomes of invasive group A streptococcal infections. Nat Med. 2002;8: 1398–404. doi:10.1038/nm800

372. Asanuma H, Thompson a H, Iwasaki T, Sato Y, Inaba Y, Aizawa C, et al. Isolation and characterization of mouse nasal-associated lymphoid tissue. J Immunol Methods. 1997;202: 123–31. Available: http://www.ncbi.nlm.nih.gov/pubmed/9107301

373. Koornstra PJ, de Jong FI, Vlek LF, Marres EH, van Breda Vriesman PJ. The Waldeyer ring equivalent in the rat. A model for analysis of oronasopharyngeal immune responses. Acta Otolaryngol. 1991;111: 591–9. Available: http://www.ncbi.nlm.nih.gov/pubmed/1887785

374. Kuper CF, Koornstra PJ, Hameleers DM, Biewenga J, Spit BJ, Duijvestijn AM, et al. The role of nasopharyngeal lymphoid tissue. Immunol Today. 1992;13: 219–24. Available: http://www.ncbi.nlm.nih.gov/pubmed/1627250

375. Park H, Francis KP, Yu J, Cleary PP. Membranous Cells in Nasal-Associated Lymphoid Tissue: A Portal of Entry for the Respiratory Mucosal Pathogen Group A *Streptococcus*. J Immunol. 2003;171: 2532–2537.

376. Alam FM, Turner CE, Smith K, Wiles S, Sriskandan S. Inactivation of the CovR/S virulence regulator impairs infection in an improved murine model of *Streptococcus pyogenes* naso-pharyngeal infection. PLoS One. 2013;8: e61655. doi:10.1371/journal.pone.0061655

377. Kasper KJ, Zeppa JJ, Wakabayashi AT, Xu SX, Mazzuca DM, Welch I, et al. Bacterial Superantigens Promote Acute Nasopharyngeal Infection by *Streptococcus pyogenes* in a Human MHC Class II-Dependent Manner. PLoS Pathog. 2014;10: e1004155. doi:10.1371/journal.ppat.1004155

378. Alam FM, Bateman C, Turner CE, Wiles S, Sriskandan S. Non-invasive monitoring of *Streptococcus pyogenes* vaccine efficacy using biophotonic imaging. PLoS One. 2013;8: e82123. doi:10.1371/journal.pone.0082123

379. Park H-S, Costalonga M, Reinhardt RL, Dombek PE, Jenkins MK, Cleary PP. Primary induction of CD4 T cell responses in nasal associated lymphoid tissue during group A streptococcal infection. Eur J Immunol. 2004;34: 2843–53. doi:10.1002/eji.200425242

380. Wang B, Dileepan T, Briscoe S, Hyland K a, Kang J, Khoruts A, et al. Induction of TGF-beta1 and TGF-beta1-dependent predominant Th17 differentiation by group A streptococcal infection. Proc Natl Acad Sci U S A. 2010;107: 5937–42. doi:10.1073/pnas.0904831107

381. Fan X, Wang X, Li N, Cui H, Hou B, Gao B, et al. Sortase A induces Th17-mediated and antibody-independent immunity to heterologous serotypes of group A streptococci. PLoS One. 2014;9: e107638. doi:10.1371/journal.pone.0107638

382. Park H-S, Cleary PP. Active and passive intranasal immunizations with streptococcal surface protein C5a peptidase prevent infection of murine nasal mucosa-associated lymphoid tissue, a functional homologue of human tonsils. Infect Immun. 2005;73: 7878–7886. doi:10.1128/IAI.73.12.7878

383. Stricker T, Navratil F, Sennhauser FH. Vulvovaginitis in prepubertal girls. Arch Dis Child. 2003;88: 324–6. doi:10.1136/adc.88.4.324

384. Berkelman RL, Martin D, Graham DR, Mowry J, Freisem R, Weber JA, et al. Streptococcal wound infections caused by a vaginal carrier. JAMA. 1982;247: 2680–2. Available: http://www.ncbi.nlm.nih.gov/pubmed/7043001

385. Stamm WE, Feeley JC, Facklam RR. Wound infections due to group A *Streptococcus* traced to a vaginal carrier. J Infect Dis. 1978;138: 287–92. Available: http://www.ncbi.nlm.nih.gov/pubmed/359723

386. Sheen TR, Jimenez A, Wang N-Y, Banerjee A, van Sorge NM, Doran KS. Serine-rich repeat proteins and pili promote *Streptococcus agalactiae* colonization of the vaginal tract. J Bacteriol. 2011;193: 6834–42. doi:10.1128/JB.00094-11

387. Jerse AE. Experimental gonococcal genital tract infection and opacity protein expression in estradiol-treated mice. Infect Immun. 1999;67: 5699–708. Available: http://www.ncbi.nlm.nih.gov/pubmed/10531218

388. Fidel PL, Lynch ME, Sobel JD. Candida-specific Th1-type responsiveness in mice with experimental vaginal candidiasis. Infect Immun. 1993;61: 4202–7. Available: http://www.ncbi.nlm.nih.gov/pubmed/8406809

389. Watson ME, Nielsen H V, Hultgren SJ, Caparon MG. Murine vaginal colonization model for investigating asymptomatic mucosal carriage of *Streptococcus pyogenes*. Infect Immun. 2013;81: 1606–17. doi:10.1128/IAI.00021-13

390. Cusumano ZT, Watson ME, Caparon MG. *Streptococcus pyogenes* arginine and citrulline catabolism promotes infection and modulates innate immunity. Infect Immun. 2014;82: 233–42. doi:10.1128/IAI.00916-13

391. Stevens DL, Bryant a. E, Hackett SP, Chang A, Peer G, Kosanke S, et al. Group A streptococcal bacteremia: the role of tumor necrosis factor in shock and organ failure. J Infect Dis. 1996;173: 619–26. doi:10.1093/infdis/173.3.619

392. Nasser W, Beres SB, Olsen RJ, Dean M a., Rice K a., Long SW, et al. Evolutionary pathway to increased virulence and epidemic group A *Streptococcus* disease derived from 3,615 genome sequences. Proc Natl Acad Sci. 2014;111: E1768–E1776. doi:10.1073/pnas.1403138111

393. Olsen RJ, Sitkiewicz I, Ayeras AA, Gonulal VE, Cantu C, Beres SB, et al. Decreased necrotizing fasciitis capacity caused by a single nucleotide mutation that alters a multiple gene virulence axis. Proc Natl Acad Sci U S A. 2010;107: 888–93. doi:10.1073/pnas.0911811107

394. Flores AR, Jewell BE, Olsen RJ, Shelburne S a, Fittipaldi N, Beres SB, et al. Asymptomatic carriage of group A *Streptococcus* is associated with elimination of capsule production. Infect Immun. 2014; doi:10.1128/IAI.01788-14

395. Taranta A, Spagnuolo M, Davidson M, Goldstein G, Uhr JW. Experimental streptococcal infections in baboons. Transplant Proc. 1969;1: 992–3. Available: http://www.ncbi.nlm.nih.gov/pubmed/5406380

396. Ashbaugh CD, Moser TJ, Shearer MH, White GL, Kennedy RC, Wessels MR. Bacterial determinants of persistent throat colonization and the associated immune response in a primate model of human group A streptococcal pharyngeal infection. Cell Microbiol. 2000;2: 283–92. Available: http://www.ncbi.nlm.nih.gov/pubmed/11207585

397. VANACE PW. Experimental streptococcal infection in the rhesus monkey. Ann N Y Acad Sci. 1960;85: 910–30. Available: http://www.ncbi.nlm.nih.gov/pubmed/13780084

398. Watson RF, Rothbard S, Swift HF, Technical Assistance of Gilbert de Mello. Type-specific protection and immunity following intranasal inoculation of monkeys with group A hemolytic streptococci. J Exp Med. 1946;84: 127–42. Available: http://www.ncbi.nlm.nih.gov/pubmed/19871558

399. Krushak DH, Zimmerman RA, Murphy BL. Induced group A beta-hemolytic streptococcic infection in chimpanzees. J Am Vet Med Assoc. 1970;157: 742–4. Available: http://www.ncbi.nlm.nih.gov/pubmed/5452082

400. Zimmerman RA, Krushak DH, Wilson E, Douglas JD. Human streptococcal disease syndrome compared with observations in chimpanzees. II. Immunologic responses to induced pharyngitis and the effect of treatment. J Infect Dis. 1970;122: 280–9. doi:10.1093/infdis/122.4.280

401. Sumby P, Tart AH, Musser JM. A non-human primate model of acute group a *Streptococcus* pharyngitis. Methods Mol Biol. 2008;431: 255–267.

402. FRIOU GJ. Experimental infection of the upper respiratory tract of young chimpanzees with group A hemolytic streptococci. J Infect Dis. 1950;86: 264–74. Available: http://www.ncbi.nlm.nih.gov/pubmed/15415631

403. Virtaneva K, Graham MR, Porcella SF, Hoe NP, Su H, Graviss EA, et al. Group A *Streptococcus* gene expression in humans and cynomolgus macaques with acute pharyngitis. Infect Immun. 2003;71: 2199–207. doi:10.1128/IAI.71.4.2199

404. Shea PR, Virtaneva K, Kupko JJ, Porcella SF, Barry WT, Wright F a, et al. Interactome analysis of longitudinal pharyngeal infection of cynomolgus macaques by group A *Streptococcus*. Proc Natl Acad Sci U S A. 2010;107: 4693–8. doi:10.1073/pnas.0906384107

405. Zhu L, Olsen RJ, Nasser W, Beres SB, Vuopio J, Kristinsson KG, et al. A molecular trigger for intercontinental epidemics of group A *Streptococcus*. J Clin Invest. 2015;125: 3545–59. doi:10.1172/JCI82478

406. Shelburne S a, Sumby P, Sitkiewicz I, Okorafor N, Granville C, Patel P, et al. Maltodextrin utilization plays a key role in the ability of group A *Streptococcus* to colonize the oropharynx. Infect Immun. 2006;74: 4605–14. doi:10.1128/IAI.00477-06

407. Gryllos I, Cywes C, Shearer MH, Cary M, Kennedy RC, Wessels MR. Regulation of capsule gene expression by group A *Streptococcus* during pharyngeal colonization and invasive infection. Mol Microbiol. 2001;42: 61–74.

408. Cunningham MW. Post-Streptococcal Autoimmune Sequelae: Rheumatic Fever and Beyond [Internet]. *Streptococcus pyogenes*: Basic Biology to Clinical Manifestations. 2016. Available: http://www.ncbi.nlm.nih.gov/pubmed/26866235

409. Cunningham MW. Rheumatic fever, autoimmunity, and molecular mimicry: the streptococcal connection. Int Rev Immunol. 2014;33: 314–29. doi:10.3109/08830185.2014.917411

410. Massell BF, Michael JG, Amezcua J, Siner M. Secondary and apparent primary antibody responses after group A streptococcal vaccination of 21 children. Appl Microbiol. 1968;16: 509–18. Available: http://www.pubmedcentral.nih.gov/articlerender.fcgi?artid=547450&tool=pmcentrez&rendertype=abstract

411. Massell BF, Honikman LH, Amezcua J. Rheumatic fever following streptococcal vaccination. Report of three cases. JAMA. 1969;207: 1115–9. Available: http://www.ncbi.nlm.nih.gov/pubmed/5818242

412. Lancefield RC. Persistence of type-specific antibodies in man following infection with group A streptococci. J Exp Med. 1959;110: 271–92. Available: http://www.ncbi.nlm.nih.gov/pubmed/13673139

413. Lancefield RC. Current knowledge of type-specific M antigens of group A streptococci. J Immunol. 1962;89: 307–13. Available: http://www.ncbi.nlm.nih.gov/pubmed/14461914

414. Dale JB. Group A streptococcal vaccines. Infect Dis Clin North Am. 1999;13: 227–43, viii. Available: http://www.ncbi.nlm.nih.gov/pubmed/10198801

415. Dale JB, Chiang EY, Lederer JW. Recombinant tetravalent group A streptococcal M protein vaccine. J Immunol. 1993;151: 2188–94. Available: http://www.ncbi.nlm.nih.gov/pubmed/8345202

416. Dale JB, Simmons M, Chiang EC, Chiang EY. Recombinant, octavalent group A streptococcal M protein vaccine. Vaccine. 1996;14: 944–8. Available:

http://www.ncbi.nlm.nih.gov/pubmed/8345202

417. Hu MC, Walls M a, Stroop SD, Reddish M a, Beall B, Dale JB. Immunogenicity of a 26-valent group A streptococcal vaccine. Infect Immun. 2002;70: 2171–2177. doi:10.1128/IAI.70.4.2171

418. Dale JB, Penfound T a., Chiang EY, Walton WJ. New 30-valent M protein-based vaccine evokes cross-opsonic antibodies against non-vaccine serotypes of group A streptococci. Vaccine. Elsevier Ltd; 2011;29: 8175–8178. doi:10.1016/j.vaccine.2011.09.005

419. McNeil S a, Halperin S a, Langley JM, Smith B, Warren A, Sharratt GP, et al. Safety and immunogenicity of 26-valent group a *Streptococcus* vaccine in healthy adult volunteers. Clin Infect Dis. 2005;41: 1114–1122.

420. Kotloff KL, Corretti M, Palmer K, Campbell JD, Reddish M a, Hu MC, et al. Safety and immunogenicity of a recombinant multivalent group a streptococcal vaccine in healthy adults: phase 1 trial. JAMA. 2004;292: 709–715.

421. Shulman ST, Tanz RR, Dale JB, Beall B, Kabat W, Kabat K, et al. Seven-year surveillance of north american pediatric group a streptococcal pharyngitis isolates. Clin Infect Dis. 2009;49: 78–84. doi:10.1086/599344

422. Luca-Harari B, Darenberg J, Neal S, Siljander T, Strakova L, Tanna A, et al. Clinical and microbiological characteristics of severe *Streptococcus pyogenes* disease in Europe. J Clin Microbiol. 2009;47: 1155–65. doi:10.1128/JCM.02155-08

423. Engel ME, Muhamed B, Whitelaw AC, Musvosvi M, Mayosi BM, Dale JB. Group A streptococcal emm type prevalence among symptomatic children in Cape Town and potential vaccine coverage. Pediatr Infect Dis J. 2014;33: 208–10. doi:10.1097/INF.0b013e3182a5c32a

424. Dale JB, Penfound T a, Tamboura B, Sow SO, Nataro JP, Tapia M, et al. Potential coverage of a multivalent M protein-based group A streptococcal vaccine. Vaccine. Elsevier Ltd; 2013;31: 1576–81. doi:10.1016/j.vaccine.2013.01.019

425. Bessen D, Fischetti VA. Synthetic peptide vaccine against mucosal colonization by group A streptococci. I. Protection against a heterologous M serotype with shared C repeat region epitopes. J Immunol. 1990;145: 1251–6. Available: http://www.ncbi.nlm.nih.gov/pubmed/1696296

426. Batzloff MR, Hayman W a, Davies MR, Zeng M, Pruksakorn S, Brandt ER, et al. Protection against group A *Streptococcus* by immunization with J8-diphtheria toxoid: contribution of J8- and diphtheria toxoid-specific antibodies to protection. J Infect Dis. 2003;187: 1598–608. doi:10.1086/374800

427. Guilherme L, Faé KC, Higa F, Chaves L, Oshiro SE, de Barros SF, et al. Towards a Vaccine Against Rheumatic Fever. Clin Dev Immunol. Hindawi Publishing Corporation; 2006;13: 125–132. doi:10.1080/17402520600877026

428. Guilherme L, Postol E, Freschi de Barros S, Higa F, Alencar R, Lastre M, et al. A vaccine against S. *pyogenes*: design and experimental immune response. Methods.

Elsevier Inc.; 2009;49: 316–21. doi:10.1016/j.ymeth.2009.03.024

429. Pandey M, Batzloff MR, Good MF. Mechanism of protection induced by group A *Streptococcus* vaccine candidate J8-DT: contribution of B and T-cells towards protection. PLoS One. 2009;4: e5147. doi:10.1371/journal.pone.0005147

430. Sheel M, Pandey M, Good MF, Batzloff MR. Correlation between bioluminescence and bacterial burden in passively protected mice challenged with a recombinant bioluminescent M49 group A *Streptococcus* Strain. Clin Vaccine Immunol. 2010;17: 127–33. doi:10.1128/CVI.00256-09

431. Pandey M, Wykes MN, Hartas J, Good MF, Batzloff MR. Long-term antibody memory induced by synthetic peptide vaccination is protective against *Streptococcus pyogenes* infection and is independent of memory T cell help. J Immunol. 2013;190: 2692–701. doi:10.4049/jimmunol.1202333

432. Hayman WA, Brandt ER, Relf WA, Cooper J, Saul A, Good MF. Mapping the minimal murine T cell and B cell epitopes within a peptide vaccine candidate from the conserved region of the M protein of group A *Streptococcus*. Int Immunol. 1997;9: 1723–33. Available: http://www.ncbi.nlm.nih.gov/pubmed/9418133

433. Steer AC, Carapetis JR, Dale JB, Fraser JD, Good MF, Guilherme L, et al. Status of research and development of vaccines for *Streptococcus pyogenes*. Vaccine. Elsevier Ltd; 2016; 6–11. doi:10.1016/j.vaccine.2016.03.073

434. De Amicis KM, Freschi de Barros S, Alencar RE, Postól E, Martins CDO, Arcuri HA, et al. Analysis of the coverage capacity of the StreptInCor candidate vaccine against *Streptococcus pyogenes*. Vaccine. Elsevier Ltd; 2014;32: 4104–10. doi:10.1016/j.vaccine.2013.08.043

435. Postol E, Alencar R, Higa FT, Freschi de Barros S, Demarchi LMF, Kalil J, et al. StreptInCor: a candidate vaccine epitope against S. *pyogenes* infections induces protection in outbred mice. PLoS One. 2013;8: e60969. doi:10.1371/journal.pone.0060969

436. Guerino MT, Postol E, Demarchi LMF, Martins CDO, Mundel LR, Kalil J, et al. HLA class II transgenic mice develop a safe and long lasting immune response against StreptInCor, an anti-group A *Streptococcus* vaccine candidate. Vaccine. Elsevier Ltd; 2011;29: 8250–8256. doi:10.1016/j.vaccine.2011.08.113

437. Roggiani M, Stoehr J a, Olmsted SB, Matsuka Y V, Pillai S, Ohlendorf DH, et al. Toxoids of streptococcal pyrogenic exotoxin A are protective in rabbit models of streptococcal toxic shock syndrome. Infect Immun. 2000;68: 5011–7. Available: http://www.ncbi.nlm.nih.gov/pubmed/10948118

438. McCormick JK, Tripp TJ, Olmsted SB, Matsuka Y V, Gahr PJ, Ohlendorf DH, et al. Development of streptococcal pyrogenic exotoxin C vaccine toxoids that are protective in the rabbit model of toxic shock syndrome. J Immunol. 2000;165: 2306–2312.

439. Ulrich RG. Vaccine based on a ubiquitous cysteinyl protease and streptococcal pyrogenic exotoxin A protects against *Streptococcus pyogenes* sepsis and toxic shock. J Immune Based Ther Vaccines. BioMed Central; 2008;6: 8.

doi:10.1186/1476-8518-6-8

440. Sriskandan S, Ferguson M, Elliot V, Faulkner L, Cohen J. Human intravenous immunoglobulin for experimental streptococcal toxic shock: bacterial clearance and modulation of inflammation. J Antimicrob Chemother. 2006;58: 117–24. doi:10.1093/jac/dkl173

441. Rajagopalan G, Patel R, Kaveri S V, David CS. Comment on: Human intravenous immunoglobulin for experimental streptococcal toxic shock: bacterial clearance and modulation of inflammation. J Antimicrob Chemother. 2007;59: 157-9-60. doi:10.1093/jac/dkl430

442. Schrage B, Duan G, Yang LPH, Fraser JD, Proft T. Different preparations of intravenous immunoglobulin vary in their efficacy to neutralize streptococcal superantigens: implications for treatment of streptococcal toxic shock syndrome. Clin Infect Dis. 2006;43: 743–6. doi:10.1086/507037

443. Kapur V, Maffei JT, Greer RS, Li LL, Adams GJ, Musser JM. Vaccination with streptococcal extracellular cysteine protease (interleukin-1 beta convertase) protects mice against challenge with heterologous group A streptococci. Microb Pathog. 1994;16: 443–50. doi:10.1006/mpat.1994.1044

444. Sabharwal H, Michon F, Nelson DC, Dong W, Fuchs K, Manjarrez RC, et al. Group A *Streptococcus* (GAS) carbohydrate as an immunogen for protection against GAS infection. J Infect Dis. 2006;193: 129–135.

445. Cleary PP, Matsuka Y V, Huynh T, Lam H, Olmsted SB. Immunization with C5a peptidase from either group A or B streptococci enhances clearance of group a streptococci from intranasally infected mice. Vaccine. 2004;22: 4332–4341. doi:10.1016/j.vaccine.2004.04.030

446. Chen X, Li N, Bi S, Wang X, Wang B. Co-Activation of Th17 and Antibody Responses Provides Efficient Protection against Mucosal Infection by Group A *Streptococcus*. PLoS One. 2016;11: e0168861. doi:10.1371/journal.pone.0168861

447. Kawabata S, Kunitomo E, Terao Y, Nakagawa I, Kikuchi K, Totsuka K, et al. Systemic and mucosal immunizations with fibronectin-binding protein FBP54 induce protective immune responses against *Streptococcus pyogenes* challenge in mice. Infect Immun. 2001;69: 924–30. doi:10.1128/IAI.69.2.924-930.2001

448. Zhang X, Song Y, Li Y, Cai M, Meng Y, Zhu H. Immunization with Streptococcal Heme Binding Protein (Shp) Protects Mice Against Group A *Streptococcus* Infection. Adv Exp Med Biol. 2017;6: 57–66. doi:10.1007/5584_2016_198

449. Kasper KJ. Systematic Assessment of the Contribution of Superantigens to Nasopharyngeal Colonization in a Mouse Model of Streptococcal Infection [Internet]. The University of Western Ontario. 2013. Available: http://ir.lib.uwo.ca/etd/1120

450. Ferretti JJ, McShan WM, Ajdic D, Savic DJ, Savic G, Lyon K, et al. Complete genome sequence of an M1 strain of *Streptococcus pyogenes*. Proc Natl Acad Sci U S A. 2001;98: 4658–63. doi:10.1073/pnas.071559398

451. McCool TL, Cate TR, Moy G, Weiser JN. The immune response to pneumococcal proteins during experimental human carriage. J Exp Med. 2002;195: 359–65. doi:10.1084/jem.20011576

452. Syrjänen RK, Kilpi TM, Kaijalainen TH, Herva EE, Takala a K. Nasopharyngeal carriage of *Streptococcus pneumoniae* in Finnish children younger than 2 years old. J Infect Dis. 2001;184: 451–9. doi:10.1086/322048

453. Zhang Z, Clarke TB, Weiser JN. Cellular effectors mediating Th17-dependent clearance of pneumococcal colonization in mice. J Clin Invest. 2009;119: 1899–909. doi:10.1172/JCI36731

454. Kasper KJ. Functional Characterization of Streptococcal Superantigen Low-Affinity MHC Class II Binding Interfaces. The University of Western Ontario. 2007.

455. Chau TA, McCully ML, Brintnell W, An G, Kasper KJ, Vinés ED, et al. Toll-like receptor 2 ligands on the staphylococcal cell wall downregulate superantigen-induced T cell activation and prevent toxic shock syndrome. Nat Med. 2009;15: 641–8. doi:10.1038/nm.1965

456. Kapust RB, Tözsér J, Fox JD, Anderson DE, Cherry S, Copeland TD, et al. Tobacco etch virus protease: mechanism of autolysis and rational design of stable mutants with wild-type catalytic proficiency. Protein Eng. 2001;14: 993–1000. doi:10.1093/protein/14.12.993

457. Nabozny BGH, Baisch JM, Cheng S, Coggrovefi D, Grifl MM, Luthra IIHS, et al. HLA-DQ8 Transgenic Mice are Highly Susceptible to Collagen-Induced Arthritis: A Novel Model for Human Polyarthritis. J Exp Med. 1996;183: 27–37.

458. Sirard J-C, Fayolle C, de Chastellier C, Mock M, Leclerc C, Berche P. Intracytoplasmic delivery of listeriolysin O by a vaccinal strain of Bacillus anthracis induces CD8-mediated protection against *Listeria monocytogenes*. J Immunol. 1997;159: 4435–43. Available: http://www.ncbi.nlm.nih.gov/pubmed/9379042

459. Zeppa JJ, Wakabayashi AT, Kasper KJ, Xu SX, Haeryfar SMM, McCormick JK. Nasopharyngeal Infection of Mice with *Streptococcus pyogenes* and In Vivo Detection of Superantigen Activity. Methods Mol Biol. 2016;1396: 95–107. doi:10.1007/978-1-4939-3344-0_8

460. Puchta A, Verschoor CP, Thurn T, Bowdish DME. Characterization of inflammatory responses during intranasal colonization with *Streptococcus pneumoniae*. J Vis Exp. 2014; e50490. doi:10.3791/50490

461. Pavlidis P, Noble WS. Matrix2png: a utility for visualizing matrix data. Bioinformatics. 2003;19: 295–6. doi:10.1093/bioinformatics/19.2.295

462. Roggiani M, Stoehr JA, Leonard BA, Schlievert PM. Analysis of toxicity of streptococcal pyrogenic exotoxin A mutants. Infect Immun. 1997;65: 2868–75. Available: http://www.ncbi.nlm.nih.gov/pubmed/9199461

463. Lee KH, Wucherpfennig KW, Wiley DC. Structure of a human insulin peptide-

HLA-DQ8 complex and susceptibility to type 1 diabetes. Nat Immunol. 2001;2: 501–7. doi:10.1038/88694

464. Li PL, Tiedemann RE, Moffat SL, Fraser JD. The superantigen streptococcal pyrogenic exotoxin C (SPE-C) exhibits a novel mode of action. J Exp Med. 1997;186: 375–83. Available: http://www.ncbi.nlm.nih.gov/pubmed/9236189

465. Steer AC, Dale JB, Carapetis JR. Progress toward a global group a streptococcal vaccine. Pediatr Infect Dis J. 2013;32: 180–2. doi:10.1097/INF.0b013e318281da11

466. Cunningham MW. *Streptococcus* and rheumatic fever. Curr Opin Rheumatol. 2012;24: 408–16. doi:10.1097/BOR.0b013e32835461d3

467. Lozano R, Naghavi M, Foreman K, Lim S, Shibuya K, Aboyans V, et al. Global and regional mortality from 235 causes of death for 20 age groups in 1990 and 2010: a systematic analysis for the Global Burden of Disease Study 2010. Lancet (London, England). 2012;380: 2095–128. doi:10.1016/S0140-6736(12)61728-0

468. Norrby-Teglund A, Ihendyane N, Kansal R, Basma H, Kotb M, Andersson J, et al. Relative neutralizing activity in polyspecific IgM, IgA, and IgG preparations against group A streptococcal superantigens. Clin Infect Dis. 2000;31: 1175–82. doi:10.1086/317423

469. Norrby-Teglund A, Muller MP, Mcgeer A, Gan BS, Guru V, Bohnen J, et al. Successful management of severe group A streptococcal soft tissue infections using an aggressive medical regimen including intravenous polyspecific immunoglobulin together with a conservative surgical approach. Scand J Infect Dis. 2005;37: 166–72. doi:10.1080/00365540410020866

470. Linnér A, Darenberg J, Sjölin J, Henriques-Normark B, Norrby-Teglund A. Clinical efficacy of polyspecific intravenous immunoglobulin therapy in patients with streptococcal toxic shock syndrome: a comparative observational study. Clin Infect Dis. 2014;59: 851–7. doi:10.1093/cid/ciu449

471. Poindexter NJ, Schlievert PM. Suppression of immunoglobulin-secreting cells from human peripheral blood by toxic-shock-syndrome toxin-1. J Infect Dis. 1986;153: 772–9. Available: http://www.ncbi.nlm.nih.gov/pubmed/3512737

472. Hofer MF, Newell K, Duke RC, Schlievert PM, Freed JH, Leung DY. Differential effects of staphylococcal toxic shock syndrome toxin-1 on B cell apoptosis. Proc Natl Acad Sci U S A. 1996;93: 5425–30. Available: http://www.pubmedcentral.nih.gov/articlerender.fcgi?artid=39262&tool=pmcentrez&rendertype=abstract

473. Stohl W, Lynch DH, Starling GC, Kiener PA. Superantigen-driven, CD8+ T cell-mediated down-regulation: CD95 (Fas)-dependent down-regulation of human Ig responses despite CD95-independent killing of activated B cells. J Immunol. 1998;161: 3292–8. doi:10.4049/jimmunol.0903296

474. Stohl W, Elliott JE, Lynch DH, Kiener PA. CD95 (Fas)-based, superantigen-dependent, CD4+ T cell-mediated down-regulation of human in vitro immunoglobulin responses. J Immunol. 1998;160: 5231–8. Available:

http://www.ncbi.nlm.nih.gov/pubmed/9605118

475. Kupz A, Zedler U, Stäber M, Kaufmann SHE. A Mouse Model of Latent Tuberculosis Infection to Study Intervention Strategies to Prevent Reactivation. PLoS One. 2016;11: e0158849. doi:10.1371/journal.pone.0158849

476. Foxwell AR, Kyd JM, Karupiah G, Cripps AW. CD8+ T cells have an essential role in pulmonary clearance of nontypeable *Haemophilus influenzae* following mucosal immunization. Infect Immun. 2001;69: 2636–2642. doi:10.1128/IAI.69.4.2636-2642.2001

477. Li Z, Zhang C, Zhou Z, Zhang J, Zhang J, Tian Z. Small intestinal intraepithelial lymphocytes expressing CD8 and T cell receptor γδ are involved in bacterial clearance during *Salmonella enterica* serovar Typhimurium infection. Infect Immun. 2012;80: 565–74. doi:10.1128/IAI.05078-11

478. Malley R, Trzcinski K, Srivastava A, Thompson CM, Anderson PW, Lipsitch M. CD4+ T cells mediate antibody-independent acquired immunity to pneumococcal colonization. Proc Natl Acad Sci U S A. 2005;102: 4848–53. doi:10.1073/pnas.0501254102

479. Siegel SJ, Weiser JN. Mechanisms of Bacterial Colonization of the Respiratory Tract. Annu Rev Microbiol. 2015;69: 425–44. doi:10.1146/annurev-micro-091014-104209

480. Tsatsaronis J a, Walker MJ, Sanderson-Smith ML. Host Responses to Group A *Streptococcus*: Cell Death and Inflammation. PLoS Pathog. 2014;10: e1004266. doi:10.1371/journal.ppat.1004266

481. Malott RJ, Keller BO, Gaudet RG, McCaw SE, Lai CCL, Dobson-Belaire WN, et al. *Neisseria gonorrhoeae*-derived heptose elicits an innate immune response and drives HIV-1 expression. Proc Natl Acad Sci U S A. 2013;110: 10234–9. doi:10.1073/pnas.1303738110

482. Gaudet RG, Sintsova A, Buckwalter CM, Leung N, Cochrane A, Li J, et al. Innate Immunity. Cytosolic detection of the bacterial metabolite HBP activates TIFA-dependent innate immunity. Science. 2015;348: 1251–5. doi:10.1126/science.aaa4921

483. Gaudet RG, Gray-Owen SD. Heptose Sounds the Alarm: Innate Sensing of a Bacterial Sugar Stimulates Immunity. Kline KA, editor. PLOS Pathog. 2016;12: e1005807. doi:10.1371/journal.ppat.1005807

484. Lupp C, Robertson ML, Wickham ME, Sekirov I, Champion OL, Gaynor EC, et al. Host-mediated inflammation disrupts the intestinal microbiota and promotes the overgrowth of *Enterobacteriaceae*. Cell Host Microbe. 2007;2: 119–29. doi:10.1016/j.chom.2007.06.010

485. Hirano T, Kodama S, Kawano T, Suzuki M. Accumulation of Regulatory T Cells and Chronic Inflammation in the Middle Ear in a Mouse Model of Chronic Otitis Media with Effusion Induced by Combined Eustachian Tube Blockage and Nontypeable *Haemophilus influenzae* Infection. Infect Immun. 2015;84: 356–64. doi:10.1128/IAI.01128-15

486. Taylor AL, Llewelyn MJ. Superantigen-induced proliferation of human CD4+CD25- T cells is followed by a switch to a functional regulatory phenotype. J Immunol. 2010;185: 6591–8. doi:10.4049/jimmunol.1002416

487. Taylor AL, Cross ELA, Llewelyn MJ. Induction of contact-dependent CD8(+) regulatory T cells through stimulation with staphylococcal and streptococcal superantigens. Immunology. 2012;135: 158–67. doi:10.1111/j.1365-2567.2011.03529.x

488. Stjernquist-Desatnik A, Prellner K, Schalén C. High recovery of *Haemophilus influenzae* and group A streptococci in recurrent tonsillar infection or hypertrophy as compared with normal tonsils. J Laryngol Otol. 1991;105: 439–41. doi:10.1017/S002221510011624X

489. Agren K, Andersson U, Nordlander B, Nord CE, Linde A, Ernberg I, et al. Upregulated local cytokine production in recurrent tonsillitis compared with tonsillar hypertrophy. Acta Otolaryngol. 1995;115: 689–96. doi:10.3109/00016489509139388

490. Agren K, Brauner A, Andersson J. *Haemophilus influenzae* and *Streptococcus pyogenes* group A challenge induce a Th1 type of cytokine response in cells obtained from tonsillar hypertrophy and recurrent tonsillitis. ORL J Otorhinolaryngol Relat Spec. 1998;60: 35–41. Available: http://www.ncbi.nlm.nih.gov/pubmed/9519380

491. Xu SX, Kasper KJ, Zeppa JJ, McCormick JK. Superantigens Modulate Bacterial Density during *Staphylococcus aureus* Nasal Colonization. Toxins (Basel). 2015;7: 1821–1836. doi:10.3390/toxins7051821

492. Sumby P, Porcella SF, Madrigal AG, Barbian KD, Virtaneva K, Ricklefs SM, et al. Evolutionary origin and emergence of a highly successful clone of serotype M1 group a *Streptococcus* involved multiple horizontal gene transfer events. J Infect Dis. 2005;192: 771–82. doi:10.1086/432514

493. Chatellier S, Ihendyane N, Kansal RG, Khambaty F, Basma H, Norrby-Teglund A, et al. Genetic relatedness and superantigen expression in group A *Streptococcus* serotype M1 isolates from patients with severe and nonsevere invasive diseases. Infect Immun. 2000;68: 3523–34. doi:10.1128/IAI.68.6.3523-3534.2000

Appendices

Appendix 1. Human ethics approval certification.

Western Research

Research Ethics

Western University Health Science Research Ethics Board
HSREB Annual Continuing Ethics Approval Notice

Date: June 29, 2016
Principal Investigator: Dr. John McCormick
Department & Institution: Schulich School of Medicine and Dentistry\Microbiology & Immunology,Western University

Review Type: Delegated
HSREB File Number: 1268
Study Title: Molecular architecture of streptococcal superantigen/T cell receptor interactions
Sponsor: Canadian Institutes of Health Research

HSREB Renewal Due Date & HSREB Expiry Date:
Renewal Due -2017/06/30
Expiry Date -2017/07/21

The Western University Health Science Research Ethics Board (HSREB) has reviewed the Continuing Ethics Review (CER) Form and is re-issuing approval for the above noted study.

The Western University HSREB operates in compliance with the Tri-Council Policy Statement Ethical Conduct for Research Involving Humans (TCPS2), the International Conference on Harmonization of Technical Requirements for Registration of Pharmaceuticals for Human Use Guideline for Good Clinical Practice (ICH E6 R1), the Ontario Freedom of Information and Protection of Privacy Act (FIPPA, 1990), the Ontario Personal Health Information Protection Act (PHIPA, 2004), Part 4 of the Natural Health Product Regulations, Health Canada Medical Device Regulations and Part C, Division 5, of the Food and Drug Regulations of Health Canada.

Members of the HSREB who are named as Investigators in research studies do not participate in discussions related to, nor vote on such studies when they are presented to the REB.

The HSREB is registered with the U.S. Department of Health & Human Services under the IRB registration number IRB 00000940.

Ethics Officer, on behalf of Dr. Joseph Gilbert, HSREB Chair

Ethics Officer: Erika Basile ___ Katelyn Harris___ Nicole Kaniki___ Grace Kelly ___ Vikki Tran ___ Karen Gopaul ___

Western University, Research, Support Services Bldg., Rm. 5150
London, ON, Canada N6G 1G9 t. 519.661.3036 f. 519.850.2466 www.uwo.ca/research/ethics

Appendix 2. Animal ethics approval certification.

Western

AUP Number: 2011-088
AUP Title: Vaccine development for colonization and sepsis of Streptococcus pyogenes
Yearly Renewal Date: 06/01/2015

The YEARLY RENEWAL to Animal Use Protocol (AUP) 2011-088 has been approved, and will be approved for one year following the above review date.

1. This AUP number must be indicated when ordering animals for this project.
2. Animals for other projects may not be ordered under this AUP number.
3. Purchases of animals other than through this system must be cleared through the ACVS office. Health certificates will be required.

REQUIREMENTS/COMMENTS
Please ensure that individual(s) performing procedures on live animals, as described in this protocol, are familiar with the contents of this document.

The holder of this Animal Use Protocol is responsible to ensure that all associated safety components (biosafety, radiation safety, general laboratory safety) comply with institutional safety standards and have received all necessary approvals. Please consult directly with your institutional safety officers.

Submitted by: Kinchlea, Will D
on behalf of the Animal Use Subcommittee

Appendix 3. Vaccination with SpeA$_{N20A/Y100A}$ elicits an antibody-dependent bimodal phenotype.

A. HLA-DR4/DQ8 mice were vaccinated with SpeA$_{N20A/Y100A}$ and intranasally infected with 10^8 CFU of *S. pyogenes* MGAS8232. Data points represent CFU from the cNT of individual mice 48 hours post infection. Horizontal bars represent the mean. Horizontal dotted line indicates limit of detection. **B.** Serum was collected 24 hours prior to infection and used to assess IgG antibody titres using ELISA ($n \geq 3$). Data represented as the mean ± SEM. Significance determined by Student's *t* test (***, $P < 0.001$). The cNT bacterial load and anti-SpeA IgG titre data have already been reported (Figure 17B and C, respectively).

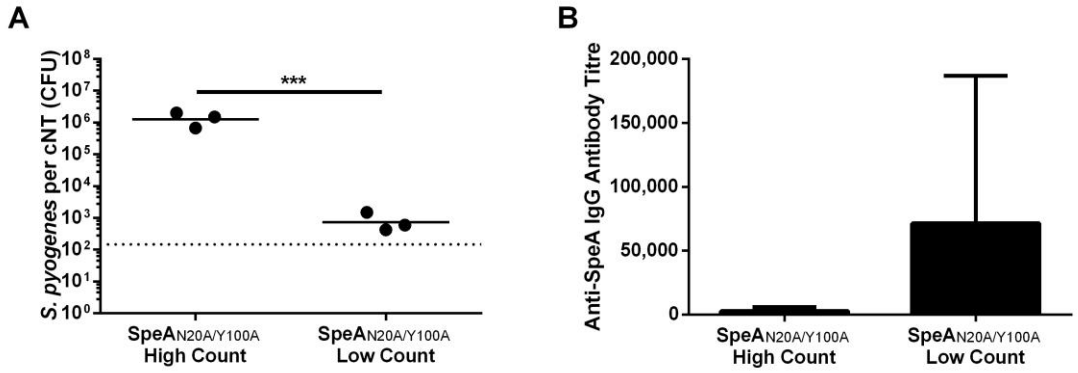

Appendix 4. Cytokine response from complete nasal turbinates during streptococcal infection after indicated treatment.

Mice were treated with T cell depleting antibodies (CD4 [GK1.5], CD8 [YTS 169.4] or combination), an isotype control (LTF-2) or wild-type SAg vaccination (SpeA or SEB) or control (sham) and infected intranasally with either 10^8 CFU *S. pyogenes* MGAS8232 or 10^7 *S. pneumoniae* P1121. Sacrifice occurred 48 hours later and complete nasal turbinates (cNT) homogenates were analyzed for multiple cytokines and chemokines (Th1-type [**A**]; Th2-type cytokines [**B**]; Treg cytokines [**C**]; Th17 cytokines [**D**]; chemokines [**E**]; or growth factors [**F**]). Data represents the mean ± SEM of cNT cytokine/chemokine concentration (pg mL^{-1}) ($n \geq 3$ mice per group). Significance was determined by one-way ANOVA with Dunnett's multiple comparison post-hoc test (*S. pyogenes*) or Student's *t* test (*S. pneumoniae*) (*, $P < 0.05$; **, $P < 0.01$; ***, $P < 0.001$).

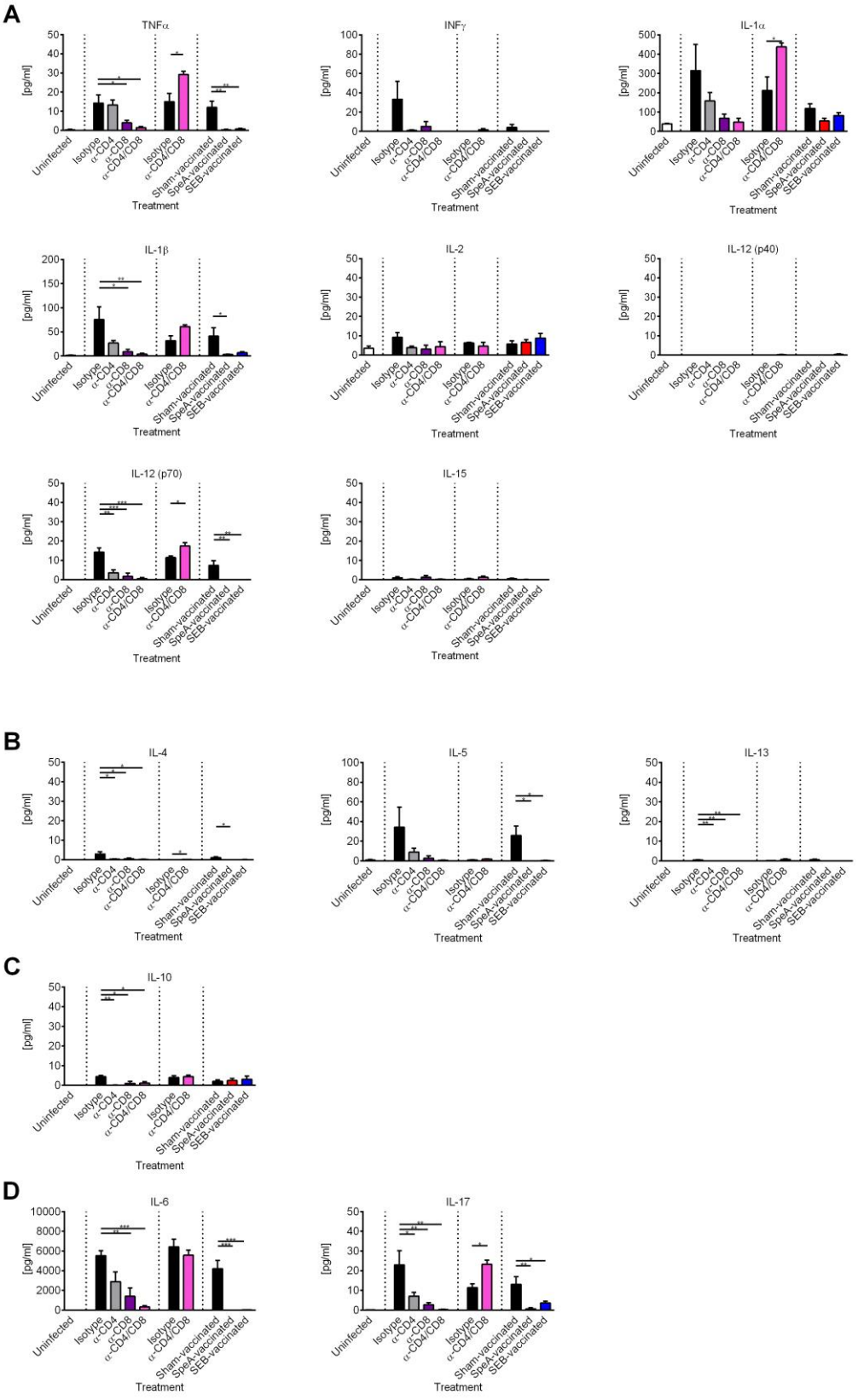
A
TNFα
INFγ
IL-1α
IL-1β
IL-2
IL-12 (p40)
IL-12 (p70)
IL-15
B
IL-4
IL-5
IL-13
C
IL-10
D
IL-6
IL-17
[pg/ml]
Treatment
Uninfected
Isotype
α-CD4
α-CD8
α-CD4/CD8
Isotype
α-CD4/CD8
Sham-vaccinated
SpeA-vaccinated
SEB-vaccinated

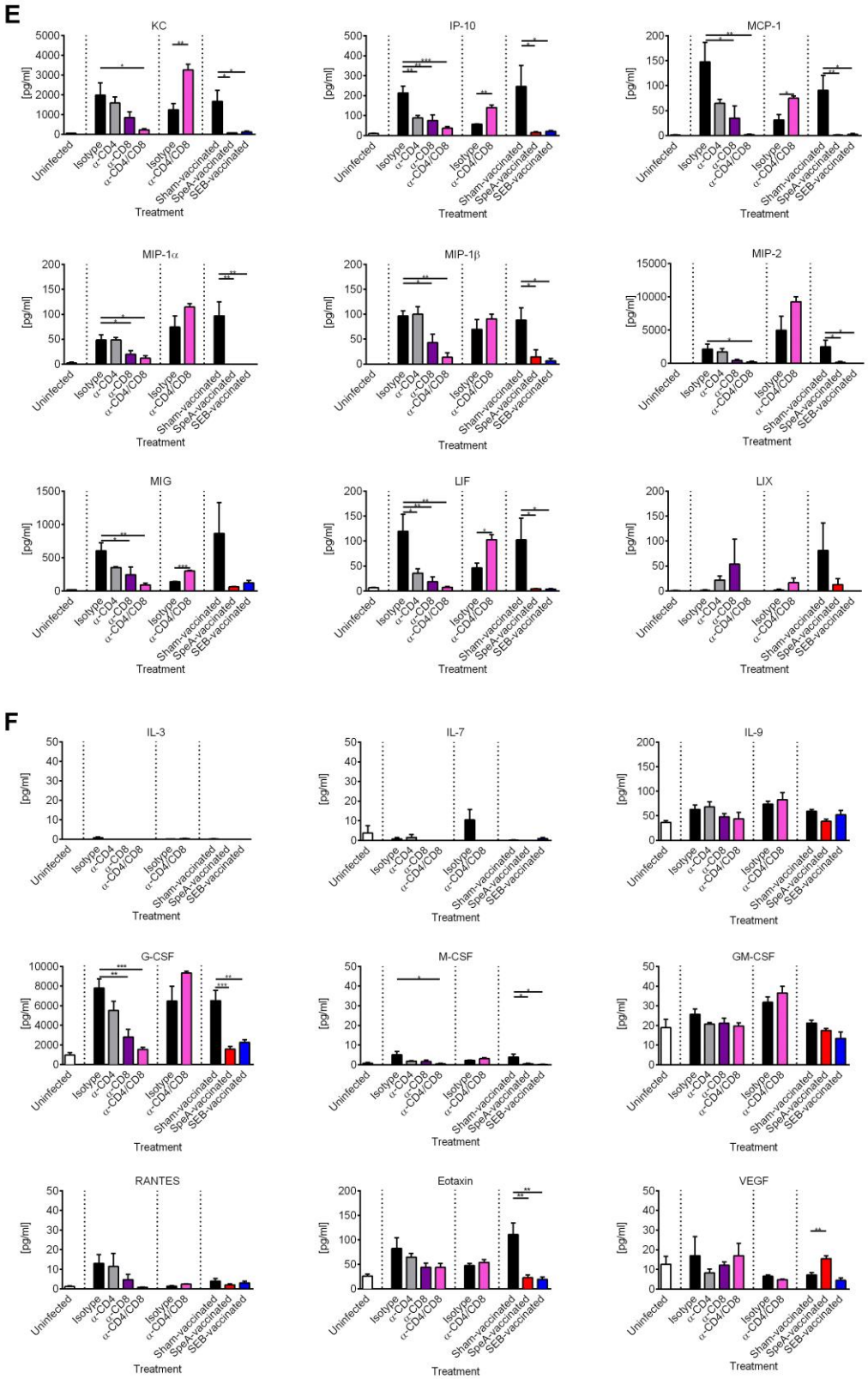
E
KC
IP-10
MCP-1
MIP-1α
MIP-1β
MIP-2
MIG
LIF
LIX
F
IL-3
IL-7
IL-9
G-CSF
M-CSF
GM-CSF
RANTES
Eotaxin
VEGF
[pg/ml]
Uninfected
Isotype
α-CD4
α-CD8
α-CD4/CD8
Sham-vaccinated
SpeA-vaccinated
SEB-vaccinated
Treatment

Curriculum Vitae

Joseph John Zeppa, BMSc.

Education

2011 – present	Doctor of Philosophy Candidate (Ph.D.) Department of Microbiology and Immunology, Schulich School of Medicine and Dentistry, The University of Western Ontario, London, Ontario
2007 – 2011	Bachelor of Medical Sciences (BMSc.), Honors Specialization in Microbiology and Immunology The University of Western Ontario, London, Ontario

Research Experience

2011 – present	**Ph.D. Candidate**, Department of Microbiology and Immunology, The University of Western Ontario, London, Ontario Thesis: *T cell involvement during Streptococcus pyogenes host-pathogen interactions and preventative vaccination strategies*
2010 – 2011	**Summer Laboratory Technician**, Laboratory of Dr. John McCormick, The University of Western Ontario, London, Ontario
2010 – 2011	**4th Year Honors Thesis Project**, Department of Microbiology and Immunology, The University of Western Ontario, London, Ontario Thesis: *Engineer single-chain MHC class II molecules as novel inhibitors for bacterial superantigens*
2009 – 2010	**Work Study Student**, Laboratory of Dr. John McCormick, The University of Western Ontario, London, Ontario

Honours and Awards

2016	Dr. Frederick W. Luney Graduate Travel Award in Microbiology and Immunology, The University of Western Ontario ($2,000)
2016	Graduate Ambassador Award, Canadian Society of Microbiologists ($1,500)
2015 – 2016	Ontario Graduate Scholarship ($15,000)
2015	Second Place Oral Presentation Award, London Health Research Day, London, Ontario ($600)

2015 Dr. Frederick W. Luney Graduate Travel Award in Microbiology and Immunology, The University of Western Ontario ($2,000)

2014 Terry Beveridge Poster Award, Top Student Poster Presentation – Infection and Immunity, 64th Annual Canadian Society of Microbiologists /International Union of Microbiological Societies Joint Meeting, Montreal, Quebec ($500)

2014 Travel Award, 114th General Meeting of the American Society for Microbiology, Boston, Massachusetts ($500)

2014 Travel Award, 64th Annual Canadian Society of Microbiologists/International Union of Microbiological Societies Joint Meeting, Montreal, Quebec ($500)

2013 – 2014 Ontario Graduate Scholarship ($15,000)

2013 Dr. John Robinson Graduate Scholarship, Department of Microbiology and Immunology, The University of Western Ontario, London, Ontario ($1,200)

2013 Dr. Frederick W. Luney Graduate Entrance Fellowship, The Department of Microbiology and Immunology, The University of Western Ontario, London, Ontario ($2,500)

2011 – 2016 Western Graduate Research Scholarship, The University of Western Ontario, London, Ontario ($37,288.53)

2011 Microbiology and Immunology Graduate Entrance Scholarship, The Department of Microbiology and Immunology, The University of Western Ontario, London, Ontario ($2,000)

2009 – 2011 Dean's Honor List, The University of Western Ontario, London, Ontario

Publications and Presentations

Publications

Zeppa, J. J., I. Mohorovic, S. M. M. Haeryfar and J. K. McCormick. 2017. Acute nasopharyngeal infection by *Streptococcus pyogenes* requires superantigen-responsive Vβ-specific T cells. Submitted.

Armstrong, B. D., C. A. Herfst, N. C. Tonial, A. T. Wakabayashi, **J. J. Zeppa** and J. K. McCormick. 2016. Identification of a two-component Class IIb bacteriocin in *Streptococcus pyogenes* by recombinase-based *in vivo* expression technology. *Sci. Rep.* 6: 36233.

Zeppa, J. J., A. T. Wakabayashi, K. J. Kasper, S. X. Xu, S. M. Mansour Haeryfar, and J. K. McCormick. 2016. Nasopharyngeal infection of mice with *Streptococcus pyogenes* and *in vivo* detection of superantigen activity. *Method Mol. Biol.* 1396: 95-107.

Xu, S. X., K. J. Kasper, **J. J. Zeppa**, and J. K. McCormick. 2015. Superantigens modulate bacterial density during *Staphylococcus aureus* nasal colonization. *Toxins* (Basel). 7: 1821-1836.

Xu, S. X., K. J. Gilmore, P. A. Szabo, **J. J. Zeppa**, M. L. Baroja, S. M. M. Haeryfar, and J. K. McCormick. 2014. Superantigens Subvert the Neutrophil Response To Promote Abscess Formation and Enhance *Staphylococcus aureus* Survival *in vivo*. *Infect. Immun.* 82: 3588–98.

Kasper, K. J., **J. J. Zeppa**, A. T. Wakabayashi, S. X. Xu, D. M. Mazzuca, I. Welch, M. L. Baroja, M. Kotb, E. Cairns, P. P. Cleary, S. M. M. Haeryfar, and J. K. McCormick. 2014. Bacterial Superantigens Promote Acute Nasopharyngeal Infection by *Streptococcus pyogenes* in a Human MHC Class II-Dependent Manner. *PLoS Pathog.* 10: e1004155.

Anantha, R. V., K. J. Kasper, K. G. Patterson, **J. J. Zeppa**, J. Delport, and J. K. McCormick. 2013. Fournier's gangrene of the penis caused by *Streptococcus dysgalactiae* subspecies *equisimilis*: case report and incidence study in a tertiary-care hospital. *BMC Infect. Dis.* 13: 381.

Oral Presentations

2016 **Joseph J. Zeppa**, Katherine J. Kasper, Delfina M. Mazzuca, Ivor Mohorovic, S. M. Mansour Haeryfar and John K. McCormick. Nasopharyngeal infection by *Streptococcus pyogenes* requires superantigen-responsive T cells. CSM Graduate Ambassador Award Presentation 2 – The University of British Columbia, Vancouver, British Columbia

2016 **Joseph J. Zeppa**, Katherine J. Kasper, Delfina M. Mazzuca, Ivor Mohorovic, S. M. Mansour Haeryfar and John K. McCormick. Nasopharyngeal infection by *Streptococcus pyogenes* requires superantigen-responsive T cells. American Society for Microbiology Conference on Streptococcal Genetics, Washington, D.C.

2016 **Joseph J. Zeppa**, Katherine J. Kasper, Delfina M. Mazzuca, Ivor Mohorovic, S. M. Mansour Haeryfar and John K. McCormick. Nasopharyngeal infection by *Streptococcus pyogenes* requires superantigen-responsive T cells. CSM Graduate Ambassador Award Presentation 1 – The University of Toronto, Toronto, Ontario

2015 **Joseph J. Zeppa**, Katherine J. Kasper, Adrienne T. Wakabayashi, Delfina M. Mazzuca, S. M. Mansour Haeryfar and John K. McCormick. Vaccine approaches targeting colonization by *Streptococcus pyogenes*. 8th

International Conference on Gram-Positive Microorganisms, Montecatini Terme, Tuscany, Italy

2015 **Joseph J. Zeppa**, Katherine J. Kasper, Adrienne T. Wakabayashi, Delfina M. Mazzuca, S. M. Mansour Haeryfar and John K. McCormick. Vaccine approaches targeting colonization by *Streptococcus pyogenes*. Southwestern Ontario Pathogenesis Meeting, Guelph, Ontario

2015 **Joseph J. Zeppa**, Katherine J. Kasper, Adrienne T. Wakabayashi, Delfina M. Mazzuca, S. M. Mansour Haeryfar and John K. McCormick. Vaccine approaches targeting colonization by *Streptococcus pyogenes*. London Health Research Day, London, Ontario
Second Place Oral Presentation Award

2014 **Joseph J. Zeppa**, Katherine J. Kasper, Adrienne T. Wakabayashi, Delfina M. Mazzuca, S. M. Mansour Haeryfar and John K. McCormick. Vaccine approaches targeting colonization by *Streptococcus pyogenes*. Talks on Fridays Student Development and Recognition Program, St. Joseph's Health Care, Lawson Health Research Institute, London, Ontario

2014 **Joseph J. Zeppa**, Katherine J. Kasper, Adrienne T. Wakabayashi, Delfina M. Mazzuca, S. M. Mansour Haeryfar and John K. McCormick. Vaccine approaches targeting colonization by *Streptococcus pyogenes*. 64th Annual Canadian Society of Microbiologists/International Union of Microbiological Societies Joint Meeting, Montreal, Quebec

2014 **Joseph J. Zeppa**. Stopping the Scourge of Strep Throat. Three Minute Thesis, The University of Western Ontario, London, Ontario

Poster Presentations

2016 **Joseph J. Zeppa**, Katherine J. Kasper, Delfina M. Mazzuca, Ivor Mohorovic, S. M. Mansour Haeryfar and John K. McCormick. Nasopharyngeal infection by *Streptococcus pyogenes* requires superantigen-responsive T cells. 66th Annual Canadian Society of Microbiologists General Meeting, Toronto, Ontario

2016 **Joseph J. Zeppa**, Katherine J. Kasper, Delfina M. Mazzuca, Ivor Mohorovic, S. M. Mansour Haeryfar and John K. McCormick. Nasopharyngeal infection by *Streptococcus pyogenes* requires superantigen-responsive T cells. Banff Conference of Infectious Disease, Banff, Alberta

2015 **Joseph J. Zeppa**, Katherine J. Kasper, Adrienne T. Wakabayashi, Delfina M. Mazzuca, S. M. Mansour Haeryfar and John K. McCormick. Vaccine approaches targeting colonization by *Streptococcus pyogenes*. Canadian Student Health Research Forum, Winnipeg, Manitoba

2015 **Joseph J. Zeppa**, Katherine J. Kasper, Adrienne T. Wakabayashi, Delfina M. Mazzuca, S. M. Mansour Haeryfar and John K. McCormick. Vaccine approaches targeting colonization by *Streptococcus pyogenes*. Department of Microbiology and Immunology 2015 Retreat, Grand Bend, Ontario

2014 **Joseph J. Zeppa**, Katherine J. Kasper, Adrienne T. Wakabayashi, Delfina M. Mazzuca, S. M. Mansour Haeryfar and John K. McCormick. Vaccine approaches targeting colonization by *Streptococcus pyogenes*. 64th Annual Canadian Society of Microbiologists/International Union of Microbiological Societies Joint Meeting, Montreal, Quebec
Terry Beveridge Poster Award – Top Student Poster Presentation – Infection and Immunity

2014 **Joseph J. Zeppa**, Katherine J. Kasper, Adrienne T. Wakabayashi, Delfina M. Mazzuca, S. M. Mansour Haeryfar and John K. McCormick. Vaccine approaches targeting colonization by *Streptococcus pyogenes*. American Society for Microbiology 114th General Meeting, Boston, Massachusetts

2014 **Joseph J. Zeppa**, Katherine J. Kasper, Delfina M. Mazzuca, S. M. Mansour Haeryfar and John K. McCormick. Vaccine approaches targeting colonization by *Streptococcus pyogenes*. London Health Research Day, London, Ontario

2013 **Joseph J. Zeppa**, Katherine J. Kasper, Delfina M. Mazzuca, S. M. Mansour Haeryfar and John K. McCormick. Vaccine approaches targeting colonization by *Streptococcus pyogenes*. Infection and Immunity Research Forum, London, Ontario

2013 **Joseph J. Zeppa**, Katherine J. Kasper, Delfina M. Mazzuca, S. M. Mansour Haeryfar and John K. McCormick. Vaccine approaches targeting colonization by *Streptococcus pyogenes*. London Health Research Day, London, Ontario

2012 **Joseph J. Zeppa**, Katherine J. Kasper, Delfina M. Mazzuca, S. M. Mansour Haeryfar and John K. McCormick. Vaccine approaches targeting colonization by *Streptococcus pyogenes*. Infection and Immunity Research Forum, London, Ontaio

Scholarly and Professional Activities

Teaching Experience

2016 Lecturer: Microbiology and Immunology 3500B: Biological and Social Determinants of Disease – Lecture on Rheumatic Heart Disease
Department of Microbiology and Immunology, The University of Western Ontario, London, Ontario

2012 – 2016 Teaching Assistant: Microbiology and Immunology 3600/3620G: Immunology Laboratory
Department of Microbiology and Immunology, The University of Western Ontario, London, Ontario

Mentorship and Supervision

2013 – 2017 4th Year Honors Thesis Student Mentor
Laboratory of Dr. John McCormick, The Department of Microbiology and Immunology, The University of Western Ontario, London, Ontario
Students: Akshay Sule (2016 – 2017)
Jacklyn Hurst (2015 – 2016)
Annamarie Edwards (2013 – 2014)

2011 – 2017 Work Study Supervisor
Laboratory of Dr. John McCormick, The Department of Microbiology and Immunology, The University of Western Ontario, London, Ontario

Select Volunteer Experiences

2015 – 2016 Retiring with Strong Minds – Strong Bones, Strong Minds, Strong Muscles
2015 American Society for Virology General Meeting Volunteer, The University of Western Ontario, London, Ontario
2012 – 2016 Department of Microbiology and Immunology Undergraduate Education Committee
2011 – 2016 Microbiology and Immunology Department Representative, University Open Houses
2011 – 2016 Department of Microbiology and Immunology Social Committee Member
2011 – 2013 Let's Talk Science Classroom Volunteer
2010 – 2016 Infection and Immunity Research Forum Conference Organizer

Memberships

2013 – present Canadian Society for Immunology
2013 – present Canadian Society of Microbiologists
2013 – present American Society for Microbiology